RADIATIVE HEAT TRANSMISSION FROM NON-LUMINOUS GASES. COMPUTATIONAL STUDY OF THE EMISSIVITIES OF WATER VAPOR AND CARBON DIOXIDE.

by

Ihab Hanna Farag

B.S. (with Honor), Cairo University, Giza
Egypt (1967)

S.M., Massachusetts Institute of Technology (1970)

Ch.E., Massachusetts Institute of Technology (1971)

Submitted in Partial Fulfillment of the

Requirements for the Degree of

Doctor of Science

at the

Massachusetts Institute of Technology

August 1976

Signature of Author _____

Department of Chemical Engineering August 1976

Certified by: _____

Adel F. Sarofim, Thesis Supervisor

_____

Hoyt C. Hottel, Thesis Supervisor

Approved by: _____

Glenn C. Williams, Chairman
Department Committee on Graduate Students

ABSTRACT

RADIATIVE HEAT TRANSMISSION FROM NON-LUMINOUS GASES. COMPUTATIONAL STUDY OF THE EMISSIVITIES OF WATER VAPOR AND CARBON DIOXIDE.

by

Ihab H. Farag

Submitted to the Department of Chemical Engineering
on August , 1976, in partial fulfillment of the
requirements for the degree of Doctor of Science.

Published spectral data on the emission/absorption characteristics of water vapor and carbon dioxide gases, which are generally in the form of the absorption coefficient and the mean line spacing averaged over same spectral interval have been compiled and studied. Different gas band models were studied and the gas statistical model have been adopted as the present model for emissivity and absorptivity calculation. Total emissivity and absorptivity data of carbon dioxide, water vapor and their mixture by various investigators have been complied, corrected to a common partial pressure of zero and total pressure of one atmsophere and critically reviewed. Spectral data of carbon dioxide were modified to include the 10 and 2 micron bands, which are of importance at high temperatures. Computed emissivities of carbon dioxide were compared to experimental data to construct the recommended emissivity charts for carbon dioxide at $p_c = 0$, $P_t = 1$ atm. Comparison of corrected experimental water vapor emissivities with computed using the Ludwig et. al. (1973) spectral tabulations necessitated the modification of the rotation band absorptive coefficient to include the more recent tabulations of McClatchey et. al. (1972) at 300 and 600 K. Computed emissivities are compared to experimental and rules for constructing the recommended emissivity charts for water vapor at $p_w = 0$, $P_t = 1$ atm. are presented and implemented. Pressure broadening correction factor charts are presented both in a set of general plots and a set of Engineering plots. Overlap correction charts due to superimposed spectral radiation bands are presented in two different sets of plots at $p_c = p_w = 0$ and $P_t = 1$ atm. Pressure boradening correction of the overlap correction is discussed and a "Grey gas" approximation proposed in the work is discussed.

Ludwig, C. D., W. Malkmus, T. E. Reardon and J. A. L. Thomson (1973) 'Handbook of Infrared Radiation from Combustion Gases', Ed. R. Goulard and J. A. L. Thomson, NASA SP-3080, Washington, D. C.

McClatchey, R. A., R. W. Fenn, T. E. A. Selby, F. E. Volz and J. S. Garing (1972) 'Optical Properties of the Atmosphere', Third Edition, AFCRL-72-0497, Bedford, Mass.

Thesis Supervisors: Hoyt C. Hottel
Adel F. Sarofim

Department of Chemical Engineering
Massachusetts Institute of Technology
Cambridge, Massachusetts 02139

August 1976

Professor Irving Kaplan
Secretary of the Faculty
Massachusetts Institute of Technology
Cambridge, Massachusetts 02139

Dear Professor Kaplan:

In accordance with the regulations of the faculty, I herewith submit a thesis entitled "Radiative Heat Transmission from Non-Luminous Gases. Computational Study of the Emissivities of Water Vapor and Carbon Dioxide", in partial fulfillment of the requirements for the degree of Doctor of Science in Chemical Engineering at the Massachusetts Institute of Technology.

Respectfully submitted,

Ihab H. Farag

ACKNOWLEDGEMENTS

My utmost gratitude to Professor Adel F. Sarofim for his invaluable advice, great willingness, continued encouragement and considerable time he gave me.

My deepest gratitude to Professor Hoyt C. Hottel for the enormous amount of time he spent with me, the invaluable advice, comments, and suggestions he gave me.

Thanks are also due to Professor Glenn C. Williams for his valuable comments, suggestions, advice, and effort in providing financial support.

I am very grateful to the Chemical Engineering Department for providing me with financial aid in the form of Instructorship and free computer time on its two computers.

My thanks are extended to Mrs. Sharon W. Brown for her enthusiasm and dedication in typing my thesis.

I am most indebted to my parents for their continuous confidence and encouragement throughout my studies.

Finally, my utmost praise is to my wife, Madiha, whose patience, continuous encouragement, and great understanding were immeasurable. Not only did she not mind being lonely on many long nights, but she continually provided me love, affection, and encouragement.

To

My

Madiha

TABLE OF CONTENTS

Title Page	1
Abstract	2
Letter of Transmittal	3
Acknowledgements	4
Table of Contents	6
List of Figures	10
List of Tables	15
Chapter 1 Summary	16
1.1 Intorduction	16
1.2 Basic Definitions	17
1.3 Spectral Data	21
1.3.1 Water Vapor	21
1.3.2 Carbon Dioxide	22
1.4 Results and Discussion	22
1.4.1 Carbon Dioxide	22
1.4.2 Pressure Broadening Correction Factor of Carbon Dioxide	28
1.4.3 Water Vapor	30
1.4.4 Pressure Broadening Correction Factor of Water Vapor	35
1.4.5 Overlap Correction	36
1.4.6 Pressure Broadening Correction of Overlap Correction and Emissivity of Mixture	40
Chapter 2 Introduction	42
2.1 Preface	42
2.2 Theoretical Considerations	43
2.2.1 Single Line Emission	43

TABLE OF CONTENTS (continued)

2.3 Equations of Radiative Transfer in Nonscattering Media 47

2.4 Transmissivity 47

2.5 Collision Line Width 49

2.5.1 Introduction 49

2.5.2 Effect of Pressure 49

2.5.3 Effect of Temperature 51

Chapter 3 Homogeneous Gases 55

3.1 Introduction 55

3.2 Thin Gas Approximation 55

3.3 Grey Gas Approximation 56

3.4 Non-Overlapping Lines Approximation 57

3.5 Integrated Emissivities 57

3.6 Total Emissivity and Absorptivity 58

3.7 Band Models 59

3.7.1 Elsasser Model for Collision-Broadened Lines Having Lorentz Shape 59

3.7.2 Random Band Models 60

3.7.2.1 Exponential Line Strength Distribution 60

3.7.3 High Pressure Limit of Emissivity 62

3.7.4 Lower Limit of Gas Emissivity 62

3.8 Pressure Broadening Correction Factor 63

3.9 Emissivity for a Mixture of Water Vapor and Carbon Dioxide 66

Chapter 4 Spectral and Total Emission Data 68

4.1 Water Vapor 68

4.1.1 Introduction 68

TABLE OF CONTENTS (continued)

4.1.2 Total Emissivity Measurement 68

4.1.2.1 Sources of Errors 68

4.1.2.1.1 Atmospheric Absorption 68

4.1.2.1.2 Knowledge of Exact Temperature 68

4.1.2.1.3 Stray Radiation 69

4.1.2.1.4 Determination of Path Length 69

4.1.2.1.5 Radiometric Errors 69

4.1.2.1.6 Partial Pressure Errors 69

4.1.2.1.7 Edge Cooling Effect 69

4.1.2.2 Schmidt 70

4.1.2.3 Mangelsdorf 70

4.1.2.4 Smith 72

4.1.2.5 Eckert 74

4.1.2.6 Eberhardt 77

4.1.2.7 Falckenberg 80

4.1.2.8 Elsasser 80

4.1.2.9 Brooks 81

4.1.2.10 Egbert 83

4.1.3 Spectral Data of Water Vapor 84

4.1.3.1 Introduction 84

4.2 Carbon Dioxide 107

4.2.1 Introduction 107

4.2.2 Total Emissivity Measurements 107

4.2.2.1 Rubens and Ladenberg 107

4.2.2.2 Hottel and Mangelsdorf 107

4.2.2.3 Hottel and Smith 109

TABLE OF CONTENTS (continued)

4.2.2.4 Eckert 109

4.2.2.5 Akhunov et al. 112

4.2.3 Spectral Data 115

4.2.4 Calculation of Band Contributions 128

4.3 Mixtures of Carbon Dioxide and Water Vapor 131

4.3.1 Introduction 131

4.3.2 Mixture Measurements 131

4.3.2.1 Hottel and Mangelsdorf 131

4.3.2.2 Eberhardt 133

4.3.2.3 Millard 133

4.3.2.4 Fishenden 133

4.3.2.5 Eckert 137

4.3.2.6 Sarofim 137

4.3.2.7 Hines and Edwards 139

Chapter 5 Results and Discussion 142

5.1 Results and Discussion of Carbon Dioxide 142

5.2 Pressure Broadening Correction Factor of Carbon Dioxide 153

5.3 Water Vapor 164

5.4 Pressure Broadening Correction Factor of Water Vapor 174

5.5 Overlap Correction 194

5.6 Pressure Broadening Correction of Overlap Correction and Emissivity of Mixture 214

Chapter 6 Conclusions and Recommendations 222

Nomenclature 223

References 225

LIST OF FIGURES

4.1.2-2	Schmidt Water Vapor Data	71
4.1.2.3-1	Hottel and Mangelsdorf Water Vapor Data	73
4.1.2.4-1	Hottel and Smith Water Vapor Data	75
4.1.2.5-1	Eckert Water Vapor Data L = 10.2 cm.	76
4.1.2.5-2	Eckert Water Vapor Data L = 65.4 cm.	78
4.1.2.6-1	Eberhardt Water Vapor Data	79
4.1.2.8-1	Water Vapor Data of Falckenberg, Elsasser, and Brooks	82
4.1.3.1-1	Effect of Temperature on Integrated Band Intensities of the 1.9, 4.3, 2.7, and 6.3 Micron Bands of Water Vapor	91
4.1.3.1-2	Tejwani and Varanasi Water Vapor Absorption Coefficient at 400 K	94
4.1.3.1-3	Tejwani and Varanasi Water Vapor Absorption Coefficient at 600 K	95
4.1.3.1-4	Tejwani and Varanasi Water Vapor Absorption Coefficient at 800 K	96
4.1.3.1-5	Tejwani and Varanasi Water Vapor Absorption Coefficient at 1000 K	97
4.1.3.1-6	Tejwani and Varanasi Water Vapor Absorption Coefficient at 1200 K	98
4.1.3.1-7	Spectral Absorption Coefficients of McClatchey et. al. and General Dynamics of the Rotation Band of Water Vapor at 300 K	100
4.1.3.1-8	Spectral Absorption Coefficients of Benedict, Palmer, Hettner , and Stauffer of the Rotation Band of Water Vapor at Room Temperature	101
4.1.3.1-9	Comparison of Spectral Water Vapor Absorption Coefficient in the Rotation Band at 600 K of General Dynamics and the Present Recommended Values	104

LIST OF FIGURES (continued)

4.1.3.1-10	Spectral Absorption Coefficients of the Rotation Band as Used in the Present Work	105
4.2.2.1-1	Absorptivity of Carbon Dioxide at 20 C. Data of Hertz and Ruben and Ladenburg	108
4.2.2.2-1	Hottel and Mangelsdorf Carbon Dioxide Data	110
4.2.2.4-1	Eckert's Carbon Dioxide Data	111
4.2.3-1	Effect of Temperature on the Integrated Band Intensities of the 1.9, 2.7, and 4.3 Micron Bands of CO_2	117
4.2.3-2	Effect of Temperature on the Integrated Band Intensity of the 10μ CO_2 Band	126
4.3.2.1-1	Hottel and Mangelsdorf Data on Overlap Correction	132
4.3.2.2-1	Mixture Emissivity (Eberhardt Data)	134
4.3.2.3-1	Mixture Emissivity (Millard Data)	135
4.3.2.4-1	Mixture Emissivity (Fishenden Data)	136
4.3.2.6-1	Sarofim's Calculated Overlap Correction	138
5.1-1	Smoothed Hottel and Smith Carbon Dioxide Emissivities, T = 1710, 1810, 1910, 2010, 2210, and 2310 K	143
5.1-2	Carbon Dioxide Emissivity (computed and experimental), pL = .1, .3, .8, 2, 5, 10, 30, 80 and 200 cm. atm.	144
5.1.3	Carbon Dioxide Emissivity (computed and experimental), pL - 1., .2, .5, 1, 3, 8, 20, 50, 100 and 300 cm. atm.	145
5.1-4	Recommended Carbon Dioxide Emissivity Chart p_c = 0, P_t = 1 atm. (ε v.s. T)	150
5.1-5	Recommended Carbon Dioxide Emissivity Chart p_c = 0, P_t = 1 atm. (ε v.s. pL)	151

LIST OF FIGURES (continued)

5.2-1	Pressure Broadening Correction Factor of CO_2 at 500 K	155
5.2-2	Pressure Broadening Correction Factor of CO_2 at 1000 K	156
5.2-3	Pressure Broadening Correction Factor of CO_2 at 1500 K	157
5.2-4	Pressure Broadening Correction Factor of CO_2 at 2000 K	158
5.2-5	Pressure Broadening Correction Factor of CO_2 at 2500 K	159
5.2-6	Pressure Broadening Correction Factor of CO_2 at 500 K and Total Pressure of One Atmosphere	160
5.2-7	Pressure Broadening Correction Factor of CO_2 at 1000 K and Total Pressure of One Atmosphere	161
5.3-1	Effect of Pressure Boradening Correction on the Scatter in the Raw Data of Water Vapor at 756 K	165
5.3-2	Experimental Water Vapor Emissivities at 294, 644, 867, 1300 and 1811 K	166
5.3-3	Experimental Water Vapor Emissivities at 417, 756, and 1517 K	167
5.3-4	Experimental Water Vapor Emissivities at 522, 978, and 1389 K	168
5.3-5	Recommended Water Vapor Emissivities	171
5.3-6	Smoothed Computed Water Vapor Emissivities	172
5.4-1	Water Vapor Pressure Broadening Correction Factor at 500 K	177
5.4-2	Water Vapor Pressure Broadening Correction Factor at 750 K	178
5.4-3	Water Vapor Pressure Broadening Correction Factor at 1000 K	179

LIST OF FIGURES (continued)

5.4-4	Water Vapor Pressure Broadening Correction Factor at 1500 K	180
5.4-5	Water Vapor Pressure Broadening Correction Factor at 2000 K	181
5.4-6	Water Vapor Pressure Broadening Correction Factor at 2500 K	182
5.4-7	Water Vapor Pressure Broadening Correction Factor at 1500 K (same scale as 5.4-1)	183
5.4-8	Water Vapor Pressure Broadening Correction Factor at 2000 K (same scale as 5.4-1)	184
5.4-9	Water Vapor Pressure Broadening Correction Factor at 2500 K (same scale as 5.4-1)	185
5.4-10	Water Vapor Presure Broadening Correction Factor at 500 K and P_t = 1 atm.	187
5.4-11	Water Vapor Pressure Broadening Correction Factor at 750 K and P_t = 1 atm.	188
5.4-12	Water Vapor Pressure Broadening Correction Factor at 1000 K and P_t = 1 atm.	189
5.4-13	Water Vapor Pressure Broadening Correction Factor at 1500 K and P_t = 1 atm.	190
5.4-14	Water Vapor Pressure Broadening Correction Factor at 2000 K and P_t = 1 atm.	191
5.4-15	Water Vapor Pressure Broadening Correction Factor at 2500 K and P_t = 1 atm.	192
5.4-16	Effect of Temperature on Water Vapor Pressure Correction Factor	193
5.5-1	Comparison of Present Computed and Eckert's Emissivity Overlap Correction at 260 F	195
5.5-2	Comparison of Present Computed and Eckert's Emissivity Overlap Correction at 1000 F	196
5.5-3	Comparison of Present Computed and Eckert's Emissivity Overlap Correction at 1700 F	197
5.5-4	Comparison of Present Computed Mixture Emissivities and Millard's Data	199

LIST OF FIGURES (continued)

5.5-5	Comparison of Present Computed Mixture Emissivities and Fishenden Data	200
5.5-6	Emissivity Overlap Correction Against Temperature, $p_c = 0$, $p_w = 0$, $P_t = 1$ atm., $p_w/p_c = 1$ (solid line), $p_w/p_c = 2$ (dashed)	205
5.5-7	Emissivity Overlap Correction Against Temperature, $p_c = 0$, $p_w = 0$, $P_t = 1$ atm., $p_w/p_c = 1/3$ (solid line), $p_w/p_c = 4$ (dashed)	206
5.5-8	Emissivity Overlap Correction Against Temperature, $p_c = 0$, $p_w = 0$, $P_t = 1$ atm., $p_w/p_c = 1/9$ (solid line), $p_w/p_c = 9$ (dashed)	207
5.5-9	Emissivity Overlap Correction Against $p_w/(p_w + p_c)$, $p_w = 0$, $p_c = 0$, $P_t = 1$ atm., and $T = 500$ K	208
5.5-10	Emissivity Overlap Correction Against $p_w/(p_w + p_c)$, $p_w = 0$, $p_c = 0$, $P_t = 1$ atm., and $T = 1000$ K	209
5.5-11	Emissivity Overlap Correction Against $p_w/(p_w + p_c)$, $p_w = 0$, $p_c = 0$, $P_t = 1$ atm., and $T = 1500$ K	210
5.5-12	Emissivity Overlap Correction Against $p_w/(p_w + p_c)$, $p_w = 0$, $p_c = 0$, $P_t = 1$ atm., and $T = 2000$ K	211
5.5-13	Emissivity Overlap Correction Against $p_w/(p_w + p_c)$, $p_w = 0$, $p_c = 0$, $P_t = 1$ atm., and $T = 2500$ K	212
5.6-1	Effect of Temperature on Pressure Broadening of the Overlap Correction and Mixture Emissivity	216
5.6-2	Effect of Water Vapor Partial Pressure on Pressure Broadening of the Overlap Correction and Mixture Emissivity	218
5.6-3	Effect of Total Pressure on Pressure Broadening of the Overlap Correction and Mixture Emissivity	219

LIST OF TABLES

1.4.1-1	Experimental Conditions of Carbon Dioxide Emissivity Measurements	23
1.4.1-2	Recommended Emissivities of Carbon Dioxide	29
1.4.3-1	Experimental Conditions of Water Vapor Emissivity Measurements	31
4.1.3.1-1	Goldstein Integrated Intensities of Water Vapor (± 10%)	88
4.1.3.1-2	Water Vapor Integrated Band Intensities at 300 K cm^{-2} $atm^{-1}_{(STP)}$	90
4.2.2.5-1	CO_2 Data of Akhunov et. al. (1972)	113
4.2.3-1	Integrated Band Intensities of the 2, 2.7, 4.3, 10 and 15 Micron Bands of Carbon Dioxide (cm^{-2} atm^{-1} at STP at 300 K)	118
4.2.3-2	Integrated Band Intensities of Carbon Dioxide Spectral Data Used in the Present Work	127
4.2.4-1	Band Contribution Factors (Δf) in Carbon Dioxide Emission	129
4.3.2.7-1	Comparison of Absorptivities and Absorptivities Overlap Corrections of Carbon Dioxide and Water Vapor Mixture	140
5.1-1	Recommended Emissivities of Carbon Dioxide	152
5.2-1	Numerical Values of Coefficients of Equation $b_{CO_2, T} = ap_{CO_2} + cp_{H_2O} + ep_{N_2} + dp_{O_2} + ep_{H_2} + fp_{CO}$	162
5.4-1	Numerical Values of Coefficients of Equation $b_{H_2O, T} = ap_{H_2O} + cp_{N_2} + dp_{CO_2} + ep_{O_2} + fp_{H_2} + gp_{CO}$	176
5.5-1	Comparison of Emissivities, Absorptivities and Absorptivity Overlap Correction of CO_2 - H_2O Mixtures	202

1. Summary

1.1. Introduction

The basis for calculating the radiative transfer from the combustion products of hydrocarbon fuels has long been the emissivity charts for carbon dioxide and water vapor developed by Hottel and coworkers (1954, 1967). These charts were generated from measurements at M.I.T. and elsewhere (Hottel and Mangelsdorf (1935), Hottel and Egbert (1941, 1942), Egbert (1942), Schmidt (1932), Eckert (1937), Smith (1935), Eberhardt (1936) and Brooks (1940, 1941)) of total radiation from heated mixtures of CO_2 and H_2O at one atmosphere and from limited available spectral data at low temperatures (Schmidt (1913), Hertz (1911)). Considerable effort was subsequently expended in the 60's, partly motivated by the interests in rocket plume radiation, on developing experimental data and theoretical models for calculating the spectral emissivities of combustion products, but these spectral data were not critically tested against the earlier total emissivity measurements and have had relatively little impact on the procedures for calculating furnace performance. In view of the current interest in improved methods for analyzing the thermal efficiency of furnaces and the trend in combustion equipment to higher temperatures and pressures than those covered by the early investigators, it is timely to develop a new set of emissivity charts based on a critical assessment of all available existing spectral and total emissivity data and models and to develop total emissivity charts to cover the wide range of temperatures and pressures of current interest.

1.2. Basic Definitions

The spectral transmissivity, the complement of the emissivity, is given by Beer's law of attenuation, i.e.

$$\tau_w = \exp(-k_w pL) \tag{1.2-1}$$

where τ_w is the spectral transmissivity, k_w the spectral absorption coefficient and pL is the absorbing matter. It follows that the spectral emissivity or absorptivity is given by

$$\alpha_w = \varepsilon_w = 1 - \tau_w = 1 - \exp(-k_w pL) \tag{1.2-2}$$

The total emissivity may be obtained by the integration of the spectral emissivities weighted by the black body Planck function over all wave numbers w, i.e.

$$\varepsilon = \int_0^\infty \varepsilon_w E_w^0 \, dw / \int_0^\infty E_w^0 \, dw \tag{1.2-3}$$

$$= \int_{\text{all bands}} \varepsilon_w E_w^0 \, dw / \sigma T^4 \tag{1.2-4}$$

and the total absorptivity by the integration of the spectral emissivity weighted by the Planck function evaluated at the source temperature over all wave numbers, i.e.

$$\alpha = \int_0^\infty \varepsilon_w E_w^0 (T_s) \, dw / \sigma T_s^4 \tag{1.2-5}$$

Due to the very rapid variation of k_w with w and the lack of sufficiently high resolution spectral data the integrations of equations (1.2.4) and (1.2.5) on a line-by-line basis is not possible. An adequate representation of spectral emissivities is provided by models which average the spectrum over narrow intervals containing several lines. The model adopted here, the statistical or random model, assumes that the spectral lines are randomly distributed within a wave number and that the line strength

(area under a k_w - w curve) followed an exponential distribution. Goody (1952) showed that this model yeilded a transmissivity in a wave number interval Δw given by

$$\tau_{\Delta w} = \exp\left[-\frac{S_0}{d_0}\, pL\, (1 + \frac{S_0}{4b}\, pL)^{-1/2}\right] \qquad (1.2\text{-}6)$$

$\tau_{\Delta w}$, therefore, is a function of the average line strength S_0, the mean line spacing d_0 and the gas half width b. The term S_0/d_0 is sometimes termed the absorption coefficient k, and the ratio b/d_0 is termed the fine structure parameter.

The gas statistical model was found to give good representation of the measured emissivities at high temperatures in spectral intervals of 5 - 25 cm^{-1} and is used in the present investigation for the calculation of spectral emissivities. The published spectral tabulation of water vapor and of carbon dioxide list the absorption coefficients and the reciprocal of the mean line spacing 1/d in wave number intervals of 5 - 25 cm^{-1}.

The line half width is taken to be independent of the wave number and is a function of the partial pressure of the different gaseous species in the gas mixture and the absolute temperature. Benedict et al. (1956) recommended the form

$$b_a = b^*_{a,\,273}\, p_a \left(\frac{273}{T}\right) + \sqrt{\frac{273}{T}}\ \Sigma\, b_{i,\,273}\, p_i \qquad (1.2\text{-}7)$$

where the subscript a refers to the absorbing gas. For water vapor, Equation (1.2-7) becomes

$$b_{H_2O} = 0.44 \left(\frac{273}{T}\right) p_{H_2O} + \sqrt{\frac{273}{T}}\ (0.09\, p_{H_2O} + 0.09\, p_{N_2} + 0.13\, p_{CO_2} + 0.04\, p_{O_2} + 0.05\, p_{H_2} + 0.10\, p_{CO}) \qquad (1.2\text{-}8)$$

which may be approximated for engineering purposes, or for a mixture of water vapor and nitrogen only to

$$b_{H_2O} = 0.44 \left(\frac{273}{T}\right) p_{H_2O} + \sqrt{\frac{273}{T}} \; (0.09 \; P_t) \qquad (1.2\text{-}9)$$

For carbon dioxide, the half width is given by

$$b_{CO_2} = \sqrt{\frac{273}{T}} \; (0.07 \; p_{H_2O} + 0.07 \; p_{N_2} + 0.09 \; p_{CO_2} + 0.069 \; p_{O_2} + 0.08 \; p_{H_2} + 0.06 \; p_{CO}) \qquad (1.2\text{-}10)$$

which may be approximated by

$$b_{CO_2} = \sqrt{\frac{273}{T}} \; (0.02 \; p_{CO_2} + 0.07 \; P_t) \qquad (1.2\text{-}11)$$

Both gases have a spectrum consisting of a number bands separated by transparent intervals. From the above definitions, it is clear that

$$\varepsilon = f_1 \; (T, \; pL, \; p_a, \; P_t) \qquad (1.2\text{-}12)$$

or, introducing Equations (1.2-7),(1.2-9) and(1.2-11),

$$\varepsilon = f_2 \; (T, \; pL, \; b) \qquad (1.2\text{-}13)$$

The effect of the absorbing, or emitting gas, partial pressure and total pressure, which may be combined as the half width, on the radiation of gas is termed Pressure Broadening. To facilitate the representation of the emissivity charts, it has become conventional to eliminate the effect of p_a and P_t by defining a standard emissivity at zero partial pressure and one atmosphere total pressure, and then developing a pressure broadening correction C_F factor to obtain the emissivity at a given temperature, pL but with a p_a different from zero and/or P_t different from 1.

$$C_F = \frac{\varepsilon \; (T, \; pL, \; p_a, \; P_t)}{\varepsilon \; (T, \; pL, \; p_a = 0, \; P_t = 1 \text{ atm})} \qquad (1.2\text{-}14)$$

Clearly,

$$C_F = C_F\,(T,\ pL,\ b) \qquad (1.2\text{-}15)$$

and its graphical representation requires a family of families of curves. The half width corresponding to the standard condition of $p_a = 0$ and $P_t = 1$ atm., termed the standard half width and is given by

$$b_{ST,\ H_2O} = 0.09\sqrt{\frac{273}{T}} \quad \text{for water vapor} \qquad (1.2\text{-}16)$$

$$b_{ST,\ CO_2} = 0.07\sqrt{\frac{273}{T}} \quad \text{for carbon dioxide} \qquad (1.2\text{-}17)$$

Therefore $C_F > 1$ when $b > b_{ST}$

$C_F = 1$ when $b = b_{ST}$

$C_F < 1$ when $b < b_{ST}$

For a mixture of two gases that emit in spectral bands that do not overlap significantly, the total emissivity of the mixture can be obtained by adding the total emissivities of the two gases. In the case of water vapor, where the major radiation comes from the 20, 6.3, and 2.7 micron bands, and of carbon dioxide where the major contribution to its radiation comes from the 15, 4.3 and 2.7 micron bands overlap in the 2.7 micron band and the partial overlap in the 15 micron band will result in a reduction $\Delta\varepsilon$ in the emissivity of the mixture.

$$\varepsilon_{c\,+\,w} = \varepsilon_c + \varepsilon_w - \Delta\varepsilon \qquad (1.2\text{-}18)$$

$\Delta\varepsilon$ is termed the overlap correction.

Assuming that the lines of both carbon dioxide and water vapor are randomly distributed the spectral transmissivity of a mixture will be given by

$$\tau_{c\,+\,w}(w) = \tau_c(w)\ \tau_w(w) \qquad (1.2\text{-}19)$$

Substituting $\tau = 1 - \varepsilon$ and using Equation (1.2-18) gives

$$\Delta\varepsilon(w) = \varepsilon_c(w)\ \varepsilon_w(w) \qquad (1.2\text{-}20)$$

In words, for this limiting behavior spectral overlap correction is the product of the spectral emissivities of the two radiating gases.

Integrating Equation (1.2-20) over the spectrum gives

$$\Delta\varepsilon = \int_{\bar{w}} \varepsilon_c(w)\ \varepsilon_w(w)\ E(w)\ dw/\sigma T^4$$

$$= \frac{1}{\sigma T^4} \sum \varepsilon_c(w)\ \varepsilon_w(w)\ E(w)\ \Delta w \qquad (1.2\text{-}21)$$

The overlap correction is a function of four variables,

$$\Delta\varepsilon = f\ \left(T,\ [p_c + p_w]L,\ \frac{p_w}{p_w + p_c},\ P_t\right) \qquad (1.2\text{-}22)$$

By analogy to total emissivity $\Delta\varepsilon$ may be evaluated at standard conditions of $p_w = p_c = 0$ and $P_t = 1$ atm. and a pressure broadening correction factor $C_{\Delta\varepsilon}$ developed.

$$C_{\Delta\varepsilon} = f_4\ \left(T,\ [p_c + p_w]L,\ \frac{p_w}{p_w + p_c},\ p_w,\ P_t\right) \qquad (1.2\text{-}23)$$

which is a function of five variables. Effort in computation and exposition may be saved by use of the following approximations

$$C_{\Delta\varepsilon} = C_{\varepsilon_w}\ C_{\varepsilon_c}\ , \qquad (1.2\text{-}24)$$

making use of the overlap correction charts of each gas. As will be shown later, this approximation yields adequate accuracy.

1.3. Spectral Data

1.3.1. Water Vapor

Recent publications listing the experimental or theoretical spectral constants of water vapor in a wave number and temperature regions of

interest (wave numbers from about 50 to 10,000 cm^{-1} and temperatures from 300 to 3000 K) are numerous. The most complete set is that published by Ludwig et al. (1966, 1968 and 1973) which cover the spectral region from 37.5 through 9312.5 cm^{-1} in 371 successive 25 cm^{-1} intervals; the average spectral absorption coefficient (S/d) and the reciprocal of the mean line spacing (1/d) at STP are listed for each interval at temperatures of 300, 600, 1000, 1500, 2000, 2500 and 3000 K. Early computations in this thesis indicated that absorption coefficients for the rotation band were in error at low temperatures. A critical review and comparison of available rotation band spectral data resulted in the replacement of Ludwig's spectral data from a wave number w of 425 to 1000 cm^{-1} with the more recent tabulation of McClatchey (1972, 1973) at 300 K. The k's at 600 K were similarly updated. The tabulation of Ludwig et al. was used in all other parts of the spectrum.

1.3.2. Carbon Dioxide

Extensive band absorption data were published. The most extensive spectral constants for the 15 micron, 4.3 micron and 2.7 micron bands are those published by Ludwig et. at. (1966, 1968 and 1973) and are used in the present work. Their data did not include the weak 2 and 10 micron bands. Edwards (1963) spectral data were utilized to provide the 2 and 10 micron band spectral data used in the present work after being smoothed in the temperature and in the wave number direction and integrated to check the band intensity values.

1.4. Results and Discussion

1.4.1. Carbon Dioxide

The conditions for which total emissivity data are available for carbon dioxide are summarized in Table 1.4.1-1. The most comprehensive

Table 1.4.1-1

Experimental Conditions of Carbon Dioxide Emissivity Measurements

Investigator	Gas Used	T Gas K	Path Length cm.	p_c atm.	p_cL cm.atm.	Background T K
Rubens & Ladenberg (1905)	CO_2	293	1-400	1.	1-400	Room
Mangelsdorf (1935)	CO_2 + air 1 atm.	294-1320	51.2	.002-1	1-51.2	90-1633
Smith (1935)	CO + O_2 CO + air 1 atm	1682 2355	15-40	.25-.35	1.3-14.9	294
Eckert (1937)	CO_2 + N_2 1 atm	678-1533 373-673 373	10.2 65.2 295.6	.01 1.	.5-190	297
Akhunov et. al. (1972)	CO_2	673-1070	10-26.5	1.02-21.42	10.2 to 297.33	Room

measurements were those by Hottel and Mangelsdorf (1935), Hottel and Smith (1935) and Eckert (1937). Mangelsdorf used a furnace of path length of 51.2 cm. which was defined by a concentration traverse and used hot, dry, carbon dioxide free air as a windowless boundary to confine the radiating gas. Some of his measurements, especially the low pL ones might have suffered from atmospheric absorption. The emissivities he reported at 2480 F were not data points, but values obtained by extrapolations from absorption measurements of radiation from black body at 2480 F. Eckert, in his measurements, confined the radiating gas mixture with atmospheric air containing water vapor and carbon dioxide introducing the possibility of atmospheric absorption. Smith's measurements were obtained in a system continuously flushed with CO_2-free H_2O-free air, but it was later decided that some carbon dioxide or water vapor absorption might have occured in a short open coupling between the flushed radiometer and the flushed burner end. Akhunov et al. estimated an error in their experiments to be between 4.5 to 7.5 percent.

In order to check the consistency of the different independent experimenters and to check the agreement between the present computed emissivities and the experimental results it was necessary to reduce all data to a common basis of $p_c = 0$ and $P_t = 1$ atm. The correction was achieved by computing the pressure broadening correction factor at T and pL corresponding to each experimental point and use it to normalize the data to $p_c = 0$ and $P_t = 1$ atm. The above step compensated, to the extent that the present model predicts the correct C_F, for the variation of p_c and P_t between different experiments. The resulting corrected ε's are functions only of T and p_cL. The use of a power relation in the form

$$\frac{\varepsilon_1}{\varepsilon_2} = \left(\frac{pL_1}{pL_2}\right)^n$$

allowed the elimination of the pL variation among the different experimenters. The above procedure was used to normalize experimental data of Hottel and Mangelsdorf, Eckert and Akhunov to obtain plots of the emissivity versus the absolute temperature for pL's from 0.1 to 300 cm. atm. and a temperature range of 400 to 1700 K. For purposes of clarity, the data were plotted in two different figures, only figure 5.1-2 will be discussed here. It includes Hottel and Mangelsdorf correction emissivities denoted by + at pL's of 0.1, 0.3, 0.8, 2., 5., 10., 30. and 80. cm. atm. Eckert's emissivities, denoted by X are plotted for the same pL's over a temperature range of 400 to 600 K and for the same pL's up to 10 cm. atm. for temperatures of 700 to 1500 K; Akhunov data, shown as *, are plotted for pL's of 10, 30, 80, and 200 cm. atm. over a temperature range of 670 to 1070 K. Emissivities computed using the present model and using Edwards and Balakrishnan's model are plotted on the same graph at the same pL's over a temperature range of 300 to 2200 K and are denoted 0 and - respectively. In order to include Smith's (1935) high temperature carbon dioxide data, it was necessary to smooth his data. The first step was to calculate the pressure broadening correction factor for each of his data points and reduce his data to $p_c = 0$ and $P_t = 1$ atm. The normalized data were grouped together for temperature intervals of 100 K between 1710 and 2310 K. Emissivity was plotted versus pL and smooth curves for any chosen temperature were drawn with the guidance of the data points at the other temperatures. Emissivities read from the smoothed curves at pL = 1, 2, 3, 5, 8 and 10 cm. atm. were included in the graph. The figures show a break in the curves

going through Eckert's smoothed points between 600 and 700 K. This is because Eckert's data points between 400 and 600 K were measured in a furnace of length 65.4 cm. while his data at 700 K and above were measured using a 10.2 cm. furnace. The break in the curve diminishes with increasing pL and diappears around 2 cm. atm. In comparing the different curves, one should be cognisant that Edwards and Balakrishnan did not place much confidence in the accuracy of their model for the fifteen micron bnad. Therefore, curves going through computed points of Edwards were not extended below 480 K. At low pL's (0.1, 0.2 cm. atm.) there is a marked discrepancy between the data of Eckert and Hottel and Mangelsdorf. Eckert's curve is quite high, while the H & M curve is quite low compared to the present computations and to Edwards computation in the range 1000-1500 K. Eckert's emissivities are almost twice as high as H & M's. Therefore, in constructing the smoothed carbon dioxide emissivity, it is not unjustifiable to give Eckert and H & M curves very little weight at pL's of 0.1 and 0.2 cm. atm.

One of the explanations for discrepancies between different sets of data is that Mangelsdorf's low pL measurements might have suffered from atmospheric absorption. At low pL's and temperatures below 500 K Mangelsdorf had no experimental data. The extrapolation of his line to 300 K was made possible by the use of the measurements of Rubens and Landeburg and Hertz over a pL range of 0.1 to 50 cm. atm. The agreement between Ruben's data and the present computations is good at all temperatures below 350 K. The figures also show that between 900 and 1100 K and between pL = 30 and 100 cm. atm. the agreement between Akhunov data and Edwards and Balakrishnan's model is good. In the same temperature

range and at pl = 20 cm.atm. the lines representing the data of Akhunov Eckert and Hottel and Mangelsdorf coincide. In the 1200-1300 K region the lines representing Edwards, Eckert, Hottel and Mangelsdorf and the present computations are close together for pL = 1 to 30 cm.atm. At the high temperature end (1200 to 2000 K) the emissivities predicted from Edwards and Balakrishnan's model and the present computations parallel each other with the present values being consistently high; in this range the emissivities of Hottel and Mangelsdorf are much closer to those from Edwards and Balakrishnan model. The figures also show a change in slope at 1200 K of the curves fitted to the present computations. This behavior is not evident in the emissivities recommended by Hottel and Mangelsdorf or Edwards and Balakrishnan. Smoothing curves fitted to the present computations could change the emissivities by as much as six percent at the bend. Based on the above discussion, some preliminary rules were set as guidances in constructing the new chart of the emissivity of carbon dioxide against the temperature. At 1600 K the curves of Hottel and Mangelsdorf and of Edwards and Balakrishnan each is to be given double the weight of the present computed values. The curves of Eckert should be ignored because of the marked discrepancies at 1500 K. At points of closest agreement of different curves use the same weighting. At 700 and 800 K equal weight should be given to all four curves at pL greater than 0.2 cm.atm. At pL = 0.2 and 0.1 cm.atm. the mean of Edwards and present computed emissivities should be used. After applying the above rules and eliminating any irregularities the emissivities were cross plotted versus

the pL to insure their smoothness. From the latter curves the preliminary curves of the emissivity against the temperature were slightly adjusted. The final curves smoothed in both directions (Temperature and pL) shown in figure 5.1-4 were then used to compute the final working plot. The final smoothed emissivities are presented in table 1.4.1-2.

1.4.2 Pressure Broadening Correction Factor of Carbon Dioxide

The standard emissivity charts were drawn at p_c = 0 and P_t = 1. atm. The pressure broadening correction factor charts were developed as a function of the gas temperature, pL and half width. In theory, a family of families of curves are needed for graphical presentation. It was decided to present the correction factor at five discrete temperatures of 500, 1000, 1500, and 2000 K. Figure 5.2-1 is a plot of the carbon dioxide pressure broadening correction factor at 500 K against the pL in cm.atm. for half width values of .01,.02,.03,.05,.07, .1, .2, .3, .5, .7, 1., 2. and 10 cm^{-1}. The correction factor is unity for all pL's at the "standard" half width. Similar plots were developed at temperatures of 500, 1000, 1500, 2000 and 2500 K. The new chart, termed the engineering pressure broadening correction factor chart is presented in figure 5.2-6 for a gas temperature of 500 K. Similar plots were developed at 1000 K.

The carbon dioxide factor falls off rapidly with increasing temperature. The maximum correction for p_c = 0.2 atm. is 1.1 percent at 500 K, and 0.92% at 1000 K. Additional computations indicate a maximum correction for p_c = 0.2 atm. of 0.23% at 1500 K. The correction becomes very small and presentation of any charts for furnace applications at temperatures above 1000 K is unwarranted.

TABLE 1.4.1-2

RECOMMENDED EMISSIVITIES OF CARBON DIOXIDE

PL CM.ATM.	EMISSIVITY OF CARBON DIOXIDE AT TEMP. OF (K)								
	300	400	600	800	1000	1200	1400	1600	1800
.05	.00955	.00811	.0113	.0121	.00980	.00732	.00540	.00403	.00291
.09	.01555	.0131	.0177	.0185	.0159	.01255	.00946	.00702	.00516
.10	.0170	.0142	.0189	.0202	.0176	.0138	.0105	.00788	.00583
.12	.0191	.01585	.02055	.02245	.01955	.01562	.0121	.00915	.00681
.15	.0221	.0184	.0230	.0254	.0225	.0184	.0144	.0111	.00831
.20	.0265	.0221	.0264	.0295	.0267	.0222	.0177	.0138	.01055
.25	.0300	.0250	.0291	.0316	.030	.0251	.0202	.0160	.0123
.30	.0320	.0276	.0314	.0352	.0326	.0277	.0224	.0179	.0139
.35	.0357	.0302	.0336	.0375	.0350	.0301	.0242	.0195	.0153
.40	.0382	.0325	.0357	.0398	.0371	.0321	.0260	.0210	.0166
.45	.0403	.0345	.0375	.0416	.0390	.0338	.0276	.0223	.0178
.50	.0426	.0365	.0391	.0435	.0410	.0355	.0291	.0235	.0189
.60	.0465	.0400	.0421	.0466	.0438	.0382	.0316	.0257	.0208
.70	.0498	.0430	.0448	.0493	.0465	.0406	.0336	.0275	.0225
.80	.0528	.0457	.0471	.0519	.0490	.0430	.0361	.0296	.02425
.90	.0558	.0484	.0495	.0544	.0513	.0451	.0380	.0313	.0258
1.	.0584	.0503	.0514	.0562	.0532	.0470	.0398	.0329	.0271
1.20	.0630	.0544	.0550	.0601	.0570	.0502	.0427	.0358	.0294
1.5	.0683	.0597	.0593	.0649	.0620	.0549	.0470	.0394	.03255
1.8	.0730	.0638	.0629	.0682	.0658	.0588	.0505	.04265	.0355
2.	.0758	.0661	.0650	.0708	.0681	.0611	.0527	.0446	.0371
2.2	.0781	.0682	.0670	.0730	.0701	.0632	.0546	.0465	.0387
2.5	.0814	.0710	.0698	.0759	.0733	.0664	.0572	.0489	.0408
2.8	.0843	.0737	.0720	.0784	.0760	.0692	.0599	.0513	.0428
3.	.0858	.0751	.0732	.080	.0776	.0709	.0617	.0528	.0440
3.2	.0877	.0767	.0747	.0813	.0793	.0726	.0630	.0539	.0453
3.5	.0899	.0788	.0763	.0834	.0818	.0749	.0652	.0560	.0471
3.8	.0921	.0806	.0780	.0852	.0839	.0771	.0674	.0579	.0488
4.	.0931	.0820	.0791	.0861	.0851	.0787	.0688	.0591	.0499
4.5	.0962	.0850	.0819	.0890	.0883	.0819	.0711	.0621	.0524
5.	.0990	.0872	.0840	.0918	.0912	.0850	.0749	.0648	.0548
5.5	.102	.0895	.0860	.0940	.0940	.0878	.0778	.0671	.0570
6.	.104	.0918	.0879	.0959	.0968	.0901	.0801	.0696	.0589
6.5	.106	.0937	.0897	.0980	.0990	.0928	.0827	.0718	.0605
7.	.108	.0956	.0912	.0998	.1010	.0951	.0850	.0738	.0623
7.5	.110	.0976	.0927	.1015	.1030	.0969	.0870	.0758	.06440
8.	.112	.0988	.0940	.103	.105	.0988	.0889	.0775	.0656
8.5	.1135	.1010	.0952	.1045	.1070	.1010	.0905	.0795	.0672
9.	.1148	.1025	.0969	.1060	.1085	.1025	.0922	.0812	.0690
9.5	.1162	.1035	.0980	.1075	.1105	.1040	.0940	.0828	.0702
10.	.1175	.1050	.0991	.1085	.1120	.1060	.0957	.0843	.0719
12.	.1235	.1095	.1035	.1135	.1175	.1120	.1015	.0900	.0769
15.	.1288	.1155	.1085	.1190	.1250	.1195	.1090	.0967	.0835
18.	.1350	.1200	.1133	.1245	.1310	.1255	.1150	.1020	.0889
20.	.1385	.123	.1162	.128	.134	.129	.118	.105	.0920
25.	.1455	.129	.1220	.1345	.1410	.1360	.1250	.1120	.0992
30.	.1520	.1337	.1265	.1395	.1460	.1420	.131	.1170	.1045
35.	.1565	.1370	.1310	.1440	.1505	.1475	.1355	.1220	.1095
40.	.1605	.141	.1350	.1475	.1545	.1520	.1400	.1265	.1138
45.	.1645	.144	.1380	.1520	.1580	.1555	.1438	.1305	.1175
50.	.167	.147	.142	.154	.1605	.159	.1475	.134	.121
55.	.171	.150	.1440	.1575	.1640	.1625	.1502	.1370	.1240
60.	.1735	.1520	.1475	.1605	.1665	.1650	.1535	.1395	.1265
70.	.1785	.1560	.1520	.1650	.1720	.1700	.1585	.1445	.1315
80.	.1825	.1595	.1560	.170	.1760	.1755	.1635	.1495	.1365
90.	.1856	.1635	.1600	.1740	.1798	.1795	.1670	.1530	.1403
100.	.188	.166	.164	.177	.183	.182	.171	.157	.142
120.	.1930	.1715	.170	.1830	.1885	.1885	.1775	.1635	.1480
150.	.1990	.1780	.1780	.1910	.1970	.1968	.1860	.1720	.1555
200.	.205	.1860	.1865	.2025	.2060	.2065	.1970	.1830	.1665
250.	.2105	.1925	.1970	.2100	.2140	.2150	.2055	.1910	.1745
300.	.215	.198	.203	.215	.219	.220	.211	.1975	.182
500.	.224	.2130	.224	.2305	.2325	.234	.230	.2180	.1980
1000.	.234	.2330	.252	.2545	.255	.256	.257	.2470	.2245

1.4.3. Water Vapor

The result on water vapor are less conclusive than those on carbon dioxide. The extent of experimental data is shown in Table 1.4.3-1. Schmidt (1932) utilized pure steam with p_w = 1 atm. His measurements could have been slightly inaccurate due to cold edges and to some atmospheric absorption. Mangelsdorf's (1935) measured ε_w using a fixed path length of 51.2 cm. and his measurements might have suffered from atmospheric absorption. His reported emissivities at 2270 F (1517 K) were extrapolations from absorptivities measurements using a black body at 2270 F. Smith (1935) measured the radiation from CO_2 flames and from CO_2 - H_2O mixtures calculated ε_{H_2O} by subtracting the CO_2 effect from the mixture measurements without the proper overlap correction. His temperatures might have error as much as 50 F and his measurements might have suffered from atmospheric absorption. Eckert (1937) utilized furnaces of three different path lengths claiming an error of not more than 2 - 3% in p_w. His measurements might have suffered from edge cooling effects and some atmospheric absorption. Eberhardt measured the radiation from a steel reheating furnace with a path length of 14 ft. (426.7 cm.). The combustion gases contained both CO_2 and H_2O. He subtracted the CO_2 and $\Delta\varepsilon$ contribution estimated from Hottel and Mangelsdorf's charts, which might have introduced errors. His measurements suffered from edge cooling effect and some atmospheric absorption.

Falckenberg (1938, 1939) measured the emission from the atmosphere at 20 C. Elsasser (1940, 1941) constructed a heat radiation telescope to measure the emission from moist air for distances from 3 cm. to 315 meters. His gas boundary was poorly defined and the moixture content along his path showed large fluctuations. Some variation of air temperature along his line of sight was possible. Brooks (1941) measured the radiation from

Table 1.4.3-1

Experimental Conditions of Water Vapor Emissivity Measurements

Investigator	Gas Used	T Gas K	Path Length cm.	p_w atm.	p_wL cm. atm.	Background
Schmidt (1932)	Pure steam	395-1233	.91-18.3	1	.91-18.3	
Mangelsdorf (1935)	Steam - air at 1 atm.	294-1302	51.2	.006-1.	.305-51.2	90-1567
Smith (1935)	CO_2-H_2O at 1 atm	1644 1811	12.7-20.4	.11-.13	1.3-2.6	
Eckert (1937)	Steam - N_2 1 atm.	394- 1533	10.2, 65.2, 295.7	.1- 1.	1-295.7	
Falckenberg (1939)	Atmosphere	293	66 → 1000	.01	.66 → 10.02	
Elsasser (1940, 1941)	Atmosphere	293	3 → 32000	.005-.015	.25-522	
Brooks (1941)	Atmosphere	294	5 → 585	.006	.3-3.2	
Egbert (1942)	Steam - Air 1 atm.	294-978	1.83, 23.5, 7.77, 203.3 406.3	.005-1	.009-406.3	90-1389
General Dynamics (1967)	Burned mix $H_2 + O_2$	1200 3000	60.9-609		60.9 609	

laboratory air. His gas boundary was not well defined. Egbert (1942) improved the system designed by Mangelsdorf by the use of purged atmosphere between the furnace and the radiometer to flush absorbing gases. He estimated an error of less than 5% in his ε_w measurements. His flow pattern were not as carefully controlled as Mangelsdorf's. His reported emissivities at 2040 F (1389 K) were extrapolations from his absorptivity measurements. Earlier calculations in the present study attempted to establish the consistency of the data of different investigators carried out at p_w = 1 atm. and therefore p_wL = L, corresponding to the conditions in Schmidt's measurements. All experimenters were found to report emissivities at p_w = 1 atm., which agreed to within 5 to 9%. In order to effectively compare the experimental data, it was decided to reduce all points to a common basis of p_w = 0 and P_t = 1 atm.The correction was achieved by computing C_F corresponding to each point. In many cases the difference in emissivity of the raw data taken at different p_w's was as much as 30%. The use of the present computed correction factor brought the points to within 10% of each other. This was a good measure of the validity of C_F computed using the present model. The corrected emissivities were grouped at temperatures of 294, 417, 522, 644, 756, 867, 978, 1300, 1389, 1517 and 1811 K. The corrected emissivities at each of three or four temperatures were plotted versus pL on one chart together with the computed emissivities. At low temperatures, e. g. 294 K, the computed values were much higher than experimental at low pL's (less than 2 cm. atm.) while at high pL's (>100 cm. atm.) the computed values were lower by more than a factor of 2. The agreement between the experimental data of most investigators in the pL range 5 →100 cm. atm. was within 10% indicating the consistency of their data at temperatures of 417 → 978 K. The agreement

is not very good at room temperature. The consistency of the experimental data was a strong factor in deciding to give the computed values little weight in the range of good agreement of different experimenters. In extrapolating the ε v.s. pL curve outside the range of experiments the slope of the computed curves was used as a guidance. The resulting smooth emissivities were cross plotted against the temperature to insure their smoothness. The smoothed curves are shown as the dotted lines in Figure 5.3-5 . The disagreement of computed and experimental emissivities at 294 K necessitated the modification of the rotation band spectral tabulation by including the more recent tabulation of McClatchey et al. (1972, 1973) form w = 425 cm^{-1} to 1000 cm^{-1} at 300 K and by interpolation from McClatchey's data at 300 K to Ludwig et al.'s tabulation at T > 1000 K to get the spectral absorption coefficients at 600 K in the same interval. These modifications resulted in a much closer agreement of computed and experimental emissivities at temperatures below 600 K, and especially at 294 K. A review of the smoothed experimental data was done resulting in alternative smooth curves that are higher at the low pL end of the ε v.s. pL plots. The new lines were cross plotted versus the temperature and smoothed in both directions. The resulting smooth lines are shown as the solid lines in figure 5.3-5 Whenever a solid and a dotted line coincide a solid line is drawn.

The results permit the identification of regions of agreement and disagreement between different measurements of the total emissivity of water vapor. For pL's of 5 to 200 cm. atm. at 417 K, 5 - 100 cm. atm. at 522 K, 10 - 100 cm atm. at 644 K and 5 - 200 cm. atm. at temperatures of 756 to 867 K the emissivities measured in different equipment and by different investigators agree to wihin 9% when reduced to a common p_w of

zero and P_t of 1 atm. In this range of agreement the computed values based on a modification of Ludwig et al. (1973) data differ from the mean of the experimental data by about 9 to 10%. The variations increasing with increasing temperature and decreases from a positive to a negative deviation with increasing p_wL. The values computed from the model of Edwards and Balakrishnan are generally below the values computed using the present modification of Ludwig et al. especially at the low and high temperature ends. At low pL's the experimental data of Hottel and Mangelsdorf and of Egbert show more scatter (30%) and differ from the computed values by as much as 48% at pL = 0.5 cm. atm. and 30% at pL = 1 cm. atm. It is apparent that a number of uncertainties remain. The most complete models are those developed from Ludwig et al. and Edwards and Balakrishnan of which the former appears to be more reliable. The computations from this model it must be recognized differ from well established total emissivity data by -9% to +10% in the region where the total emissivity measurements are reliable. At this stage no reliable estimate of the uncertainty of using the present model at low pL's and high temperatures is available. This is an area which needs resolution.

1.4.4. Pressure Broadening Correction Factor of Water Vapor

The standard emissivity charts were drawn at zero water vapor partial pressure and a total pressure of one atmosphere. To use those charts at conditions other than $p_w = 0$ and $P_t = 1$ atm., the pressure broadening correction factor charts were developed as a function of the gas temperature, pL and half width. It was decided to present the correction facotr at six temperatures of 500, 750, 1000, 1500, 2000 and 2500 K in the form of C_F versus the pL with the half width as a parameter. Figure 5.4-1 is a sample plot of the water vapor pressure broadening correction factor at 500 K against pL in cm. atm. for half width values of 0.01, 0.02, 0.03, 0.05, 0.07, 0.1, 0.2, 0.3, 0.5, 0.7, 1., 2. and 10 cm^{-1}. The correction factor is unity for all pL's at the "standard half width. As in the case of carbon dioxide the "Engineering pressure boradening correction factor charts" are presented for water vapor partial pressures of 0.02 to 0.2 atm., total pressure of 1 atm. at the same six temperatures. Figure 5.4-10 is a sample plot of the "Engineering charts" at 500 K.

To obtain the correction factors at temperatures other than those for which the charts are given, a linear interpolation of C_F v.s. T using the correction factors at the nearest two temperatures is recommended. To estimate the error introduced by the use of linear interpolation the correction factors at pL's of 1, 10 and 100 cm. atm., p_w's of 0.04, 0.1 and 0.2 atm. are plotted against the temperature in Figure 5.4-16 which shows that the use of linear interpolation may introduce a maximum error in C_F of less than a couple of percent.

An example of the application of the working charts is the case of a gas turbine combustor at 1500 K at 20 atm. total pressure and a 15 cm. chamber. Assuming a 10 percent mole fraction of water vapor gives

p_w = 2 atm., $p_w L$ = 30 cm.atm. at 1500 K

$$b_{1500} = 0.0801\ p_w + 0.0384\ P_t$$
$$= 0.0801 * 2 + 0.0384 * 20 = 0.928\ cm^{-1}.$$

Next the correction factor is read from the C_F chart at 1500 K, $p_w L$ = 30 cm.atm. and b = 0.928 as 1.235 approximately. This indicates that pressure broadening is responsible for an increase of 23.5% in the water vapor emissivity when the total pressure increases from 1 to 20 atm.

1.4.5 Overlap correction

Spectral emissivities of water vapor and carbon dioxide gases were measured at elevated temperatures by Ferriso et al. (1964) but since both gases were optically thin, the overlap correction was practically zero.

The classic example of the overlap correction is the chart developed by Hottel by cross plotting data calculated by Eckert from then available low-temperature low-resolution absorption spectra of water vapor and carbon dioxide. Comparison of the present computed overlap corrections and the Eckert charts at a temperature of 260 F (400 K) is shown in figure 5.5-1 for pl's of .75,1,1.5,2,3 and 5 ft. atm. Similar comparisons were made at 1000 F (811 K) and 1700 F (1200 K). The curves show agreement generally on the location of the maximum of the curves. At 260 F and $p_w/(p_w+p_c)$ of 0.5 or less the computed overlap corrections are consistently higher than Eckert's. At $p_w/(p_w+p_c)$ of 0.6 and above the computed values are higher than Eckert's at pL less than 1.5 ft. atm., and are lower at higher pL's. At 1000 F the computed overlap corrections are higher than Eckert's values at pL's greater than 2 ft. atm. At 1700 F the computed overlap corrections are lower than Eckert's values at pL's less than 3 ft. atm. The important

point here is that the disagreement between the two sets of curves is never more than 50% at all temperatures and pL's of 0.75 ft. atm. and higher. Considering that Eckert charts were published by Hottel to be a temporary measure of the overlap correction disagreements of this magnitude are not surprising.

Hines and Edwards (1968) investigated the use of band model for calculation of absorption of radiation by mixtures of water vapor, carbon dioxide and nitrogen as an inert gas. Their results are shown in table 5.5-1, which includes the results of Hottel, "HOTTEL", modified Hottel, "MOD HCH", Penner and Varanasi, "P+V" and the present computed absorptivities, emissivities and overlap corrections of the mixtures. Hines and Edwards absorptivities and overlap corrections are denoted "BAND" while those based on summing experimentally measured band absorptions are denoted "EXPTL". The "HOTTEL" values were the values of gas absorptivities predicted for the experimental conditions by the graphical correlations of Hottel and Egbert (1942) and listed by Hines and Edwards. They modified Hottel's extrapolated data to include contributions of the medium strength bands 1.87 and 1.38 microns of water vapor and the 2.0 micron band of CO_2. This was done by replacing the absorptivity overlap correction of Hottel by one calculated by Hines and Edwards using the approximations of Penner and Varanasi (1966). The "P+V" values are overlap corrections calculated by Hines and Edwards based on the model of Penner and Varanasi (1966) in which they used a harmonic oscillator approximation and rigid rotator band profiles. For computation purposes the source temperature was taken as 1700 F (2160 R). The table shows good agreements in general between the present absorptivities and the values listed for others. The agreement is

better for higher gas temperatures (1470 and 1475 R). In comparing the absorptivities overlap corrections it is clear that the agreement is excellent between the present values and those recently published by Edwards and Hines. Both sets are in good agreement with Penner and Varanasi corrections when the water vapor mole fraction is three or more times that of carbon dioxide. The agreement of the present overlap corrections with those of Edwards and Hines and of Penner and Varanasi is important in as much as it provides an independent check of the present values.

The best agreement between the four sets of overlap corrections occurs at $p_c + p_w \simeq 1$ atm. and $p_w/p_c \simeq 3$. This is because the overlap correction of Hottel closely represent conditions in which the partial pressure of water vapor and $(p_c + p_w)L$ are high enough to cause the water vapor to act as a black body over the 2.7 micron band of carbon dioxide.

It is possible to conclude from the above mentioned comparisons that the present model is suitable for the computation of overlap corrections. The standard conditions of zero partial pressure of water vapor, zero partial pressure of carbon dioxide, and a total pressure of one atmosphere were selected. The overlap correction is, therefore, a function of the gas absolute temperature, the ratio of p_w/p_c and the $(p_c + p_w)L$ product. Presentation of the overlap corrections, therefore, requires a family of families of curves. In order to cover the widest possible range, the results of the present computed overlap corrections were presented in several plots. The solid lines in Figure 5.5-6 represent the computed overlap corrections for an equimolal mixture of water vapor and carbon dioxide plotted against the temperature from 300 to 2500 K for pL's of 20, 50, 100, 200, and 500 cm. atm. The dashed

lines are for $p_w/p_c = 2$. Similar plots were developed for p_w/p_c values of 1/3, 4, 1/9, and 9. Figure 5.5-9 is a plot of the overlap correction against the fraction $p_w/(p_w + p_c)$ for pL's of 20, 50, 100, 200, and 500 cm. atm. at 500 K. Similar plots were developed for temperatures of 1000, 1500, 2000, and 2500 K. The low temperature end of the curves (less than 1000 K) is a strong function of the spectral data of the water vapor rotation band and of the fifteen micron band of carbon dioxide. It was pointed out earlier that the water vapor rotation band spectral constants tabulated by General Dynamics were not adequate at 300 and 600 K. The spectral tabulation of McClatchey was used at 300 K and the constants at 600 K were obtained by interpolation. If and when better spectral data of the water vapor rotation band become available, it will be possible to update the charts in the range $T < 1000$ K.

Two approximations to the overlap correction were investigated. The first is the grey gas approximation in which the overlap correction becomes the product of the individual emissivities or absorptivities. For temperatures of 278 to 2500 K, pL's of 3 to 240 cm. atm. the grey gas overlap corrections were off by a factor ranging from 2 to 60, but the maximum deviation in the mixture emissivities was about 11%.

The second approximation was that of Hadvig (1964) who found that the product $\varepsilon_{c+w} T$ was a function of $(p_c + p_w)L$ only over a restricted temperature range and pL ranges. At temperatures of 1500, 2000, 2500, and 3500 R and pL ranging from 0.2 to 4 ft. atm. the deviation of mixture emissivities calculated using Hadvig's approximation and the present computed emissivities was within 20 percent.

1.4.6. Pressure Boradening Correction of Overlap Correction and Emissivity of Mixture

The effect of pressure broadening on overlap correction should be more than its effect on the emissivities of individual gases, especially at temperatures below 800 K when most of the contribution to the overlap correction is form the overlapping region of the wings of the fifteen micron band of carbon dioxide and the rotation band of water vapor. This is because broadening increases the strength of the wings of each gas; therefore, the broadening of the individual bands will greatly increase the wave length region in which overlap is important. In the case of the 2.7 micron band where the carbon dioxide band is completely contained within that of water vapor the broadening effect would not probably be a strong function of pressure and may even decrease with increasing pressure as a consequence of the decrease in the effective absorption coefficient of the water vapor band in the region of overlap. The proposed approximate pressure broadening correction facotr of the overlap correction is given by

$$C_{\Delta_\varepsilon} = C_{\varepsilon_w} C_{\varepsilon_C} \qquad (1.4.6\text{-}1)$$

and the mixture emissivity would, therefore, be given by

$$\varepsilon_{mix} = C_{\varepsilon_w} \varepsilon_{w,\,0} + C_{\varepsilon_C} \varepsilon_{C,\,0} - C_{\varepsilon_w} C_{\varepsilon_C} \Delta\varepsilon_0 \qquad (1.4.6\text{-}2)$$

Equations (1.4.6-1) and 1.4.6-2) would be exact if the gases were grey.

To show the validity of the approximation Figure 5.6-1 shows the effect of temperature on three types of computed correction factors, $C_{\Delta\varepsilon}$ exact, $C_{\Delta\varepsilon}$ proposed (grey gas) and $C_{\varepsilon_{mix}}$ at P_t = 1 atm., $p_w = p_c = 0.5$, $p_{c+w}L$ = 4 ft. atm. in a temperature range of 500 to 3500 R (278 to 1944 K). As anticipated, the exact $C_{\Delta\varepsilon}$ is larger than the

proposed grey gas approximation C_{ε_W} C_{ε_C} at temperatures below 1500 R (833 K). For temperatures above 1500 R the approximation seems to be good. In the temperature range 500 to 1500 R the present approximation may be used with the understanding that it may underestimate the correction factor.

The effect of partial pressure variation on the computed exact correction factor to the overlap correction, the computed proposed grey gas approximate correction factor to the overlap correction and the computed exact correction facotr to the emissivity of the mixture is shown in Figure 5.6-2 for a temperature of 1500 K, pL = 50 cm. atm., p_c/p_w = 1 and P_t = 1 atm. The figure shows the close agreement of the present proposed approximation. Figure 5.6-3 shows the computed effect of total pressure on the three types of corrections for an equimolal mixture of carbon dioxide and water vapor, pL = 50 cm. atm. and zero partial pressures of water vapor and carbon dioxide. An increase in the total pressure from 1 atm. to 20 atm., in the range of turbines increases the overlap correction and the mixture emissivity by about 56 and 25 percent respectively. The present proposed approximation results in an increase of about fifty percent in the overlap correction and twenty-six percent in mixture emissivity.

The above comparison indicates the importance of the pressure broadening correction for the overlap corrections. In spite of the very limited comparisons shown in the present investigation the use of the grey gas appxoimation proposed in the present study and represented by equations 1.4.6-1 and 1.4.6-2 is recommended with caution. It is to be regarded as a preliminary estimate of the correction.

2. Introduction

2.1. Preface

Engineers have long recognized the importance of infrared radiation from gases, especially at high temperatures where the radiation from such gases such as carbon dioxide and water vapor may be much larger than the convective heat transfer. Hottel, recognizing the importance of infrared emission, conducted several studies and investigations at M.I.T. in the 30's, 40's and 50's, measuring the radiation from non Luminous gaseous flames. Experiemnts were conducted by others, e.g. Schmidt, Eckert, and others; but the final recommendations by the different investigators for the emissivities of water vapor and carbon dioxide were not in agreement. Hottel critically analyzed all the available data and constructed the well-known emissivity charts of water vapor and carbon dioxide.

The progress of rocket and space technology has given new momentum to research in this area. In recent years, several detailed spectral data of water vapor and of carbon dioxide were published, and a better understanding of the radiation from gases was achieved. Therefore, it is timely to critically evaluate the new spectral data and their use in calculating gas radiation. The present thesis was undertaken with the objectives of selecting the best available spectral data and model for water vapor and carbon dioxide radiation, setting up a model to compute gas emissivities and absorptivities, analyzing the experimental data on water vapor and carbon dioxide emission critically and comparing them with the computed values using the present model in an effort to update the emissivity charts of water vapor and of carbon

dioxide to include the new spectral information and to cover a wider range. Additional objectives were to develop pressure broadening correction factor charts for each of the two gases and charts for estimating the overlap correction due to superimposed radiation of water vapor and carbon dioxide.

2.2. Theoretical Considerations

The problem of predicting the thermal radiation of a gas molecule using quantum mechanics is a complex one. Only heteropolar gases can emit or absorb radiation in the infrared. Except for rare and elementary gases, all others are heteropolar to some extent. Of these gases, water vapor and carbon dioxide are the most important gases for radiative heat transfer calculations. They exist in the products of combustion of all common fossil fuels as well as in the atmosphere.

2.2.1. Single Line Emission

From the quantum mechanics point of view, an atom or a molecule radiates or absorbs energy whenever it goes from one energy level to a different one giving rise to a spectral line.

The frequency variation of the spectral intensity of a single line may be generally described by a simple bell shaped curve. Consequently, two constants are needed to describe the line, e.g. area and width. Three factors may affect the shape of a spectral line. These are:

1. The finite natural radiative life time of the molecule, sometimes called the natural life time line broadening.
2. The translational motion of the molecule, called the Droppler

line broadening.

3. Collisions with other molecules, called collision line broadening.

In flame systems the collision broadening is dominant. The width of a spectral line is, therefore, governed by random collisions between molecules. The spectral contour of a particular line is defined by an absorption coefficient k_w which reaches its maximum value at a characteristic wave number w_0. When k_w is plotted against the wave number w a bell shaped curve is obtained. The line strength S is defined as

$$S = \int_{-\infty}^{+\infty} k_w dw \qquad (2.2.1\text{-}1)$$

S is the area under the k-w curve and is a measure of the total line absorption when the self absorption is neglected. A second constant is required to describe the shape of the curve. This is the line width, 2b, defined as the width of the line, in units of wave number, when the absorption coefficient reaches half its maximum value. The line shape can be approximated by the so-called Lorentz form, which is

$$k_w = \frac{Sb}{\pi} \frac{1}{(w - w_0)^2 + b^2} \qquad (2.2.1\text{-}2)$$

In order to perform calculations of gas emission accurately it is necessary to measure S and b for each collision broadened line. At the temperatures and pressures that characterize most practical flames the line widths tend to be much smaller than the width of the entire spectrum, which is of the order of 3000 cm^{-1}. Measurement of very small

line widths is a very difficult task even with high-resolution instruments, therefore, indirect approximate techniques were developed. These are the band model techniques which are used in the present work and will be described later.

A term commonly used when describing spectral line radiation from homogeneous media is the equivalent width A_i. This is defined as the wave number integral of the spectral absorptivity α_w defined as

$$\alpha_w = 1 - \exp(-k_w \ pL) \qquad (2.2.1\text{-}3)$$

where k_w is the monochromatic absorption coefficient and pL is the absorbing gas partial-pressure-length product. Therefore

$$A = \int \alpha_w \, dw = \int (1 - \exp[-k_w \, pL] \, dw \qquad (2.2.1\text{-}4)$$

A may be thought of as the wave number interval in which a black body (a totally absorbing surface) will have the same absorption as the spectral line.

For a Lorentz-shape line the equivalent width is given by

$$A = 2\pi b \, f(x) \qquad (2.2.1\text{-}5)$$

where $x = SpL/2\pi b$ (2.2.1-6)

and $f(x)$, the Ladenbrug-Reiche function, is

$$f(x) = x \exp(-x) [I_0(x) + I_1(x)] \qquad (2.2.1\text{-}7)$$

where I_0 and I_1 are the modified Bessel functions of orders zero and one respectively.

The evaluation of the Ladenburg-Reiche function is a time consuming calculation. Several approximation formulas and series representations have been proposed. A very useful one and easy to evaluate is

$$f(x) \simeq \frac{x}{\sqrt{1 + \frac{\pi}{2} x}} \qquad (2.2.1\text{-}8)$$

The present calculations indicated that the deviation of the above

formula is not more than 7.5% for all x values, with the maximum occuring at an $x \simeq 0.8$.

More recent work indicates that the deviation could be reduced to less than 0.5% by adding a term to the above approximation:

$$f(x) \simeq \frac{1}{\sqrt{1 + \frac{\pi}{2} x}} + \frac{0.07\ x^3}{(1 + 0.5\ x^2)} \qquad (2.2.1\text{-}9)$$

The equivalent width A can be approximated as

$$A = 2\pi b\ f\left(\frac{SpL}{2\pi b}\right) \simeq \frac{SpL}{\sqrt{1 + \frac{SpL}{4b}}} \qquad (2.2.1\text{-}10)$$

This simple relation is valid only in a homogeneous media and is exact for a statistical band model with an exponential S distribution, as will be discussed later. In the general case, however, temperature, pressure, and partial pressure of absorbing gas vary along a line of sight and the media is termed inhomogeneous. In this case the equivalent line width can be written as

$$A = \int_{\Delta w} \left(1 - \exp\left[-\int_{-\infty}^{s} k(w, s')\, \rho(s')\, ds'\right]\right) dw \qquad (2.2.1\text{-}11)$$

which involves two integrations, one over the distance s, the other over the line spectral interval Δw.

The Curtis-Godson model is a two-parameter approximation for an inhomogeneous media. It represents the equivalent width of a single line along inhomogeneous path, along which S and b may vary, in terms of the equivalent width of a single line for a homogeneous path using some appropriately defined terms: The effective strength S_e and the effective half-width b_e. Considering a case of a path through several isothermal slabs the equivalent S_e and b_e may be defined in terms of the

S_i and b_i in region i of optical thickness u_i of a single Lorentz line as

$$S_e \equiv \sum_i S_i u_i / \sum_i u_i \qquad (2.2.1\text{-}12)$$

$$b_e \equiv \sum S_i b_i u_i / \sum S_i u_i \qquad (2.2.1\text{-}13)$$

and the Curtis-Godson approximation of the equivalent width is

$$A = 2\pi b_e \, f\left(\frac{S_e u}{2\pi b_e}\right) \qquad (2.2.1\text{-}14)$$

where $u = \sum_i u_i \qquad (2.2.1\text{-}15)$

This approximation is exact in certain limiting cases, e.g. when the absorption at the line center is either very strong or very weak.

2.3. Equation of Radiative Transfer in Nonscattering Media

The differential equation describing the spectral radiance as a function of the distance s is an non scattering medium in local thermodynamics equilibrium is

$$\frac{\partial E_w(w, s)}{\partial s} = - k(w, s)E(w, s)\rho(s) + k(w, s)\rho(s)E_w^0(w, s) \qquad (2.3\text{-}1)$$

where k(w, s) is the absorption coefficient, $\rho(s)$ is the local density of the absorbing matter, E(w, s) is the spectral radiance and $E_w^0(w, s)$ is the spectral radiance of a blackbody at the same temperature.

2.4. Transmissivity

For a gas volume between positions s_1, s_2 the monochromatic transmissivity is defined as:

$$\tau(w) = \exp\left[-\int_{s_1}^{s_2} k(w, s)\, \rho(s)\, ds\right] \qquad (2.4\text{-}1)$$

and the absorptivity is defined as

$$\alpha(w) = 1 - \exp\left[-\int_{s_1}^{s_2} k(w,s)\ \rho(s)\ ds\right]$$

$$= 1 - \tau(w) \qquad (2.4\text{-}2)$$

2.5. Collision Line Width

2.5.1. Introduction

It has been known that the presence of a non absorbing gas in a certain spectral region can affect the absorptivity or the emissivity of a gas or a species that absorbs radiation in that spectral region. This results from the pressure broadening of the spectral lines of the absorbing gas by the nonabsorbing species.

Broadening is determined by the force between molecules. When two molecules collide, the process of emission or absorption is interrupted. The result of many such random interruptions is a spreading of frequencies associated with a particular transition. This spread of frequencies is determined by a line shape. The Lorentz line shape results from an assumption of rigid particles and is generally applied to all collision-broadened lines.

The second important class of interactions occurs when two highly polar molecules having large permanent electric dipole moments interact strongly if they are in neighboring rotational states. This is termed "resonant-dipole" collision. This effect has to be taken into consideration when studying highly polar molecules like water or hydrogen halides.

Two intensive properties affect the collision broadening: pressure and temperature.

2.5.2. Effect of Pressure

It has been established that the line half width b is linearly dependent upon the pressure. The general expression of the half width

can be expressed as

$$b = \sum_i b_{0i} p_i = (\Sigma\, b_{0i}\, Y_i)\, P_t \qquad (2.5.2\text{-}1)$$

where P_t is the total pressure, p_i and Y_i are the partial pressure and the mole fraction, respectively, of component i of the gaseous mixture and b_{0i} is the line half width due to a one atmosphere pressure.

In case of a single gas the molecules could collide with each other resulting in a self-broadening effect the b of which may be expressed as

$$b = b_0 p \qquad (2.5.2\text{-}2)$$

It is believed that although the half-widths of individual spectral lines are different, the variation from line to line may be small, and an average value may be acceptable for most heat transfer calculation.

Burch et al. (1962) introduced the term self broadening coefficient γ which is the ratio of the self broadening half-width to the nitrogen-broadened b

$$b = b_x p_x + b_N p_N = b_N \left(Y_N + \frac{b_x}{b_N} Y_x\right) P_t$$

$$= b_N (1 - Y_x + \gamma\, Y_x)\, P_t = b_N (1 + [\gamma - 1]\, Y_x)\, P_t \qquad (2.5.2\text{-}3)$$

where $\gamma = b_x / b_N$ (2.5.2-4)

Defining an equivalent pressure P_e as

$$P_e = (1 + [\gamma - 1]\, Y_x)\, P_t\,, \qquad (2.5.2\text{-}5)$$

the line half-width equation may be expressed as

$$b = b_N P_e \qquad (2.5.2\text{-}6)$$

2.5.3. Effect of Temperature

The ambient temperature T has an important effect on the collision process. According to the kinetic theory of gases

$$b_0 \propto T^{-1/2}; \text{ or } b_0 \propto 1/\sqrt{T}$$

The reciprocal square root dependence, although based on simplistic theory, has been verified by experiment. A better form, however, may be obtained by writing

$$b_0 \propto T^{-n}$$

where n may differ from 0.5.

The situation for self broadening beteeen resonant alike molecules is different. In this case, Benedict et al. (1956) recommended that the contribution to the line width $b^*_{0_x}$ for resonant collisions may be expressed as

$$b^*_{0_x} \propto T^{-n^*} \quad \text{where } n^* \simeq 1.$$

The temperature dependence of the self broadening between nonresonant alike molecules is analogous to that for foreign gas broadening and can be approximated by

$$b_{0_x} \propto T^{-n} \quad \text{and } n \simeq 0.5$$

It is, therefore, possible to write a general formula for the collision half width of an absorbing gas x as

$$b_x = b^*_{x,\,273}\, p_x \left(\frac{273}{T}\right) + \sqrt{\frac{273}{T}} \sum_{i=1}^{m} b_{i,\,273}\, p_i \qquad (2.5.3\text{-}1)$$

where the summation is taken over all gaseous species m including the absorbing gas x itself. In case of water vapor gas, a high polar molecule, the half width can be expressed as

$$b_{H_2O} = b^{*H_2O}_{H_2O,\ 273}\ p_{H_2O}\ \left(\frac{273}{T}\right) + \sqrt{\frac{273}{T}} \sum_{i=1}^{m} \left(b^{H_2O}_{i,\ 273}\ p_i \right) \qquad (2.5.3\text{-}2)$$

For a mixture of water vapor and nitrogen only at a total pressure of P_t

$$b_{H_2O} = b^{*H_2O}_{H_2O,\ 273}\ p_{H_2O}\ \left(\frac{273}{T}\right) + \sqrt{\frac{273}{T}} \left(b^{*H_2O}_{H_2O,\ 273}\ p_{H_2O} + b^{*H_2O}_{N_2,\ 273} \left[P_t - p_{H_2O}\right] \right) \qquad (2.5.3\text{-}3)$$

the self broadening coefficient γ is

$$\gamma_{H_2O} = \frac{\sqrt{\frac{273}{T}}\ b^{*H_2O}_{H_2O,\ 273} + b^{H_2O}_{H_2O,\ 273}}{b^{H_2O}_{N_2,\ 273}} \qquad (2.5.3\text{-}4)$$

Reports by the Space Science Lab (1966, 1967) and by Ludwig et. al (1968) listed preliminary data on the individual half widths for different broadening molecules with the absorbing molecule being water vapor or carbon dioxide at standard conditions of temperature and pressure. Their data is summarized in Table 2.5.3-1 in units of reciprocal centimeter. Utilizing these values to calculate the self broadening coefficient of water vapor results in

$$\gamma_{H_2O} = \frac{0.44\ \sqrt{273/T} + 0.09}{0.09} \simeq 4.9 \sqrt{\frac{273}{T}} + 1 \qquad (2.5.3\text{-}5)$$

$$\simeq 5.9 \text{ at } 273 \text{ K}$$

$$\simeq 3.09 \text{ at } 1500 \text{ K}$$

$$\simeq 2.48 \text{ at } 3000 \text{ K}$$

Clearly, γ_{H_2O} is a strong function of temperature. It is also clear that self broadening becomes weaker at high temperatures.

TABLE 2.5.3-1

Collision-broadened Line Half Widths

at STP in cm^{-1}

Broadener Gas	Absorbing Gas	
	H_2O	CO_2
H_2O Resonant	0.44	-
H_2O Nonresonant	(0.09)	(0.07)
N_2	0.09	0.07
CO_2	0.12	0.09
O_2	0.04	0.069
H_2	(0.05)	0.08
CO	(0.10)	(0.06)

Values in parenthesis are guesses.

In the case of carbon dioxide the resonant collision self broadening term can drop out i.e.

$$b_{CO_2} = \sqrt{\frac{273}{T}} \sum_{i=1}^{m} b_{i,\,273}^{CO_2} \; p_i \qquad (2.5.3\text{-}6)$$

For a mixture of carbon dioxide and nitrogen at a total pressure p_i

$$b_{CO_2} = \sqrt{\frac{273}{T}} \left(b_{CO_2,\,STP}^{CO_2} \; p_{CO_2} + b_{N_2,\,STP}^{CO_2} \left[P_t - p_{CO_2} \right] \right) \qquad (2.5.3\text{-}7)$$

$$\gamma_{H_2O} = \frac{b_{CO_2,\,STP}^{CO_2}}{b_{N_2,\,STP}^{CO_2}} \simeq \frac{0.09}{0.07} \simeq 1.3 \qquad (2.5.3\text{-}8)$$

The self broadening coefficient is not a function of temperature and is less than γ_{H_2O} indicating a much stronger self broadening in water vapor than in carbon dioxide, especially at low temperatures.

It should be stated here that although some of the b values given by Ludwig et al. were guesses, their sensitivity analysis for the line half width indicated that such crude representation could yield reasonably accurate representation of the spectra and while it is difficult to assign a specific error limit to the table values Ludwig et al. estimated overall error limits in the calculations of spectral emissivities to be within ± 20 percent. This is accepted as is in the present work.

3. Homogeneous Gases

3.1. Introduction

For a homogeneous gas the radiative transfer equation may be expressed as

$$E_w(w,u) = \int_{-\infty}^{u} E_w^0(w,u') \frac{\partial}{\partial u'} \tau(w, u', u)\, du' \qquad (3.1\text{-}1)$$

where u is the absorbing matter and

$$du = \rho ds \qquad (3.1\text{-}2)$$

For a gas with a uniform temperature

$$E_w = E_w^0 (w, T) (1 - \tau [w, u]) \qquad (3.1\text{-}3)$$

where $\tau(w,u) = \exp(-k[w]u)$ (3.1-4)

Generally, the absoprtion coefficient varies rapidly with the wave number, making it necessary to integrate the radiative transfer equation at a very large number of wave number to get a precise value of $\int E_w(w,u)du$. To facilitate this procedure, the so-called band-models were developed.

3.2. Thin Gas Approximation

A weakly absorbing gas simplifies the calculations. In this case the absorptivity is small, and the monochromatic transmissivity is very close to 1 at all frequencies,

i.e. $k\,u << 1$ for all wave numbers (3.2-4)

Therefore,

$$E_w(w,u) \simeq E_w^0(w,u)\, k\,(w)\, u \qquad (3.2\text{-}2)$$

$$E_w(w,u)\,dw \simeq \int_{\Delta w} E_w^0\,(w,u)\;k\;(w)\;u\;dw$$

$$\simeq E_w^0\,(w_0,T)\;u\int_{\Delta w} k\;(w)\;dw \qquad (3.2\text{-}3)$$

the absorptivity is

$$\alpha_w = 1 - \exp\left[-\int k\;(w)\;dw\right]$$

$$= 1 - \exp\,(-ku) \simeq k_w u \qquad (3.2\text{-}4)$$

and the total absorptivity for a unit absorbing matter, or the band strength

$$\beta = \int_{\Delta w} k_w\,du \qquad (3.2\text{-}5)$$

Therefore

$$\int_{\Delta w} E_w(w,u)\,dw \simeq E_w^0\,(w_0,\,T)\;u\;\beta \qquad (3.2\text{-}6)$$

where w_0 is a mean wave number.

3.3 Grey Gas Approximation

A grey gas is one that has a constant monochromatic absorption coefficient over a wide range of wave numbers. In this case

$$\int_{\Delta w} E_w(w,u)\,dw = [1 - \exp\,(-\overline{k}_w)]\int_{\Delta w} E_w^0\,(w,u)\,dw \qquad (3.3\text{-}1)$$

when a gas is not really grey but this approximation is made $\overline{k}$ becomes a mean absorption coefficient defined as

$$\overline{k} = \frac{1}{\Delta w}\int_{\Delta w} k\;(w)\;dw \qquad (3.3\text{-}2)$$

It is noteworthy to mention that most of the combustion gases are non-grey.

3.4. Non-Overlapping Lines Approximation:

When the spectrum of a gas consists of very narrow non-overlapping lines, the radiance integrated over a wave number range Δw may be approximated as a summation

$$\int_{\Delta w} E_w (w, u)\, dw \simeq \sum_i E_w (w_i, u) \int_{\Delta w} (1 - \exp [k(w)u])\, dw$$

$$\simeq \sum_i E_w (w_i, u)\, A_i (w) \qquad (3.4\text{-}1)$$

where $A_i(u)$ is the equivalent width of the $i^{\underline{th}}$ line in the interval Δw.

This approximation may be used for calculation of integrated radiance in case the following two conditions are satisfied:

1. $k (w)\, u << 1$ between each neighboring lines.
2. The equivalent width of the lines should be small enough that the Plank function can be assumed constant across a single line.

The Grey gas approximation and the non overlapping lines approximation provide an upper limit to the integrated radiance.

3.5. Integrated Emissivities

For a homogeneous gas at uniform temperature

$$E_w = E_w^0 (w, T) [1 - \tau (w, u)] = E_w^0 (w, T)\, \varepsilon (w, u) \qquad (3.5\text{-}1)$$

The integrated radiance in a spectral band Δw is

$$\int_{\Delta w} E_w\, dw = \int_{\Delta w} E_w^0 (w, T)\, \varepsilon (w, u)\, dw \qquad (3.5\text{-}2)$$

Assuming a mean value of the spectral radiance E_w^0 evaluated at at average wave number $\bar{w}$

$$\int_{\Delta w} E_w dw = E_w^0 (\bar{w}, T) \int_{\Delta w} \varepsilon (w, u)\, dw \qquad (3.5\text{-}3)$$

$\int_{\Delta w} \varepsilon (w, u)\, dw$ is termed the integrated emissivity and equals

$$\int_{\Delta w} (1 - \exp [-k(w)u])\, dw \leq u \int_{\Delta w} k(w)\, dw = \beta u \qquad (3.5\text{-}4)$$

where β is the band strength. This provides an upper limit of the integrated emissivity at large path lengths and is the thin gas approximation, i. e. when $ku << 1$.

3.6. Total Emissivity and Absorptivity

The monochromatic rate of emission for a homogeneous gas at uniform temperature is

$$E_w = E_w^0 (w, T)\, \varepsilon(w, u) \qquad (3.6\text{-}1)$$

The total rate of emission is

$$\int_0^\infty E_w(w,T)\, dw = \int_0^\infty E_w^0 (w,T)\, \varepsilon(w, T)\, dw \qquad (3.6\text{-}2)$$

For a black body the total rate of emission at the same temperature is

$$\int_0^\infty E_w^0 (w, T)\, dw = \sigma T^4 \qquad (3.6\text{-}3)$$

The total emissivity is defined as the ratio of the total rate of emission to that of a black body at the same temperature, i.e.

$$\varepsilon_T = \frac{\int_0^\infty E_w^0 (w, T)\, \varepsilon(w, T)\, dw}{\int_0^\infty E_w^0 (w, T)\, dw} = \frac{1}{\sigma T^4} \int_0^\infty E_w^0 (w, T)\, \varepsilon(w, T)\, dw \qquad (3.6\text{-}4)$$

In case of a gas having a spectrum consisting of a number of bands separated by transparent intervals of wave numbers, the integration may be replaced with a summation over all bands, i.e.

$$\varepsilon_T = \frac{1}{\sigma T^4} \sum_{j=1}^{\infty} E_{w_{ij}}\, \varepsilon_{w_{ij}}\, \Delta w_j \qquad (3.6\text{-}5)$$

The summation is taken over all intervals where the absorption coefficient is not zero. The term $E_{w_j} \Delta w_j$ represents the black body emissive power of the wave number interval Δw.

Similarly, the total absorptivity may be defined as

$$\alpha_T = \frac{1}{\sigma T_s^4} \int_0^\infty \varepsilon(w, T)\, E_w^0\, (w, T_s)\, dw \qquad (3.6\text{-}5)$$

$$= \frac{1}{\alpha T_s^4} \sum_j \varepsilon_{w_{i,j}}\, E_{w_{i,j}}\, (T_s)\, \Delta w_j \qquad (3.6\text{-}7)$$

where T_s is the absolute temperature of the source.

3.7. Band Models

Band models are mathematical approximations of a smiplified structure that fairly represent the real spectrum of a gas and takes a reasonable computing time.

3.7.1. Elsasser Model for Collision-broadened Lines having Lorentz Shape

At moderately low temperature the spectrum of a diatomic gas consist mainly of lines of almost constant intensity and spacing that it may be possible to represent the spectrum by a series of infinite number of equally spaced identical lines. When the line is collision broadened, the model is termed Elsasser model, in which the absorption coefficient may be represented as

$$k\,(w) = \sum_{n=0}^{\infty} \frac{Sb/\pi}{b^2 + (w - nd)^2} \qquad (3.7.1\text{-}1)$$

where S and b are the line strength and half width, and d is the line spacing.

This model is not expected to give good representation at high temperature where many high-resolution spectra indicated irregular line intensities or spacings. To represent such spectrum it is possible to assume a model in which the location of any line is statistically independent of other lines. These models ahve been developed and are termed Random band models.

3.7.2 Random Band Models

In these models the location as well as the strength of the spectral lines are described by a probability distribution, with all lines having the same shape. This permits the separation of integrals over wave number, strength and path. The simplest form of random models is the case in which it is possible to assume all lines to be of equal strength S, and randomly distributed with a mean line spacing of d.

In this case, the mean absorptivity of the band may be given as

$$\bar{\alpha} \equiv \int \alpha(w)dw = 1 - \exp\left(-\frac{A(s)}{d}\right) \qquad (3.7.2\text{-}1)$$

where A(s) is the equivalent width of a single line. If the real spectrum have a small variation in line strength it may still be possible to use the equal strength random band model if an average strength of the lines is used.

3.7.2.1. Exponential Line Strength Distribution

Real gases, expecially at high temperature, exhibit spectral lines with varying strength. It is, therefore, necessary to introduce a probability distribution for the line strength. A common form is the exponential distribution, which, according to Goody (1952), can be expressed as

$$P(S) = \frac{4}{\pi S_0} \exp\left(\frac{-4S}{\pi S_0}\right) \qquad (3.7.2.1\text{-}1)$$

Using this distribution, Goody showed that the mean absorptivity $\bar{\alpha}$ is

$$\bar{\alpha} = \int_{\text{band}} \alpha(w)dw = 1 - \exp\left\{-\frac{S_0 u}{d_0}\left(1 + \frac{S_0 u}{4b}\right)^{-1/2}\right\} \qquad (3.7.2.1\text{-}2)$$

and the transmissivity τ can be represented as

$$-\ln \tau = \frac{S_0 u}{d_0}\left(1 + \frac{S_0 u}{4b}\right)^{-1/2} \qquad (3.7.2.1\text{-}3)$$

A plot of $-\ln \tau$ v.s. u is termed curve of growth. According to Goody's equation, the curve of growth will have two assymptotic regions:

At low u as $u \to 0$ $\quad -\ln \tau \simeq \frac{S_0 u}{d_0}$

This is known as the linear assymptotic region.

At high u as $u \to \infty$ $\quad -\ln \tau = 2\frac{(S_0 bu)^{1/2}}{d_0}$

which is known as the square root assymptotic region. It is, therefore, theoretically possible to determine the values of S_0, d_0 and b by measuring τ at very short and very long path lengths.

The term S_0/d_0 is sometimes termed the absorption coefficient k, and the ratio b/d_0 is termed the fine structure parameter a. The curve of growth equations of the Goody model, also known as the gas statistical model, may be written as

$$-\ln \tau = (S_0/d_0)\, u\left(1 + \frac{(S_0/d_0)u}{4(b/d_0)}\right)^{-1/2} = ku\left(1 + \frac{ku}{4a}\right)^{-1/2} \qquad (3.7.2.1\text{-}4)$$

Ludwig et al. (1966) found that the gas statistical model gives a good representation of the measured emissivities at high temperatures. This model can be used to calculate the mean gas transmissivity τ_w or

emissivity ε_w over a spectral interval of about 5 - 25 cm^{-1}. This interval is sufficiently large to justify the use of the statistical model, which is used in the present work.

3.7.3. High Pressure Limit of Emissivity

As the gas temperature increases the number of spectral lines increases sharply. At high temperatures there are many more lines in the spectrum than at low temperature. This is especially noticed in the water vapor. Therefore, the fine structure gets filled up at high temperatures. The upper limit of the emissivity is termed the "high pressure limit" and is expressed as

$$\varepsilon_w = 1 - \exp(-[S/d]u) = 1 - \exp(-ku) \qquad (3.7.3\text{-}1)$$

$$\varepsilon_T = \frac{1}{\sigma T^4} \int_0^\infty (1 - \exp[-ku])\, E^0(w, T)\, dw \qquad (3.7.3\text{-}2)$$

This should provide an approximate upper limit to the total emissivity at a given temperature T and optical path length u.

3.7.4. Lower Limit of Gas Emissivity

It was discussed earlier that the presence of a non absorbing gas in a certain spectral region can affect the absorptivity or the emissivity of the absorbing gas in that spectral region. This is especially noticeable in water vapor and to a much lesser extend in carbon dioxide. At a given gas temperature and optical path length the total emissivity change as the partial pressure of the absorbing gas varies. Generally, ε_T increases as p_a increases. The lower limit of gas emissivity is calculated assuming $p_a = 0$, or alternatively the furnace length is

infinite, at a given temperature and $p_a L$ product. In fact, the Hottel water vapor emissivity may be considered lower limit of ε_{H_2O} at a total pressure of one atmosphere. In the present work, the non absorbing gas was taken as nitrogen, unless otherwise specifically stated.

3.8. Pressure Broadening Correction Factor

The spectral and total emissivities of water vapor and carbon dioxide depend very much upon the product of the partial pressure of the absorbing gas times the path length, the absolute temperature of the gas, and to some extent on the partial pressure of the absorbing gas which in turn affects the line half width. In an earlier section, the equation for calculating the half width, b as a function of the gas temperature, total pressure P_t and the partial pressure of existing gases was derived. For a gas at a total pressure P_t containing only a mixture of water vapor at a partial pressure of p_w and nitrogen gas the line half width equation reduces to

$$b = 0.44\, p_w \left(\frac{273}{T}\right) + (0.09) P_T \sqrt{\frac{273}{T}} \qquad (3.8\text{-}1)$$

or

$$b/P_t = 0.44\, Y_w \left(\frac{273}{T}\right) + (0.09) \sqrt{\frac{273}{T}} \qquad (3.8\text{-}2)$$

where Y_w is the mole fraction of water vapor. Equation 3.8-2 permits the graphical presentation of b/P_t in a plot versus the absolute temperature with the water mole fraction as a parameter. The Hottel standards emissivity charts of water vapor are plotted at a total pressure of one atmosphere and a zero partial pressure of water vapor. The standard emissivity charts for carbon dioxide gas should similarly be plotted at P_t = 1 atm. and p_c = 0.

The ratio of the line half width when the gas is pure steam, i.e. when the water vapor pressure equals to the total pressure to that at a

zero partial pressure is

$$b_p/b_0 = 1 + \frac{44}{9}\sqrt{\frac{273}{T}} \simeq 1 + 4.9\sqrt{\frac{273}{T}}\ , \qquad (3.8\text{-}3)$$

$$\simeq 5.9 \text{ at } 273 \text{ K},$$

$$\simeq 2.8 \text{ at } 2000 \text{ K}. \qquad (3.8\text{-}5)$$

These ratios are valid for all pressures at which collision broadening is dominant. Clearly the effect of pressure broadening on half width decreases as the gas temperature increases. In addition, at high temperatures the number of spectral lines increases rapidly saturating the spectrum causing the broadening effect on emissivity to decrease.

The minimum half width for water vapor is for a zero partial pressure

$$b_{min} = 0.09\ P_t\sqrt{\frac{273}{T}} \qquad (3.8\text{-}6)$$

The maximum half width is for pure steam

$$b_{max} = 0.44\ P_t\ (\frac{273}{T}) + 0.09\ P_t\sqrt{\frac{273}{T}} \qquad (3.8\text{-}7)$$

It is possible to define a standard half width as that evaluated at a $p_w = 0$ and $P_t = 1$ atm.

$$b_{st} = 0.09\sqrt{\frac{273}{T}} \qquad (3.8\text{-}8)$$

For a given b at a given total pressure P_t the water vapor partial pressure may be calculated from the relation

$$P_w = 2.273\ b(\frac{T}{273}) - 0.205\ P_t\sqrt{\frac{T}{273}} \qquad (3.8\text{-}9)$$

$$\text{and } b_{min} \leq b \leq b_{max}$$

The pressure broadening correction factor C is defined as the ratio, for

a fixed water-vapor-partial-pressure-length product, of the total gas emissivity at given values of water vapor partial pressure and total pressure to that at zero partial pressure and a total gas pressure of one atmosphere. Clearly, C is a function of the gas temperature, the gas absorbing matter pL and the line half width of the absorbing gas, which will be simply termed the "half width." The latter is assumed not to be a function of the wave number w.

When the absorbing gas is carbon dioxide and nitrogen is the inert gas the line half width is given by

$$b = \sqrt{\frac{273}{T}}\ (0.02\ p_c + 0.07\ P_t) \qquad (3.8\text{-}10)$$

or

$$\frac{b}{P_t} = \sqrt{\frac{273}{T}}\ (0.02\ Y_c + 0.07) \qquad (3.8\text{-}11)$$

where Y_c is the mole fraction of carbon dioxide.

The minimum, maximum, and standard gas half width may be expressed as

$$b_{min} = 0.07\ \sqrt{273/T}\ P_t \qquad (3.8\text{-}12)$$

$$b_{max} = 0.09\ \sqrt{273/T}\ P_t \qquad (3.8\text{-}13)$$

$$b_{ST} = 0.07\ \sqrt{273/T} \qquad (3.8\text{-}14)$$

The ratio of the maximum to the miminum value of carbon dioxide half width is given by

$$b_{max}/b_{min} = 9/7 \simeq 1.3, \qquad (3.8\text{-}15)$$

independent of the gas temperature and total pressure.

3.9. Emissivity for a Mixture of Water Vapor and Carbon Dioxide

For a mixture of gases of different spectral bands that do not overlap significantly, the total emissivity of the mixture can be obtained by adding the total emissivities of the different species present. In the case of mixtures involving water vapor and carbon dioxide where the two species overlap significantly in the 2.7 micron band and partially in the 15 micron band some of the water vapor emission in those bands is absorbed by carbon dioxide and vice versa. The result is a total emissivity that is less than the sum of the two species calculated separately. The amount by which the sum of the total emissivities of carbon dioxide and water vapor, each evaluated as if the other gas were transparent, has to be reduced to obtain the total emissivity of the mixture is termed the overlap correction $\Delta\varepsilon$. Therefore,

$$\varepsilon_{c+w} = \varepsilon_c + \varepsilon_w - \Delta\varepsilon \tag{3.9-1}$$

The combined spectral transmissivity in a spectral interval Δw centered around a wave number w may be expressed by

$$\tau(w) = f(\tau_c[w], \tau_w[w]) \tag{3.9-2}$$

where $f(\tau_c, \tau_w)$ represent an appropriate band model value of the transmissivity of the mixture of water vapor and carbon dioxide. Assuming random occupancy of wave number intervals, one obtains

$$f(\tau_c, \tau_w) = \tau_c\tau_w \tag{3.9-3}$$

Therefore

$$\tau(w) = \tau_c(w)\tau_w(w) \tag{3.9-4}$$

$$1 - \varepsilon_{c+w}(w) = (1 - \varepsilon_c[w])\,(1 - \varepsilon_w[w])$$

and $$\Delta\varepsilon(w) = \varepsilon_c(w)\varepsilon_w(w) \tag{3.9-5}$$

$\Delta\varepsilon(w)$ is the monochromatic overlap correction. Integrating over the spectrum gives the following expression for the overlap correction $\Delta\varepsilon$.

$$\Delta\varepsilon = \int_{w} \varepsilon_c(w)\ \varepsilon_w(w)\ E(w)\ dw\ /\ \sigma T^4$$

$$= \frac{1}{\sigma T^4} \Sigma\ \varepsilon_c(w)\ \varepsilon_w(w)\ E(w)\ \Delta w \qquad (3.9\text{-}6)$$

Clearly, $\Delta\varepsilon = f\ (p_c,\ p_w,\ L,\ T,\ P_t)$

$$\text{or} = f\ (p_c,\ p_w,\ L,\ T) \quad \text{at constant } P_t \qquad (3.9\text{-}7)$$

Hottel proposed a different arrangement of the variable in an attempt to reduce the four variable dependency to three by writing

$$\Delta\varepsilon = f\ \left(\frac{p_w}{p_c + p_w},\ p_w L + p_c L,\ T\right) \qquad (3.9\text{-}8)$$

Similarly, for the absorptivity overlap correction $\Delta\alpha$

$$\Delta\alpha(w) = \varepsilon_c(w)\ \varepsilon_w(w) = \Delta\varepsilon(w) \qquad (3.9\text{-}9)$$

$$\Delta\alpha = \frac{1}{\sigma T_s^4} \sum_{\text{all bands}} \varepsilon_c(w)\ \varepsilon_w(w)\ E_s(w)\ \Delta w \qquad (3.9\text{-}10)$$

and $$\Delta\alpha = f\ \left(\frac{p_w}{p_c + p_w},\ p_w L + p_c L,\ T,\ T_s\right) \qquad (3.9\text{-}11)$$

$$\alpha_{c+w} = \alpha_c + \alpha_w - \Delta\alpha \qquad (3.9\text{-}12)$$

If the spectral emissivities were relatively constant over the wave number of integration the overlap correction could be written as

$$\Delta\varepsilon = \varepsilon_w \varepsilon_c \qquad (3.9\text{-}13)$$

and $$\Delta\alpha = \alpha_w \alpha_c \qquad (3.9\text{-}14)$$

The above approximation is sometimes termed "the Grey gas approximation".

4. Spectral and Total Emission Data

4.1. Water Vapor

4.1.1. Introduction

Water vapor is present in appreciable amounts in almost all flames. It radiates its characteristic vibration-rotation spectrum along with the other molecules formed during combustion. Numerous measurements of the spectral and total water vapor emissivities have been done. These measurements show that the spectral or total emissivity depends on the gas temperature, partial pressure, the broadening ability of the various species, the path length, and in case of the spectral emissivity, the wave number.

4.1.2. Total Emissivity Measurement

Before discussing the work of every investigator, a discussion of the source of errors involved in total emissivity measurements seems in order.

4.1.2.1. Sources of Errors

These may be

4.1.2.1.1. Atmospheric Absorption

This is due to the presence of absorbing gas or gases in the gas layer separating the radiating gas from the radiometer. This potential source of error was not considered by several investigators and could have serious effect at small values of the product of the absorbing gas partial pressure time the length.

4.1.2.1.2. Knowledge of Exact Temperature

Gas radiation calculations involve using the absolute temperature

raised to the fourth power. Any error in T can, therefore, be magnified four times approximately when calculating T^4. Errors in gas temperature measurements could be either due to a non uniform gas temperature or to a surface surrounding the gas and not being at the same temperature as the gas affecting the thermocouple used to measure T.

4.1.2.1.3. Stray radiation

Some radiation from a hot surface associated with the radiant gas may reach the thermopile introducing some uncertainty in the measured values.

4.1.2.1.4. Determination of Path Length

The hot radiating gas should be confined in a certain path length by means of a flow system giving a fairly sharp concentration gradient at the boundary of the radiating gas as no windows could be used. The thickness of the boundary layer where the concentration falls sharply, introduces possible errors in L.

4.1.2.1.5. Radiometric Errors

There are errors introduced either during calibration of radiometer or by a change in calibration with time.

4.1.2.1.6. Partial Pressure Errors

This could be due to errors in controlling partial pressure of absorbing gas. It may have some effect at very low p's and pL's.

4.1.2.1.7. Edge Cooling Effect

This results from a non uniform gas temperature at the edges of the

radiating layer where cooling may occur introducing error in the measured radiation.

4.1.2.2. Schmidt

Schmidt (1932) carried his investigation in Germany utilizing a jet of pure steam issuing from a nozzle at a velocity of about 60 ft/sec. The partial pressure of water vapor was, therefore, fixed at one atmosphere with no appreciable error. The path length was varied by using different nozzle sizes and the use of the mirrored doubling and trekling effect which permitted a path length of as long as 0.6 ft. (about 18 cm.). The experimental measurements could have been slightly inaccurate due to the cold edges, "Edge Cooling" effect. The use of mirrors to increase path lengths could have multiplied this effect. The steam temperature was not uniform. It is possible that his measurements suffered from atmospheric absorption by moisture in boundary layer air. Schmidt did not indicate a control experiment to study the possiblity of stray reflection from the background. Schmidt presented his results in three different forms: ε v.s. T (C) at pL's of 0.96, 2, 3.02, 4.02, 6., 12. and 18.2 cm., the product of εT v.s. T (C) for the same seven pL's and temperatures up to 1000 C and ε v.s. pL in cm. atm. for Temperatures of 0 to 1600 C and pL's of 0.8 to 120 cm. atm. His results are reproduced in Figure 4.1.2.2-1.

4.1.2.3. Mangelsdorf

Mangelsdorf (1935) working at M.I.T. under the supervision of Hottel measured the emission and absorption characteristics of steam-air mixtures in a fixed path length of 1.68 ft (51.2 cm.). Through his

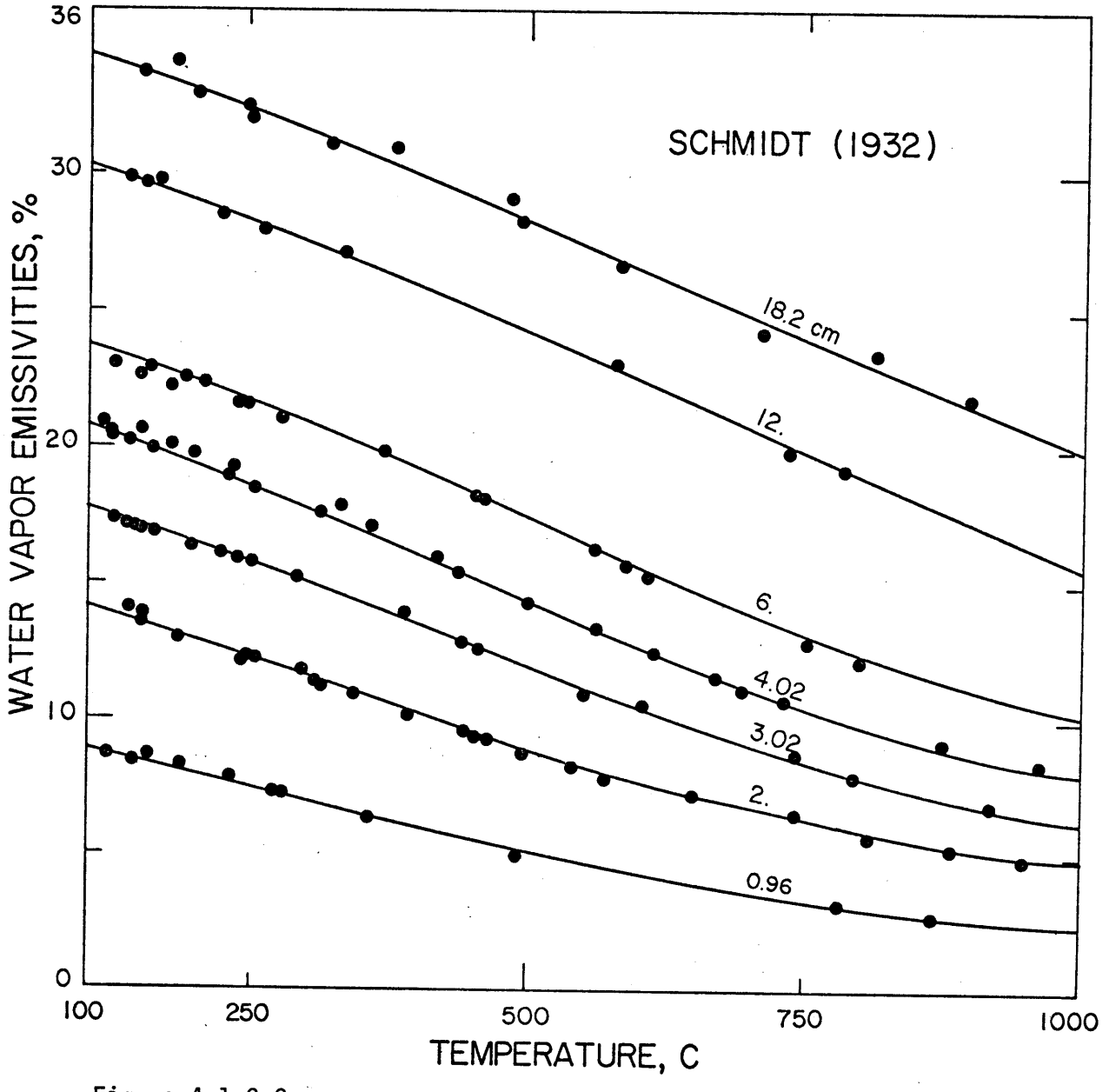
SCHMIDT (1932)
18.2 cm
12.
6.
4.02
3.02
2.
0.96
WATER VAPOR EMISSIVITIES, %
TEMPERATURE, C
0
10
20
30
36
100
250
500
750
1000

Figure 4.1.2-2

very careful experimental technique, Mangelsdorf controlled the uniformity of the gas temperature to within ± 2 F over the entire path length. Error was not more than one percent. The edge-cooling effect was avoided by defining the ends of the path length by the use of opposed-equal-momentum flow of hot dry carbon dioxide-free air with no greater than 2% error in L. Stray radiation was only 1.3% of black body radiation when black body is at the gas temperature. The presence of carbon dioxide and water vapor in the surrounding atmosphere, a one-to-two-inch path, through which the radiation travelled from the furnace to the radiometer might, however, have caused some atmospheric absorption effect. Mangelsdorf also explained the need for measurements of the gas absorption in addition to its emission. In his absorption measurement, however, Mangelsdorf mistakenly assumed that the absorption of radiation by water vapor at constant p_wL depends on the radiator temperature alone and not on the gas temperature. Figure 4.1.2.3-1 illustrates the results of the experimental measurements for pL from 0.0084 ft. atm. (.25 cm. atm.) to 1.68 ft. atm. (51.2 cm. atm.) for the temperature range 75 F to 1885 F (594 K to 1303 K). The values at 2270 F were obtained from absorptivity measurements using a radiation source at 2270 F (1517 K) at water vapor partial pressures of 0.02, 0.04, 0.08, 0.167, 0.5 and 1.0 atm.

4.1.2.4. Smith

Smith (1935) working under the supervision of Hottel measured the radiation from CO_2 flames and from CO_2 - H_2O mixtures resulting from the combustion of CO and CO - H_2 mixtures in which p_w varied from 0.11 to 0.13 atm. and path lengths for mixture measurements of 5 to 8 inches. His

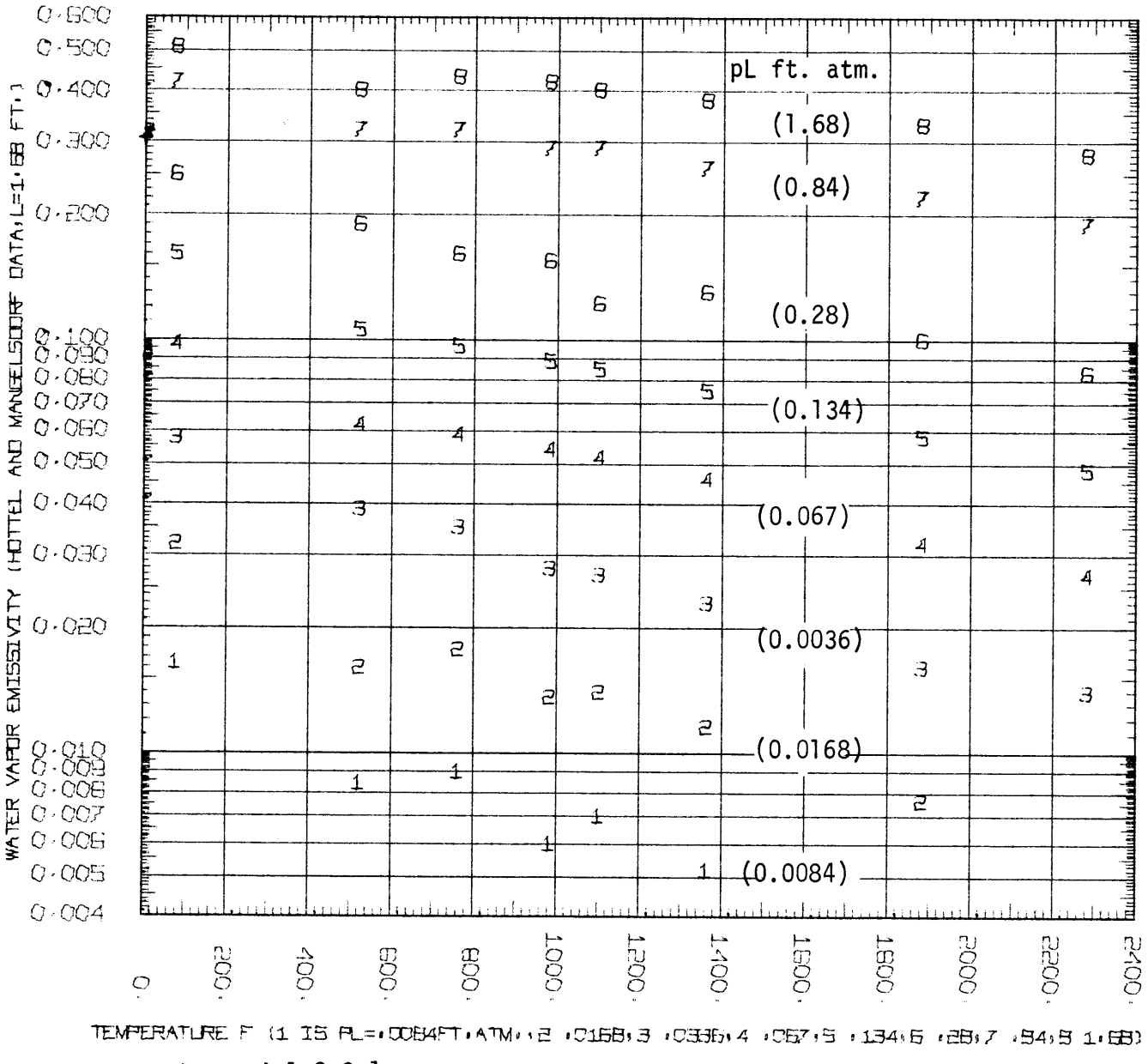

Figure 4.1.2.3-1

partial pressure was accurate to within 3% except at conditions where high temperature dissociation was possible. Temperature was measured by sodium D-line reversal method with a possible error of 50 F. His measurement might have suffered from atmospheric absorption. He measured emission from CO_2 flames and from CO_2 - H_2O mixtures, calculated the ε_{H_2O} by subtracting the CO_2 effect from the mixture measurements. His water vapor emissivities at temperatures of 2500 to 2800 F and pL's of 0.045 to 0.085 ft. at. are presented in Figure 4.1.2.4-1. His measurements were taken at 4 path lengths of 5", 5-3/4", 7" and 8" and his water vapor emissivities are the results of all measurements. An average L of 6.5" may be assumed.

4.1.2.5. Eckert

Eckert (1937) working in Germany utilized furnaces of three different path lengths. Two were backed by gold-plated mirrors to increase path lengths. The uniformity of the steam-nitrogen temperatures was good. He claimed an error of not more than 2 - 3% in absorbing gas partial pressure. There was no hot protecting air column at the end, however, thus causing edge-cooling effects and possibly resulting in lower measured water vapor emissivities. Stray radiation was about 1% of radiation from black body at gas temperature for the path length of 10.2 cm (0.334 ft.), 1.8 to 2.5% for the 65.4 cm. (2.14 ft.) furnace and about 6% for the 296 cm. (9.7 ft.) path length. The pressure of moisture between the gas furnace and radiometer could have caused some atmospheric absorption. The results of his measurements are shown for the 10.2 cm. furnace in Figure 4.1.2.5-1, in which the water vapor emissivity is plotted v.s. pL in cm. atm. for gas temperatures of 150 to 1200 C.

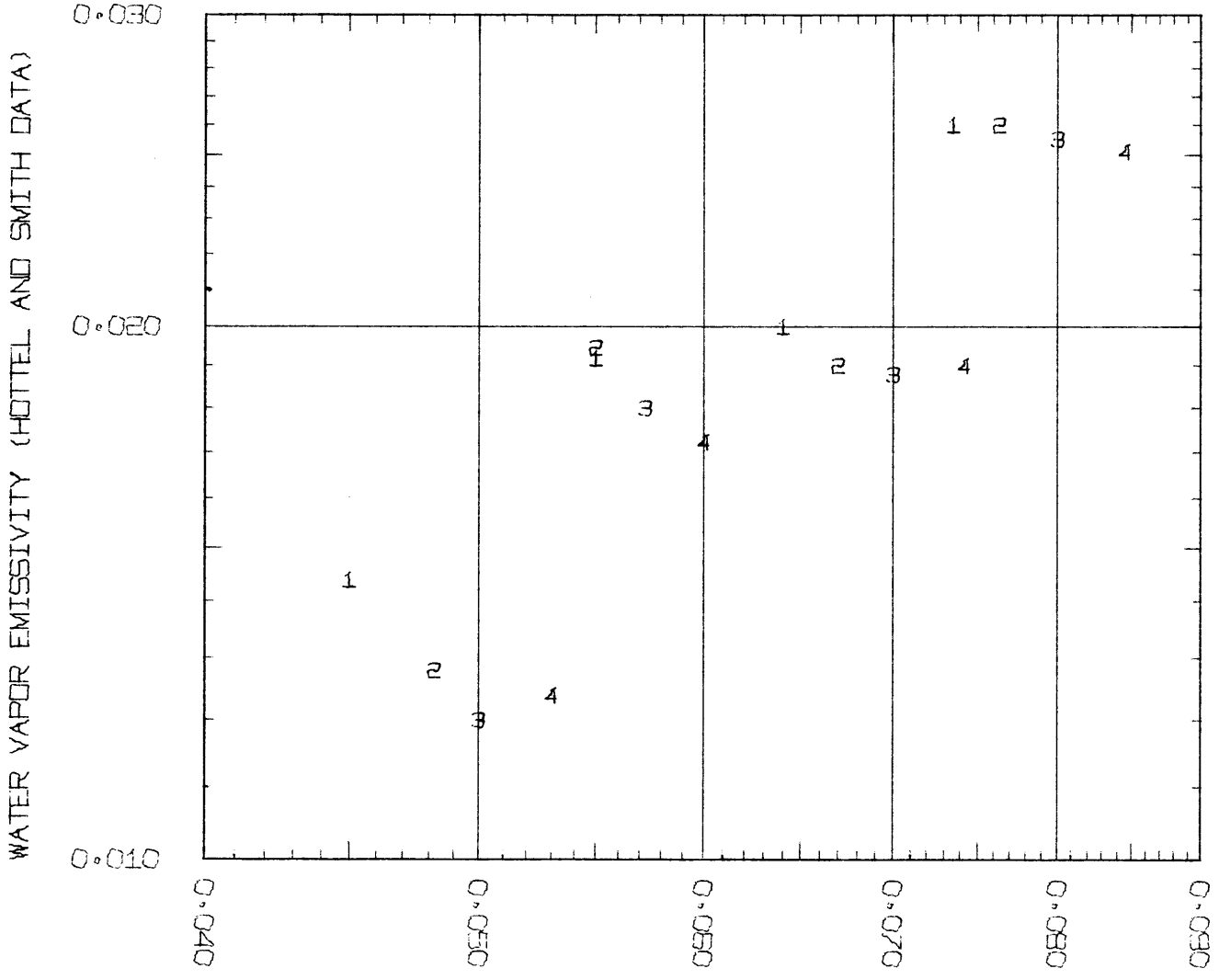

Figure 4.1.2.4-1

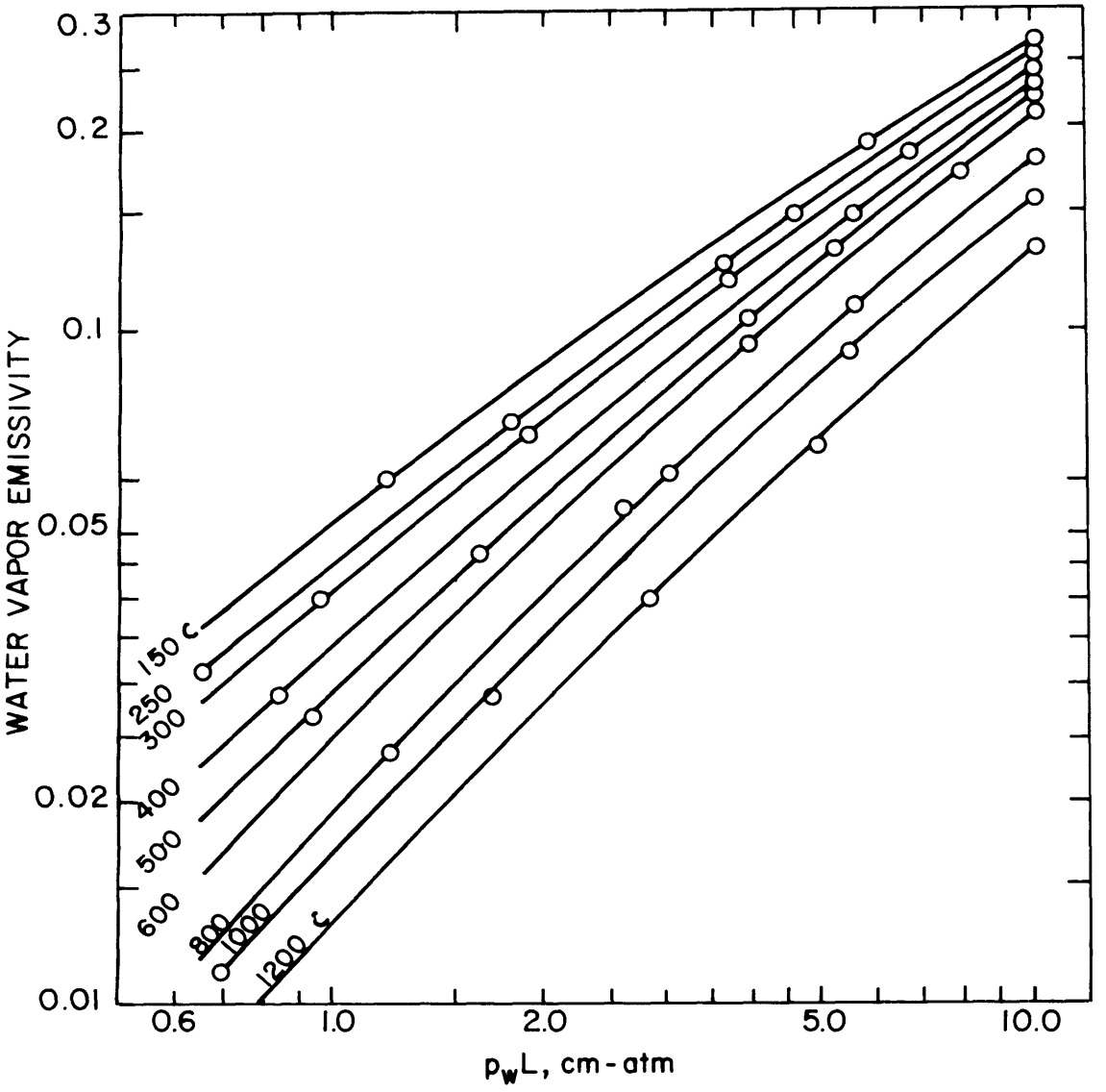

Figure 4.1.2.5-1 ECKERT WATER VAPOR DATA, L = 10.2 cm

The results of the 65.4 cm. path length are shown in Figure 4.1.2.5-2, in which the emissivity is plotted v.s. the gas temperature in C for pL's of 2, 4, 8, 17, 35 and 65.4 cm. atm. Eckert measured the water vapor emissivities at only one temperature, 100 C, using his 296 cm. furnace.

Eckert assumed the validity of Schmidt's data and proposed an allowance for the effect of water vapor partial pressure on emission from water vapor at a given pL in the form:

$$E_{p_w} = E_{p_w = 1} (p_w)^x \quad .$$

4.1.2.6. Eberhardt

Eberhardt (1936) working at M.I.T. under the supervision of Hottel measured the radiation from a steel reheating furnace with a path length of 14 ft. (426.7 cm.) in an industrial plant. The combustion gases contained both CO_2 and water vapor. The contribution of carbon dioxide to the total radiation was calculated from Hottel and Mangelsdorf's recommended charts for carbon dioxide and for overlap correction and subtracted to get the water vapor contribution. The temperature range was 1670 to 2370 F (1183 K to 1572 K) and the pL range was 1.5 to 2.5 ft. atm. (45 to 76.2 cm. atm.). The partial pressure error was not more than 1 - 4%. The temperature was fairly uniform in furnaces with the exception of a gradient at the edge which introduced the possibility of an edge cooling effect. The error in his temperature measurements was 50 - 200 F since radiant surroundings were at very low temperature and the radiating gas was at a high temperature. His measurement might have also suffered from atmospheric absorption. His water vapor emissivities are illustrated in Figure 4.1.2.6-1 for temperatures of 1600 to 2400 F

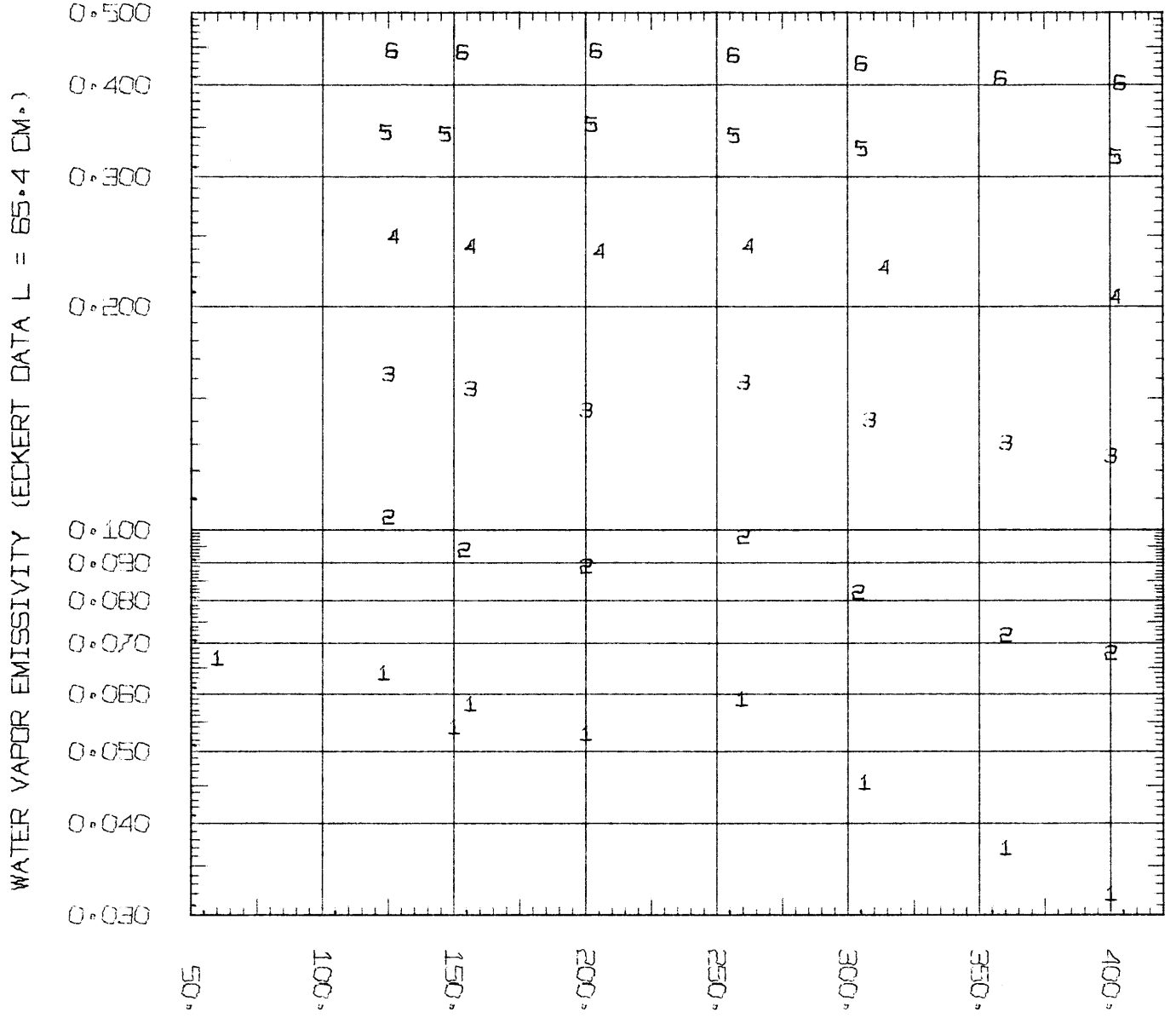

Figure 4.1.2.5-2 TEMPERATURE C (1 IS PL=2 CM.ATM.,2 4,3 8,4 17,5 35,6 65.4 CM.ATM.)

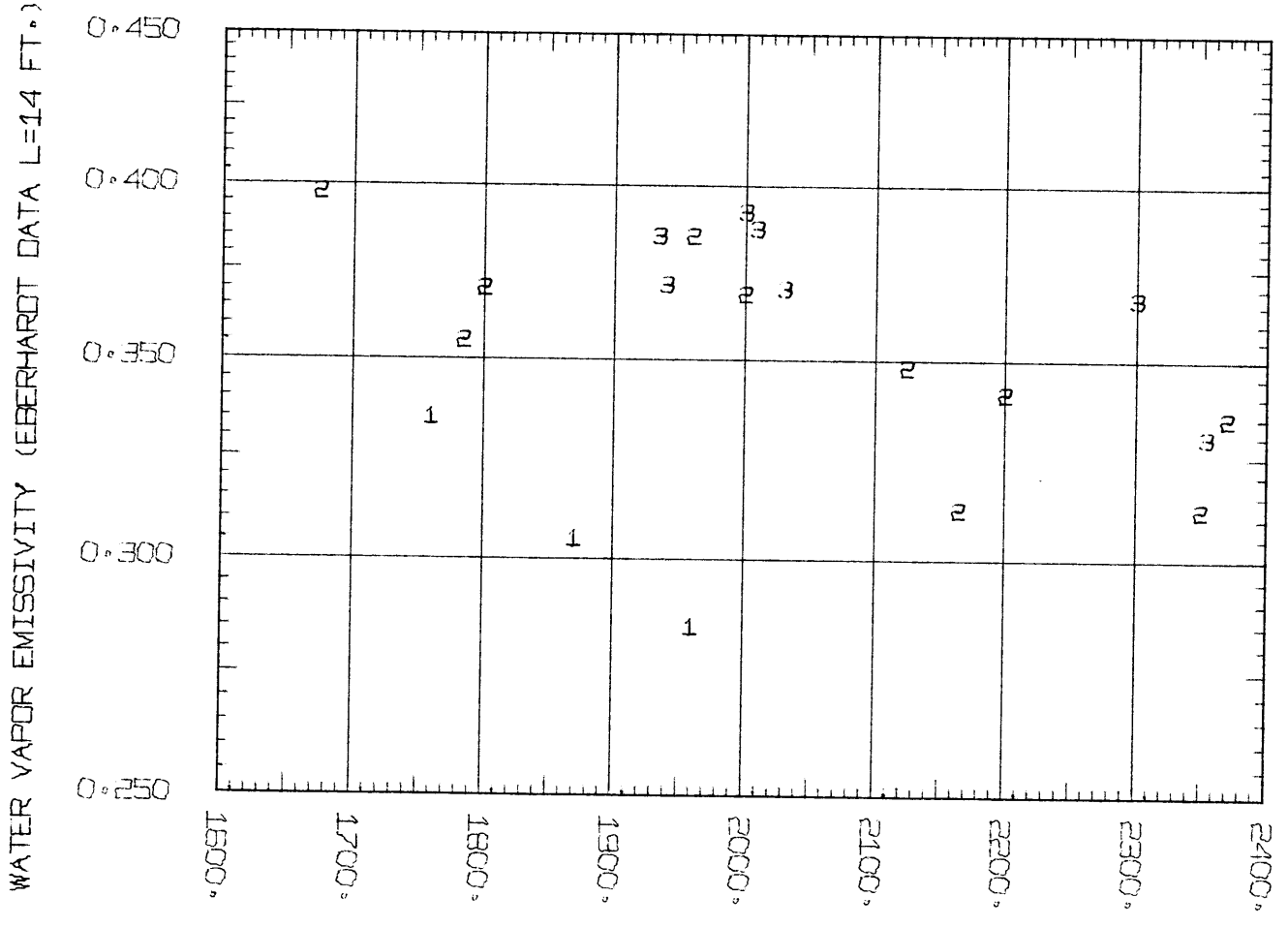

Figure 4.1.2.6-1

4.1.2.7. Falckenberg

Falkenberg (1938, 1939) was interested in the emission of the atmosphere. He adopted a method developed by Hottel and Mangelsdorf (1935) in which the intensity of the radiation coming from a column of moist air, free from carbon dioxide, was measured with a black body chilled by liquid air as background. Since the thermal emission of the chilled balck body was negligible, Falckenberg obtained the total emission of a moist column. His measurements covered a limited range at 20 C. He expressed his optical path length as gm/cm^2. To convert the pL into the units of cm. atm. the following factor was used

$$\frac{1\ gm}{cm^2} * \frac{1\ gm\ mole}{M\ gm} * T\ K * R\ \frac{cm^3 atm}{gm\ mole\ K}\ , \text{ where}$$

M is the molecular weight of water vapor = 18, and R is the gas constant = 82.07 $(cm)^3$ (atm) $(gm\ mole)^{-1}$ $(K)^{-1}$. Substituting with the above values and T = 293 K gives

$1\ gm/cm^2$ = 1335.92 cm. atm.

Falckenberg's three data points are shown in Figure 4.1.2.8-1 with Elsasser's water vapor data.

4.1.2.8. Elsasser

Working at CALTECH Elsasser (1940, 1941) measured the infrared emission of the atmosphere. He constructed a heat radiation telescope to measure the emission from moist air for distances ranging from 3 meters to 50 meters and up to 120 meters by combining the heat radiation telescope with an astronomical mirror. His minimum path length was 13 cm. and

his maximum was 315 meters. Elsasser used the method of Hottel and Mangelsdorf (1935) in determining the emissivity of moist air. His measurements of the moisture contents showed large fluctuations which can not be easily ascribed to errors of measurements. The water vapor pressure varied from 0.005 to 0.015 atm. There was a vertical gradient in the moisture content of the atmosphere due to turbulence and evaporation. In determining the path length his gas boundary was poorly defined but the error should be negligible at very large pL lengths. Some variation of air temperature along his line of sight was possible. Elsasser presented his data in the form of a semi-log plot of the emissivity (linear scale) versus the pL in gram/cm^2 (log scale). His data points as read by the author of the present work from his 3.8 cm X 8.4 cm plot is replotted using full logarithmic scale and after converting his pL's into cm. atm. at 20 C in Figure 4.1.2.8-1 the accuracy in reading his data points, especially the low emissivities values is not very good. His data shows some scatter.

4.1.2.9. Brooks

Brooks (1941) working at M.I.T. with Hottel carried out several measurements of water vapor motivated by his interest in nocturnal radiation. He used a sensitive radiometer to sight through the laboratory air upon either of two black bodies, one filled with liquid air, the other with hot water. His path length was the distance between the black body and the radiometer which varied from 1.5 to 20 ft. Clearly, his gas boundary was not well defined. Stray radiation was of no problem since the gas and the radiometer were at the same temperature. The calibration of his radiometer is believed to be unreliable. Egbert (1942)

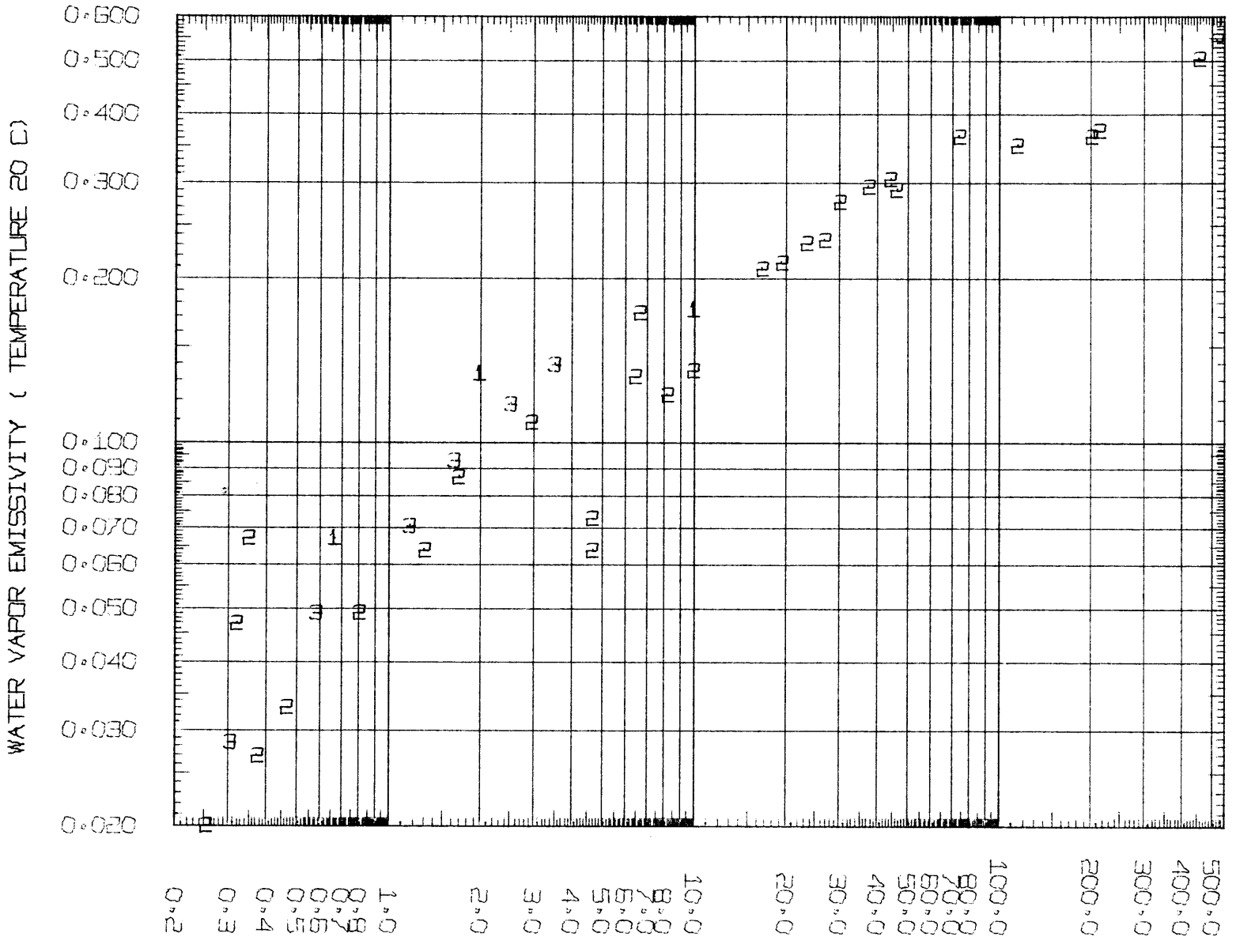

Figure 4.1.2.8-1

corrected Brooks atmospheric data to allow for the absorption by atmosphere carbon dioxide to obtain the water vapor emissivities at 70 F which are plotted in Figure 4.1.2.8-1 for pL's of 0.30 to 3.7 cm. atm. and a constant water vapor partial pressure of 0.006 atm.

4.1.2.10. Egbert

Egbert (1942) working at M.I.T. under the supervision of Hottel utilized a system with a design somewhat similar to Mangelsdorf except that he included the use of a purged atmosphere between the furnace and the radiometer to flush absorbing gases. He used five different path lengths L = 0.006 (1.83), 0.77 (23.5), 2.55 (77.7), 6.67 (203.3) and 13.33 ft. (406.3 cm.) at gas temperatures of 70 - 1300 F (294 - 978 K). The path length of 406.3 cm. was obtained by placing a gold mirror in his furnace of maximum useful length of 203.3 cm. The partial pressure of water vapor was determined to within 1 - 3 percent of its actual value, except for few values below 0.02 atm. His path length was within 1% at 203.3 cm. and 5% at 23.5 cm, and as much as 30% at the shortest path length of 1.83 cm. Temperature errors were ± 3 F except for the 23.5 cm. furnace when the error was as high as 10 F. Stray radiation was constant for any given path length. Egbert estimated an overall error in water vapor emissivity of less than five percent.

The probable error in determining gas absorptivity was greater since this involved taking the difference of two large numbers. Egbert's experimental runs were not as carefully controlled as Mangelsdorf's. His flow patterns were under poorer control and the data were far more ragged. He did cover a wide range of L, p, and T which compensated in large means for the raggedness of his data. His water vapor data are

shown in the composite figures in the section of water vapor results and discussion. Extrapolation of absorptivity curves for a source at 2040 F and L = 2.55 ft. (77.7 cm.) to a gas temperature of 2040 F were used by Egbert to determine the approximate values of water emissivities at 2040 F. Similarly his absorptivity measurements using a black body source at 70 F were used to approximate the water vapor emissivities at 70 F.

4.1.3. Spectral Data of Water Vapor

4.1.3.1. Introduction

The H_2O molecule is a non-linear triatomic molecule having three different values of moments of inertia about its principal areas. This causes the approximate theoretical methods for predicting spectral emissivities of diatmoic and linear polyatmoic molecule not to be directly applicable. Detailed line-by-line calculations have been made for water molecule at low temperatures, around 300 K, but extending these calculations to high temperatures is not possible with the available knowledge of the structure of the H_2O molecule. It is, therefore, necessary to get all necessary spectral data or band model parameters for water at high temperatures by means of experimental measurements. Recent publications listing the experimental or theoretical spectral constants of water vapor in a wave number region of about 50 to 10,000 cm^{-1} and covering a temperature range from 300 to 3000 K include those by Benedict and Kaplan (1959 and 1964), Ferriso et al. (1964, 1966), Gates et al. (1964), Goldman and Oppenheim (1965), Goldstein (1964), Goody (1964), Howard et al. (1956),

Ludwig et al. (1965, 1966, 1968, 1973), Malkmus (1962, 1967), McClatchey et al. (1972), Palmer (1957, 1959, 1960), Selby et al. (1972), Smith (1969), Stauffer and Walsh (1966), Stull et al. (1964), Tien (1967) and Wyatt et al. (1964). The experimental spectra were measured by different techniques and cover optical depths from 0.2 to 120 cm. atm., total pressures between 0.07 to about 10 atm., but the range of parameters covered at any one temperature was limited. Only a few of the pertinent articles will be reviewed here.

Howard, Burch and Williams (1956) used a multiple pass cell to study the infrared absorption of water vapor and carbon dioxide under simulated atmospheric conditions. They determined the band absorption for the carbon dioxide bands at 15, 5.2, 4.8, 4.3, 2.7, 2.0, 1.6 and 1.4 microns with pL's of 1 - 1000 cm. atm. for the strong bands and of 100 - 8600 cm. atm. for the weak bands. They also measured the band absorption of water vapor bands at 6.3, 3.2, 2.7, 1.87, 1.38, 1.1 and 0.94 micron with a water vapor absorber concentration range of 0.004 to 3.8 cm. of precipitable water. Assuming an average temperature of 290 K and an ideal gas gives 1 pr. cm. of water $\simeq$ 1322.24 cm. atm. resulting in a p_wL range covered of 5.2 to 5025 cm. atm. (approximately). They fitted their data in two forms:

$$\text{weak band fit} \quad \int A_w dw = cu^{1/2} (P + p)^k \qquad (4.1.3.1\text{-}1)$$

$$\text{strong band fit} \quad \int A_w dw = C + D \log_{10} u + K \log (P + p) \qquad (4.1.3.1\text{-}2)$$

Their results are in the form of tables of c, k, C, D and K for each band. Their results of the 2.7 micron band of water vapor were later extrapolated to cover the wings of the band by Ferriso and Ludwig (1964)

in order to obtain an integrated band intensity, reported by them as 120 cm^{-2} atm^{-1} normalized to STP.

Howard et al. also applied the gas statistical model to water vapor at room temperature and 1 atm. total pressure and found good agreement over a wide range of optical depths.

Palmer (1957, 1959, 1960) studied and measured the transmission of radiation through water vapor - nitrogen mixture in the spectral region 20 to 50 microns, i. e. 500 to 200 cm^{-1}. Palmer used an experimental set up which he termed the "Big Tube". It was a 100 ft. long absorption cell with a diameter of 3 ft. The optical path consisted of six passes through the cell, or an absorption path of 19600 cm. The spectrometer was purged and dried to insure water-vapor free carbon-dioxide-free air and was slightly pressurized to prevent influx of wet air. He covered a partial pressure range of .00015 to .01 atm. approximately. He reported his experimental spectral transmission at spectral intervals of 10 cm^{-1} in the range 500 to 320 cm^{-1} and at intervals of 5 cm^{-1} in the range of 340 to 200 cm^{-1}. His data included p_w atm., P_t, T C, and the measured spectral transmission.

Palmer's data as presented can not be used as is in the present work or for comparison with other's results. It was necessary to reduce his data by fitting his experimental transmission in a given spectral region to a curve of growth form, i. e.

$$\left(\frac{u}{-\ln\tau}\right)^2 = \frac{1}{k^2} + \frac{1}{4ak}\,\frac{1}{u} \quad . \qquad (4.1.3.1\text{-}3)$$

A direct fit is not possible because of variation of partial pressures of water vapor and nitrogen. Using the equation of the water vapor line half width:

$$b = 0.44\ p_w\ (\frac{273}{T}) + 0.09\sqrt{\frac{273}{T}}\ P_t \qquad (4.1.3.1\text{-}4)$$

$$a = b/d \qquad (4.1.3.1\text{-}5)$$

the curve of growth equation becomes

$$(\frac{u}{-\ln\tau})^2 = \frac{1}{k^2} + \frac{d}{4K}\ \frac{1}{bu} \qquad (4.1.3.1\text{-}6)$$

A least square fit of Palmer's spectral data in the form of $(\frac{u}{-\ln\tau})^2$ versus $\frac{1}{bu}$ should result in a straight line with an intersection of $\frac{1}{k^2}$ and a slope of $\frac{d}{4K}$ which permits the calculation of the absorption coefficient k and the reciprocal line spacing 1/d.

Goldstein (1964) used a specially designed isothermal, high-temperature absorption cell supplied with water vapor from a liquid water reservoir submerged in a constant temperature oil bath to study the infrared intensities and absorption coefficients of water vapor in the 6.3, 2.7, 1.87, and 1.38 micron regions at temperatures up to 1000 K. His results are shown in Table 4.1.3.1-1. His results showed that the integrated intensity for the 2.7 micron band normalized to 300 K is approximately constant in the temperature range 300 to 1000 K at $195 \pm 20\ cm^{-2}\ atm^{-1}$.

Ferriso and Ludwig (1964) used a small supersonic burner which used gaseous hydrogen and oxygen propellants to produce heated vapor test gas at the exit. They measured the spectral emission at the immediate exit of the burner where the composition, total pressure, and temperature were defined. They measured the spectral emissivities of water vapor between 2800 cm^{-1} and 4200 cm^{-1} at a total pressure of one

TABLE 4.1.3.1-1

Goldstein Integrated Intensities of Water Vapor

(± 10%)

Band Region (micron)	Temp (K)	α (cm^{-2} atm^{-1})	α Normalized to 300 K (cm^{-2} atm^{-1})	α Normalized to 273 K ($cm^{-2}atm^{-1}$)$_{STP}$
1.38	473	10.2	16.1	17.7
	673	7.3	16.3	17.9
	873	5.5	16.0	17.6
1.87	473	13.7	21.6	23.7
	673	9.7	21.8	23.9
	873	7.7	22.3	24.5
2.7	473	123.0	194.0	213.0
	673	82.4	185.0	203.0
	873	67.3	196.0	215.0
	1000	61.6	206.0	226.0
6.3	473	143.0	225.0	247.0

atmosphere is the optically thin region. They recommended an integrated intensity of the 2.7 micron band of 200 ± 20% $(cm^{-2}\ atm^{-1})_{STP}$ between 300 K and 2200 K.

Goldman and Oppenhein (1965, 1966) measured the emissivities of the 1.9 and 2.7 at 1200 K using quartz absorption cells of various lengths heated in an electric furnace up to a temperature of 1200 K. Their integrated band intensities are shown in Table 4.1.3.1-2.

Ludwig, Ferriso, Malkmus and Boynton (1965) measured the emission spectrum of water vapor between 10 and 22 microns at temperatures between 500 and 2200 K. They calculated the water vapor absorption coefficient in the range 0 - 130 cm^{-1} between temperatures of 300 and 3000 K by an approximate formulation and compared it with their measured values. The agreement is not very good, especially at the lowest temperature of 540 K. Their model predicts a k reaching a maximum at w = 190 cm^{1} at 300 K, at 220 cm^{-1} at 600 K causing the emissivity of the 15 micron band to peak at about the same wave number. They had no data at 300 K and their data at 540 K stopped at w $\simeq$ 440 cm^{-1} thus giving no support to the maxima in ε predicted by their model. The 300 K absorption coefficients of Ludwig et al. (1965) and the k's computed in the present work by least square fitting of Palmer's data are shown in Figures 4.1.3.1-7 and 4.1.3.1-8 respectively. In the interval 200 to 500 cm^{-1} both sets indicate the steadily increasing strength of the rotation band of water vapor toward long wave lengths, or small wave numbers. The theoretical calculations of Benedict as published by Goody (1964) are shown in Figure 4.1.3.1-8. His k's indicate the absorption coefficient at 300 K reaches a maximum between 120 and 240 cm^{-1} which is in good agreement with Ludwig's calculation. Integrated band intensity

TABLE 4.1.3.1-2

Water Vapor Integrated Band Intensities at 300 K cm^{-2} atm^{-1}_{STP}

20μ	6.3μ	2.7μ	1.87μ	1.38μ	1.14μ	Source
		120				Howard et al. (1956)
		210 ± 31				Jaffee and Benedict (1963)
	247 ± 10%	208 ± 10%	23.8 ± 10%	17.8 ± 10%		Goldstein (1964)
		200 ± 20%	26 ± 7%	21.2 ± 10%	1.96 ± 50%	Ferriso and Ludwig (1964)
1840	300 ± 60					Ludwig et al. (1965)
		180	21.2	17.9		Lowder (1971)
		200 ± 20%				Patch (1965)
	331	200	24.1	20.1		Edwards and Balakrishnan (1973)
	317		24.7			Benedict and Calfee (1967)
	338 + 17%					Rosenberg et al. (1970)
	338 - 6.7%					Rosenberg et al. (1970)
					0.4	Burch et al. (1966)
		220 ± 20	19.8 ± 2.7			Goldman and Oppenheim (1965)
	300	220	24	18	1	Ludwig et al. (1973)
1442.						Goody (1964)
	220 ± 10%					Goldman and Oppenheim (1960)
		235				Gates et al. (1964)
58.4	175	126	10.1	8.3	0.32	Thomson (1967)
5.7	6.33	4.74	1.75			Echigo (1967)
	250 ± 20%	230 ± 15%	26 ± 15%	21 ± 15%		Ferriso et al. (1966)

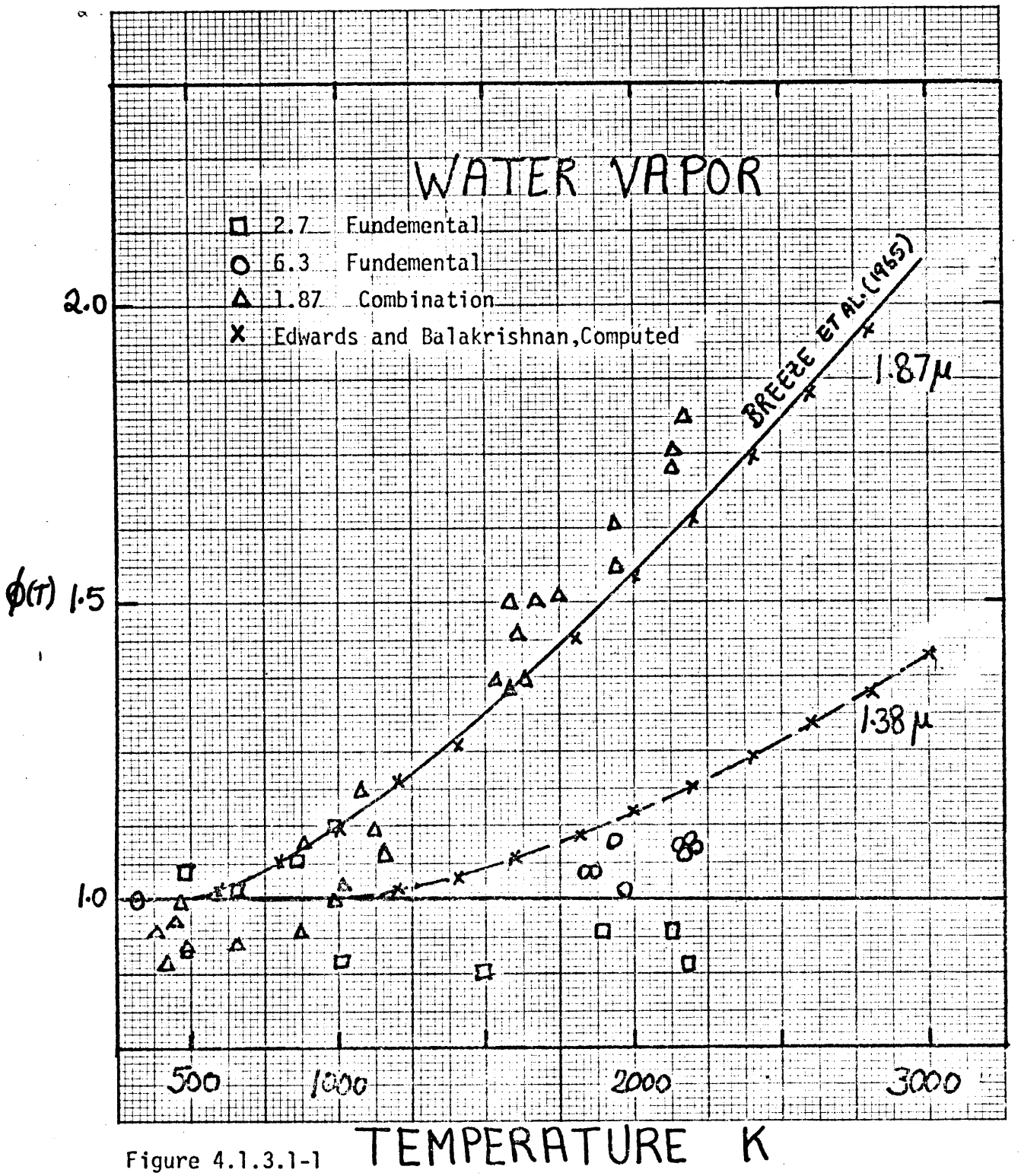

Figure 4.1.3.1-1

of the 15 micron band is 1840 cm^{-2} atm^{-1}_{STP} according to Ludwig v.s. 1442 cm^{-2} atm^{-1}_{STP} according to Benedict. These values are approximately 30 times as much as the band intensity calculated by Thomson (1967) by fitting his calculated emissivities to those of Hottel. Echigo (1967) determined the integrated band intensities for water vapor and carbon dioxide so as to coincide with Hottel total emissivities; he calculated the band intensity for the 15 micron band at an arbitrary condition at 300 K. Next he assumed the 2.7 micron and shorter bands do not contribute at 400 K and determined the integrated band intensity of the 6.3 micron by the difference between the total and the 15 micron band emissivity at 400 K. The integrated intensities of the 2.7 and 1.87 micron bands were successively determined at 600 and 800 K. Both Thomson and Echigo's values were well below those reported by other investigators. Stauffer and Walsh (1966) measured the spectral transmittances for mixtures of water vapor and nitrogen in the 14 - 20 micron region (700 to 500 cm^{-1}) of water vapor. Their data were least square fitted to a curve of growth curve and the resulting absorption coefficients in the interval 495 to 715 cm^{-1} with an interval of 55 cm^{-1} are plotted in Figure 4.1.3.1-8.

Tejwani and Varanasi (1970) extended Benedict's low temperature tabulations of spectral line intensities up to 1200 K. They computed the local mean absorption coefficent (in cm^{-1} atm^{-1}) at spectral intervals of 5 cm^{-1} from 450 cm^{-1} to 1000 cm^{-1} at 400, 600, 800, 1000, and 1200 K. They summed the spectral line intensities of all important lines which were within $\pm$ 2.5 cm^{-1} of the wave number chosen and averaged them over the spectral interval. A plot of their tabulated

spectral absorption coefficient normalized to STP for temperatures of 400, 600, 800, 1000, and 1200 K are shown in Figures 4.1.3.1-2 through 4.1.3.1-6, in which the tabulated points are joined by straight line connections. They compared the emissivities computed using their spectral constants with the experimental measurements of Ludwig et al. (1965) at the same temperatures between 10 and 22 microns. Ludwig's measurements were performed at a total pressure of 1 atm and a path length of 3.12 cm. The pL's were 0.62, 0.92, 1.10, and 1.68 cm. atm. at 590, 850, 1040 and 1640 K respectively. The agreement was reasonably good at 590 and 850 K, but the computed emissivities of Tejwani and Varanasi fell below the experimental emissivities of Ludwig et al. at 1040 K and were much lower at 1640 K.

McClatchey et al. (1972, 1973) and Selby and McClatchey (1972) provided a critical compilation of the data and models describing the optical properties of the atmosphere. They developed a computational technique in which the monochromatic transmission was assumed to follow Beer's law with an attenuation coefficient that is the sum of scattering and absorption coefficients. Their absorption coefficient followed a Laudenburg Reiche formula. The water vapor line positions were calculated from a set of energy levels which were obtained from the best available data in all spectral regions by a smoothing process which, they claimed, was partly theoretical, partly empirical. The line intensities were computed using a model they developed including modifications suggested by Benedict and Calfee (1967). They accepted the line widths of Benedict (1956), Benedict and Kaplan (1959, 1964), Benedict and Calfee (1967) and Benedict and Plyler (1954) as they were in general confirmed with more recent high-resolution spectra of air-broadened or nitrogen-

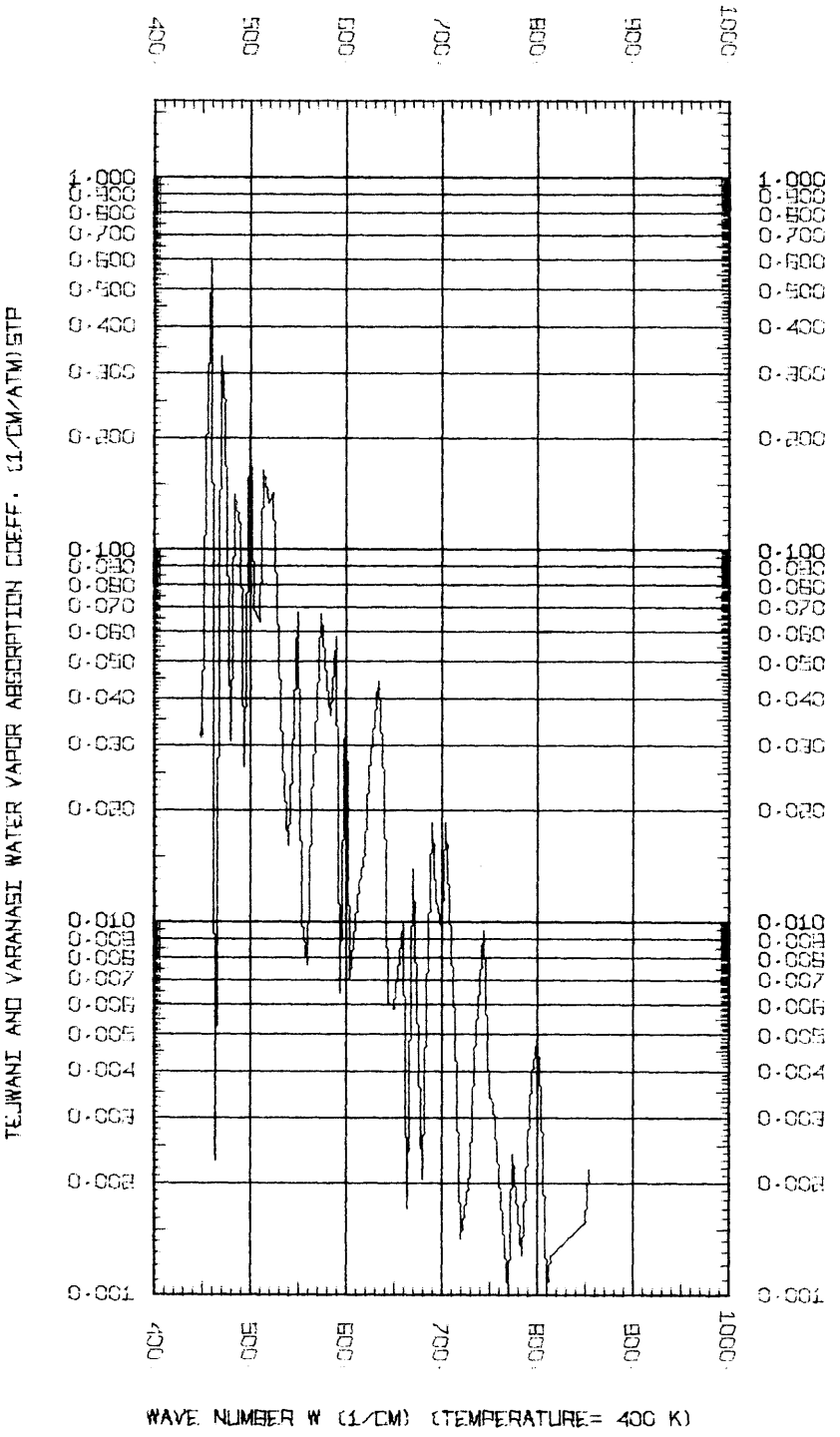

Figure 4.1.3.1-2

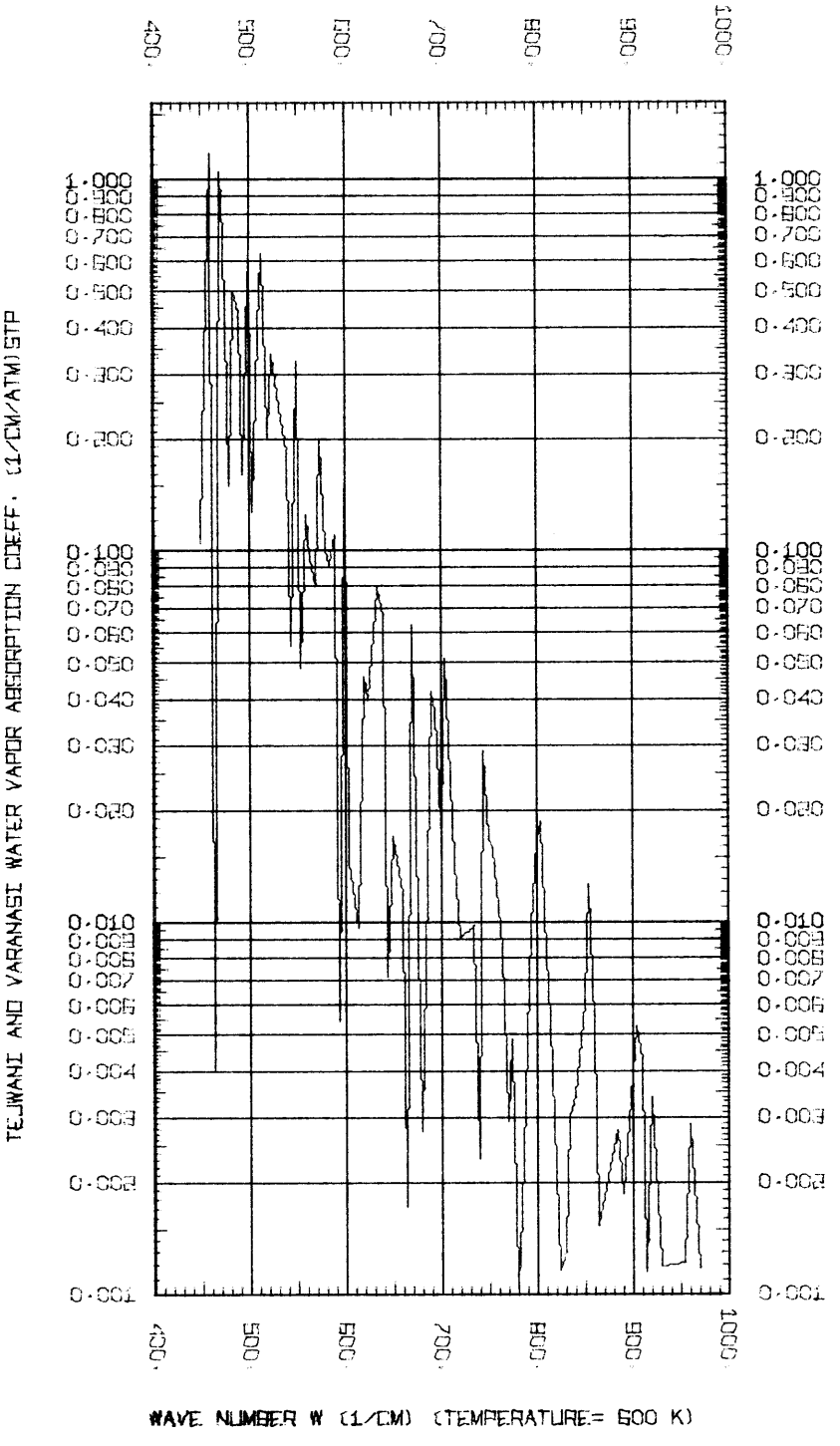

Figure 4.1.3.1-3

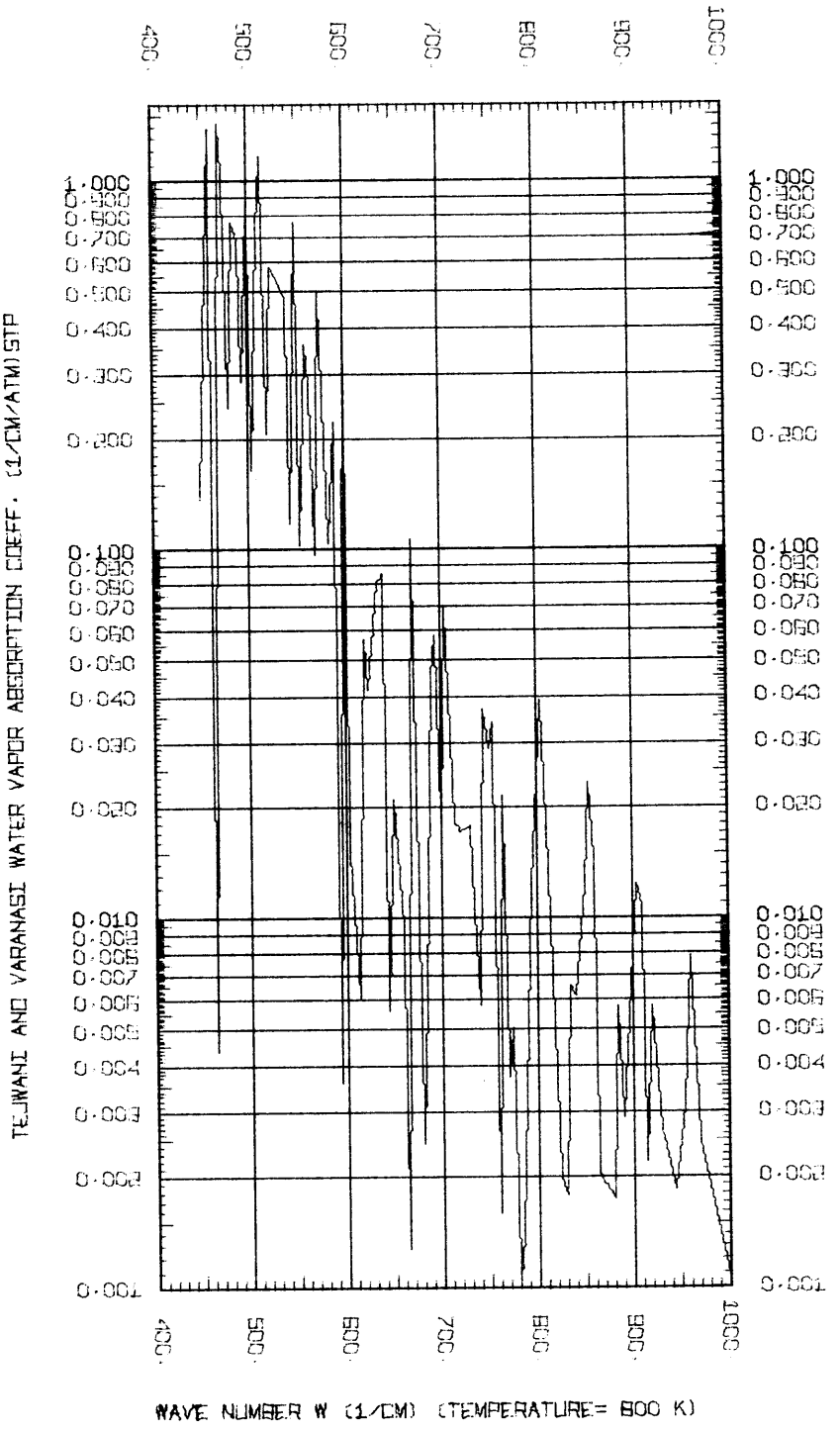

Figure 4.1.3.1-4

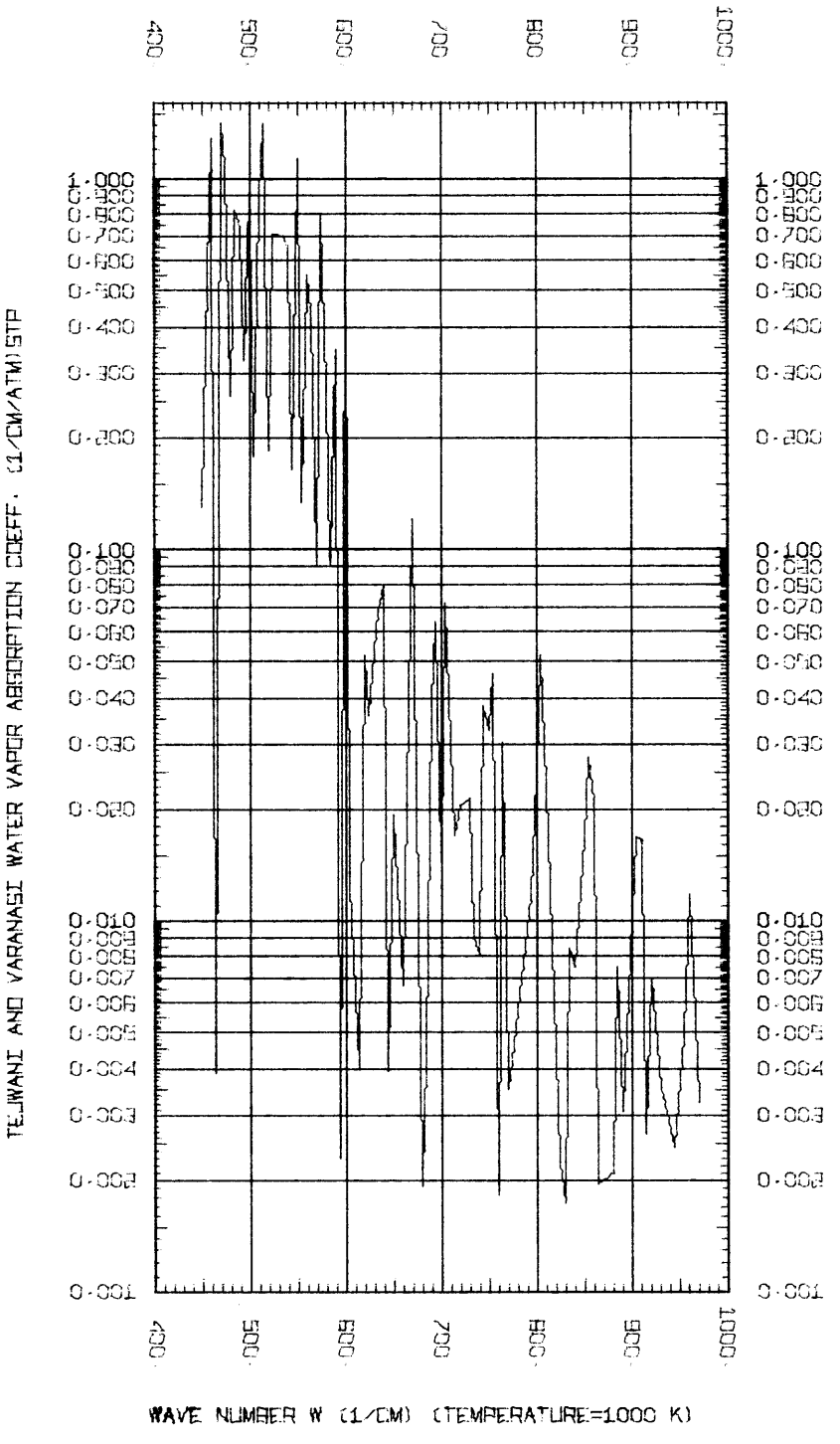

Figure 4.1.3.1-5

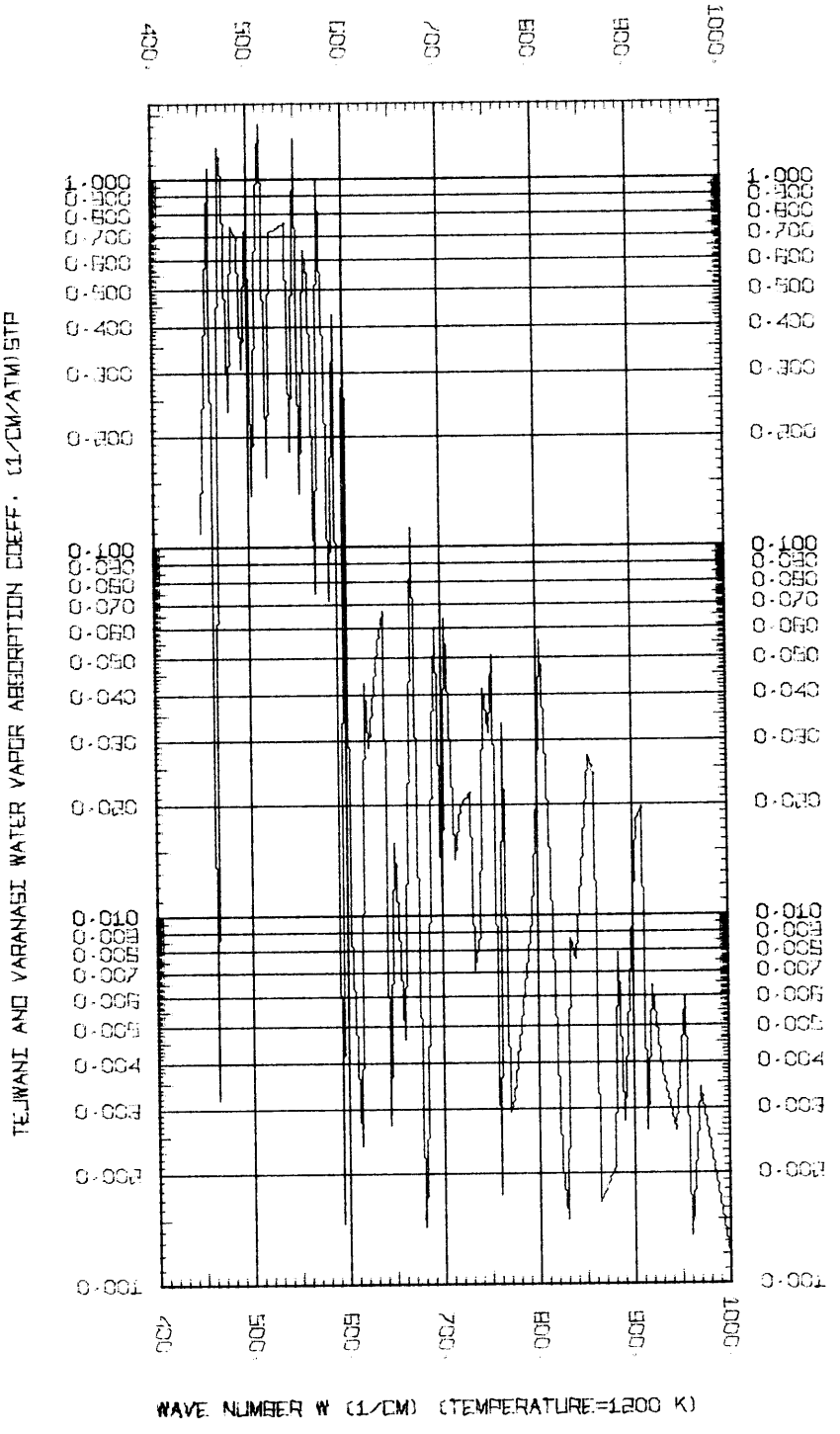

Figure 4.1.3.1-6

broadened water vapor. Their calculated spectral absorption coefficients at STP are shown in Figure 4.1.3.1-7 as a solid line connecting their tabulated values. The Figure also includes the spectral data of Breeze et al. of General Dynamics at 300 K (dashed line). For clarity purposes the absorption coefficients of Benedict, Palmer, Stauffer, and Hettner are shown separately from McClatchey et al. and the General Dynamics data in Figure 4.1.3.1-8. The curves labelled "Palmer" and "Stauffer" are the absorption coefficients fitted by the author of the present investigation to Palmer's data at 292 K, 283.4 K and 291.6 K and to Stauffer's data at 305.7 K. The spectral data of Hettner (1923) at 354 K is taken from Guerrieri (1932). It is clear that the narrow shape of the k v.s. w curve of the General Dynamics group is not supported by results of any other investigator. The figures also show the wide scatter of the spectral constants of the different experimenters thus complicating the task of selection of the absorption coefficients to be used in the present work. Although the position of the maximum k suggested by General Dynamics is not supported by experimental data, it is not too far off from a smoothed curve of Benedict's coefficients. The GD curve therefore was accepted from 50 to 220 cm^{-1}. At wave numbers greater than 220 cm^{-1} the spread of the absorption coefficients of different investigators is more than a factor of 100 in some wave numbers intervals although a factor of 10 seems a reasonable average. The discrepancy is in a range where k is low and therefore has very little effect on the integrated band intensity. It does, however, affect the dependence of the total emissivity on the pL.

A narrow band gets saturated at low pL's resulting in a total emissivity that tend to be high at low pL's and low at high pL's. A

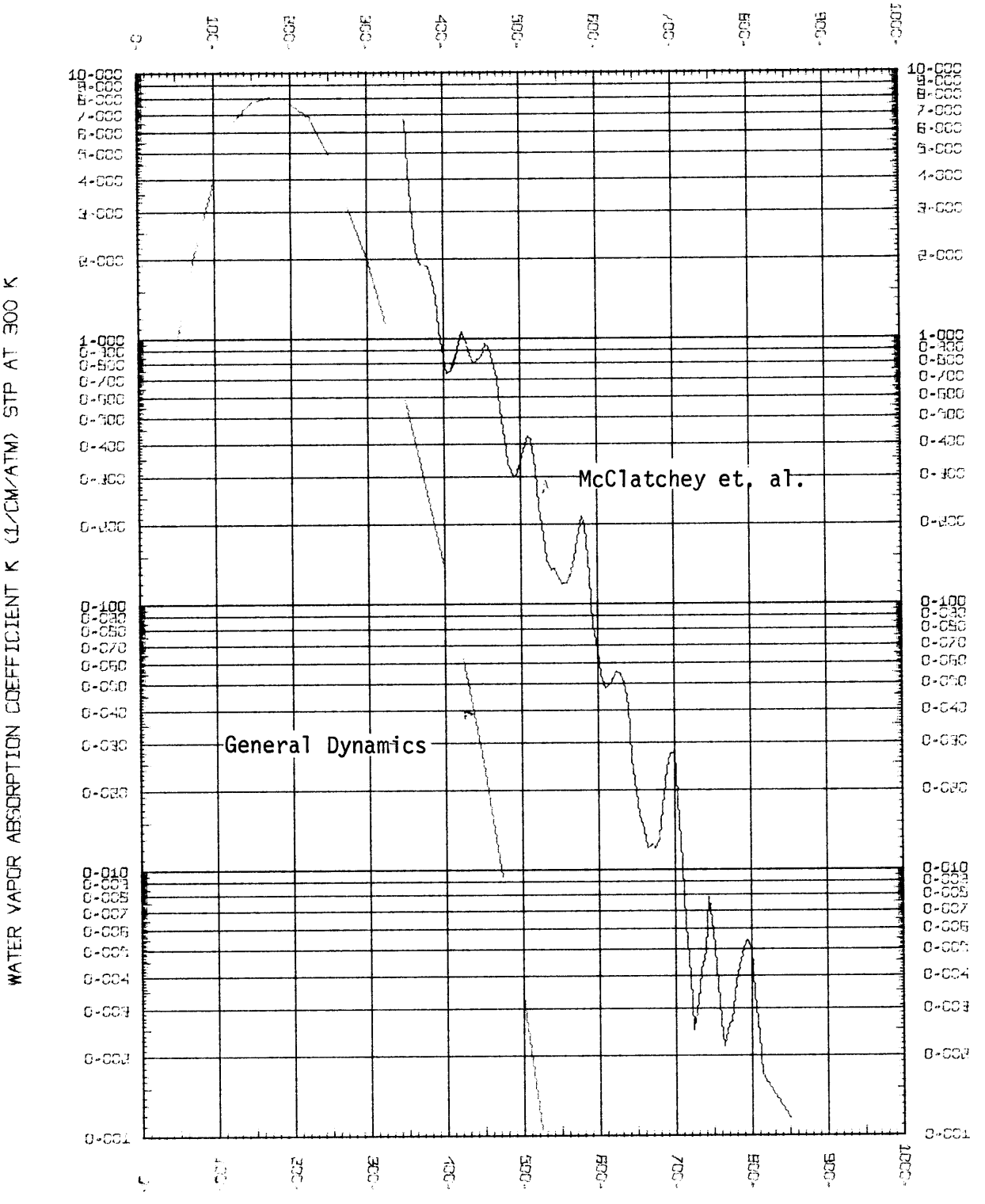

Figure 4.1.3.1-7

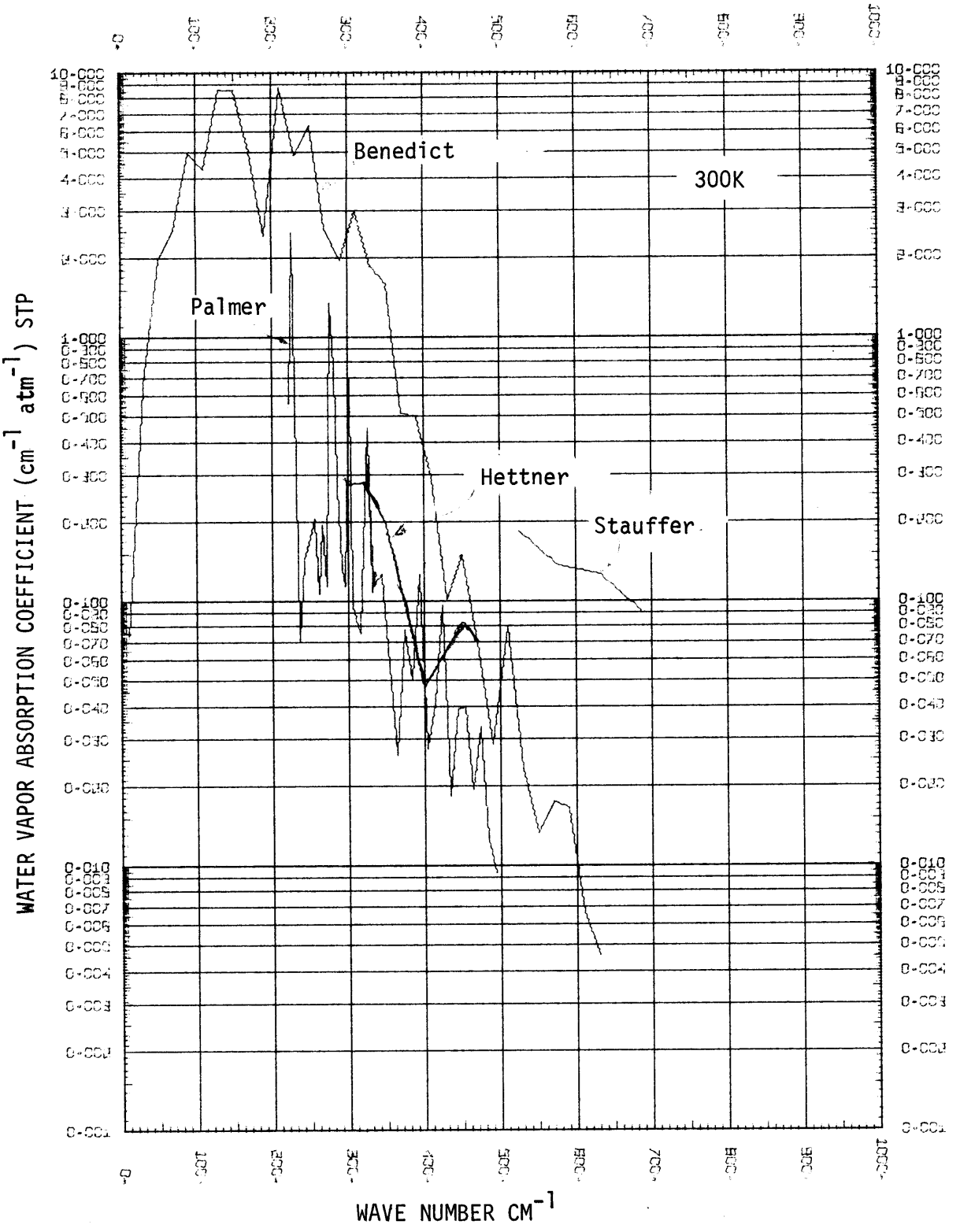

Figure 4.1.3.1-8

wide band with the same total band intensity results in a total emissivity with stronger dependency on pL at moderate and high pL's. Results of the present work showed that room temperature water vapor emissivities computed using the data tabulated by General Dynamics, i.e. Ludwig et al. and Breeze et al., were consistently higher than experimental emissivities of Schmidt, Eckert, Hottel and Mangelsdorf and Egbert at pL's less than 1 cm. atm. and were consistantly lower than experimental emissivities at pL's greater than 50 cm. atm., indicating the possibility of a correct or slightly high integrated band intensity but a narrow band assumption by Ludwig et al. In comparing the spectral data of different investigators the author decided that McClatchey et al.'s spectral data was a good representation of the water vapor molecule at wave numbers greater than 400 cm^{-1} . In order to modify Ludwig et al.'s spectral tabulations, it is necessary to maintain the same integrated band intensity within ten percent.

It was, therefore, decided to use Ludwig et al.'s spectral tabulations at 300 K from 50 to 425 cm^{-1} when the General Dynamics coefficients falls below 0.1 cm^{-1} atm^{-1} and McClatchey's absorption coefficients fall below 0.9. For wave numbers greater than or equal to 425 the absorption coefficients of McClatchey are used. The selected data for the present work are shown in Figure 4.1.3.1-10, which displays the final water vapor absorption coefficients for the fifteen micron band in the temperature range 300 to 3000 K. The absorption coefficients of the 15 micron band at 600 K of Tejwani and Varanasi were normalized to cm^{-1} atm^{-1}_{STP} and compared to the General Dynamics values. Neither set seemed to give good presentations of the desired 600 K coefficients. Both sets gave total emissivities which were higher than experiments at low pL's and lower than experiments at high pL's. In the absence of any

better method, the spectral absoprtion coefficients used in the present work at 600 K and wave numbers greater than 425 cm^{-1} were generated by plotting the absorption coefficients of each wave number interval versus the temperature using the General Dynamics values from 1000 K to 3000 K and McClatchey's value at 300 K. A tangent was drawn from the 300 K point to the curve representing the 1000 to 3000 K values. The intercept of the tangent line with the line T = 600 K was taken as the absorption coefficient of water vapor at 600 K in cm^{-1} atm^{-1}_{STP}. The present absorption coefficients at 600 K are plotted as a solid line in Figure 4.1.3.1-9 together with the General Dynamics doefficients at 600 K as a dashed line and in Figure 4.1.3.1-10 displaying the spectral constants of the water vapor 15 micron band as used in the present work. At temperatures higher than 1000 K contribution to the total emissivity of the fifteen micron band is not so significant as those of the 6.3 and 2.7 micron bands. The spectral tabulation of General Dynamics were considered adequate and are used in the present work.

Ferriso et al. (1966) of the General Dynamics group compared their tabulated values in the 6.3 micron band with those of Gates et al. (1964) at 300 and 600 K. In general, the agreement was found to be within 20%. They also compared their absorption coefficients with Oppenheim's (1965) detailed measurements in the 2.7 micron band at 1200 K, with Goldstein's (1964) absorption coefficients of the 1.38, 1.87, 2.7 and 6.3 micron bands at about 500 K and 1200 K, with Simmons et al. (1965) 2.7 micron band absorption coefficients between 700 and 1200 K. They also compared calculated spectral emissivities using their spectral tabulations with their own measured spectra of the 1.9 and 1.4 micron

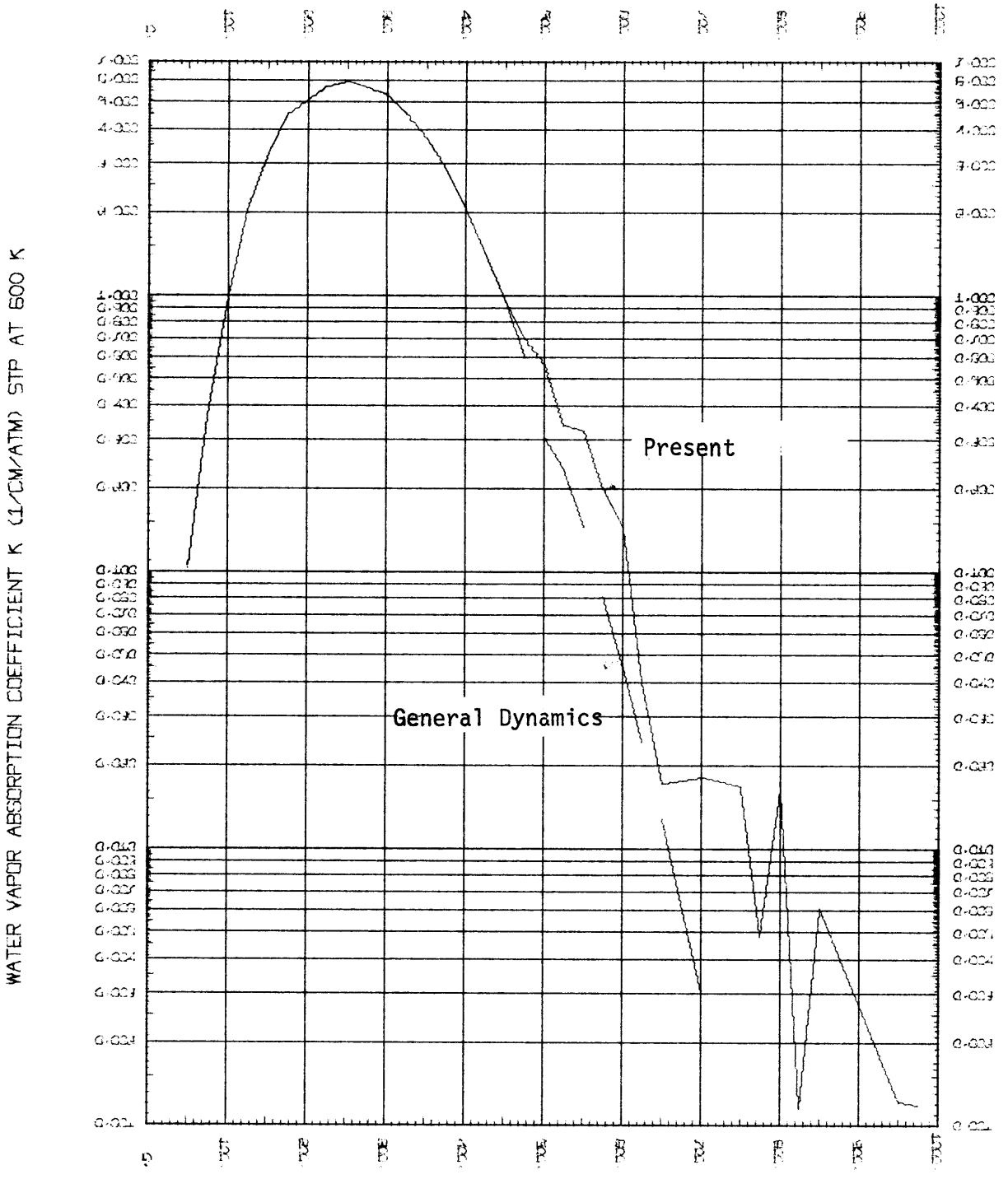

Figure 4.1.3.1-9

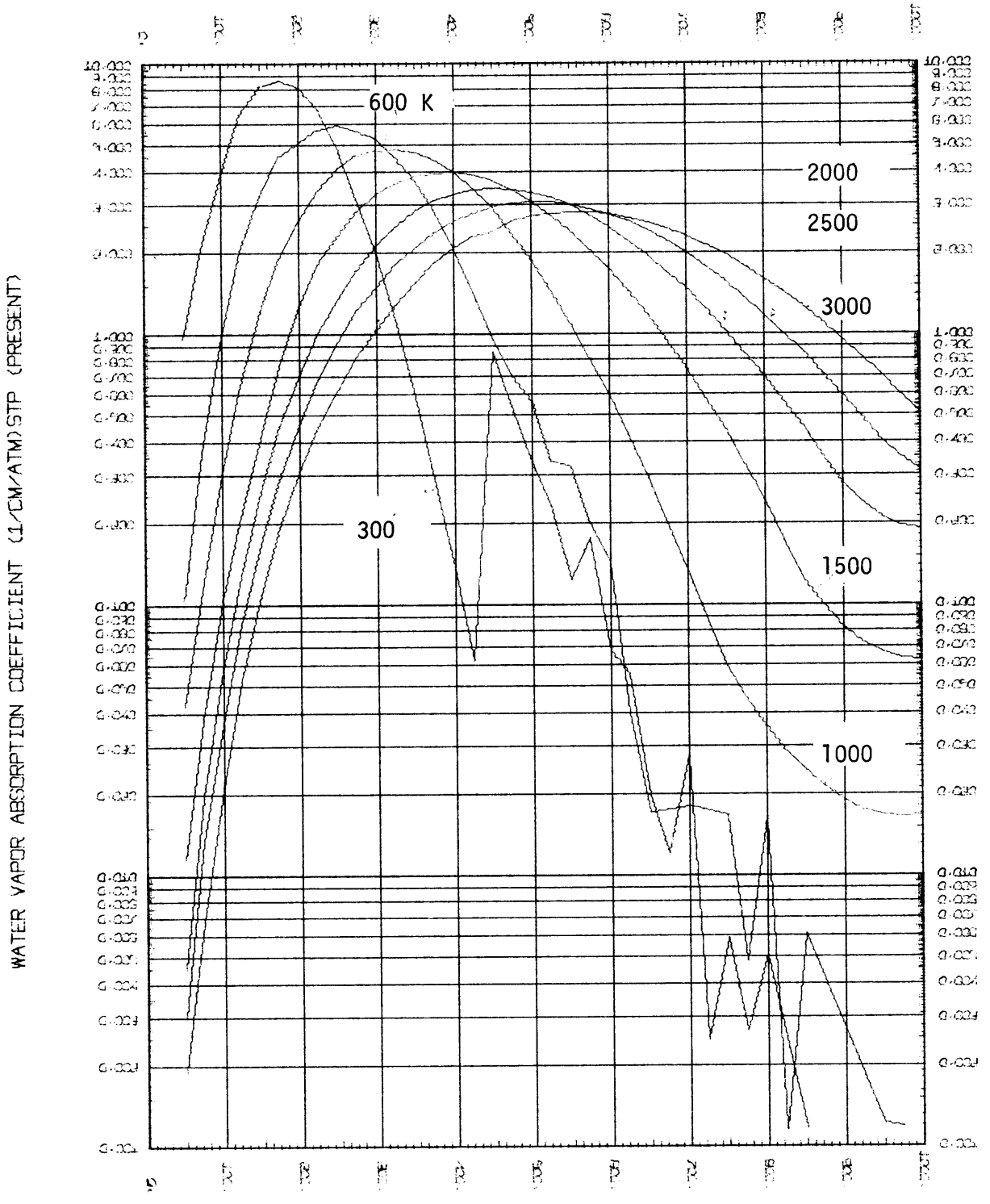

Figure 4.1.3.1-10

bands at 2200 K and 0.3 cm. atm. at STP, and with Burch and Gryvnak (1962) spectrum of the 2.7 micron band at 1200 K, 1.76 cm. atm., $p_w = P_t = 1$ atm. In general, the uncertainties were within ± 20 percent in spectral regions where k varies slowly while in rapidly varying portions of the spectrum the uncertainties were higher. The General Dynamics tabulations for the spectrum region from 1200 cm^{-1} to 9300 cm^{-1} and temperatures of 300, 600, 1000, 1500, 2000, 2500 and 3000 K were considered adequate and complete and are used in the present work.

In calculating spectral and total emissivities at temperatures other than the above seven temperatures at which the absorption coefficients and the inverse line spacings are listed, it was necessary to define an interpolating technique. Earlier computations carried by the author indicated the unsuitability of polynomial least square fitting. The technique used here is a first order Lagrange interpolation of the log of the absorption coefficient or the inverse line spacing versus the log of the absolute temperature.

4.2 Carbon Dioxide

4.2.1. Introduction

Carbon dioxide is present in appreciable amounts in almost all flames. It radiates its characteristic spectrum along with other gases formed during combustion. Numerous measurements of the spectral and total carbon dioxide have been done in addition to some theoretical work. The measurements show the total emissivity depends on the gas temperature, partial pressure, the path length and the broadening ability of various species though with less effect than the case of water vapor. Only a few of pertinent investigations will be reviewed here.

4.2.2. Total Emissivity Measurements

4.2.2.1. Rubens and Ladenburg

Rubens and Ladenburg (1905) measured the monochromatic absorptivity at room temperature of carbon dioxide layers of various thicknesses and concentration in the spectral range 12 to 18 micron. They also made direct measurement of total absorptivity of pure carbon dioxide at one atmosphere and path lengths from 1 to 400 cm. Their data points are plotted in Figure 4.2.2.1-1. The data points of Hertz (1911) are shown on the same figure. Hertz measured the long wave length absorption spectrum of carbon dioxide, which is of importance at atmospheric conditions.

4.2.2.2. Hottel and Mangelsdorf

Mangelsdorf (1935) under the supervision of Hottel at M.I.T. used a furnace of path length of 51.2 cm. The partial pressure range was 0.002 to 1.00 atm. with a gas temperature range of 294 to 1320 K and a background temperature range of 90 to 1633 K. He defined the path length

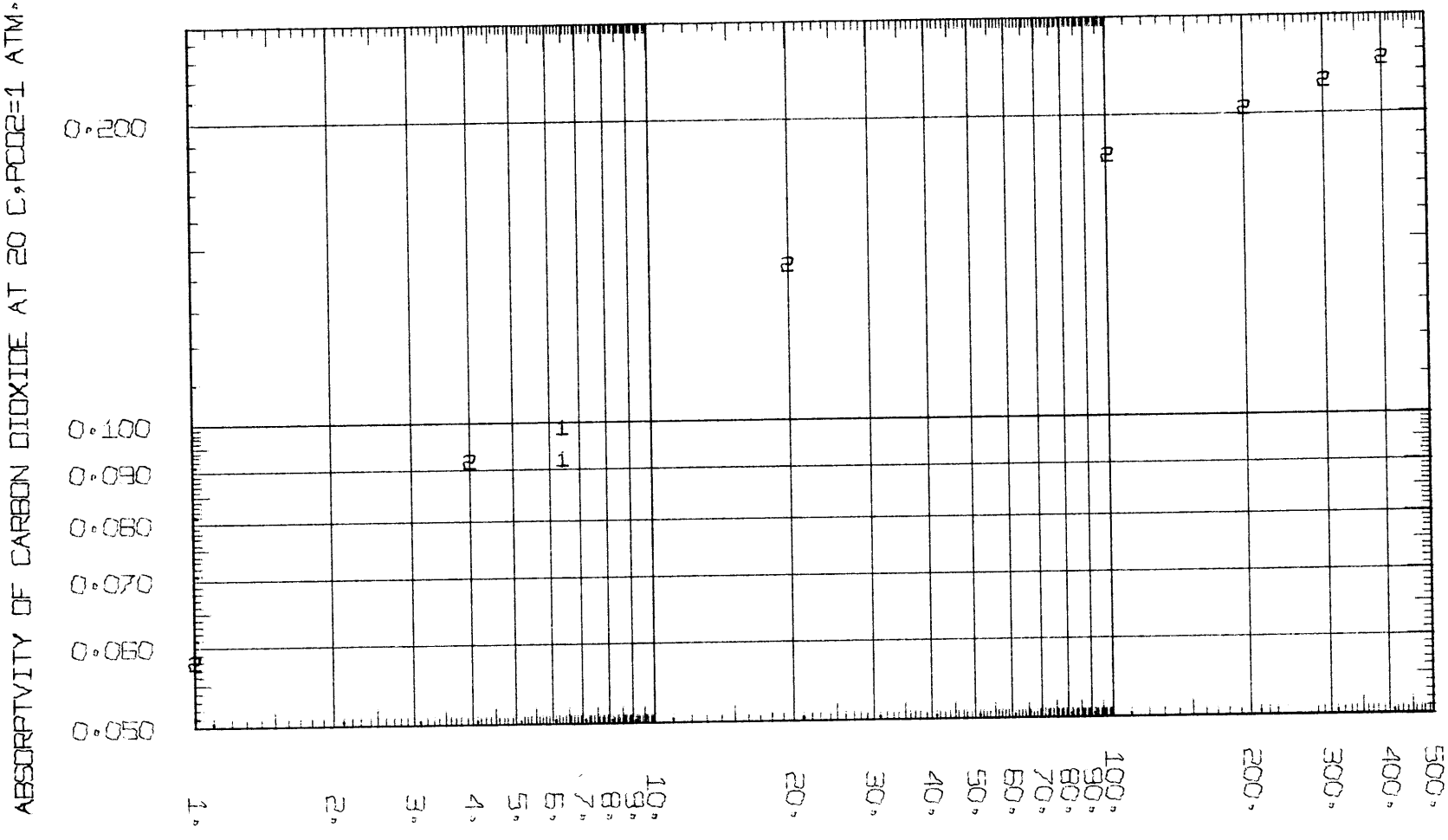

Figure 4.2.2.1-1

by a concentration traverse and used hot, dry, carbon dioxide free air as a windowless boundary to confine the radiating gas. The gas temperature was uniform to ±2 F. Some of his measurements might have suffered from atmospheric absorption. The experimental results are shown in Figure 4.2.2.2-1. The emissivities reported at 2480 F are not data points from direct measurements but are values obtained by extrapolations from absorption measurements of radiation from black body at 2480 F. Some of the data points of Rubens and Ladenburg at 70 F are also plotted.

4.2.2.3. Hottel and Smith

Smith (1935) measured the emission from combustion products of premixed flames of carbon monoxide and oxygen, and of carbon monoxide and air at a pressure of 1 atm. His temperatures, which were measured by sodium - D line reversal method, ranged from 1682 to 2355 K and the path length range was 19.5 to 40 cm. His background temperature was 294 ± 2 K.

4.2.2.4. Eckert

Eckert (1937) measured the emission of mixtures of carbon dioxide and nitrogen at a total pressure of 1 atm and path length of 10.2 cm for gas temperatures of 678 to 1533 K, 65.2 cm for 373 to 673 K and 295.6 cm at 373 K and a background temperature of 297 K. He allowed room air containing water vapor and carbon dioxide partially heated by the apparatus to form the boundary confining the radiating gas introducing the possibility of atmospheric absorption. His results are shown in Figure 4.2.2.4-1.

Hottel's (1954) recommended total emissivity chart for carbon dioxide was based on the above data. Some of the measurements, however, possibly suffered from atmospheric absorption, with the exception of the

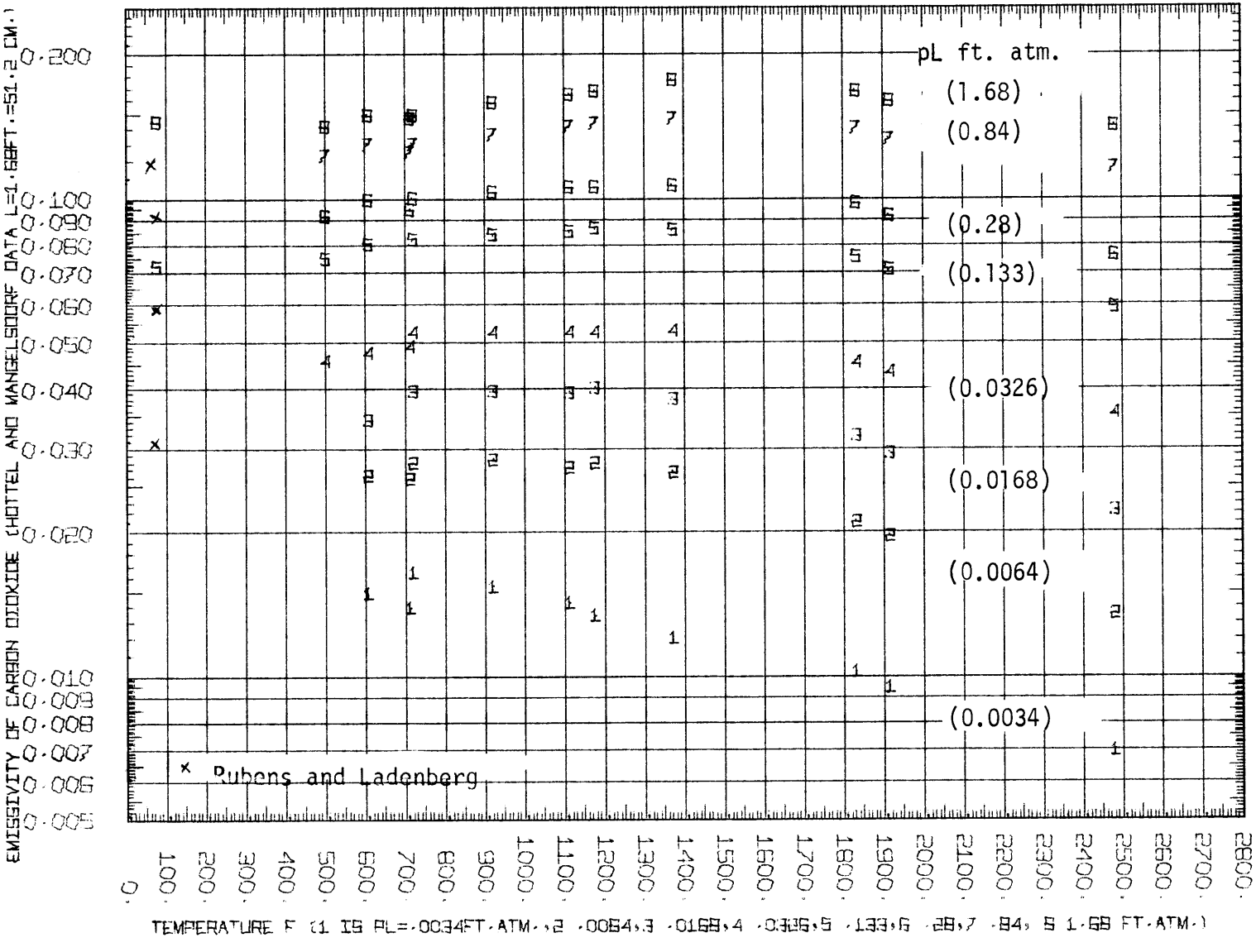

Figure 4.2.2.2-1

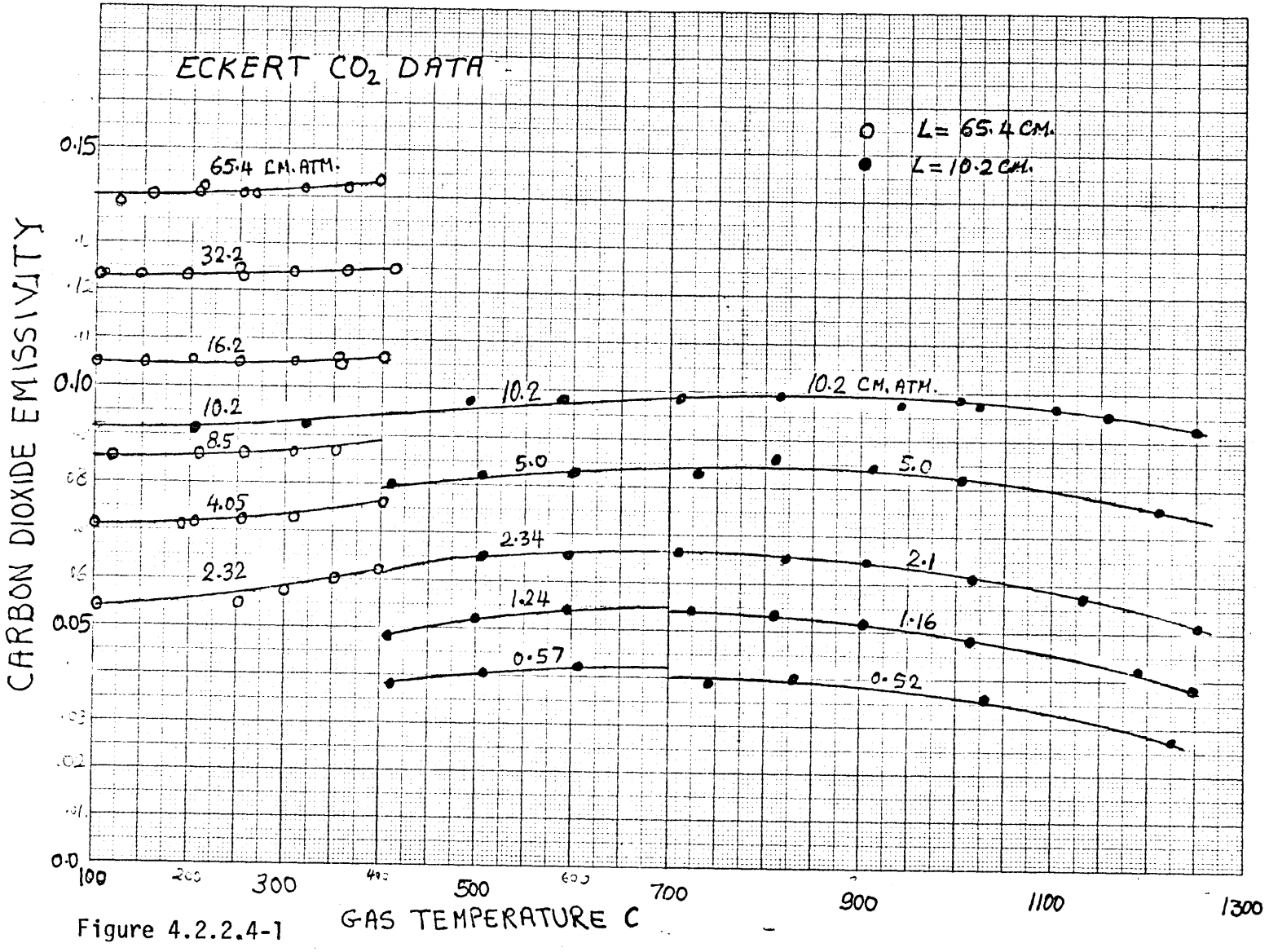

Figure 4.2.2.4-1

data of Hottel and Smith (1935) which was obtained in a system continously flushed with carbon-dioxide-free water-vapor-free air. According to Hottel it was later decided that some carbon dioxide or water vapor absorption might have occured in the short open coupling between the flushed radiometer and the flushed burner end.

4.2.2.5. Akhunov et al.

Akhunov, Panfilovich and Usmanov (1972) working in U.S.S.R. measured the emissivity of carbon dioxide at 673 - 1070 K and 1 - 21 atmospheres total pressure for layer thicknesses of 10, 16 and 26.5 cm. They used a thick-walled stainless steel tube as a working chamber in which air or carbon dioxide was heated to the required temperature. The carbon dioxide was confined, and the length was defined by the flow of carbon dioxide-free moisture-free air with equal and opposite momentum. The pressure was regulated by valves at the gas exit. The mole fraction of carbon dioxide was measured by sampling the gas by means of a moveable capillary along the axis of the chamber. The gas temperature was measured with a movable screened chromel-aluma thermocouple. They were successful in obtaining a sharp boundary and a fairly uniform gas temperature with a slight drop near the gas exit point. They estimated the error in their experiments to be between 4.5 to 7.5%. Comparisons of three of their data points at 673 K, P = 1.02 atm., L = 10, 16 and 26.5, or pL = 10.2, 16.32 and 27.03 cm atm with Hottel and Mangelsdorf (1935) shows a maximum deviation of 4%. Their data is shown in Table 4.2.2.5-1.

TABLE 4.2.2.5-1

CO_2 Data of Akhunov et. al. (1972)

P_t atm.	L cm.	p_cL cm. atm.	T K	EXP. EMIS.	PRESENT C_F	CORR. EMIS
1.02	10.0	10.20	673.	0.100	1.0089	0.0991
1.02	10.0	10.20	725.	0.100	1.0082	0.0991
1.02	10.0	10.20	770.	0.103	1.0078	0.1022
1.02	10.0	10.20	821.	0.105	1.0073	0.1042
1.02	10.0	10.20	870.	0.105	1.0069	0.1042
1.02	10.0	10.20	923.	0.108	1.0064	0.1073
1.02	10.0	10.20	975.	0.110	1.0061	0.1093
1.02	16.0	16.32	670.	0.111	1.0084	0.1100
1.02	16.0	16.32	725.	0.112	1.0080	0.1111
1.02	16.0	16.32	770.	0.112	1.0077	0.1111
1.02	16.0	16.32	821.	0.117	1.0074	0.1161
1.02	16.0	16.32	870.	0.119	1.0072	0.1181
1.02	16.0	16.32	923.	0.122	1.0069	0.1211
1.02	16.0	16.32	975.	0.122	1.0066	0.1212
1.02	16.0	16.32	1010.	0.122	1.0064	0.1212
1.02	16.0	16.32	1077.	0.122	1.0062	0.1212
1.02	26.5	27.03	673.	0.127	1.0077	0.1260
1.02	26.5	27.03	726.	0.128	1.0075	0.1270
1.02	26.5	27.03	771.	0.128	1.0074	0.1270
1.02	26.5	27.03	820.	0.130	1.0073	0.1290
1.02	26.5	27.03	871.	0.134	1.0072	0.1330
1.02	26.5	27.03	923.	0.138	1.0071	0.1370
1.02	26.5	27.03	970.	0.139	1.0070	0.1380
2.04	10.0	20.40	670.	0.128	1.0227	0.1251
2.04	10.0	20.40	725.	0.128	1.0218	0.1252
2.04	10.0	20.40	770.	0.131	1.0215	0.1282
2.04	10.0	20.40	821.	0.134	1.0207	0.1312
2.04	10.0	20.40	870.	0.136	1.0202	0.1333
2.04	10.0	20.40	923.	0.138	1.0196	0.1353
2.04	10.0	20.40	975.	0.138	1.0191	0.1354
2.04	16.0	32.64	670.	0.139	1.0208	0.1361
2.04	16.0	32.64	725.	0.140	1.0203	0.1372
2.04	16.0	32.64	770.	0.143	1.0201	0.1401
2.04	16.0	32.64	821.	0.143	1.0200	0.1401
2.04	16.0	32.64	870.	0.147	1.0199	0.1441
2.04	16.0	32.64	923.	0.150	1.0199	0.1470
2.04	16.0	32.64	975.	0.150	1.0200	0.1470
2.04	16.0	32.64	1010.	0.149	1.0201	0.1460
2.04	16.0	32.64	1077.	0.147	1.0205	0.1440
2.04	26.5	54.06	673.	0.155	1.0186	0.1521
2.04	26.5	54.06	726.	0.156	1.0182	0.1532
2.04	26.5	54.06	771.	0.156	1.0182	0.1532
2.04	26.5	54.06	820.	0.160	1.0185	0.1570
2.04	26.5	54.06	871.	0.162	1.0190	0.1589
2.04	26.5	54.06	923.	0.164	1.0197	0.1608
2.04	26.5	54.06	970.	0.165	1.0205	0.1616

TABLE 4.2.2.5-1 (continued)

P_t atm.	L cm.	p_cL cm. atm.	T K	EXP. EMIS	Present C_F	Corr. EMIS
6.12	10.0	61.20	670.	0.164	1.0263	0.1597
6.12	10.0	61.20	721.	0.166	1.0266	0.1616
6.12	10.0	61.20	772.	0.167	1.0266	0.1626
6.12	10.0	61.20	820.	0.168	1.0276	0.1634
6.12	10.0	61.20	873.	0.170	1.0291	0.1651
6.12	10.0	61.20	921.	0.171	1.0308	0.1658
6.12	10.0	61.20	973.	0.172	1.0330	0.1665
6.12	16.0	97.92	670.	0.175	1.0253	0.1706
6.12	16.0	97.92	721.	0.182	1.0252	0.1775
6.12	16.0	97.92	772.	0.182	1.0262	0.1773
6.12	16.0	97.92	820.	0.183	1.0280	0.1780
6.12	16.0	97.92	873.	0.184	1.0300	0.1786
6.12	16.0	97.92	921.	0.187	1.0339	0.1808
6.12	16.0	97.92	973.	0.188	1.0378	0.1811
6.12	16.0	97.92	1010.	0.189	1.0409	0.1815
6.12	16.0	97.92	1077.	0.188	1.0469	0.1795
6.12	26.5	162.20	666.	0.194	1.0265	0.1889
6.12	26.5	162.20	721.	0.198	1.0270	0.1927
6.12	26.5	162.20	768.	0.198	1.0296	0.1923
6.12	26.5	162.20	821.	0.200	1.0333	0.1935
6.12	26.5	162.20	870.	0.201	1.0380	0.1936
6.12	26.5	162.20	920.	0.202	1.0436	0.1935
6.12	26.5	162.20	971.	0.203	1.0275	0.1975
11.22	10.0	112.20	670.	0.188	1.0277	0.1829
11.22	10.0	112.20	723.	0.194	1.0291	0.1885
11.22	10.0	112.20	771.	0.195	1.0317	0.1890
11.22	10.0	112.20	820.	0.198	1.0353	0.1912
11.22	10.0	112.20	870.	0.198	1.0400	0.1903
11.22	10.0	112.20	922.	0.201	1.0448	0.1923
11.22	10.0	112.20	971.	0.201	1.0292	0.1952
11.22	16.0	179.50	670.	0.212	1.0289	0.2060
11.22	16.0	179.50	723.	0.216	1.0306	0.2095
11.22	16.0	179.50	771.	0.218	1.0338	0.2108
11.22	16.0	179.50	820.	0.218	1.0386	0.2098
11.22	16.0	179.50	870.	0.220	1.0386	0.2118
11.22	16.0	179.50	922.	0.224	1.0447	0.2144
11.22	16.0	179.50	971.	0.224	1.0516	0.2130
11.22	26.5	297.33	666.	0.225	1.0336	0.2176
11.22	26.5	297.33	723.	0.227	1.0317	0.2200
11.22	26.5	297.33	771.	0.230	1.0327	0.2227
11.22	26.5	297.33	826.	0.230	1.0363	0.2219
11.22	26.5	297.33	871.	0.233	1.0409	0.2238
11.22	26.5	297.33	920.	0.235	1.0478	0.2242
11.22	26.5	297.33	958.	0.236	1.0539	0.2239
21.42	16.0	342.70	670.	0.241	1.0360	0.2326
21.42	16.0	342.70	725.	0.244	1.0335	0.2360
21.42	16.0	342.70	770.	0.246	1.0348	0.2377

4.2.3. Spectral Data

Detailed line-by-line calculations are possible for carbon dioxide at low temperatures. As temperature increases the line density increases rapidly leading to the use of band models. The approximate calculations of Plass (1958, 1959) showed that the number of spectral lines with intensities greater than 10^{-7} of the intensity of the strongest line in the 4.3 micron band of carbon dioxide increased from 1400 to 300 K to 81000 at 1200 K and to 890000 at 2400 K. Considerable work has been done to give the necessary spectral constants and/or the integrated band intensities of carbon dioxide. Radiation from carbon dioxide is mainly from three strong bands 15, 4.3, and 2.7 microns. At high temperatures and high pL's the spectrum of the 4.3, 15 and 2.7 bands gets saturated and the weaker bands at 10., 9., 4.9 and 2 microns contributions become noticeable. The present calculation indicates that 20% of the total radiation from carbon dioxide at 1600 K and pL of 1000 cm. atm. is from the 2. micron bands. It is, therefore, important to include all possible information of all bands. Spectral absorption data for carbon dioxide were obtained as early as (1927) by Fues. A limited number of data for the 4.3 and 2.7 micron bands were obtained by Tingwalt (1934, 1938). Extensive band absorption data were obtained and/or published by Breeze et al. (1963, 1964, 1965), Burch et al. (1962, 1964), Edwards (1960, 1963), Flornes (1962), Ludwig et. al. (1965, 1966, 1967, 1968), Malkmus et al. (1962, 1963, 1967), Nelson (1959), Nicolet (1962), Rasool (1964), Stull et al. (1964), Thorndike (1947), Tien (1967), Tourin (1961), Varanasi and Lauer (1966), Weber et al (1951, 1959), Wolk (1967) and Yamamoto and Sasamori (1958). A summary of the

published values including recommended value in theoretical papers of integrated band intensities in (cm^{-2} atm^{-1}) normalized to STP at 300 K for the 2, 2.7, 4.3, 10 and 15 micron bands of carbon dioxide is given in Table 4.2.3-1. The total integrated intensity of a fundamental band, e.g. 15 and 4.3 micron bands of carbon dioxide, is independent of temperature while the integrated intensity of an overtone or combination band systems increase with increasing temperature [Breeze et al. (1965)]. Figure 4.2.3-1 shows the variation of the ratio ϕ, as defined as

$$\phi = \frac{\alpha(T)}{\alpha(T_0)}\frac{T}{T_0} = \frac{\alpha(T)_{STP}}{\alpha(T_0)_{STP}} ,$$

with temperature for the 4.3, 2.7 and 2 micron bands of carbon dioxide according to Breeze et al. (1965). The variation of ϕ for the same bands according to Edwards and Balakrishnan (1973) and as computed in the present work is also shown. The different recommendations for the temperature dependence are in good agreement. The data points above 1000 K were obtained by Ferriso (1962) and Ferriso and Ludwig (1964) from measurements in rocket burners and by Breeze and Ferriso (1963, 1964) and Patch (1964) from measurements made in shock tubes. The agreement in general is good. The temperature dependence of the 10 micron band system of carbon dioxide was studied and an expression for the variation of the total band intensity with temperature was given by Malkmus, Ludwig, and Ferriso (1966). The variation of α_{STP} according to their expression and as computed in the present work is shown in Figure 4.2.3-2 together with the data of different investigations.

A theoretical model for the spectral constants in the 4.3 micron band was developed by Malkmus (1963). In calculating the s/d and 1/d

EFFECT OF TEMPERATURE ON THE BAND INTENSITIES OF THE 1.9 μ, 2.7 μ AND 4.3 μ BANDS OF CO_2

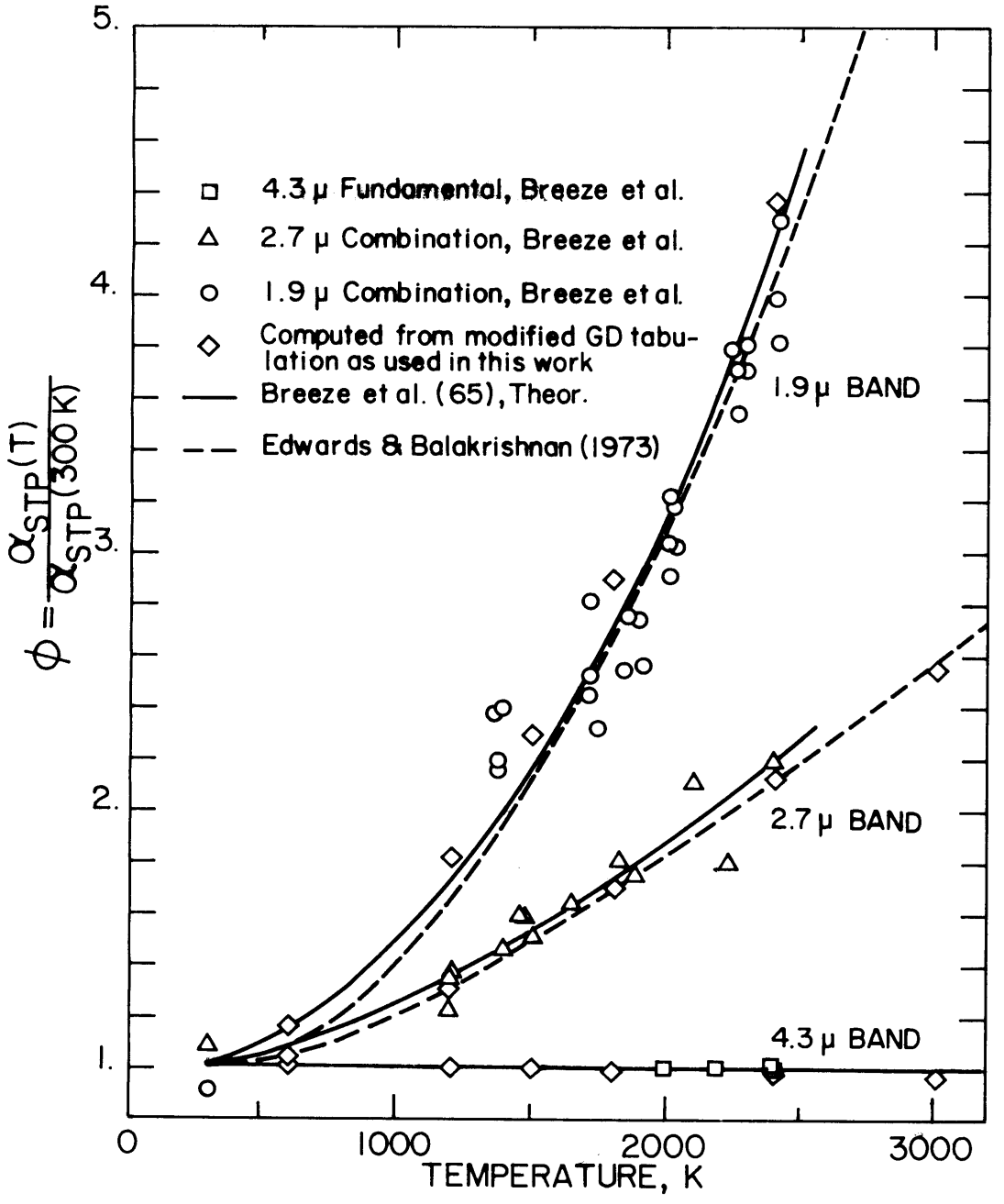

Figure 4.2.3-1

TABLE 4.2.3-1

Integrated Band Intensities of the 2, 2.7, 4.3, 10 and 15 Micron Bands of Carbon Dioxide (cm^{-2} atm^{-1} at STP at 300 K)

SOURCE	α^0 2μ	α^0 2.7μ	α^0 4.3μ	α^0 10μ	α^0 15μ
Edwards and Balakrishnan (1973)	1.30	78	2160	.0663	373
Burch et. al. (1962)				.0695 ± .016	362 ± 90
Ludwig et. al. (1966)					240 ± 36
Eggers and Crawford (1951)		66.4	2693		161 ± 20
Burch et. al. (1962)		91 ± 18	2500 ± 400		330 ± 90
Fahrenfort (1963)		80	2640, 2500		161, 220
Kaplan and Eggers (1956)					240
Fues (1927)					179
Howard and Patty (1958)					240 ± 20
Varanasi and Lauer (1966)					220 ± 10
Wolk (1967)					246
Madden (1961)					255 ± 10
Thorndike (1947)					187
Schurin (1960)			2970 ± 60		240 ± 5
Ludwig et. al. (1973)	1.6	67.	2700		240
Ferriso et. al. (1965)		67.	2970		
Benedict and Plyler (1954)			2706		
Plyler et. al. (1962)		77.8	2943		
Weber et. al. (1951)			2700		172
Martin and Barker (1932)					220 ± 22
Overend et. al. (1959)					240 ± 5
Weber (1959)				.058	
McCubbin (1966)				.043	
Malkmus et. al. (1966)				.05 ± 50%	
Kostowski (1954)				.0528 ± .0045	
Edwards (1960)				.0415 ± 40%	
Breeze et. al. (1963, 1964)	2.0				
Calfee and Benedict (1966)	1.57				

TABLE 4.2.3-1 (cont'd)

SOURCE	α^0 2μ	α^0 2.7μ	α^0 4.3μ	α^0 10μ	α^0 15μ
Burch et. al. (1964)	1.61				
Yamamoto and Sasamori (1958)					212
Penner (1959)		71.3			
Ben Arych (1967)			2700		
Oppenheim et. al. (1963)			2580		
Kunitomo et. al. (1974)			2660		
Echigo et. al. (1967)	20	30	20		28

values from his model Malkmus used the value of 2700 cm^{-2} atm^{-1} for the total band intensity obtained by Benedict and Plyler (1954) and a value of 0.064 cm^{-1} for the average line width of 300 K and 1 atm. derived from the study of Kaplan and Eggers (1956). The computed emissivities obtained by Malkmus were verified experimentally by Ferriso, Ludwig, and Acton (1966) between 2650 and 3000 K using path lengths of 1.67 and 2.34 cm. and within a wave number range of 1800 to 2450 cm^{-1}. Malkmus (1964) also developed a theoretical model for the spectral constants in the 2.7 micron band. He used Penner's (1959) value of 71.3 cm^{-2} atm^{-1} STP for the total band intensity at 300 K and Kaplan and Eggers (1956) values of 0.064 cm^{-1} for the average line half-width at 300 K and 1 atm with a $T^{-1/2}$ variation. The spectral emissivities calculated using the S/d and 1/d values from his model were in good agreement with Tourin's (1961) measurement at 1273 K, P_{CO_2} = .921, and L = 12.7 cm and with Burch, Gryvnak and Williams (1962) data at temperatures of 1200 and 1500 K, P_{CO_2} of 0.997 and 2. atm. and a path length of 7.75 cm. Ludwig, Ferriso and Acton (1966) measured the spectral emissivity of the 15 micron band of carbon dioxide in the temperature range 1000 to 2300 K. They calculated the absorption coefficient, s/d in the interval 500 to 880 cm^{-1}. The results of the calculation for the three bands were published in the form of tables by the Space Science Laboratory (1966, 1967), and by Ludwig et al. (1966, 1968, and 1973). The tabulation included the absorption coefficient k (cm^{-1} atm^{-1} STP) for the 15 micron band from w = 500 to w = 880 cm^{-1} with a step of 5 cm^{-1} at temperatures 300, 600, 1200, 1500, 1800, and 2400 K, the absorption coefficient for the 4.3 micron band (cm^{-1} atm^{-1} STP) from 1900 to 2150 cm^{-1} with a step of 10 cm^{-1} at 300,

600, 1200, 1500, 1800, 2400, and 3000 K. The absorption coefficients (cm^{-1} atm^{-1} STP) for the 2.7 micron band were listed at the same seven temperatures from 3000 to 3560 cm^{-1} with a step of 10 cm^{-1} and from 3565 to 3770 cm^{-1} with a step of 5 cm^{-1}. The fine structure parameter 1/d in cm was tabluated for the 4.3 micron band from 2000 to 2390 cm^{-1} with a step of 10 cm^{-1} at the same seven temperatures. The 1/d values listed for the 2.7 micron band were from 3080 to 3770 cm^{-1} with a step of 10 cm^{-1} at temperatures of 300, 600, 1200, 1500, and 1800 K only. No 1/d values were given for the 15 micron band. No absorption coefficient or 1/d values were listed for either the 10 micron or the 2 micron band systems. For the purpose of calculating total carbon dioxide emissivities in the present work it was necessary to use the spectral data measured by Edwards (1960, 1963), Edwards and Menard (1964), Nicolet (1963), Calfee and Benedict (1966) and Edwards and Balakrishman (1973) to fill the gaps. Edwards and Nicolet measured the spectral parameters of carbon dioxide gas in nitrogen at total pressures from 0.5 to 10 atm., temperatures from 294 to 1390 K (530 to 2500 R), mole fractions from 0.05 to 1. and pL's from 0.0004 to 5 lb/ft/ft which is approximately 0.1 to 1250 cm. atm. at STP covering a wave number range of 470 to 6180 cm-^{1}. Their integrated band intensities for the 10μ band at 300 K is included in Table 4.2.3-1 and in Figure 4.2.3-2. Using their band absorption correlations the author estimated integrated band intensities of .004, .025 and .027 cm^{-2} atm^{-1} STP at 294 K for the 7.5, 1.6 and 1.4 weak micron bands respectively. Data on the temperature dependence of the weak bands is very limited. Comparison of the above band intensities of the weak 10 and 2μ at temperature of 600 K and above, which have

numerical values above 1 cm^{-2} atm^{-1}STP show that the 7.5, 1.6, and 1.4 micron bands are very weak and their neglect is quite justifyable.

Edwards (1963) spectral data were presented in the form of k, the absorption coefficient which Edwards termed C^2, in ft^2/lb and $4b_{CO_2}/d$ (dimensionless). His k values were converted into cm^{-1} atm^{-1} by multiplying each value by 1.976/T where T is in R, or 1.976/492 to get it as cm^{-1} atm^{-1} STP. Using $b_{CO_2} = 0.07\sqrt{273/T}$ where T is in K it was possible to compute 1/d values from Edwards listings. His 2 micron band spectral data covered a spectrum range of 4800 to 5700 cm^{-1} and were very scattered when plotted as a function of the temperature for the selected wave numbers as a parameter or when cross plotted. The absorption coefficients were smoothed in both directions in the present study and then integrated to check the band intensity values. In the absence of better data for the 2 micron band, Edwards smoothed data were included in the calculation of the carbon dioxide total emissivity and absorptivity. His data for the 10 micron band were similarly treated, checked for total intensity and included in the model of the present work.

The tabluations of Malkmus et al. (1973) for the 15 micron band assigned zero values to the absorption coefficient at 1200 K between 500 and 520 cm^{-1} and from 835 to 880 cm^{-1} , and at 600 K in the range 500 - 565 cm^{-1} and from 795 to 880 cm^{-1} , and at 300 K in the range 500 - 580 and 775 to 880 cm^{-1}. Although the zeros were in the wings of the fifteen micron band, which contribute a small fraction of the total emission, they nevertheless led to some undesirable flat spots in the curves of calculated emissivity versus temperature of the 15 micron band.

The absorption coefficients, and the reciprocal of the mean line spacing 1/d at temperatures other those tabulated were obtained using Lagrange Linear interpolation of ln s/d or ln 1/d and ln T. For purposes of the program the zero values were assumed to be about 10^{-18} ($\ln 10^{-18} \simeq -40$). Clearly the interpolated value between a zero and a nonzero absorption coefficient, using logarthmic interpolation, depends on what value the zero is given. By plotting the absorption coefficients versus the absolute temperature this arbitrary value assigned to zero could be replaced with more realistic value. For example, for wave numbers of 585 and 580 cm^{-1} the curves were nearly parellel between 600 and 3000 K. There is no reason why they could not show the same trend below 600 K, yet a k of 0.0157 cm^{-1} atm^{-1} STP is given by Ludwig et al. for w = 585 cm^{-1} at 300 K while a zero is given for k at w = 580 cm^{-1}. The curve of w = 580 was extrapolated from 600 K to be with an approximately similar curvature as the one for w = 585 cm^{-1}. The extrapolated k value at 300 K for w = 580 cm^{-1} was 0.00895 cm^{-1} atm^{-1} STP. The technique of extrapolation with similar curvature was used to replace all the zeros by numerical values. This resulted in a smooth total emissivity curve for the 15 micron band. It was necessary to check the effect of this extrapolation on the total band intensity values before incorporating the new values as part of the present model. The new values had no noticeable effect on the total band intensity which was 239 at 300, 232 at 600, 240 at 1200, 246 at 1500, 242 at 1800 K and 260 cm^{-2} atm^{-1}(STP) at 2400 K. The extrapolated values were incorporated into the model to replace the zero values.

The listed absorption coefficients for the 4.3 micron band also

had some zero values. At 2400 K zeros were given in the range 1900 - 1980 cm^{-1}, at 1800 K from 1900 to 2080 cm^{-1}, at 1500 K from 1900 - 1980 cm^{-1}, at 1200 K from 1900 to 2130 cm^{-1}, at 600 K from 1900 to 2190 cm^{-1} and at 300 K from 1900 to 2240 cm^{-1}. The same technique of extrapolation based on an assumed similarity of curvature at the different wave numbers was utilized to replace the zero values. The listed k for the 2.7 micron band had zero at 2400 K from 3000 to 3080 cm^{-1}, from 3000 to 3150 cm^{-1} at 1800 K and 1500 K, from 3000 to 3100 cm^{-1} at 1200, from 3000 to 3200 cm^{-1} at 600 K and from 3000 to 3280 cm^{-1} at 300 K. The same techniques were used to replace all the zero k values. The calculated integrated band intensities using the corrected non zero absorption coefficients are plotted in Figure 4.2.3-1. Clearly, they are in very good agreement with Breeze et al. (1965) theoretical model and with Edwards and Balakrishnan (1973) model values. The integrated band intensities of the 4.3 micron spectral k's used in the present work are also plotted. The agreement is very good with both experimental and theoretical calculations of Breeze et al. The ϕ values for Edwards and Balakrishnan for the 4.3 micron band are the same as Breeze, i.e. $\phi = 1$ for all temperatures.

There were no 1/d values given for the 15 micron band. In the abscence of any data the 1/d values given at w = 2000 cm^{-1} and temperatures of 300, 600, 1200, 1500, and 1800 K were used. At 300 K the 1/d value was a constant equal to 2.553 cm^{-1} for wave numbers from 2270 to 2000 cm^{-1}. The 1/d value of 14.49 cm^{-1} at 600 K was constant from 2200 cm^{-1} to 2000. At 1200 K the 1/d value was 184.4 cm^{-1} and was constant from 2140 to 2080 cm^{-1}. At 1500 K 1/d was constant equal to 400.8 cm^{-1} for a wave number range of 2140 to 2000 cm^{-1}. At 1800 K the 1/d was

872.7 cm^{-1} for w = 2090 to 200 cm^{-1}. This justifies the use of the values of 2.593, 14.49, 184.4, 400.8 and 872.7 cm^{-1} for the 1/d values for all wave numbers less than 2000 cm^{-1} at temperatures of 300, 600, 1200, 1500, and 1800 K respectively. The 1/d values are of secondary importance in the calculation of total emissivity. The 1/d values affect the broadening correction factor, which is known to be much closer to unity than the corresponding values for water vapor. Therefore, errors introduces by casual treatment of the 1/d should not be significant. From the value 1/d = 14.49 cm^{-1} at 600 K it is evident that the line structure is so dense that an error in 1/d at 600 K and above should have a negligible influence on the total emissivity calculations.

The total band intensities of the k values used in the present work for the 10.4 micron band are shown in Figure 4.2.3-2. They are in good agreement with the theoretical model and data of Malkmus (1966) and with the data of nine other investigators. The band was assumed to extend from 900 cm^{-1} to 1150 cm^{-1}. As indicated earlier, the 1/d values were taken to be the same as the 4.3 micron band values at w = 2000 cm^{-1}. The total band intensities of the k values used in the present work and obtained from the smoothed data of Edwards are plotted in Figure 4.2.3-2. The agreement is very good with the theoretical model and data of Malkmus (1966) and with the data of nine other investigators. The band was assumed to extend from 900 cm^{-1} to 1150 cm^{-1}. As indicated earlier, the 1/d values were taken to be the same as the 4.3 micron band values at w = 2000 cm^{-1}. The total band intensities of the k values used in the present work and obtained from the smoothed data of Edwards are plotted in Figure 4.2.3-2. The agreement is very good with experimental points,

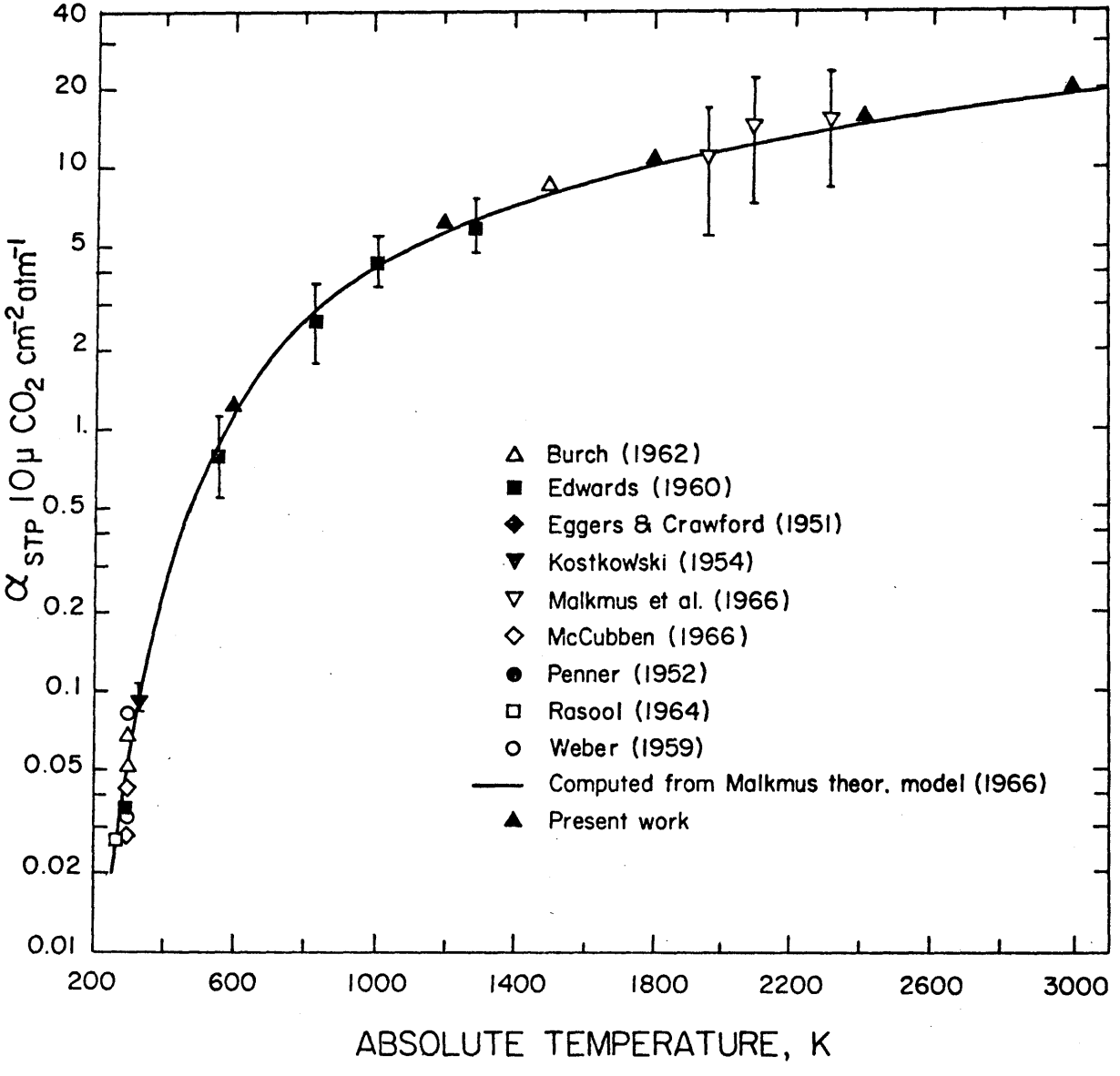
40
20
10
5
2
1.
0.5
0.2
0.1
0.05
0.02
0.01
α_{STP} 10μ CO_2 $cm^{-2}atm^{-1}$
200
600
1000
1400
1800
2200
2600
3000
ABSOLUTE TEMPERATURE, K
Burch (1962)
Edwards (1960)
Eggers & Crawford (1951)
Kostkowski (1954)
Malkmus et al. (1966)
McCubben (1966)
Penner (1952)
Rasool (1964)
Weber (1959)
Computed from Malkmus theor. model (1966)
Present work

Figure 4.2.3-2

TABLE 4.2.3-2

Integrated Band Intensities of Carbon Dioxide

Spectral Data Used in the Present Work

Temperature K	Band (in Microns)				
	15	10	4.3	2.7	2
300	239	0.0506	2952	77.8	1.47
600	233	1.262	2953	81.5	1.69
1200	240	6.365	2929	101.3	2.64
1500	246	11.13	2902	131.1	4.20
2400	262	15.93	2860	164.3	6.37
3000	262	20.5	2810	196.8	9.59

the theoretical models of Breeze et al. (1965) and of Edwards and Balakrishnan (1973). A tabulation of the band intensities of the spectral k used in the present work is shown in Table 4.2.3-2. The author believes that the spectral data of k and 1/d as selected in the present work give an adequate representation of the spectral properties of carbon dioxide.

Edwards and Balakrishnan (1973) developed what they termed as a "Universal" band absorption curve of growth which was a function of two dimensionless numbers that can be calculated either from physical constants or listed constants which were related to the type of the molecule under study. The use of this model is limited since it does not give spectral emissivities. In the present work their model was programmed separately for purposes of comparison.

4.2.4. Calculation of Band Contributions

The relative importance of each band can be estimated by assuming an average emiwsivity to each band. Consider the three strong bands of carbon dioxide: 15, 4.3, 2.7 micron bands. Assume the 15 micron band extends from 20 to 8.7 micron, the 4.3 micron band extends from 5 to 4 micron and the 2.7 extends from 3 to 2.5 micron. The total emissivity may be expressed as

$$\varepsilon = \int_0^{\infty} \varepsilon_w df_w = \int_{8.7\mu}^{20\mu} \varepsilon_w df + \int_{4\mu}^{5\mu} \varepsilon_w df + \int_{2.5\mu}^{3.0\mu} \varepsilon_w df$$

$$= \varepsilon_{15} (f_{20} - f_{8.7}) + \varepsilon_{4.3} (f_5 - f_4) + \varepsilon_{2.7} (f_3 - f_{2.5})$$

$$= \Delta f_{15}\varepsilon_{15} + \Delta f_{4.3}\varepsilon_{4.3} + \Delta f_{2.7}\varepsilon_{2.7}$$

Using table 5.1 of Hottel and Sarofim (1967) the required values of Δf

TABLE 4.2.4-1

Band Contribution Factors (Δf) in

Carbon Dioxide Emission

T K	Δf_{15}	$\Delta f_{4.3}$	$\Delta f_{2.7}$
400	.476	.0197	.0018
800	.169	.318	.0735
1200	.070	.130	.130
1600	.034	.087	.127
2000	.018	.058	.104

can be calculated at any desired temperature. Table 4.2.4-1 shows the result for temperatures of 400, 800, 1200, 1600, and 2000 K.

The present computations include the calculation of the contributions of each band to the gas emission. When those values are used with the Δf's listed in Table 4.2.4-1 it becomes possible to estimate an average emissivity of any band at specified temperatures.

4.3. Mixtures of Carbon Dioxide and Water Vapor.

4.3.1. Introduction

Mixtures of carbon dioxide and water vapor are very common in combustion products. Unfortunately, there is a limited number of measurements of the total emissivity or absorptivity from their mixtures. Clearly, the measurements depend on the gas temperature, partial pressure of each absorbing gas, the path length and the broadening ability of various species on each of the two absorbing gases. The number of experimental measurements of mixtures of carbon dioxide and water vapor is rather limited.

4.3.2. Mixture Measurements

4.3.2.1. Hottel and Mangelsdorf

The experiments of Hottel and Mangelsdorf (1935) have been discussed in the sections on water vapor and on carbon dioxide. Based on their measurements of total emissivity of each of the two gases and their mixtures, they presented data on the overlap correction $\Delta\varepsilon$ over a temperature range of 970 to 2360 R at two different pL's of 1.68 ft. atm. (51.2 cm. atm.) and 0.27 ft. atm. (8.23 cm. atm.) and $p_u/(p_w + p_c)$ ratios of 0.1, 0.5 and 0.9. Their data is shown in Figure 4.3.2.1-1. The data exhibits significant scatter and were considered by Hottel to be

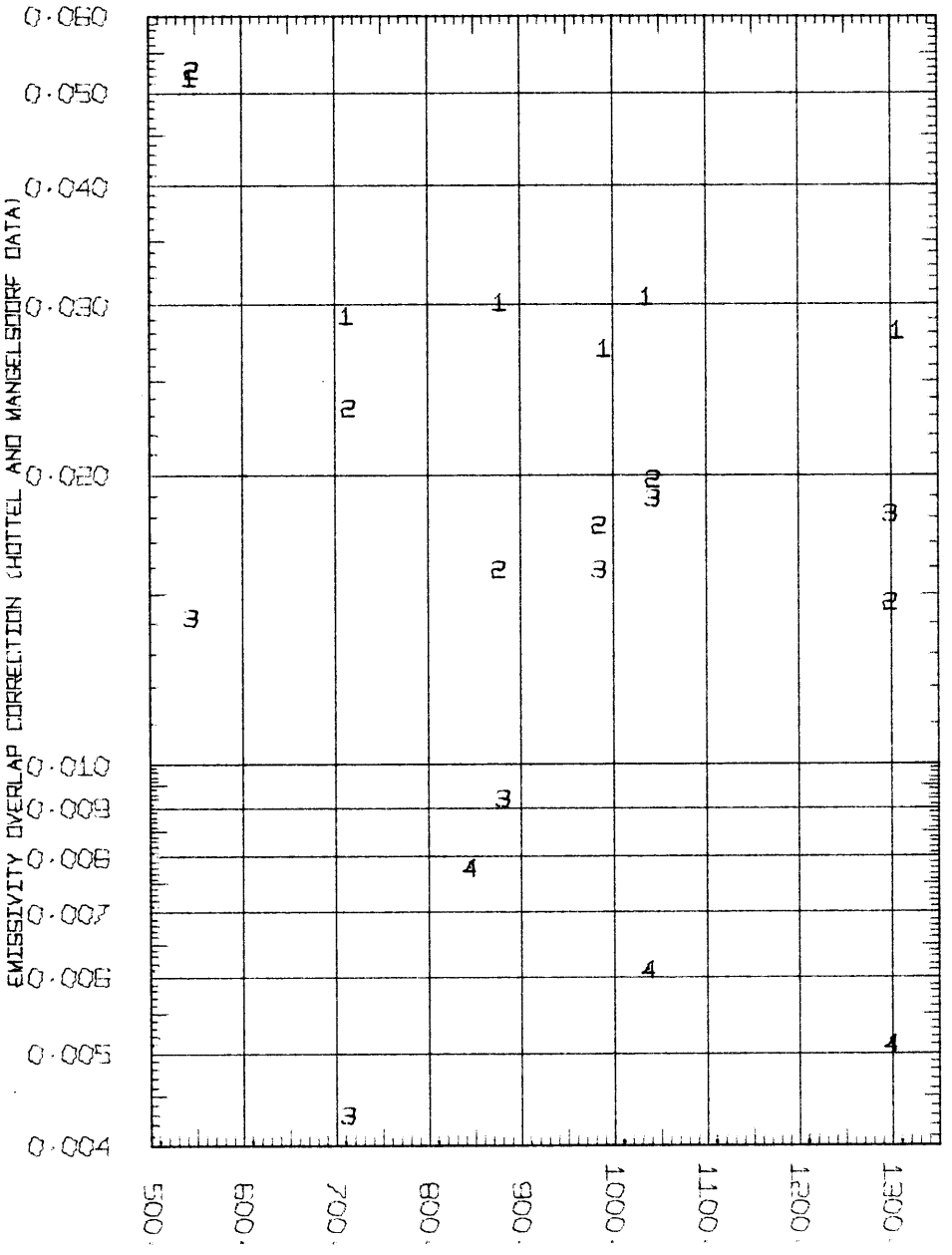

Figure 4.3.2.1-1

a temporary measure of the overlap correction.

4.3.2.2. Eberhardt

Eberhardt (1936) under the supervision of Hottel measured the heat radiation in steel reheating furnaces. His experiments were discussed in earlier sections. His data using a furnace length of 14 ft. (426.7 cm) and a ratio of p_w/p_c = 1.58 covered a temperature range of 1670 to 2380 F and pL's of 2.5 to 4.1 ft. atm. The data are shown in Figure 4.3.2.2.-1. His data shows significant scatter. Possible sources of errors in his experiments have been discussed in a previous section.

4.3.2.3. Millard

Millard (1935) working at M.I.T. under the supervision of Hottel studied the radiating characteristics of premixed flames. He measured the radiation of illuminating gas over a temperature range of 2500 to 2800 F, $(p_c + p_w)L$ = .05 to 0.12 ft. atm. at flame depths of 5, 5.75, 7, and 8 inches with an air/gas ratio of 6.99 to 8.8, $p_w \simeq$ 0.1 to 0.14 atm. and $p_c \simeq$ 0.045 to 0.055 atm. He measured the flame temperature with the sodium - D line reversal method. The total emissivity of the water-vapor-carbon dioxide mixture ($p_w/[pw + pc]$ = .705) as presented in his thesis is represented at four temperatures of 2500, 2600, 2700, and 2800 F in Figure 4.3.2.3-1.

4.3.2.4. Fishenden

Margret Fishenden (1936) working at the Imperial College in England on the radiation from Non-Luminous combustion gases measured the radiation from a combustion gas mixture of 20.5% water vapor and 7.5% carbon dioxide due to burning of town gas. She covered a temperature

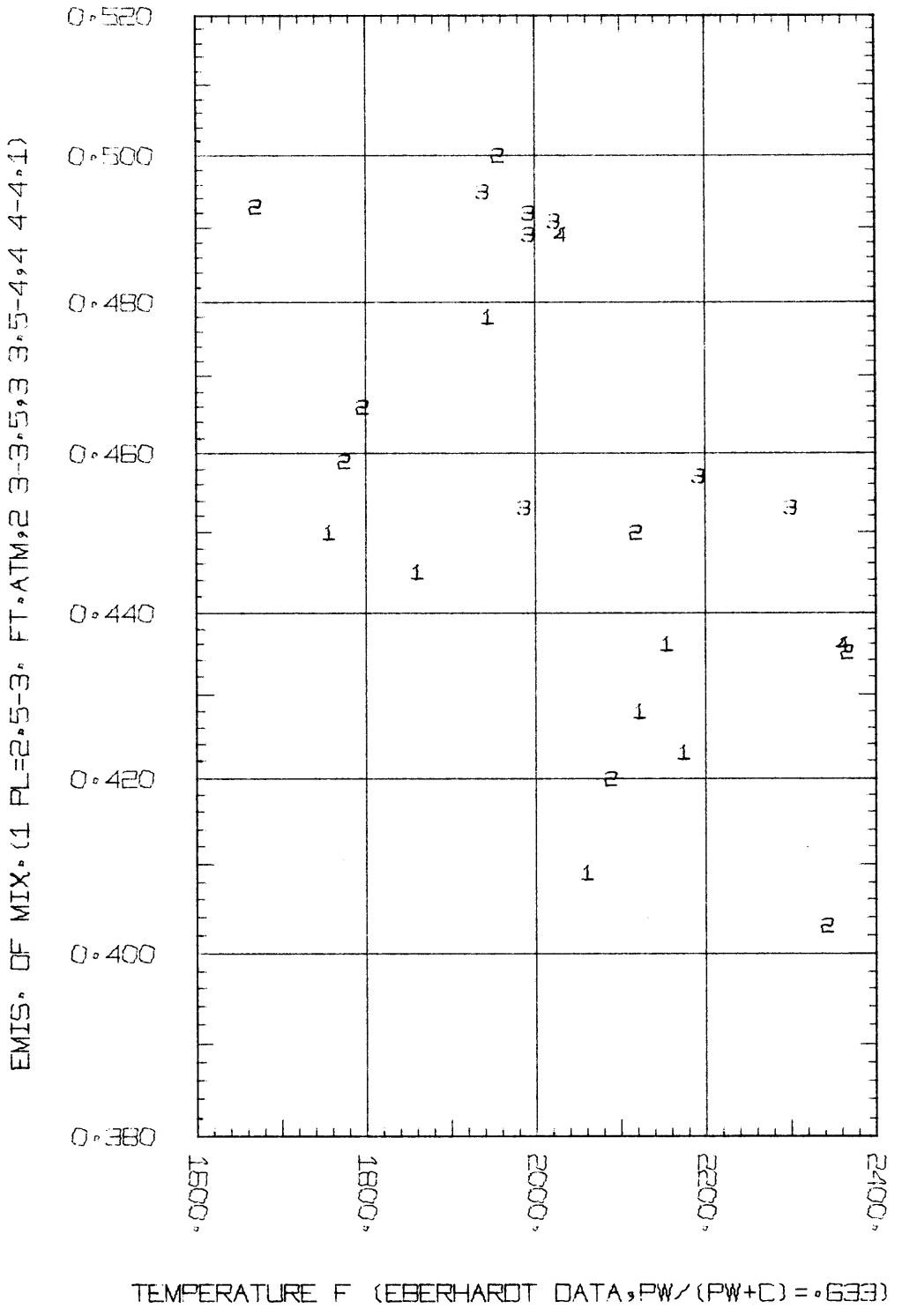

Figure 4.3.2.2-1

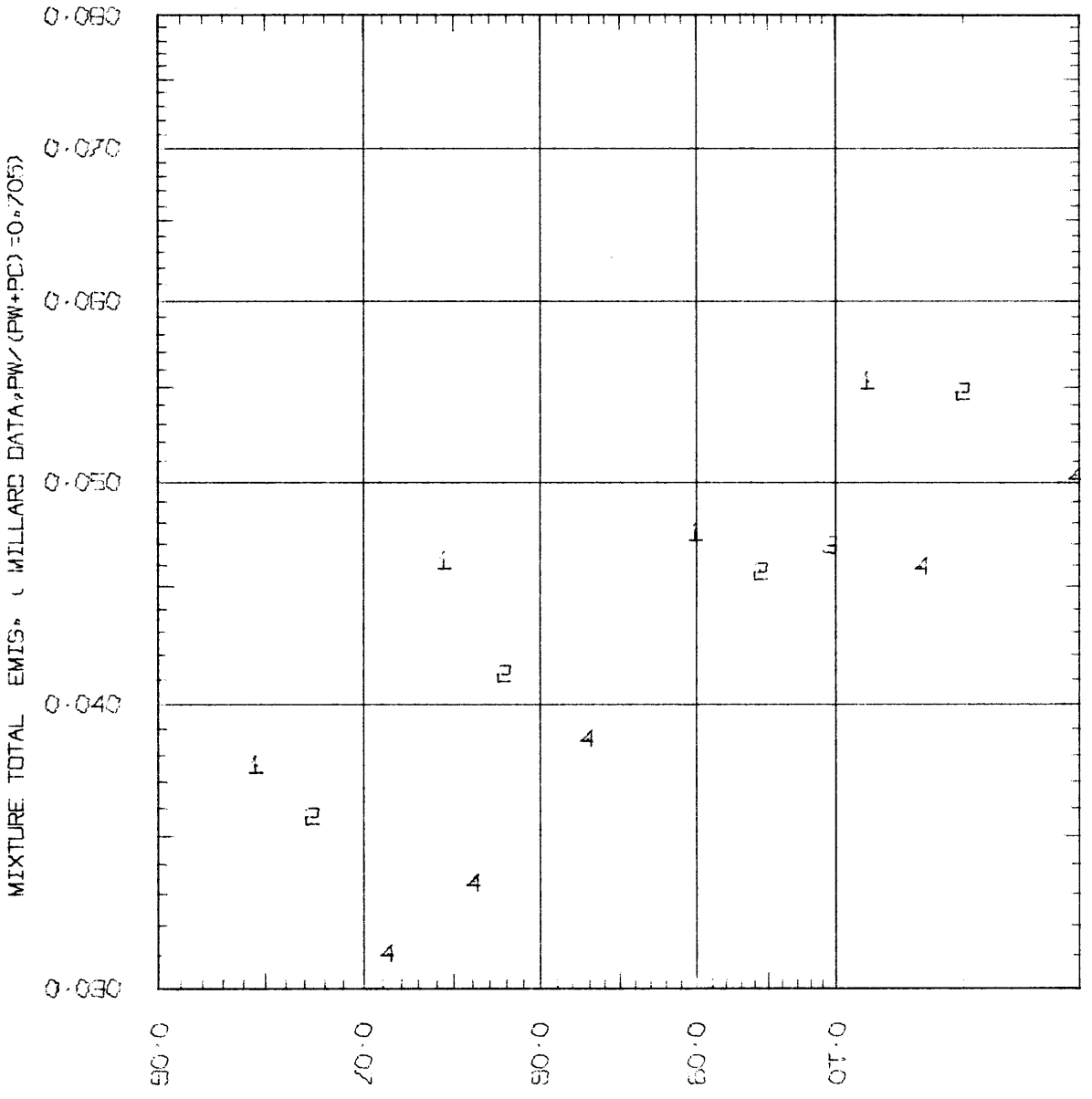

Figure 4.3.2.3-1

Figure 4.3.2.4-1 TEMPERATURE F(1 FOR PL=0.2 FT.ATM, 2 FOR 0.3 FT.ATM)

range of 600 to 2000 F and used Pt - Pt/Rh thermocouples to measure the temperature. There was, however, a considerable temperature gradient along the line of sight. Her path length was one foot, but she did not obtain very sharp boundaries to her radiating gas mixture. The stray radiation was somewhat high in her experiments and her measurements suffered from absorption by the atmosphere although she claimed that ... "A small correction had to be made for absorption by water vapor in the air between the experimental tube and the thermopile." Her data for $(P_c + P_w)L$ of 0.2 and 0.3 ft. atm. are presented in Figure 4.3.2.4-1.

4.3.2.5. Eckert

Eckert (1937) measured the radiation from water vapor and from carbon dioxide. He used monochromatic absorption data measured by Schmidt (1913) to calculate his overlap correction of the mixture emissivity. He covered a temperature range of 400 to 1200 K, $(p_c + p_w)L$ range of 10 to 200 cm. atm. The results of his calculations are plotted as dashed lines in Figures 5.5-1, 5.5-2 and 5.5-3.

4.3.2.6. Sarofim

Sarofim (1961) at M.I.T. under the supervision of Hottel studied the radiant heat transmission in enclosures. He assumed random distribution of spectral lines, which were experimentally verified by Howard et al. (1956), calculated the carbon dioxide emissivity from Edward's data and the emissivity of water vapor from Thomson's model, only at the region of overlap of the two gases. The results of Sarofim's calculations for an equimolal mixture of carbon dioxide and water vapor are reproduced in Figure 4.3.2.6-1, which includes the data by Hottel

Correction for Overlap of CO_2 and H_2O Emission Bands
(Calculated from Edwards Results and Thomsons Model)

$$p_c / (p_c + p_w) = 0.5$$

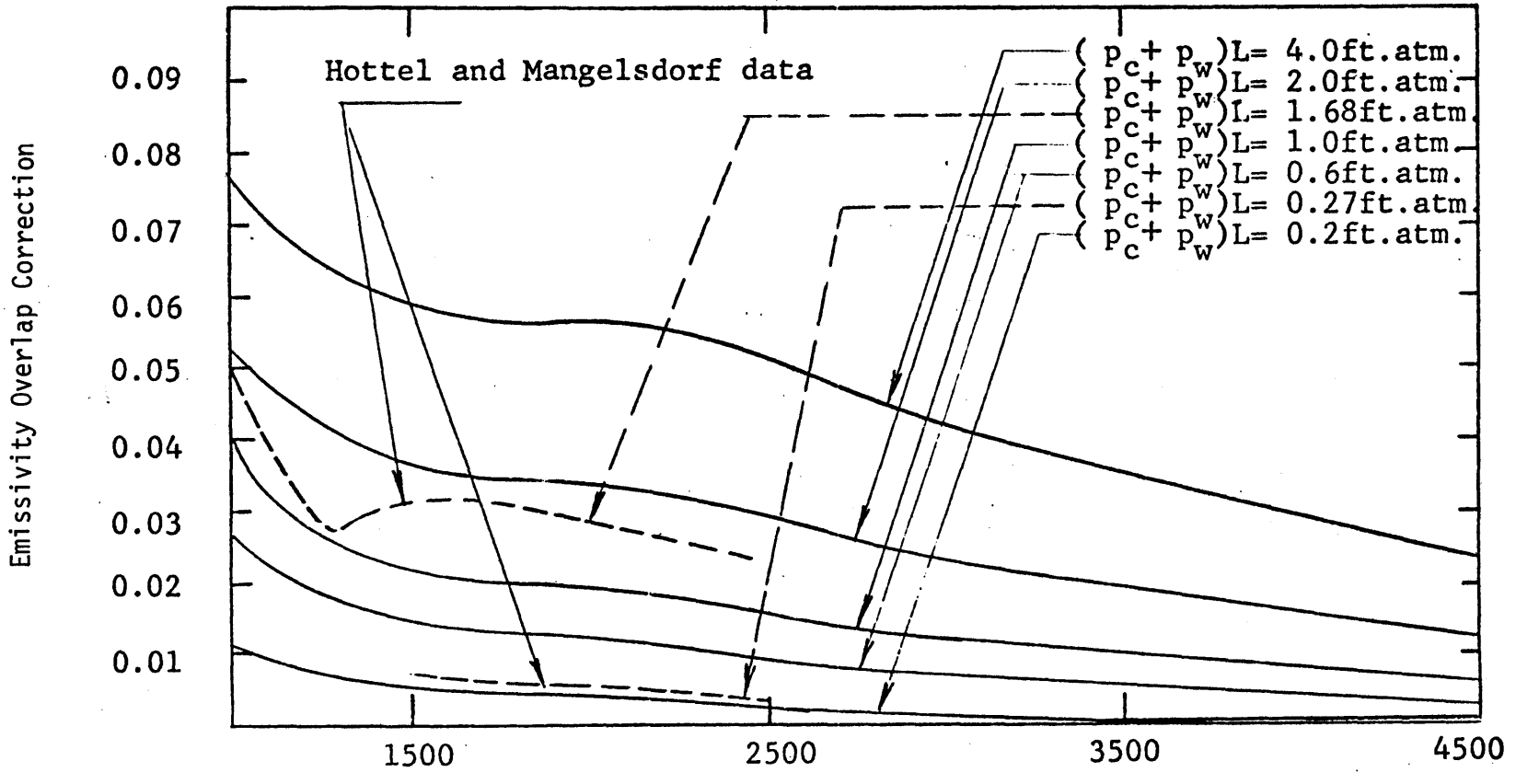

Figure 4.3.2.6-1

and Mangelsdorf as presented by Sarofim.

4.3.2.7. Hines and Edwards

Hines and Edwards (1964, 1968) studied the use of band model for calculation of absorption of infrared radiation by mixtures of water vapor, carbon dioxide and nitrogen as an inert gas. To verify theoretical calculations they made low resolution spectral absorption measurements in a 7/8 inch internal diameter stainless steel test cell with an isothermal absorbing gas path length of 15 - 24 in. They measured the wide band absorptions of carbon dioxide-water vapor-nitrogen gas mixtures at approximately 1 atm. and temperatures of about 1000 and 1500 R. Their data included the two strongest overlapping bands of 2.7 and 15 microns and the two strongest bands with minor overlapping (6.3 and 4.3 microns). Total gas absorptivities were obtained by summing the wide band absorptions weighted according to the Planck function. Their results are shown in Table 4.3.2.7-1. The "BAND" values are those recorded by Hines and Edwards using a band model equation based on Beer's law. Absorptivities based on summing experimentally measured band absorptions are denoted "EXPTL". The "HOTTEL" values were the values of gas absorptivities predicted for the experimental conditions by the graphical correlations of Hottel and Egbert (1942) and listed by Hines and Edwards who also modified Hottel's extrapolated data to include contirbutions of the medium strength bands 1.37 and 1.87 microns of water vapor and the 2.0 micron band of carbon dioxide. This was done by replacing the absorptivity overlap correction of Hottel by one calculated by Hines and Edwards using the approximations of Penner and Varanasi (1966). Mixture emissivities based on summing calculated band absorption are denoted "BAND" in the table.

TABLE 4.3.2.7-1

COMPARISON OF ABSORPTIVITIES AND ABSORPTIVITIES OVERLAP CORRECTIONS OF CARBON DIOXIDE AND WATER VAPOR MIXTURES

RUN NO	1	2	5	6	12	13	15
P ATM	1.042	1.098	1.093	1.070	1.14	1.178	1.17
TEMP R	982	990	990	1475	988	1470	1002
MOLE FRACTIONS OF							
WATER	.258	.051	.241	.250	.101	.100	.752
CO2	.254	.249	.046	.249	.099	.098	.248
ABSORBING MATTER (P(C) + P(W)) L							
FT.ATM	.686	.423	.403	.643	.292	.299	1.5
RATIO OF P(W)/ (P(W) + P(C))							
	.5037	.17	.838	.5005	.504	.505	.751
ABSORPTIVITIES							
EXPTL.	.233	.138	.206	.206	.150	.143	.332
BAND	.218	.131	.196	.197	.150	.144	.324
HOTTEL	.195	.125	.170	.190	.135	.130	.325
MOD HCH	.211	.131	.175	.204	.148	.139	.327
PRESENT	.189	.122	.169	.205	.133	.147	.298
ABSORPTIVITIES OVERLAP CORRECTIONS							
HOTTEL	.029	.011	.011	.026	.018	.013	.033
P+V	.021	.016	.006	.017	.013	.010	.029
BAND	.013	.005	.006	.012	.005	.004	.031
PRESENT	.014	.006	.006	.014	.006	.006	.026
EMISSIVITIES							
BAND	.368	.203	.348	.285	.256	.191	.520
PRESENT	.306	.190	.274	.269	.217	.195	.460

5.1. Results and Discussion of Carbon Dioxide

The gas model developed in the present work can be run for any conditions of temperature, total pressure, partial pressure and pL products to calculate the emission or absorption of carbon dioxide. The emissivity data can be plotted in several ways. A plot of the emissivity versus pL is very useful in establishing the different regimes. At low pL the slope of the curve should approach unity, which is in the linear region. At some intermediate value the slope approaches 0.5 in the square root region. At very high pL the curve approaches an assymptotic slope of zero. The problem associated with the use of an emissivity versus pL plot is that lines for different temperatures tend to cross each other, making interpolation on the temperature scale inaccurate. A plot of the emissivity versus the absolute temperature for selected pL's is preferable. The curves of different pL's do not intersect or cross each other.

Two types of comparisons are needed; one to check the consistency of the different independent experimental investigators and the second to check the agreement between the present computed emissivities and the experimental values. The experimental results of Hottel and Mangelsdorf (1935), Eckert (1937), Hottel and Smith (1935) and Akhunov (1973) have overlapping temperature range but were obtained at different conditions of total pressure, carbon dioxide partial pressure and pL product. It was necessary to reduce all data to a common total and partial pressure. This was selected to be the standard condition of zero partial pressure and a total pressure of one atmosphere. The correction to standard conditions was achieved by computing the emissivity at the temperature and pL corresponding to each

experimental point twice; once at the experimental carbon dioxide partial pressrue and total pressure, and the other at the standard condition p_c = 0 and P_t = 1.0 atm. The ratio of the two emissivities is the pressure broadening correction factor which may then be used to normalize the experimental emissivity to the standard state of p_c = 0 and P_t = 1 atm. The raw and corrected data of Akhumov et al. is shown in Table 4.2.2.5-1. The above step conpemsates, to the extent that the theoretical model predicts the correct pressure boradening correction factor, for the variation of partial and total pressure between different experiments; the resulting corrected emissivities are functions of only the gas temperature and the pL product. One of the last two variables had to be eliminated to allow comparison of data of different investigators. Although short distance interpolation in either direction (T or pL) may be acceptable, it is believed that interpolation on the basis of pL could be accomplished without introducing any appreciable error using a power relation i.e.

$$\frac{\varepsilon_1}{\varepsilon_2} = \left(\frac{pL_1}{pL_2}\right)^n ,$$

and the value of n is to be determined from the closest two data points to the pL in question. The above procedure was used to normalize experimental data to Hottel and Mangelsdorf, Eckert and Akhunov to obtain plots of the emissivity versus the absolute temperature for pL's from 0.1 to 300 cm. atm. and a temperature range of 400 to 1700 K. For purposes of clarity, the data were plotted in two different figures, 5.1-2 and 5.1-3. The first includes Hottel and Mangelsdorf corrected emissivities denoted by + at pL's of 0.1, 0.3, 0.8, 2., 5., 10., 30. and 80. cm. atm. Eckert's emissivities, denoted by X, are plotted for the

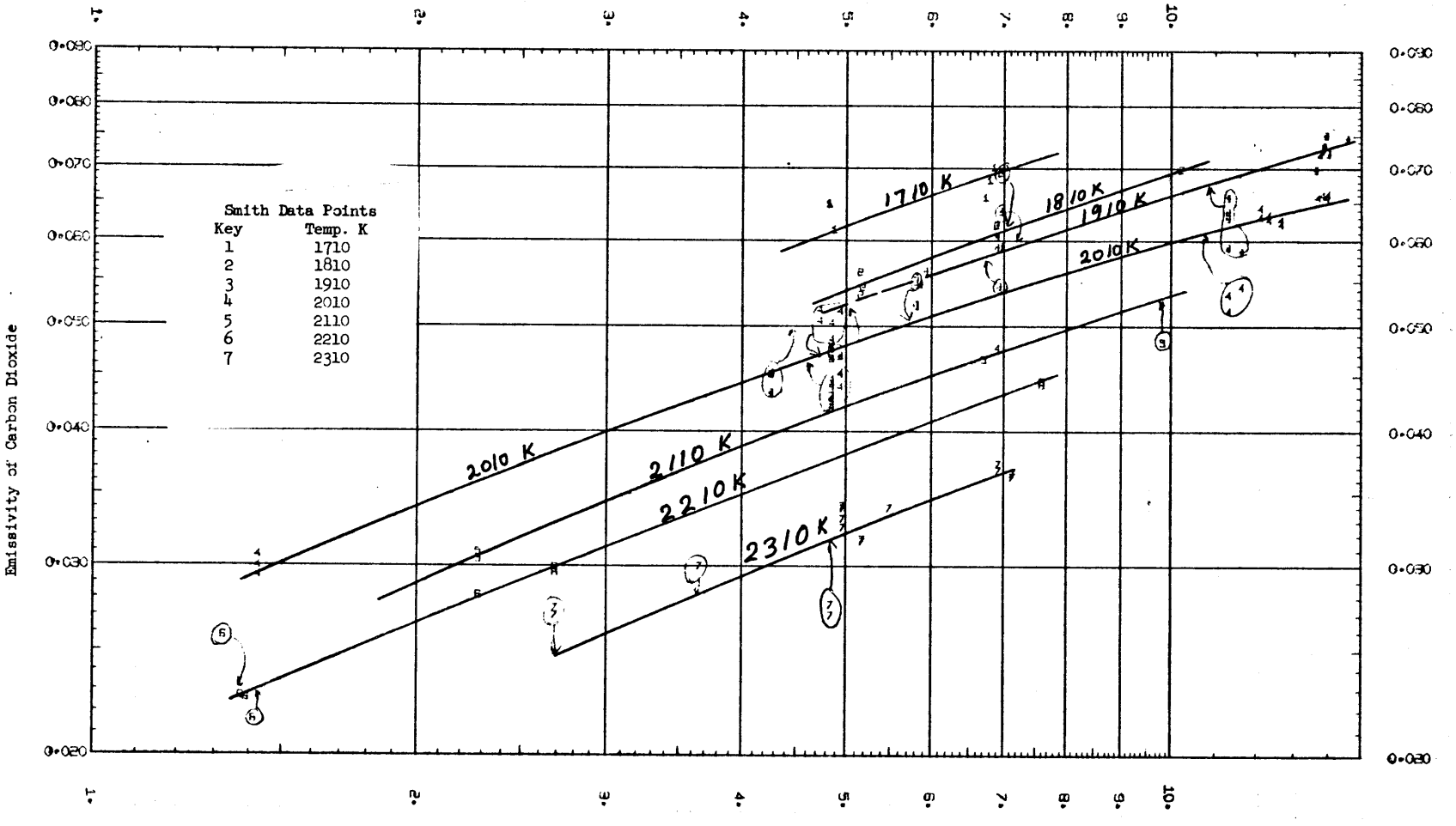

$p_c L$ cm. atm. (Hottel and Smith (1935) grouped data)

Figure 5.1-1

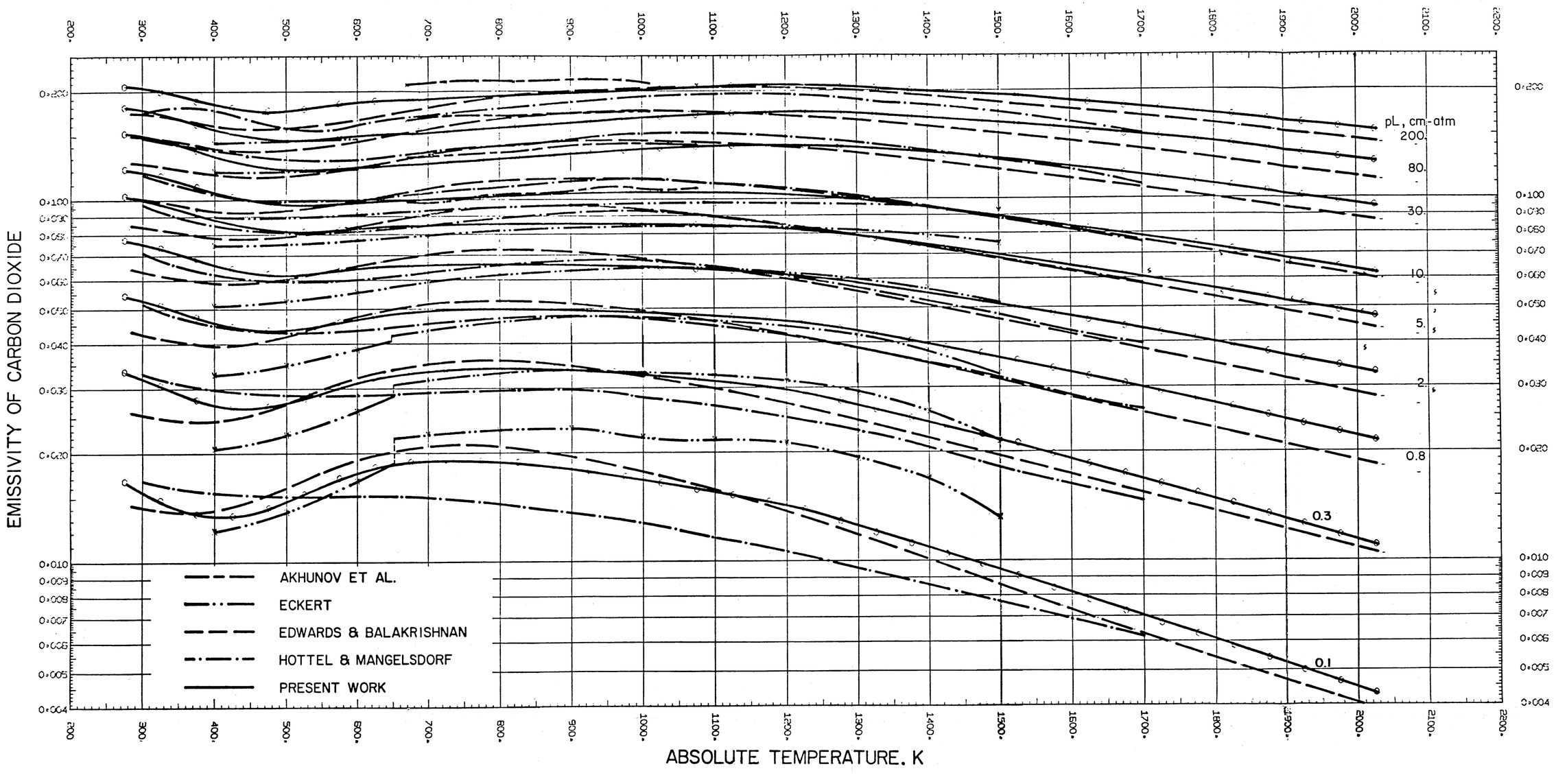
EMISSIVITY OF CARBON DIOXIDE
ABSOLUTE TEMPERATURE, K
pL, cm-atm
200.
80.
30.
10.
5.
2.
0.8
0.3
0.1
AKHUNOV ET AL.
ECKERT
EDWARDS & BALAKRISHNAN
HOTTEL & MANGELSDORF
PRESENT WORK

EMISSIVITY OF CARBON DIOXIDE

pL, cm-atm
300.
100.
50.
20.
8.
3.
1.
0.5
0.2
0.1

AKHUNOV ET AL.
ECKERT
EDWARDS & BALAKRISHNAN
HOTTEL & MANGELSDORF
PRESENT WORK

ABSOLUTE TEMPERATURE, K

same pL's over a temperature range of 400 to 600 K and for the sam pL's up to 10 cm. atm. for temperatures of 700 to 1500 K; Akhunov data, shown as *, are plotted for pL's of 10, 30, 80, and 200 cm. atm. over a temperature range of 670 to 1070 K. Emissivities computed using the present model and using Edwards and Balakrishnan's model are plotted on the same graph at the same pL's over a temperature range of 300 to 2200 K and are denoted 0 and - respectively. The second figure includes data sets of the same investigators over the same temperature ranges, but at pL's of 0.1, 0.2, 0.5, 1., 3., 8., 20., 50., 100 and 300 cm. atm. In order to include Smith's (1935) high temperature carbon dioxide data, it was necessary to smooth his data. The first step was to calculate the pressure broadening correction factor for each of his data points and reduce his data to p_c = 0 and P_t = 1 atm. The normalized data were grouped together for temperature intervals of 100 K between 1710 and 2310 K. Emissivity was plotted versus pL and smooth curves for any chosen temperature were drawn with the guidance of the data points at the other temperatures, as shown in Figure 5.1-1. Emissivities read from the smoothed curves at pL = 1, 2, 3, 5, 8, and 10 cm. atm. were included in the graph. The figures show a break in the curves going through Eckert's smoothed points between 600 and 700 K. This is because Eckert's data points between 400 and 600 K were measured in a furnace of length 65.4 cm. while his data at 700 K and above were measured using a 10.2 cm. furnace. The break in the curve diminishes with increasing pL and disappears around 2 cm. atm. In comparing the different curves, one should be cognizant that Edwards and Balakrishnan did not place much confidence in the accuracy of their model for the fifteen micron band. Therefore, curves going through computed points of Edwards were not

extended below 480 K. At low pL's (0.1, 0.2 cm. atm.) there is a marked discrepancy between the data of Eckert and Hottel and Mangelsdorf. Eckert's curve is quite high, while the H & M curve is quite low compared to the present computations and to Edwards computation in the range 1000 - 1500 K. Eckert's emissivities are almost twice as high as H & M's. Therefore, in constructing the smoothed carbon dioxide emissivity, it is not unjustiable to give Eckert and H & M curves very little weight at pL's of 0.1 and 0.2 cm. atm.

One of the explanations for discrepancies between different sets of data is that Mangelsdorf's low pL measurements might have suffered from atmospheric absorption. At low pL's and temperatures below 500 K Mangelsdorf had no experimental data. The extrapolation of his line to 300 K was made possible by the use of the measurements of Rubens and Ladenburg and Hertz over a pL range of 0.1 to 50 cm. atm. The agreement between Ruben's data and the present computations is good all temperatures below 350 K. The figures also shown that between 900 and 1100 K and between pL = 30 and 100 cm. atm. the agreement between Akhunov data and Edwards and Balakrishnan's model is good. In the same temperature range and at pL = 20 cm. atm. the lines representing the data of Akhunov, Eckert and Hottel and Mangelsdorf coincide. In the 1200 - 1300 K region the lines representing Edwards, Eckert, Hottel and Mangelsdorf and the present computations are close together for pL = 1 to 30 cm. atm. At the high temperature end (1200 to 2000 K) the emissivities predicted from Edwards and Balakrishnan's model and the present computations parallel each other with the present values being consistently high; in this range the emissivities of Hottel and Mangelsdorf are much closer to those from the Edwards and Balakrishnan model. The figures also show a

change in slope at 1200 K of the curves fitted to the present computations. This behavior is not evident in the emissivities recommended by Hottel and Mangelsdorf or Edwards and Balakrishnan. Smoothing curves fitted to the present computations could change the emissivities by as much as six percent at the bend. Based on the above discussion, some preliminary rules were set as guidances in constructing the new chart of the emissivity of carbon dioxide against the temperature. At 1600 K the curves of Hottel and Mangelsdorf and of Edwards and Balakrishnan each is to be given double the weight of the present computed values. The curves of Eckert should be ignored because of the marked discrepancies at 1500 K. At points of closest agreement of different curves use the same weighting. At 700 and 800 K equal weight should be given to all four curves at pL greater than 0.2 cm. atm. At pL = 0.2 and 0.1 cm. atm. the mean of Edwards and present computed emissivities should be used.

A piece of transparent film was placed over the semi-log graph of the emissivity of carbon dioxide against temperature shown in Figure 5.1-3 to apply the above rules, in a flexible way that would eliminate any irregularities or reversed curvatures from the smoothed plots. The next step was to cross plot emissivities read from the smoothed curves v.s. the pL to insure their smoothness. To do this, a second piece of transparent film was placed on a full logarthimic scale (10 inches cycle in both direction) and the emissivities read from the smoothed curves on first transparent film at temperatures of 300, 400, 600, 800, 1000, 1200, 1400, 1600 and 1800 K and pL's of .1, .2, .5, 1, 3, 8, 20, 50, 100 and 300 cm. atm. was plotted and smooth curves were drawn through them. From these latter curves the preliminary curves of

the emissivity against the temperature were slightly adjusted. The final curves smoothed in both directions (Temperature and pL) are shown in Figures 5.1-4 (ε v.s. T) and 5.1-5 (ε v.s. pL). The final smoothed emissivities read from Figure 5.1-5 which will be used to construct the final working plot are presented in Table 5.1-1. Although no experimental data existed at pL less than 0.1 cm. atm. or pL greater than 300 cm. atm. ε against pL curves were extrapolated to pL's of 0.05 cm. atm., 500 and 1000 cm. atm. Emissivities read at the above three pL's are presented in the table and will be shown in the final working plot as dotted lines.

RECOMMENDED CARBON DIOXIDE CHARTS

$p_e = 0$ $P_T = 1$ atm

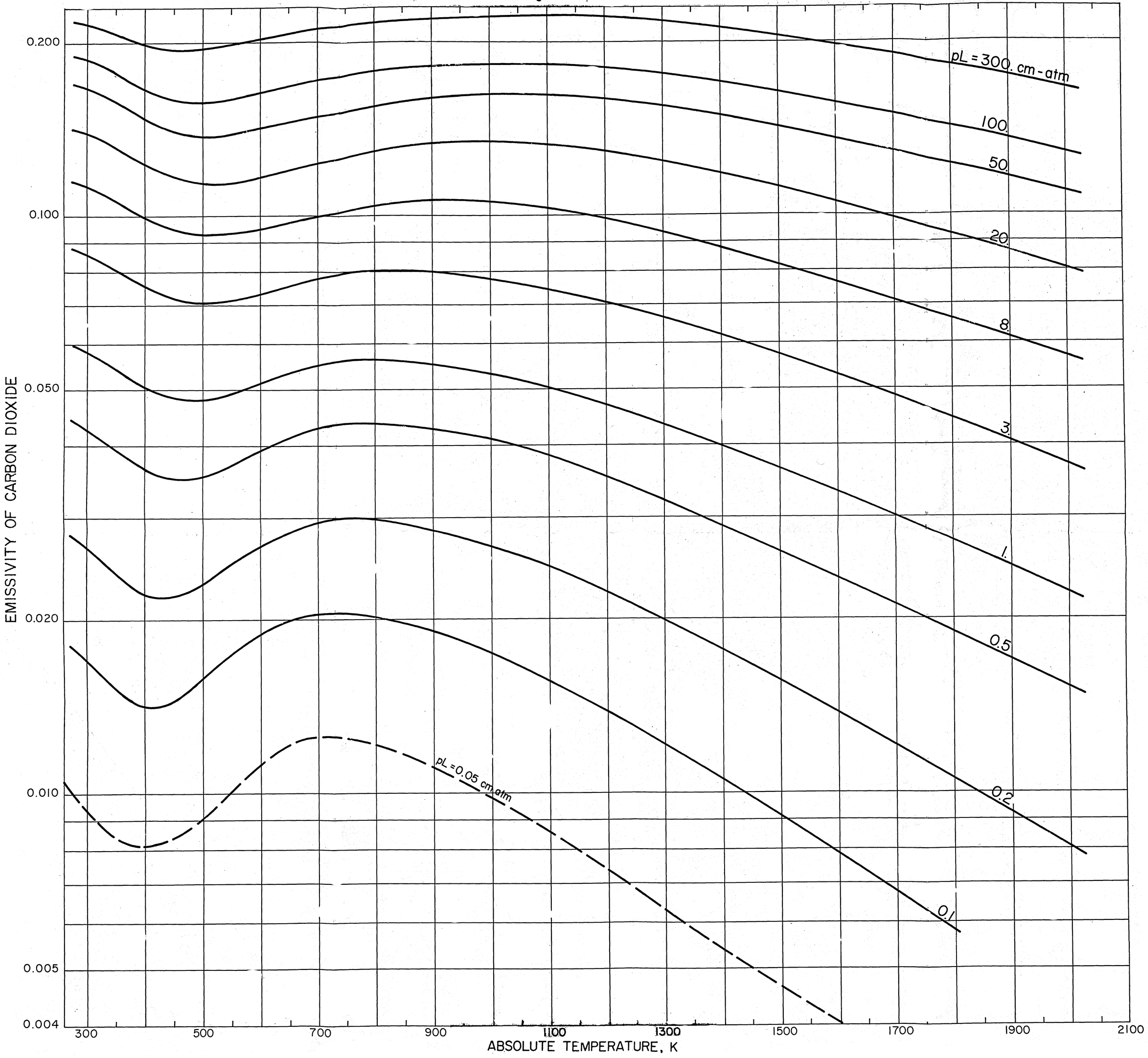

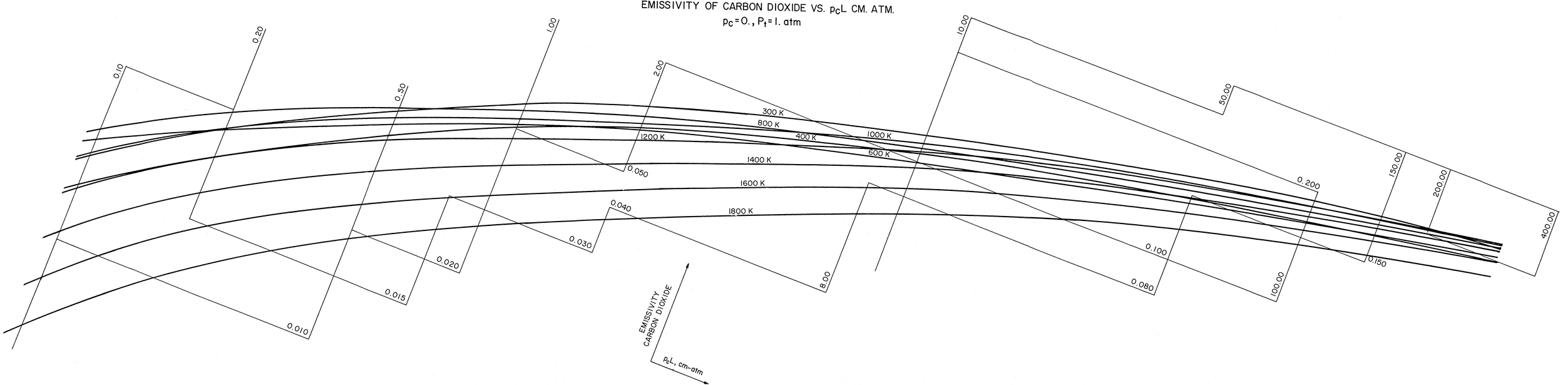
EMISSIVITY OF CARBON DIOXIDE VS. p_cL CM. ATM.
$p_c = 0.$, $P_t = 1.$ atm
0.10
0.20
0.50
1.00
2.00
10.00
50.00
150.00
200.00
400.00
300 K
800 K
400 K
1000 K
1200 K
600 K
1400 K
1600 K
1800 K
0.050
0.040
0.030
0.020
0.015
0.010
8.00
0.200
0.100
0.080
100.00
0.150
EMISSIVITY CARBON DIOXIDE
p_cL, cm-atm

TABLE 5.1-1

RECOMMENDED EMISSIVITIES OF CARBON DIOXIDE

PL CM.ATM.	EMISSIVITY OF CARBON DIOXIDE AT TEMP. OF (K)								
	300	400	600	800	1000	1200	1400	1600	1800
.05	.00955	.00811	.0113	.0121	.00980	.00732	.00540	.00403	.00291
.09	.01555	.0131	.0177	.0185	.0159	.01265	.00946	.00702	.00516
.10	.0170	.0142	.0189	.0202	.0176	.0138	.0105	.00788	.00583
.12	.0191	.01585	.02055	.02245	.01955	.01562	.0121	.00915	.00681
.15	.0221	.0184	.0230	.0254	.0225	.0184	.0144	.0111	.00831
.20	.0265	.0221	.0264	.0295	.0267	.0222	.0177	.0138	.01055
.25	.0300	.0250	.0291	.0316	.030	.0251	.0202	.0160	.0123
.30	.0320	.0276	.0314	.0352	.0326	.0277	.0224	.0179	.0139
.35	.0357	.0302	.0336	.0375	.0350	.0301	.0242	.0195	.0153
.40	.0382	.0325	.0357	.0398	.0371	.0321	.0260	.0210	.0166
.45	.0403	.0345	.0375	.0416	.0390	.0338	.0276	.0223	.0178
.50	.0426	.0365	.0391	.0435	.0410	.0355	.0291	.0235	.0189
.60	.0465	.0400	.0421	.0466	.0438	.0382	.0316	.0257	.0208
.70	.0498	.0430	.0448	.0493	.0465	.0406	.0336	.0275	.0225
.80	.0528	.0457	.0471	.0519	.0490	.0430	.0361	.0296	.02425
.90	.0558	.0484	.0495	.0544	.0513	.0451	.0380	.0313	.0258
1.	.0584	.0503	.0514	.0562	.0532	.0470	.0398	.0329	.0271
1.20	.0630	.0544	.0550	.0601	.0570	.0502	.0427	.0358	.0294
1.5	.0683	.0597	.0593	.0649	.0620	.0549	.0470	.0394	.03255
1.8	.0730	.0638	.0629	.0682	.0658	.0588	.0505	.04265	.0355
2.	.0758	.0661	.0650	.0708	.0681	.0611	.0527	.0446	.0371
2.2	.0781	.0682	.0670	.0730	.0701	.0632	.0546	.0465	.0387
2.5	.0814	.0710	.0698	.0759	.0733	.0664	.0572	.0489	.0408
2.8	.0843	.0737	.0720	.0784	.0760	.0692	.0599	.0513	.0428
3.	.0859	.0751	.0732	.080	.0776	.0709	.0617	.0528	.0440
3.2	.0877	.0767	.0747	.0813	.0793	.0726	.0630	.0539	.0453
3.5	.0899	.0788	.0763	.0834	.0818	.0749	.0652	.0560	.0471
3.8	.0921	.0806	.0780	.0852	.0839	.0771	.0674	.0579	.0488
4.	.0931	.0820	.0791	.0861	.0851	.0787	.0688	.0591	.0499
4.5	.0962	.0850	.0819	.0890	.0883	.0819	.0711	.0621	.0524
5.	.0990	.0872	.0840	.0918	.0912	.0850	.0749	.0648	.0548
5.5	.102	.0895	.0860	.0940	.0940	.0878	.0778	.0671	.0570
6.	.104	.0918	.0879	.0959	.0958	.0901	.0801	.0696	.0589
6.5	.106	.0937	.0897	.0980	.0990	.0928	.0827	.0718	.0605
7.	.108	.0956	.0912	.0998	.1010	.0951	.0850	.0738	.0623
7.5	.110	.0976	.0927	.1015	.1030	.0969	.0870	.0758	.06440
8.	.112	.0988	.0940	.103	.105	.0988	.0889	.0775	.0656
8.5	.1135	.1010	.0952	.1045	.1070	.1010	.0905	.0795	.0672
9.	.1148	.1025	.0969	.1060	.1085	.1025	.0922	.0812	.0690
9.5	.1162	.1035	.0980	.1075	.1105	.1040	.0940	.0828	.0702
10.	.1175	.1050	.0991	.1085	.1120	.1060	.0957	.0843	.0719
12.	.1235	.1095	.1035	.1135	.1175	.1120	.1015	.0900	.0769
15.	.1288	.1155	.1085	.1190	.1250	.1195	.1090	.0967	.0835
18.	.1350	.1200	.1133	.1245	.1310	.1255	.1150	.1020	.0889
20.	.1385	.123	.1162	.128	.134	.129	.118	.105	.0920
25.	.1455	.129	.1220	.1345	.1410	.1360	.1250	.1120	.0992
30.	.1520	.1337	.1265	.1395	.1460	.1420	.131	.1170	.1045
35.	.1565	.1370	.1310	.1440	.1505	.1475	.1355	.1220	.1095
40.	.1605	.141	.1350	.1475	.1545	.1520	.1400	.1265	.1138
45.	.1645	.144	.1380	.1520	.1580	.1555	.1438	.1305	.1175
50.	.167	.147	.142	.154	.1605	.159	.1475	.134	.121
55.	.171	.150	.1440	.1575	.1640	.1625	.1502	.1370	.1240
60.	.1735	.1520	.1475	.1605	.1665	.1650	.1535	.1395	.1265
70.	.1785	.1560	.1520	.1650	.1720	.1700	.1585	.1445	.1315
80.	.1825	.1595	.1560	.170	.1760	.1755	.1635	.1495	.1365
90.	.1856	.1635	.1600	.1740	.1798	.1795	.1670	.1530	.1403
100.	.188	.166	.164	.177	.183	.182	.171	.157	.142
120.	.1930	.1715	.170	.1830	.1885	.1885	.1775	.1635	.1480
150.	.1990	.1780	.1780	.1910	.1970	.1968	.1860	.1720	.1555
200.	.205	.1860	.1885	.2025	.2060	.2065	.1970	.1830	.1665
250.	.2105	.1925	.1970	.2100	.2140	.2150	.2055	.1910	.1745
300.	.215	.198	.203	.215	.219	.220	.211	.1975	.182
500.	.224	.2130	.224	.2305	.2325	.234	.230	.2180	.1980
1000.	.234	.2330	.252	.2545	.255	.256	.257	.2470	.2245

5.2. Pressure Broadening Correction Factor of Carbon Dioxide

It is well recognized that four variables are necessary to define emissivity; namely temperature, pL product, partial pressure of absorbing gas, and total pressure. As discussed earlier, these can be reduced to three independent variables by the use of the half width b, which for the case of carbon dioxide may be written as (see equation 2.5.3-6 and Table 2.5.3-1)

$$b_{CO_2,T} = \sqrt{\frac{273}{T}}\,(0.09\ p_{CO_2} + 0.07\ p_{H_2O} + 0.07\ p_{N_2} + 0.069\ p_{O_2} + 0.08\ p_{H_2} + 0.06\ p_{CO}) \qquad (5.2\text{-}1)$$

$$\text{or}\quad b_{CO_2,T} = a\ p_{CO_2} + cp_{H_2O} + cp_{N_2} + dp_{O_2} + ep_{H_2O} + fp_{CO} \qquad (5.2\text{-}2)$$

where the coefficients a, c, d, e and f are temperature dependent.

For most engineering purposes, assuming a standard half width of 0.07 cm^{-1} at STP will not introduce appreciable error. Equation (5.2-1), therefore, simplifies to

$$b_{CO_2,T} = \sqrt{\frac{273}{T}}\,(0.02\ p_c + 0.07\ P_t) \qquad (5.2\text{-}3)$$

Equation 5.2-3 would be exact if the gas mixture consisted only of carbon dioxide, water vapor and/or nitrogen. Equation (5.2-3) may be rewritten as

$$b_{CO_2,T} = P_t\sqrt{\frac{273}{T}}\,(0.02\ Y_c + 0.07) \qquad (5.2\text{-}4)$$

where Y_c is the mole fraction of carbon dioxide. Therefore, $\varepsilon_c = \varepsilon_c\,(T, pL, b)$ and the graphical presentation of the above relation requires a family of families of curves. The standard emissivity charts were drawn at $p_c = 0$ and $P_t = 1$ atm. The pressure broadening correction factor charts were developed as a function of the gas temperature, pL

and half width. In theory, a family of families of curves are needed for graphical presentation. It was decided to present the correction factor at five discrete temperatures of 500, 1000, 1500, 2000, and 2500 K. It was necessary to present the charts in a form that allows easy interpolation. Plots of the correction factor against the half width in cm^{-1} for different pL's were found to be inadequate because the partial derivative of the correction factor with respect to pL ($\partial C_F/\partial pL$) was changing signs at a pL value which was a function of the gas temperature making interpolation around the maximum point very difficult, unless the exact value of the pL at which $\partial C_F/\partial pL = 0$ is known. On the other hand, a plot of C_F against pL with the half width as a curve parameter would be satisfactory because the relation between correction factor and the half width b is monotonic. Figure 5.2-1 is a plot of the carbon dioxide pressure boradening correction factor at 500 K against the pL in cm. atm. for half width values of 0.01, .02, .03, .05, .07, .1, .2, .3, .5, .7, 1, 2 and 10 cm^{-1}. The correction factor is unity for all pL's at the "standard" half width value given by

$$b_{ST} = 0.07 \sqrt{273/T} \quad cm^{-1} \ (T \text{ in K})$$

At temperatures of 500, 1000, 1500, 2000 and 2500 K, the standard half widths are 0.015, 0.0366, 0.0299, 0.026 and 0.0231 cm^{-1} respectively. Figures 5.2-2 through 5.2-5 are the same type of plot, but at temperatures of 1000, 1500, 2000 and 2500 K. To facilitate the calculation of b to use the charts Table 5.2-1 lists the values of the coefficients a, c, d, e, and f of equation 5.2-2 at temperatures of 500, 1000, 1500, 2000 and 2500 K.

These charts are generalized and can be used for any given total and carbon dioxide partial pressure. For engineering purposes, however, these

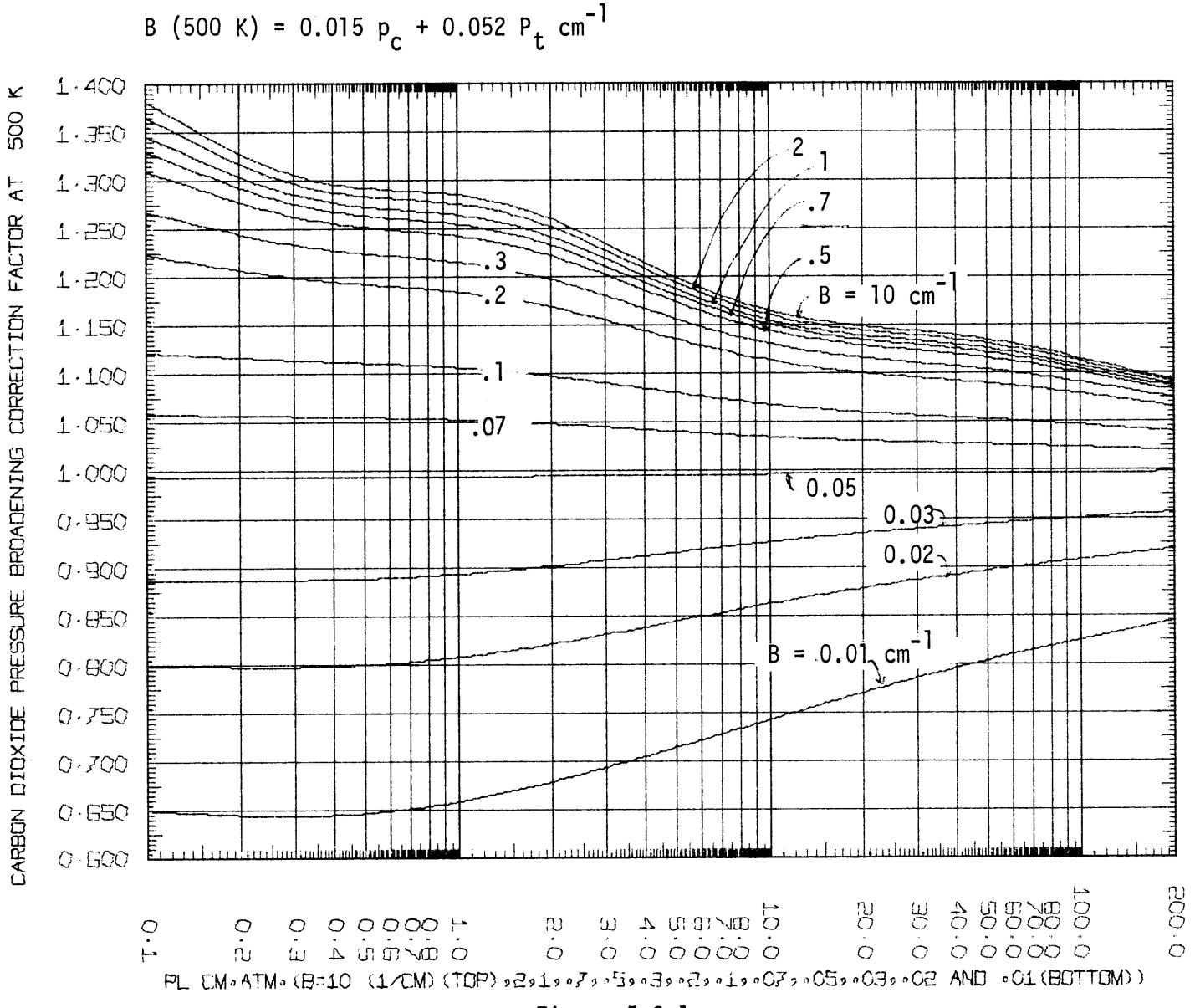
B (500 K) = 0.015 p_c + 0.052 P_t cm^{-1}
CARBON DIOXIDE PRESSURE BROADENING CORRECTION FACTOR AT 500 K
1.400
1.350
1.300
1.250
1.200
1.150
1.100
1.050
1.000
0.950
0.900
0.850
0.800
0.750
0.700
0.650
0.600
2
1
.7
.5
.3
.2
.1
.07
B = 10 cm^{-1}
0.05
0.03
0.02
B = 0.01 cm^{-1}
0.1
0.2
0.3
0.4
0.5
0.6
0.7
0.8
1.0
2.0
3.0
4.0
5.0
6.0
7.0
8.0
10.0
20.0
30.0
40.0
50.0
60.0
70.0
100.0
200.0
PL CM-ATM (B=10 (1/CM) (TOP) ,2,1,.7,.5,.3,.2,.1,.07,.05,.03,.02 AND .01(BOTTOM))

Figure 5.2-1

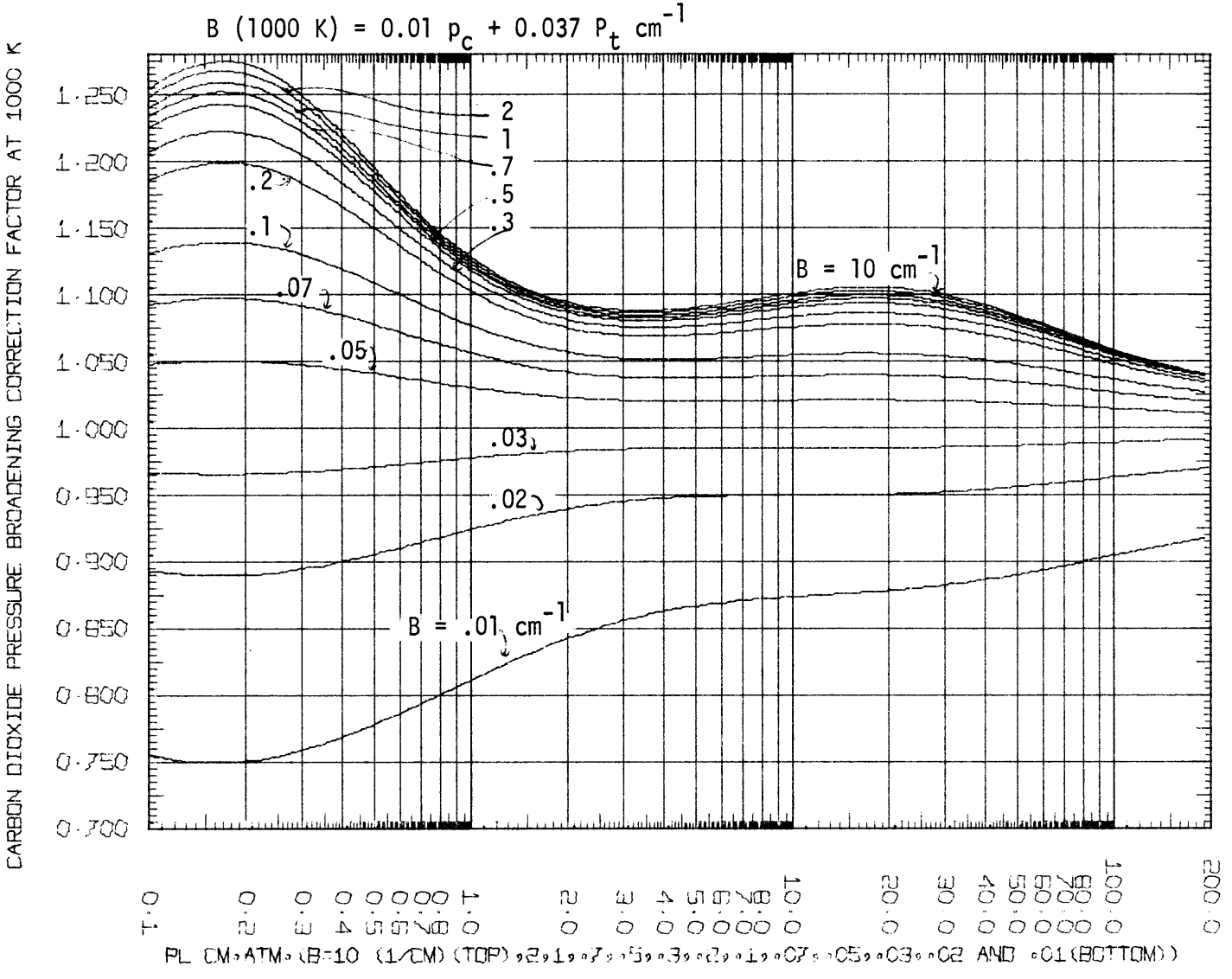
B (1000 K) = 0.01 p_c + 0.037 P_t cm^{-1}
CARBON DIOXIDE PRESSURE BROADENING CORRECTION FACTOR AT 1000 K
1.250
1.200
1.150
1.100
1.050
1.000
0.950
0.900
0.850
0.800
0.750
0.700
2
1
.7
.5
.3
.2
.1
.07
.05
.03
.02
B = 10 cm^{-1}
B = .01 cm^{-1}
0.1
0.2
0.3
0.4
0.5
0.6
0.7
0.8
1.0
2.0
3.0
4.0
5.0
6.0
7.0
8.0
10.0
20.0
30.0
40.0
50.0
60.0
70.0
100.0
200.0
PL CM-ATM (B=10 (1/CM) (TOP) .2 .1 .07 .05 .03 .02 AND .01(BOTTOM))

Figure 5.2-2

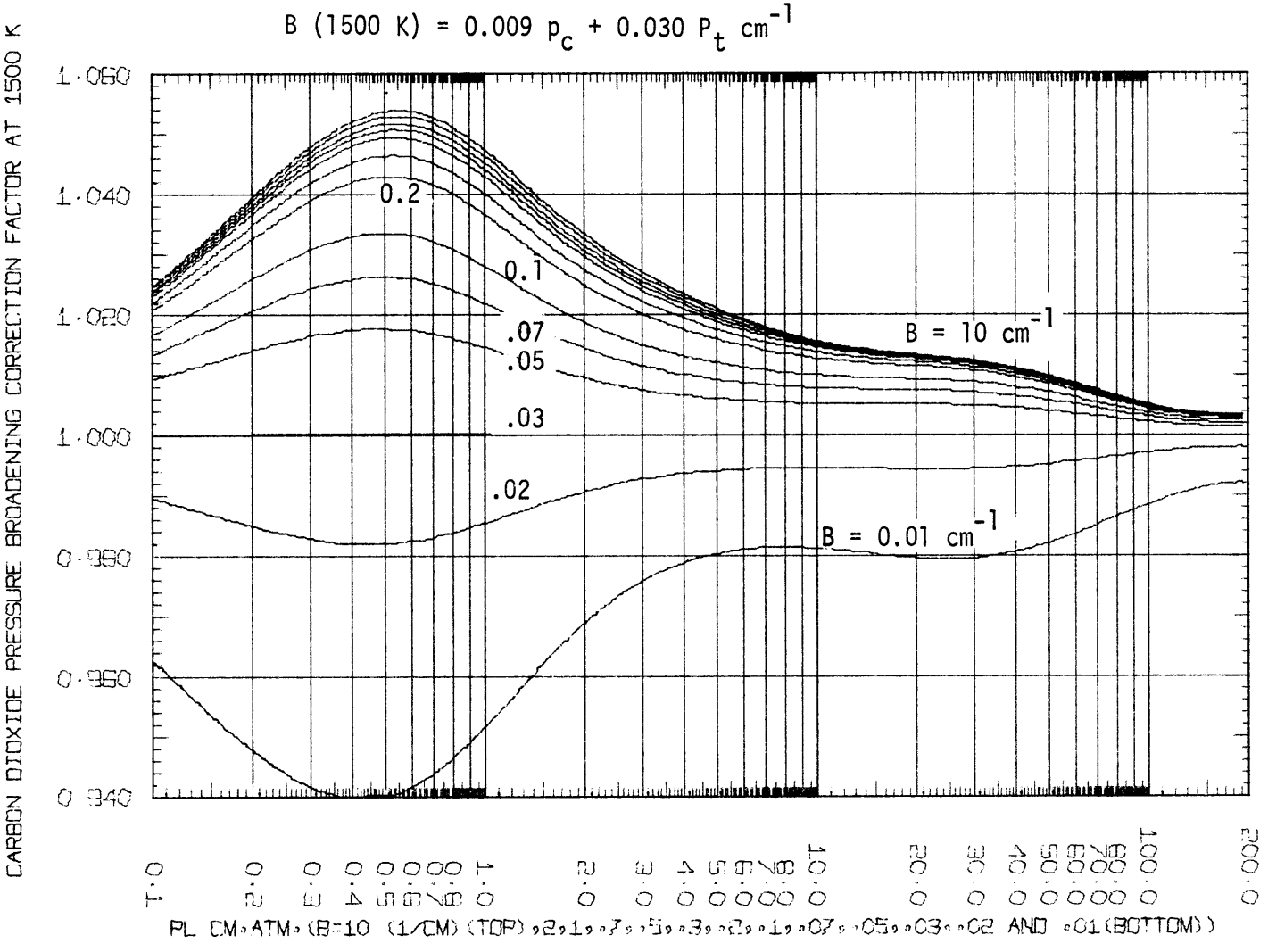
B (1500 K) = 0.009 p_c + 0.030 P_t cm^{-1}
CARBON DIOXIDE PRESSURE BROADENING CORRECTION FACTOR AT 1500 K
1.060
1.040
1.020
1.000
0.980
0.960
0.940
0.2
0.1
.07
.05
.03
.02
B = 10 cm^{-1}
B = 0.01 cm^{-1}
0.1
0.2
0.3
0.4
0.5
0.6
0.7
0.8
1.0
2.0
3.0
4.0
5.0
6.0
7.0
8.0
10.0
20.0
30.0
40.0
50.0
60.0
70.0
80.0
100.0
200.0
PL CM-ATM (B=10 (1/CM) (TOP) .2 .1 .7 .5 .3 .2 .1 .07 .05 .03 .02 AND .01(BOTTOM))

Figure 5.2-3

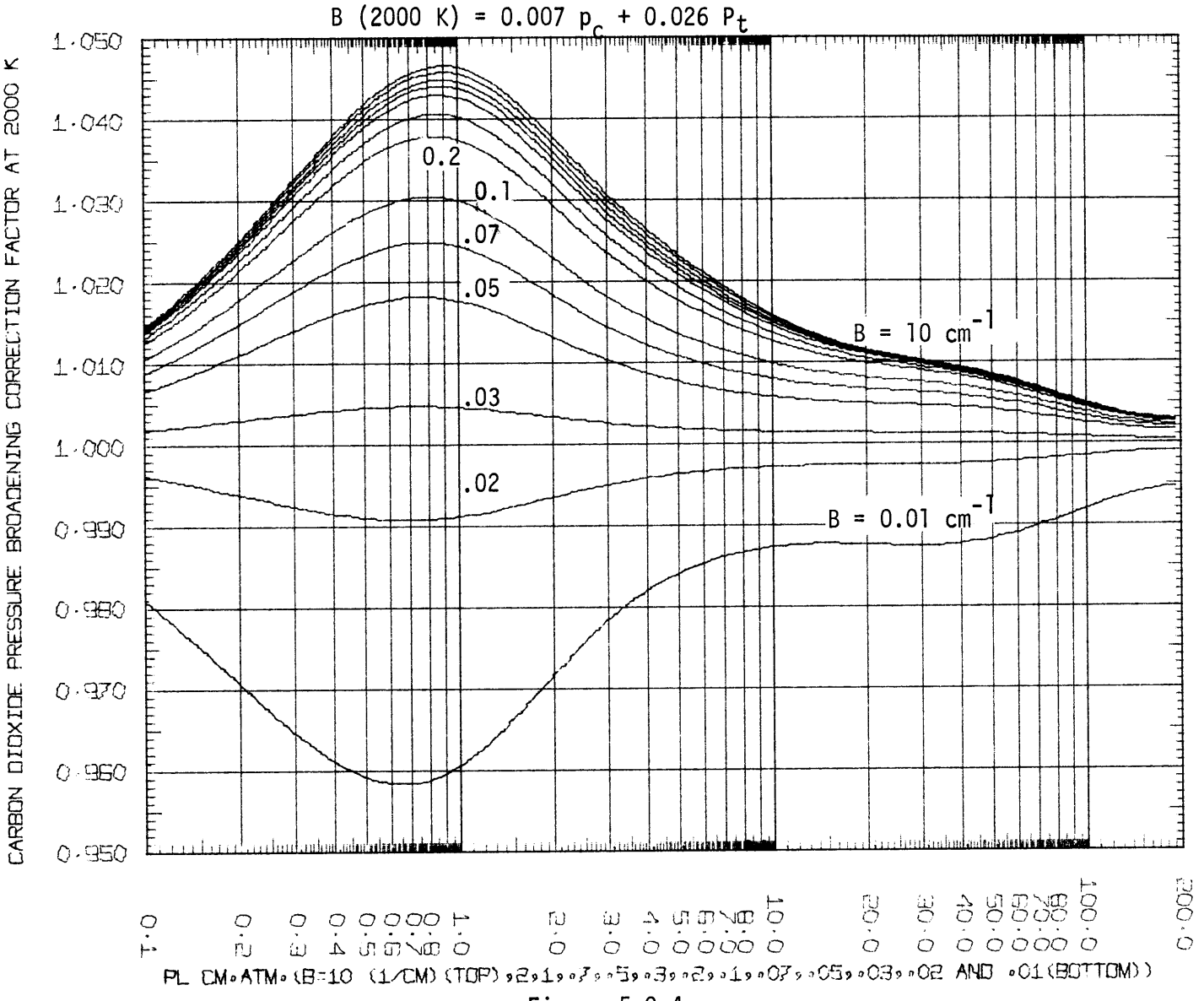
B (2000 K) = 0.007 p_c + 0.026 P_t
CARBON DIOXIDE PRESSURE BROADENING CORRECTION FACTOR AT 2000 K
1.050
1.040
1.030
1.020
1.010
1.000
0.990
0.980
0.970
0.960
0.950
0.2
0.1
.07
.05
.03
.02
B = 10 cm^{-1}
B = 0.01 cm^{-1}
0.1
0.2
0.3
0.4
0.5
0.6
0.7
0.8
1.0
2.0
3.0
4.0
5.0
6.0
7.0
8.0
10.0
20.0
30.0
40.0
50.0
60.0
70.0
100.0
200.0
PL CM•ATM•(B=10 (1/CM) (TOP),2,1,.7,.5,.3,.2,.1,.07,.05,.03,.02 AND .01(BOTTOM))

Figure 5.2-4

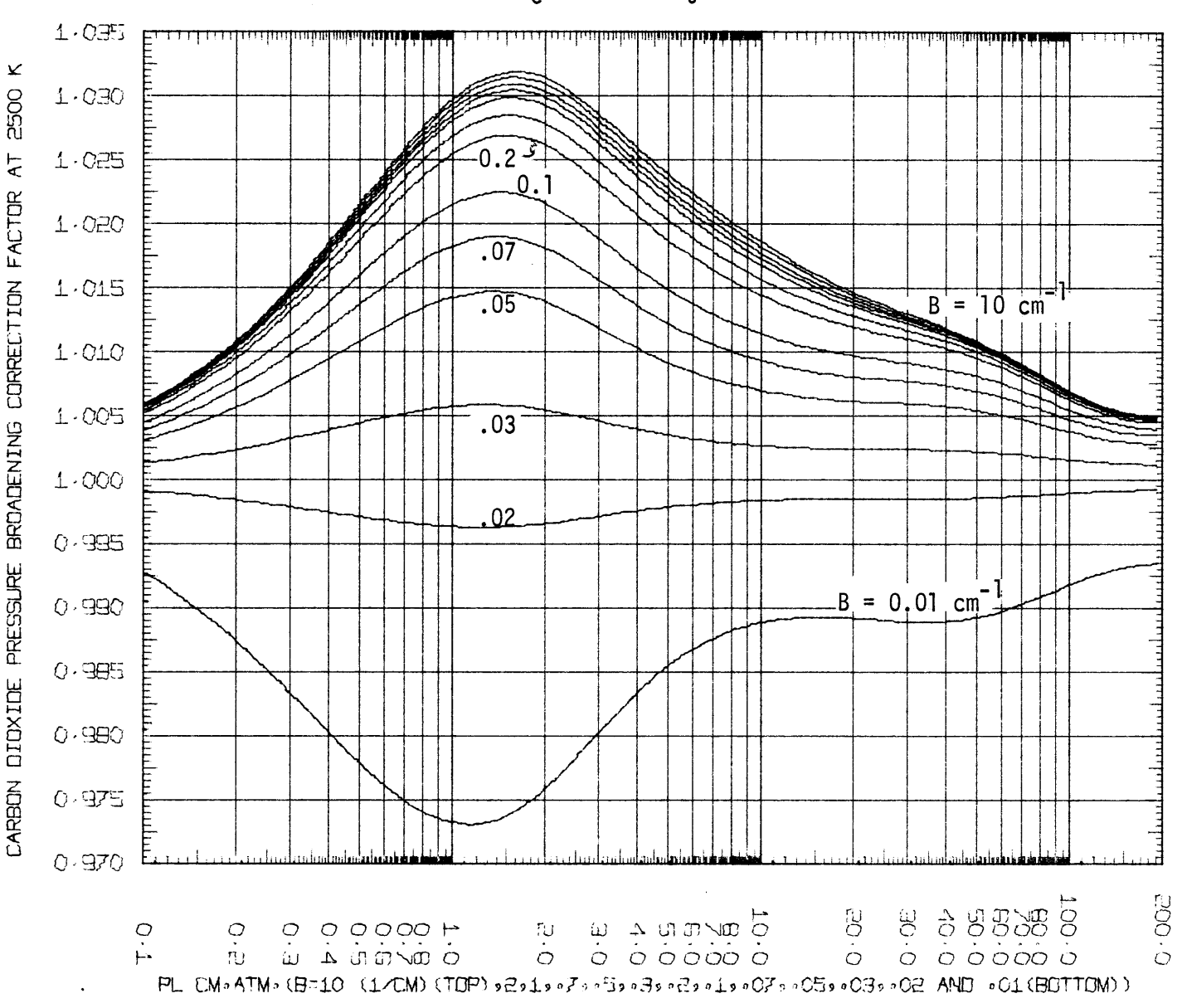
B (2500 K) = 0.0066 p_c + 0.0231 P_t
CARBON DIOXIDE PRESSURE BROADENING CORRECTION FACTOR AT 2500 K
1.035
1.030
1.025
1.020
1.015
1.010
1.005
1.000
0.995
0.990
0.985
0.980
0.975
0.970
0.2
0.1
.07
.05
.03
.02
B = 10 cm^{-1}
B = 0.01 cm^{-1}
PL CM-ATM (B=10 (1/CM) (TOP) ,2,1,.7,.5,.3,.2,.1,.07,.05,.03,.02 AND .01(BOTTOM))

Figure 5.2-5

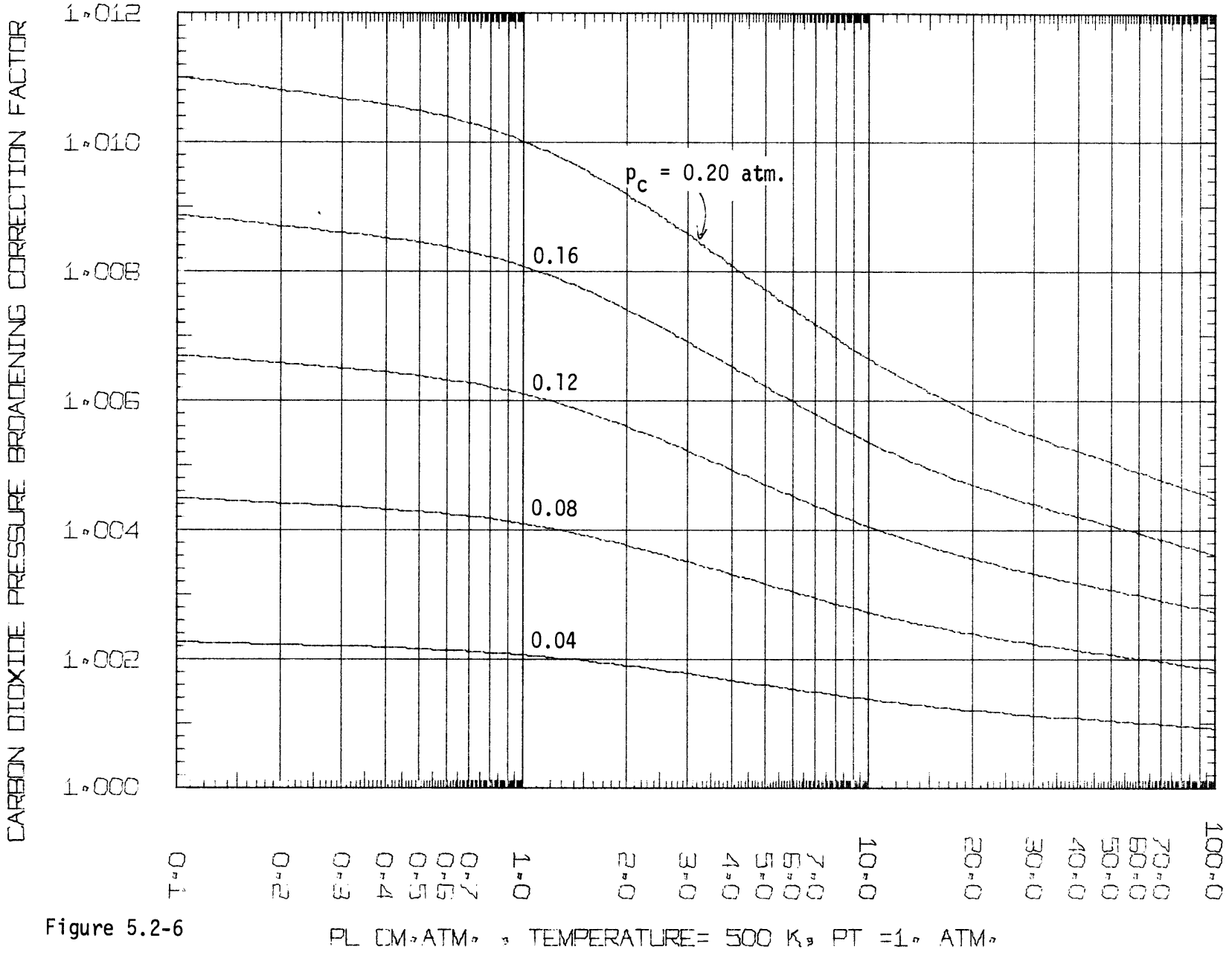
CARBON DIOXIDE PRESSURE BROADENING CORRECTION FACTOR
1.012
1.010
1.008
1.006
1.004
1.002
1.000
p_c = 0.20 atm.
0.16
0.12
0.08
0.04
0.1
0.2
0.3
0.4
0.5
0.6
0.7
1.0
2.0
3.0
4.0
5.0
6.0
7.0
10.0
20.0
30.0
40.0
50.0
60.0
70.0
100.0
PL (M-ATM) , TEMPERATURE= 500 K, PT =1. ATM)

Figure 5.2-6

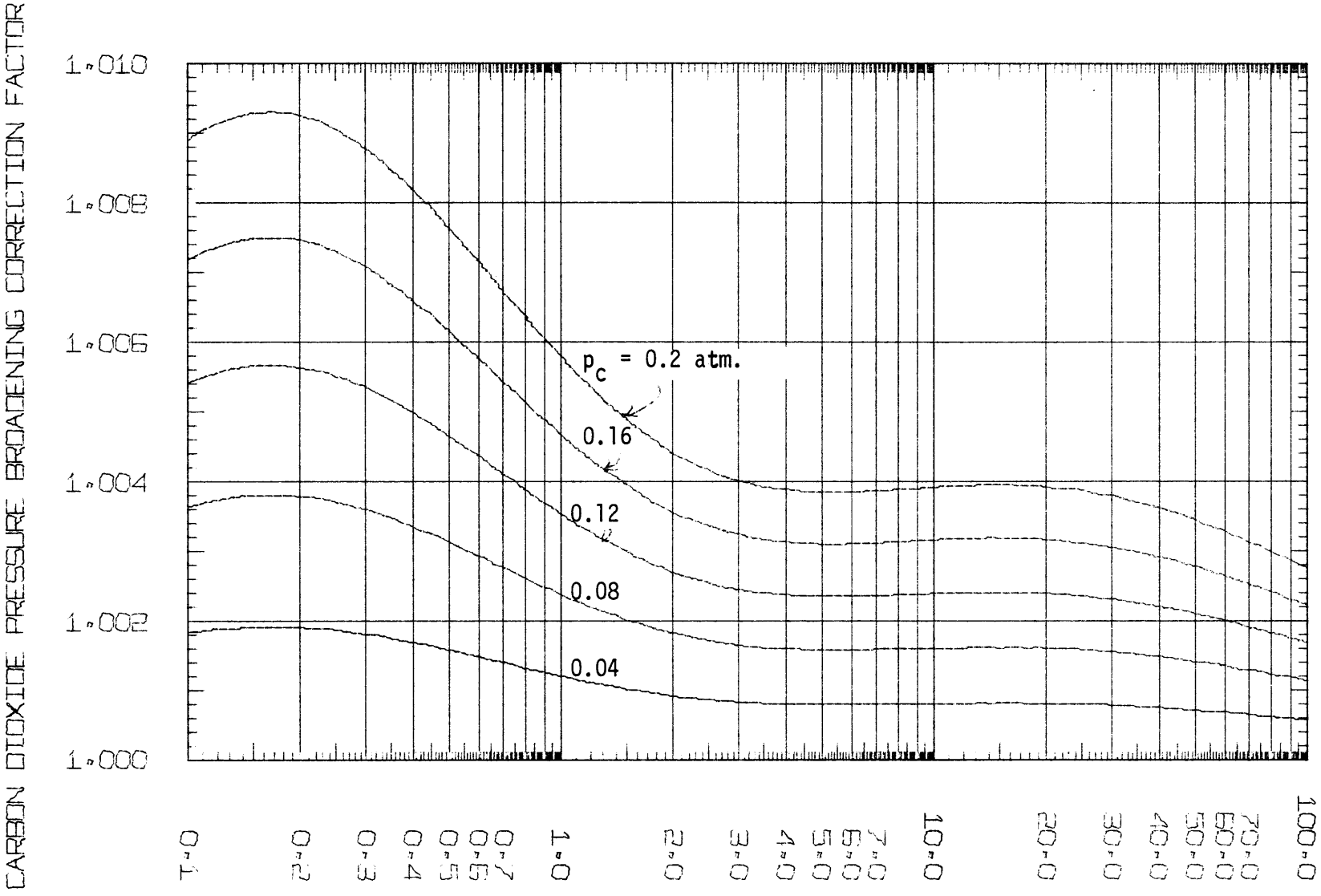
CARBON DIOXIDE PRESSURE BROADENING CORRECTION FACTOR
1.010
1.008
1.006
1.004
1.002
1.000
p_c = 0.2 atm.
0.16
0.12
0.08
0.04
0.1
0.2
0.3
0.4
0.5
0.55
0.7
1.0
2.0
3.0
4.0
5.0
7.0
10.0
20.0
30.0
40.0
50.0
60.0
75.0
100.0
PL CM-ATM, TEMPERATURE=1000 K, PT =1. ATM.

Figure 5.2-7

TABLE 5.2-1

Numerical Values of Coefficients of Equation

$$b_{CO_2,\,T} = ap_{CO_2} + cp_{H_2O} + cp_{N_2} + dp_{O_2} + ep_{H_2} + fp_{CO}$$

Temperature K	a	c	d	e	f
500	.0665	.0517	.0510	.0591	.0443
1000	.0470	.0366	.0361	.0418	.0313
1500	.0384	.0299	.0294	.0341	.0256
2000	.0333	.0259	.0255	.0296	.0222
2500	.0297	.0231	.0228	.0264	.0198

$a = 0.09\ \sqrt{273/T}$

$c = 0.07\ \sqrt{273/T} = b_{ST,\,CO_2}$

$d = 0.069\ \sqrt{273/T}$

$e = 0.08\ \sqrt{273/T}$

$f = 0.06\ \sqrt{273/T}$

charts are not very convenient. Most industrial furnaces operate around atmospheric pressure with a carbon dioxide partial pressure not exceeding 0.2 atm. These conditions represent a small section of the working charts. For practical and engineering applications the correction factors were computed as functions of the pL, carbon dioxide partial pressure in the range of .04 to .2 atm. and one atmosphere total pressure. The new charts, termed 'the engineering pressure broadening correction factor' charts are presented in Figures 5.2-6 and 5.2-7 for gas temperatures of 500 and 1000 K respectively.

Carbon dioxide correction factor falls off rapidly with increasing temperature. The maximum correction for p_c = 0.2 atm. is 1.1 percent at 500 K, and 0.92 percent at 1000 K. Additional computation indicate a maximum correction for p_c = 0.2 atm. of 0.23 percent at 1500 K. The correction factor becomes very small and presentation of any charts for furnace applications at temperatures above 1000 K is unwarranted.

An example of the application of the working charts is the case of a gas-turbine combustor operating at 1500 K at 20 atm. total pressure and a 15 cm. chamber. Assuming a 10 percent mole fraction of carbon dioxide gives p_c = 2 atm., p_cL = 30 cm. atm. The carbon dioxide emissivity read from the chart developed in the present work for p_c = 0, P_t = 1 atm., p_cL = 30 cm. atm., T = 1500 K is 0.124. Next the half width is calculated. $b = \sqrt{273/T}\, P_t\, (.02\, Y_C + .07) = \sqrt{273/1500} * 20\, (.02 * .1 + .07) = 0.614\ cm^{-1}$. From the correction chart at 1500 K, pL = 30 cm. atm. and $b = 0.614\ C_F$ is read as 1.0125, i.e. a correction of one and a quarter percent resulting is a carbon dioxide emissivity of 0.124 * 1.0125 = 0.125.

5.3. Water Vapor

The results on water vapor are less conclusive than those on carbon dioxide. Earlier calculations in the present study attempted to establish the consistency of the data of different investigators were carried out at p_w = 1 atm. and, therefore, $p_w L = L$, corresponding to the conditions of Schmidt's measurements. All experiments were found to report emissivities at p_w = 1 atm., which agreed to within 5 to 9%.

In order to effectively check the consistency of the different independent experimental measurements which had overlapping temperature range but were at different conditions of total pressure, water vapor partial pressure and pL product and to check the agreement between the present computed emissivities and the experimental data it was necessary to reduce all points to a common total and partial pressure. This was selected to be the standard condition of zero partial pressure and a total pressure of one atmosphere. The correction was achieved by computing the pressure broadening correction factor corresponding to each and every point. In many cases the difference in emissivity of the raw data taken at different p_w's was as much as 30 percent. The use of the present computed correction factor brought the points to within 10 percent. The raw water vapor emissivities at 756 K are plotted versus the pL in cm. atm. in Figure 5.3-1, which also displays the corrected emissivity corresponding to each point. The figure clearly indicates the validity of the pressure broadening correction factor computed using the present model. The corrected emissivities were grouped at temperatures of 294, 417, 522, 644, 756, 867, 978, 1300, 1389, 1517, and 1811 K. For

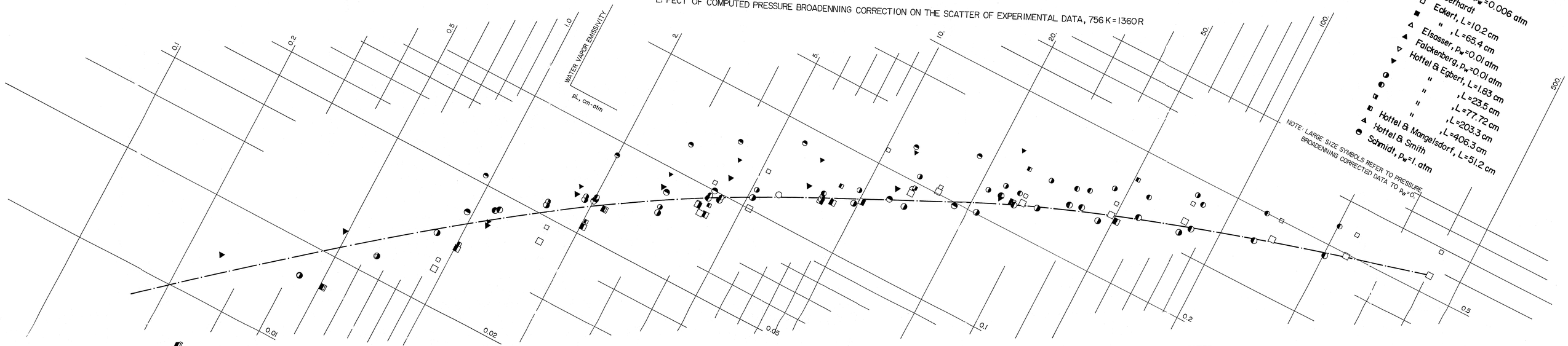
EFFECT OF COMPUTED PRESSURE BROADENNING CORRECTION ON THE SCATTER OF EXPERIMENTAL DATA, 756 K = 1360 R
WATER VAPOR EMISSIVITY
pL, cm-atm
0.1
0.2
0.5
1.0
2.
5.
10.
20.
50.
100.
500.
0.01
0.02
0.05
0.1
0.2
0.5
Brooks, p_w = 0.006 atm
Eberhardt
Eckert, L = 10.2 cm
" , L = 65.4 cm
Elsasser, p_w = 0.01 atm
Falckenberg, p_w = 0.01 atm
Hottel & Egbert, L = 1.83 cm
" , L = 23.5 cm
" , L = 77.72 cm
" , L = 203.3 cm
" , L = 406.3 cm
Hottel & Mangelsdorf, L = 51.2 cm
Hottel & Smith
Schmidt, p_w = 1. atm
NOTE: LARGE SIZE SYMBOLS REFER TO PRESSURE BROADENNING CORRECTED DATA TO p_w = 0.
SMOOTHED EXPERIMENTAL LINES PARTIALLY AFFECTED BY THE G.D. TABULATIONS

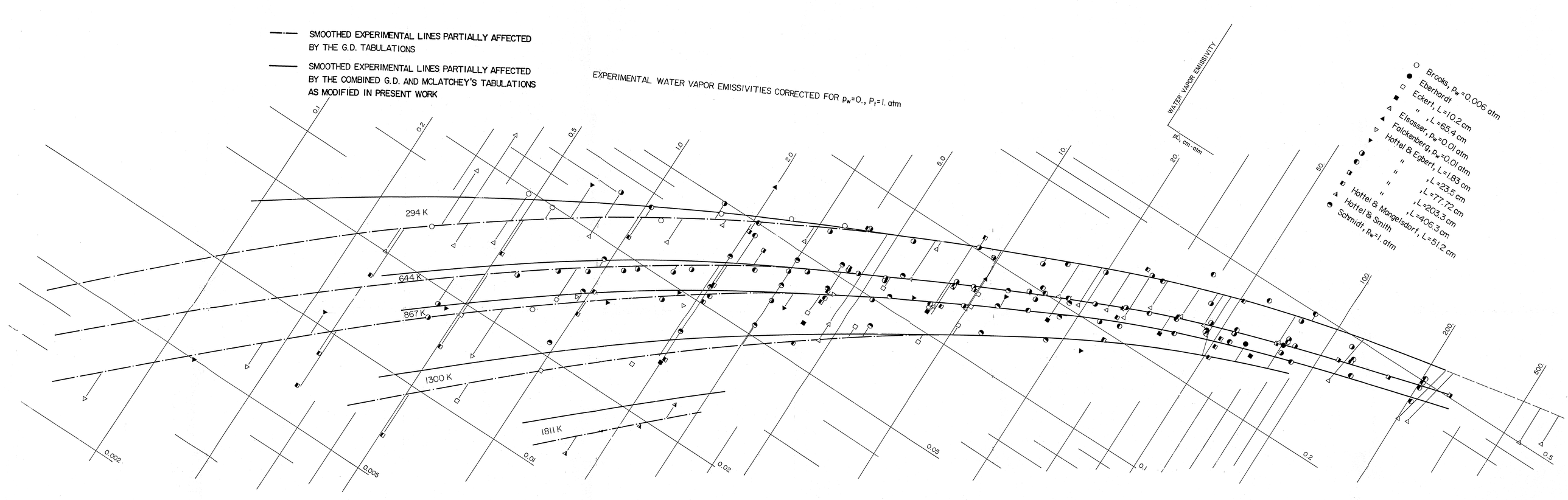
SMOOTHED EXPERIMENTAL LINES PARTIALLY AFFECTED BY THE G.D. TABULATIONS
SMOOTHED EXPERIMENTAL LINES PARTIALLY AFFECTED BY THE COMBINED G.D. AND MCLATCHEY'S TABULATIONS AS MODIFIED IN PRESENT WORK
EXPERIMENTAL WATER VAPOR EMISSIVITIES CORRECTED FOR p_w=0., P_t=1. atm
WATER VAPOR EMISSIVITY
pL, cm-atm
Brooks, p_w=0.006 atm
Eberhardt
Eckert, L=10.2 cm
" , L=65.4 cm
Elsasser, p_w=0.01 atm
Falckenberg, p_w=0.01 atm
Hottel & Egbert, L=1.83 cm
" , L=23.5 cm
" , L=77.72 cm
" , L=203.3 cm
" , L=406.3 cm
Hottel & Mangelsdorf, L=51.2 cm
Hottel & Smith
Schmidt, p_w=1. atm
294 K
644 K
867 K
1300 K
1811 K
0.1
0.2
0.5
1.0
2.0
5.0
10
20
50
100
200
500
0.002
0.005
0.01
0.02
0.05
0.1
0.2
0.5

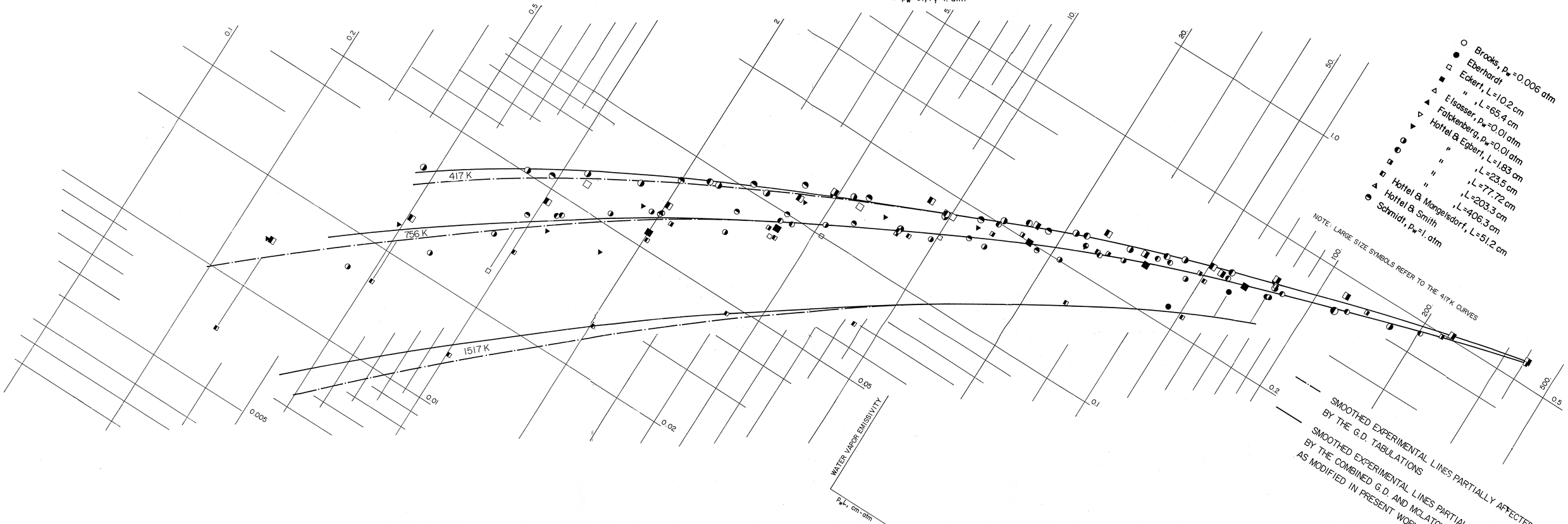
EXPERIMENTAL WATER VAPOR EMISSIVITIES CORRECTED TO p_w=0., P_t=1. atm
0.1
0.2
0.5
1.0
2
5
10
20
50.
100
200
500
0.005
0.01
0.02
0.05
0.1
0.2
0.5
417 K
756 K
1517 K
WATER VAPOR EMISSIVITY
$p_w L$, cm-atm
Brooks, p_w=0.006 atm
Eberhardt
Eckert, L=10.2 cm
" , L=65.4 cm
Elsasser, p_w=0.01 atm
Falckenberg, p_w=0.01 atm
Hottel & Egbert, L=1.83 cm
" , L=23.5 cm
" , L=77.72 cm
" , L=203.3 cm
Hottel & Mangelsdorf, L=406.3 cm
Hottel & Smith, L=51.2 cm
Schmidt, p_w=1. atm
NOTE: LARGE SIZE SYMBOLS REFER TO THE 417 K CURVES
SMOOTHED EXPERIMENTAL LINES PARTIALLY AFFECTED BY THE G.D. TABULATIONS
SMOOTHED EXPERIMENTAL LINES PARTIALLY AFFECTED BY THE COMBINED G.D. AND MCLATCHEY'S TABULATIONS AS MODIFIED IN PRESENT WORK

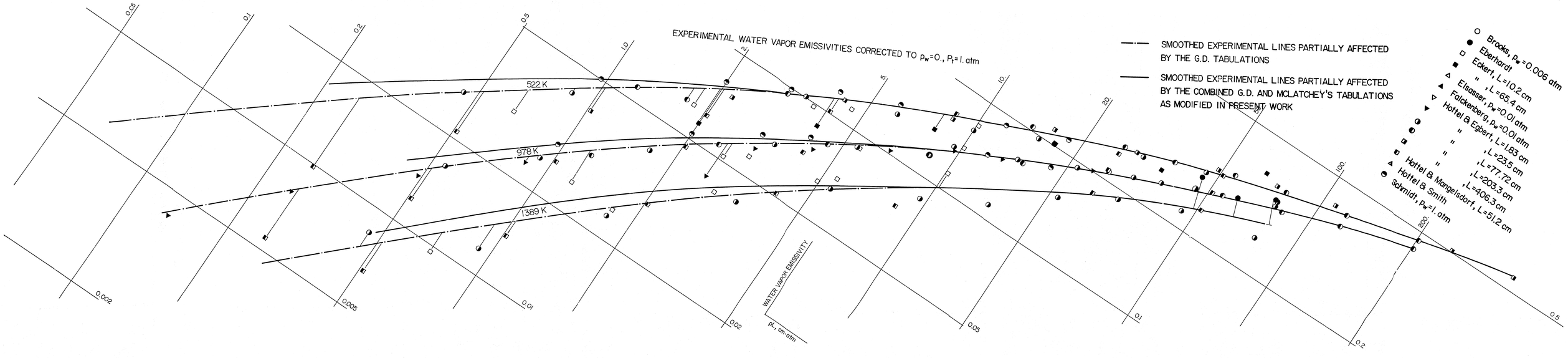
EXPERIMENTAL WATER VAPOR EMISSIVITIES CORRECTED TO p_w=0., P_t=1. atm
SMOOTHED EXPERIMENTAL LINES PARTIALLY AFFECTED BY THE G.D. TABULATIONS
SMOOTHED EXPERIMENTAL LINES PARTIALLY AFFECTED BY THE COMBINED G.D. AND MCLATCHEY'S TABULATIONS AS MODIFIED IN PRESENT WORK
522 K
978 K
1389 K
WATER VAPOR EMISSIVITY
pL, cm-atm
0.002
0.005
0.01
0.02
0.05
0.1
0.2
0.5
1.0
2
5
10
20
50
100
200
500
Brooks, p_w=0.006 atm
Eberhardt
Eckert, L=10.2 cm
" , L=65.4 cm
Elsasser, p_w=0.01 atm
Falckenberg, p_w=0.01 atm
Hottel & Egbert, L=1.83 cm
" , L=23.5 cm
" , L=77.72 cm
" , L=203.3 cm
" , L=406.3 cm
Hottel & Mangelsdorf, L=51.2 cm
Hottel & Smith
Schmidt, p_w=1. atm

purposes of clarity the data were plotted in three different plots. Figure 5.3-2 displays the corrected water vapor emissivities at 294, 644, 867, 1300 and 1811 K plotted against pL. Smooth curves were drawn to fit the experimental data. The corrected experimental emissivities at 417, 756, and 1517 K are plotted in Figure 5.3-3. Similarly the experimental emissivities at 522, 978 and 1389 K are shown in Figure 5.3-4. In order to permit easy comparison of experimental data at different temperatures and comparison with computed emissivities, Figures 5.3-4, 5.3-2 and 5.3-3 were drawn on transparent films placed on top of full logarithmic paper (10 inch cycle each direction). A piece of transparent film was used to plot the computed emissivities at the same temperatures. By overlaying the computed and experimental figures at the same temperature, it was possible to be guided by the slope of the computed curves in extrapolating the smoothed curves through the experimental points. The figures permit the identification of regions of agreement and disagreements between different measurements of the total emissivity of water vapor. For pL's of 5 to 200 cm. atm. at 417 K, 5 - 100 cm. atm. at 522 K, 10 - 100 cm. atm. at 644 K and 5 - 200 cm. atm. at temperatures of 756 to 867 the emissivities measured in different equipment and by different investigators agree to within 9% when reduced to a common p_w of zero and P_t of 1 atm. Comparison of the smoothed experimental curves with the computed emissivities indicated the computed values to be much higher than the experimental at 294 K and low pL's (less than 2 cm. atm.) while at high pL's (>100 cm. atm.) the computed values were lower by more than a facotr of 2. The agreement between the experimental data at 294 K is not very good. The consistency of the experimental data was a strong factor in deciding to give the computed values little weight in the range of good

agreement of different investigators. The resulting smooth emissivities were cross plotted against the temperature to insure their smoothness. Some minor modifications had to be made on the curves of ε v.s. p_wL to insure smoothness in both directions T and p_wL. The final smooth curves of experimental ε shown as dotted lines in Figures 5.3-2, 5.3-3, 5.3-4 and in Figure 5.3-5 in which ε is plotted against T. The line drawn to represent 0.05 cm. atm. was obtained from extrapolations of the ε v.s. p_wL curves. Figure 5.3-6 is a similar plot in which the computed emissivities are plotted against the temperature as dotted lines.

The disagreement of computed and experimental emissivities at 294 K necessitated the modification of the rotation band tabulation. Earlier attempts to include Tejwani and Varanasi spectral absorption coefficients did not result in noticeable improvements. Modification of the rotation band spectral absorption coefficients by including the more recent tabulation of McClatchey et al. from w = 425 cm^{-1} to 1000 cm^{-1} at 300 K and by interpolation from McClatchey's data at 300K to Ludwig et al's tabulation at T > 1000 K to get the spectral absorption coefficients at 600 K. These modifications resulted in a much closer agreement of computed and experimental emissivities at temperatures below 600 K, and especially at 294 K. A review of the smoothed experimental data was done resulting in alternative smooth curves that are higher at the low pL end of the ε v.s. p_wL plots. The new lines were cross plotted versus the temperature and smoothed in both directions. The resulting smooth lines are shown as solid lines in Figures 5.3-2 to 5.3-5. The modified computed emissivities are shown as solid lines in Figure 5.3-6. Whenever a solid and a dotted line coincide, a solid line is drawn.

The results show that in the range of best agreement of experimental

RECOMMENDED WATER VAPOR EMISSIVITY CHARTS

p_w=0., P_t=1. atm

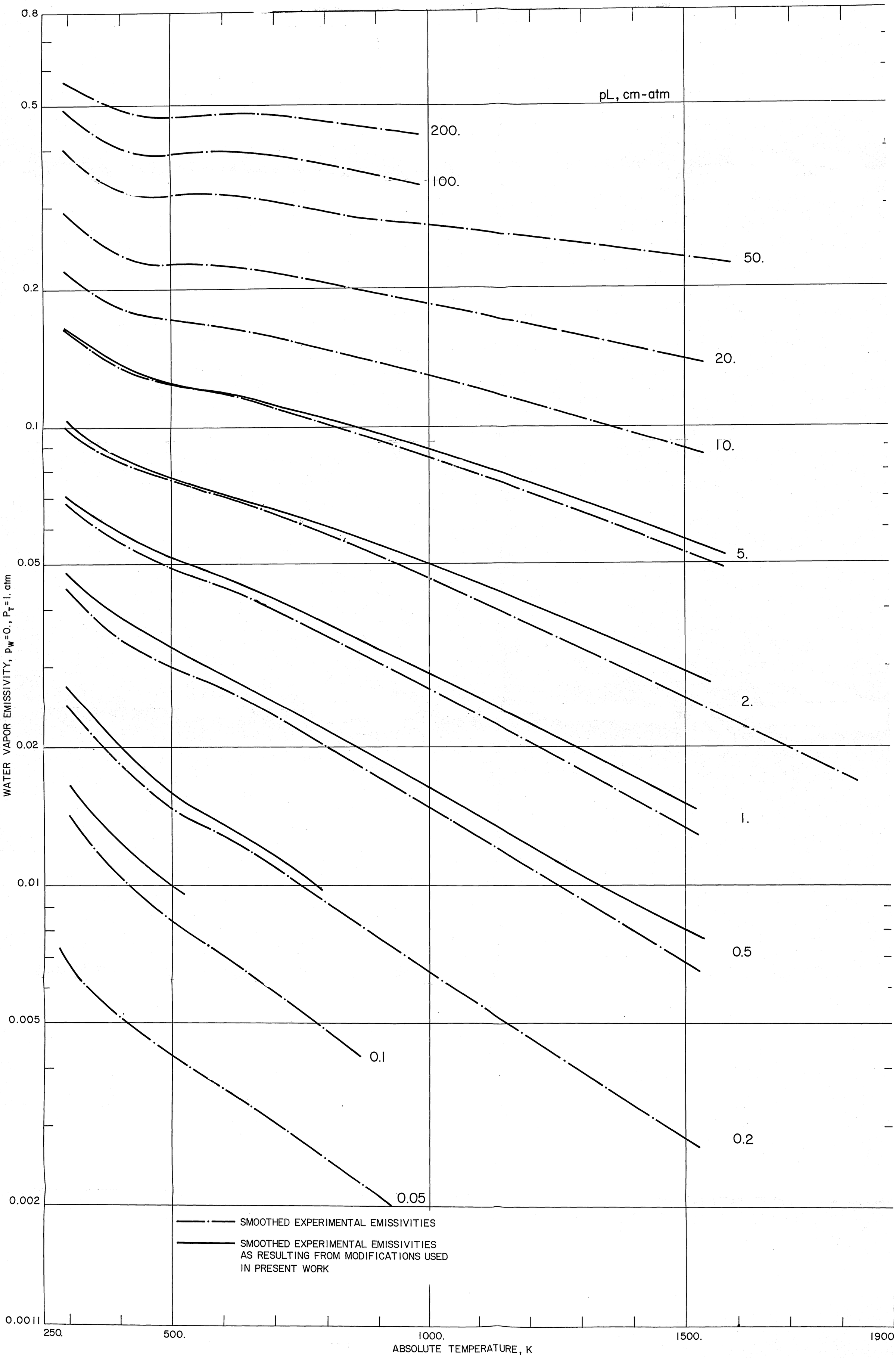

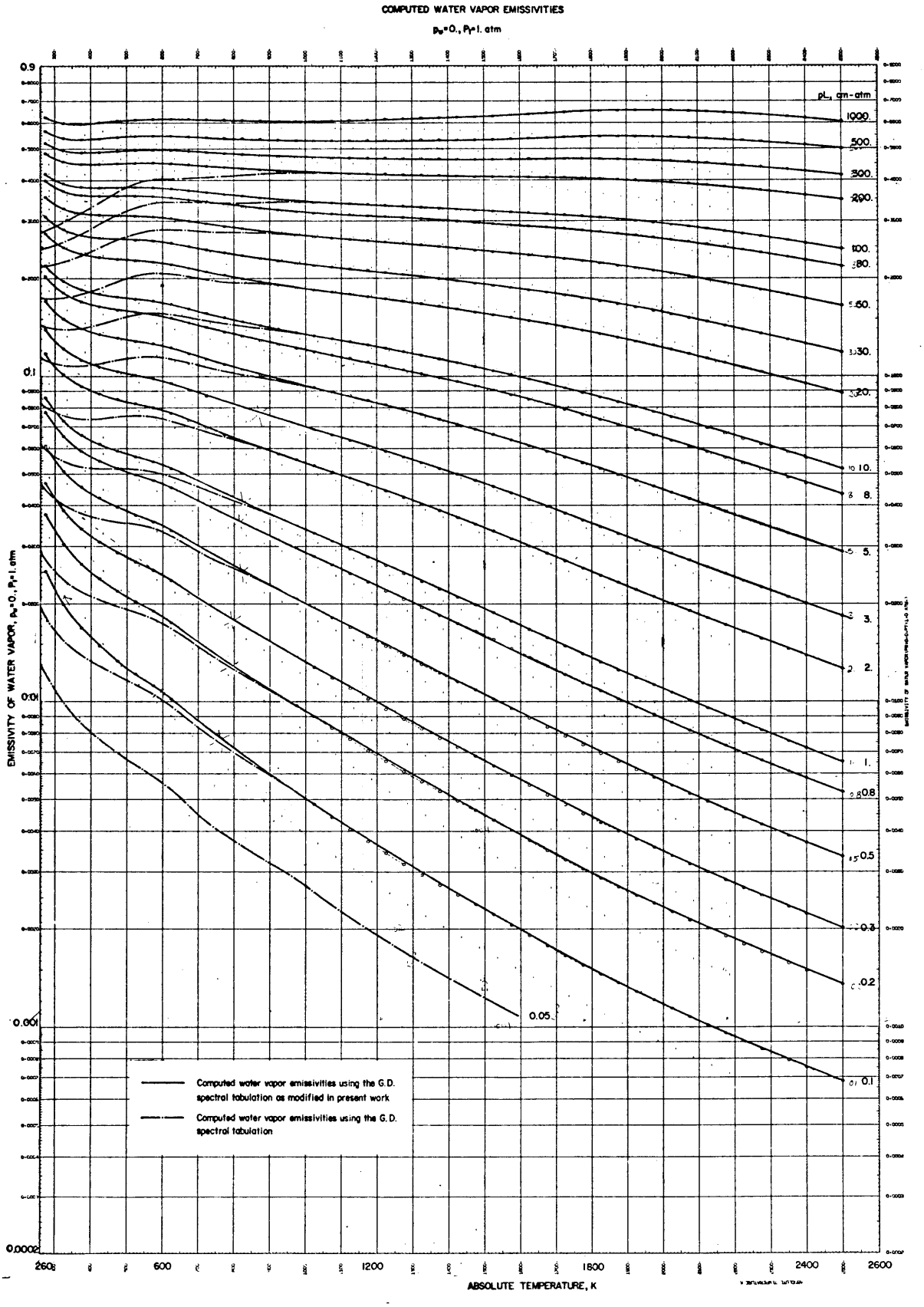
COMPUTED WATER VAPOR EMISSIVITIES
p_e=0., P_r=1. atm
EMISSIVITY OF WATER VAPOR, p_e=0., P_r=1. atm
ABSOLUTE TEMPERATURE, K
pL_r, cm-atm
1000.
500.
300.
200.
100.
80.
50.
30.
20.
10.
8.
5.
3.
2.
1.
0.8
0.5
0.3
0.2
0.1
0.05
0.9
0.1
0.01
0.001
0.0002
200
600
1200
1800
2400
2600
Computed water vapor emissivities using the G.D. spectral tabulation as modified in present work
Computed water vapor emissivities using the G.D. spectral tabulation

Figure 5.3-6

data the computed values based on a modification of Ludwig et al.'s tabulation differ from the mean of the experimental data by about 9 to 10%. The values computed from the model of Edwards and Balakrishnan are generally below the values computed using the present modification, especially at the low and high temperature ends. At low pL's, the experimental data of Hottel and Mangelsdorf and of Egbert show more scatter (30%) and differ from the computed values by as much as 48% at pL = 0.5 cm. atm. and 30% at pL = 1 cm. atm. The experimental data of Smith at 1811 K were obtained by subtracting the carbon dioxide contribution from the mixture measurements without the proper overlap correction. His measurements might have suffered from atmospheric absorption. The data of Hottel and Mangelsdorf at 1517 K were extrapolations from absorptivity measurements using a black body at 1517 K. It is apparent that a number of uncertainties remain. The most complete models are those developed from Ludwig et al. and Edwards and Balakrishnan of which the former appears to be more reliable. The computations from this model it must be recognized differ from well established total emissivity data by -9% to + 10% in the region where the total emissivity measurements are reliable. At this stage, no reliable estimate of the uncertainty of using the present model at low pL's and high temperatures is available. This is an area which needs resolution.

5.4 Pressure Broadening Correction Factor of Water Vapor

The spectral model was used to compute the pressure broadening correction factors at conditions similar to those of Scmidt, Eckert, Egbert and Mangelsdorf. A measure of the validity of the correction factors is that emissivities obtained at fixed p_wL but variable p_w in different furnaces were generally brought into closer agreement by the use of the correction factor, as discussed in Section 5.3.

As discussed in Sections 2.5 and 5.2 the pressure broadening correction factor is a function of the temperature, p_wL product and the gas half width and can be approximated by

$$b_{H_2O,\,T} = 0.44\left(\frac{273}{T}\right) p_{H_2O} + \sqrt{\frac{273}{T}}\,(0.09\, p_{H_2O} + 0.09\, p_{N_2} + 0.12\, p_{CO_2} + 0.04\, p_{O_2} + 0.05\, p_{H_2} + 0.10\, p_{CO}) \qquad (5.4\text{-}1)$$

or $$b_{H_2O,\,T} = a\, p_{H_2O} + c\, p_{N_2} + d\, p_{CO_2} + e\, p_{O_2} + f\, p_{H_2} + g\, p_{CO} \qquad (5.4\text{-}2)$$

where the coefficients a, c, d, e, f and g are temperature dependent.

For most engineering purposes assuming a standard half width of 0.09 cm^{-1} STP for all gases will not introduce appreciable error. Equation (5.4-1) therefore simplifies to

$$b_{H_2O,\,T} = \left(0.44\left(\frac{273}{T}\right) Y_{H_2O} + 0.09\sqrt{\frac{273}{T}}\right) P_t \qquad (5.4\text{-}3)$$

where Y_{H_2O} is the mole fraction of water vapor.

Therefore, the water vapor emissivity

$$\varepsilon_w = \varepsilon_w\,(T,\, pL,\, b),$$

and the graphical presentation of the above relation requires a family

of families of curves. The standard emissivity charts were drawn at zero water vapor partial pressure and a total pressure of one atmosphere. To use those charts at conditions other than $p_w = 0$ and $P_t = 1$ atm., the pressure broadening correction factor charts were developed as a function of the gas temperature, pL and half width. It was decided to present the correction factor at six temperatures of 500, 750, 1000, 1500, 2000 and 2500 K in the form of C_F versus the pL with the half width as a parameter. Figure 5.4-1 is a plot of the water vapor pressure broadening correction factor at 500 K against pL in cm. atm. for half width values of 0.01, 0.02, 0.03, 0.05, 0.07, 0.1, 0.2, 0.3, 0.5, 0.7, 1., 2. and 10 cm^{-1}. The correction factor is unity for all pL's at the "standard" half width value given by

$$b_{ST} = 0.09 \sqrt{273/T}\ cm^{-1} \qquad (T \text{ in K}).$$

Numerical values of the standard half width of water vpoar at the same six temperatures are listed in Table 5.4-1.

Figures 5.4-2 through 5.4-6 are the same type of plot, but at temperatures of 750, 1000, 1500, 2000 and 2500 K. Figures 5.4-7, 5.4-8 and 5.4-9 and the same type of plots at 1500, 2000 and 2500 K with the same scale on both axis used in Figures 5.4-1, 5.4-2 and 5.4-3 to give the reader a feel of the decrease in the magnitude, and importance of the pressure broadening with increased temperature.

To facilitate the calculation of the half width to use the charts Table 5.4-1 lists the values of the coefficients a, c ($=b_{ST}$), d, e, f and g of equation 5.4-2 at the same temperatures of the six charts.

As in the case of carbon dioxide the "engineering pressure broadening correction factor charts" are presented for water vapor partial pressures of 0.02 to 0.2 atm., total pressure of 1 atm. at the same

TABLE 5.4-1

Numerical Values of Coefficients of Equation

$$b_{H_2O,\,T} = ap_{H_2O} + cp_{N_2} + dp_{CO_2} + ep_{O_2} + fp_{H_2} + gp_{CO}$$

Temperature K	a	c (b_{ST})	d	e	f	g
500	.3067	.0665	.0887	.0296	.0369	.0739
750	.2145	.0543	.0724	.0241	.0302	.0603
1000	.1671	.0470	.0627	.0209	.0261	.0522
1500	.1185	.0384	.0512	.0171	.0213	.0427
2000	.0933	.0333	.0443	.0148	.0185	.0369
2500	.0778	.0297	.0397	.0132	.0165	.0330

$a = 0.44\ (273/T) + 0.09\ \sqrt{273/T}$

$c = 0.09\ \sqrt{273/T} = b_{ST}$

$d = 0.12\ \sqrt{273/T}$

$e = 0.04\ \sqrt{273/T}$

$f = 0.05\ \sqrt{273/T}$

$g = 0.10\ \sqrt{273/T}$

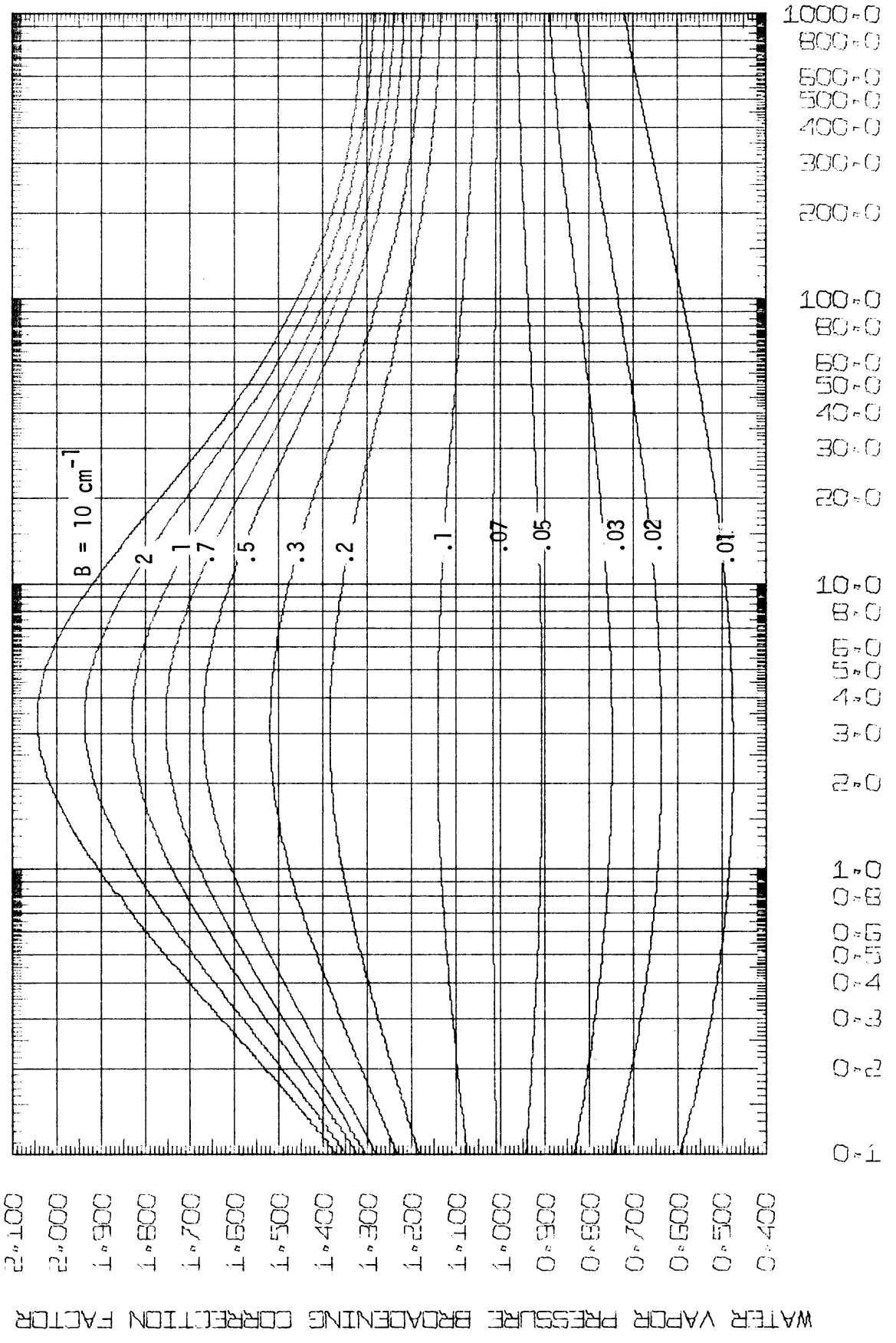
WATER VAPOR PRESSURE BROADENING CORRECTION FACTOR
2.100
2.000
1.900
1.800
1.700
1.600
1.500
1.400
1.300
1.200
1.100
1.000
0.900
0.800
0.700
0.600
0.500
0.400
B = 10 cm⁻¹
2
1
.7
.5
.3
.2
.1
.07
.05
.03
.02
.01
0.1
1
2
3
4
5
6
7
8
10
20
30
40
50
60
80
100
200
300
400
500
600
800
1000
PL CM-ATM, TEMP=500 K,B(500)=0.240 PW + 0.0665 PT

Figure 5.4-1

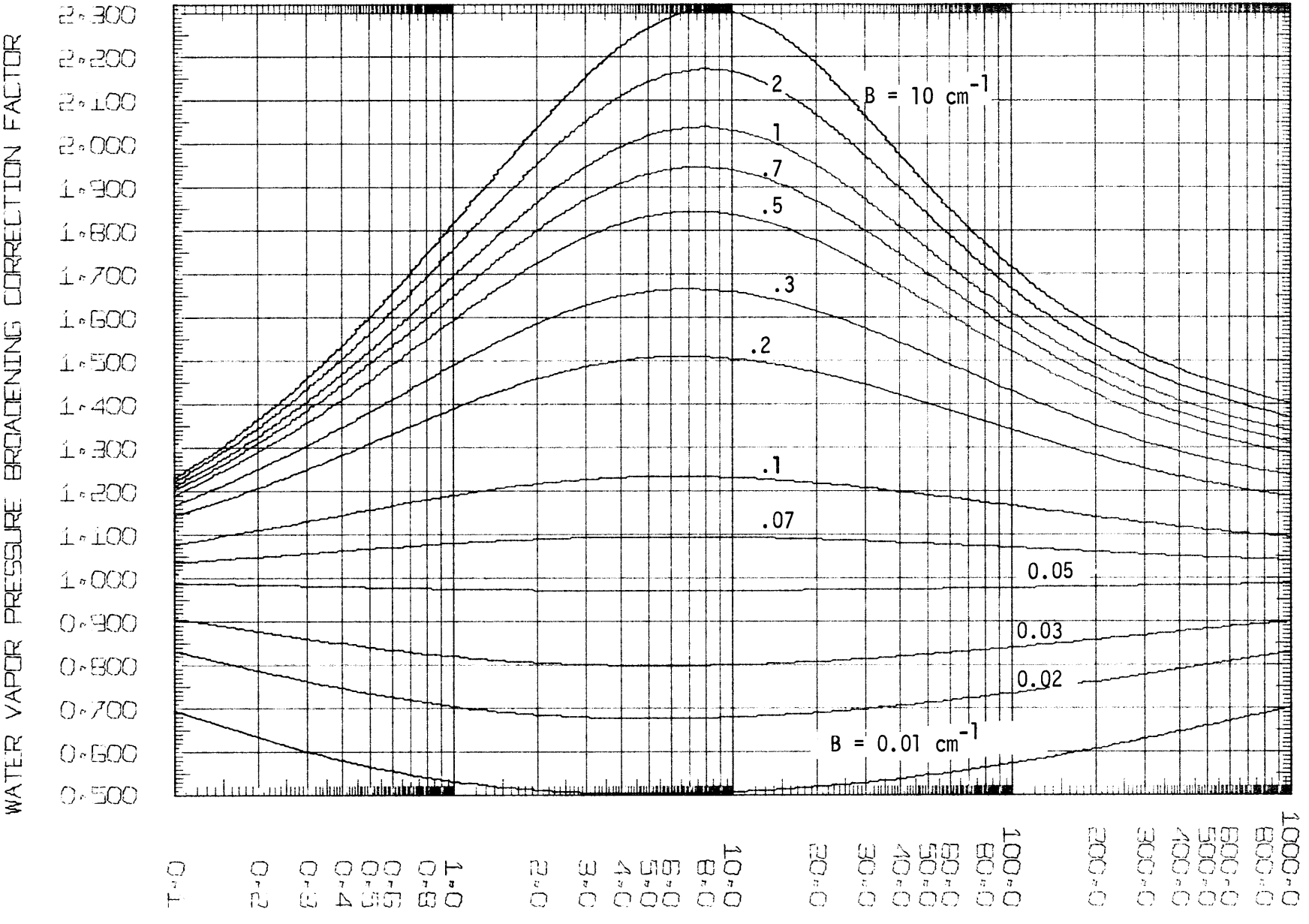

Figure 5.4-2 PL CM-ATM- -TEMP=750 K-B(750)=0-1602 PW + 0-0543 PT

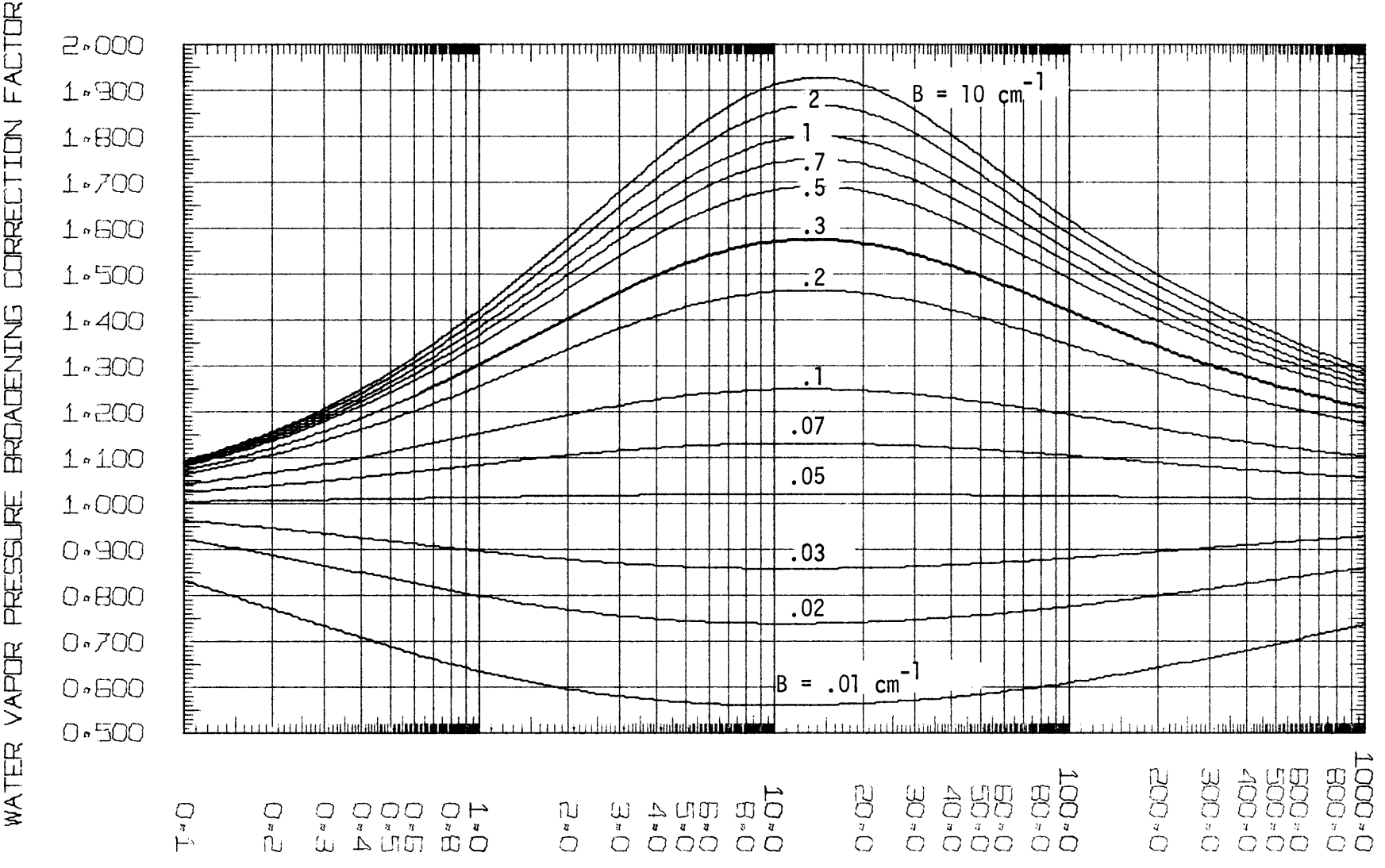

Figure 5.4-3 PL CM-ATM-,TEMP-=1000 K,B(1000)=0-1201 PW + 0-0470 PT

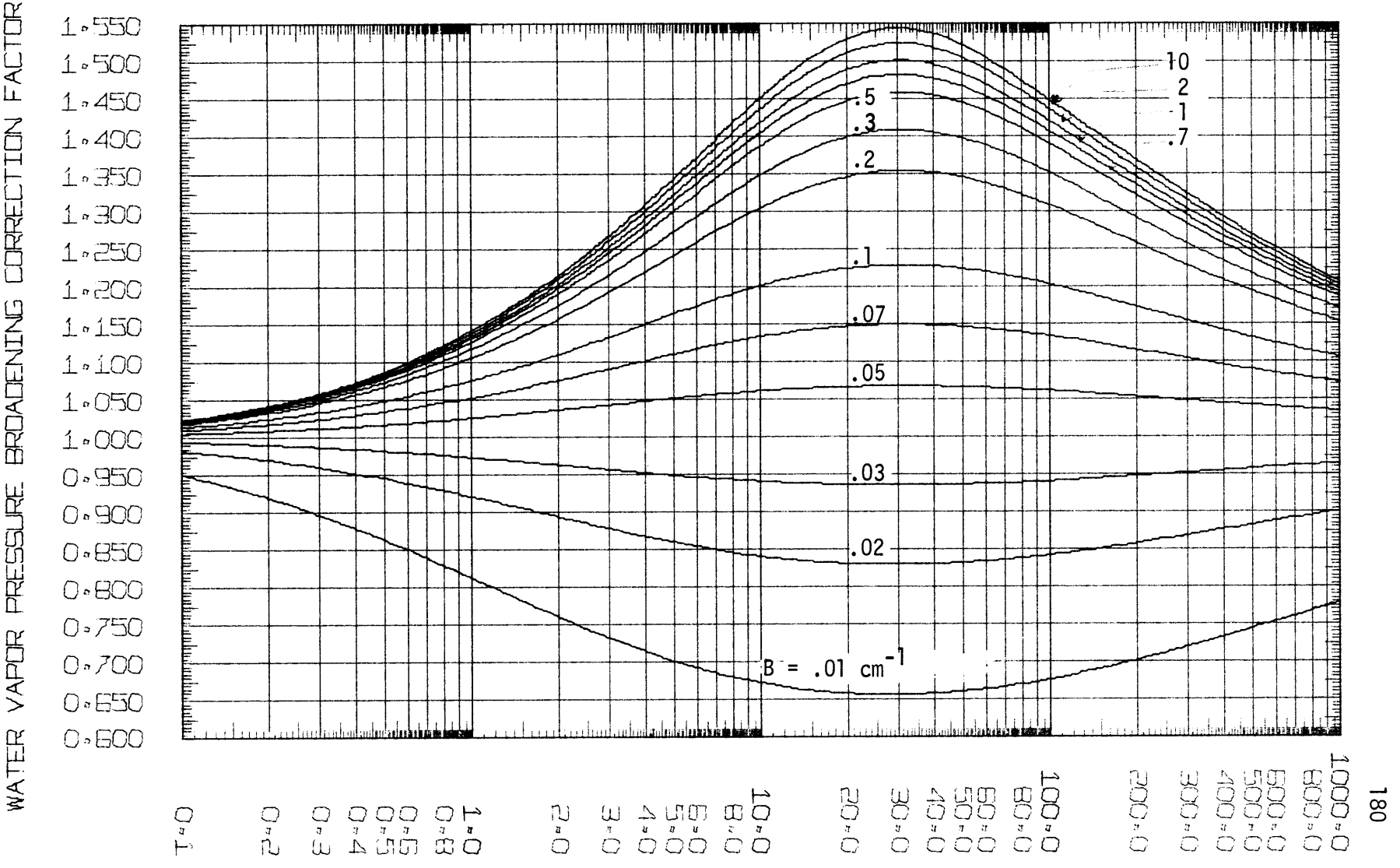

Figure 5.4-4 PL CM-ATM-,TEMP-= 1500 K,B(1500) = 0-0801 PW + 0-0384 PT

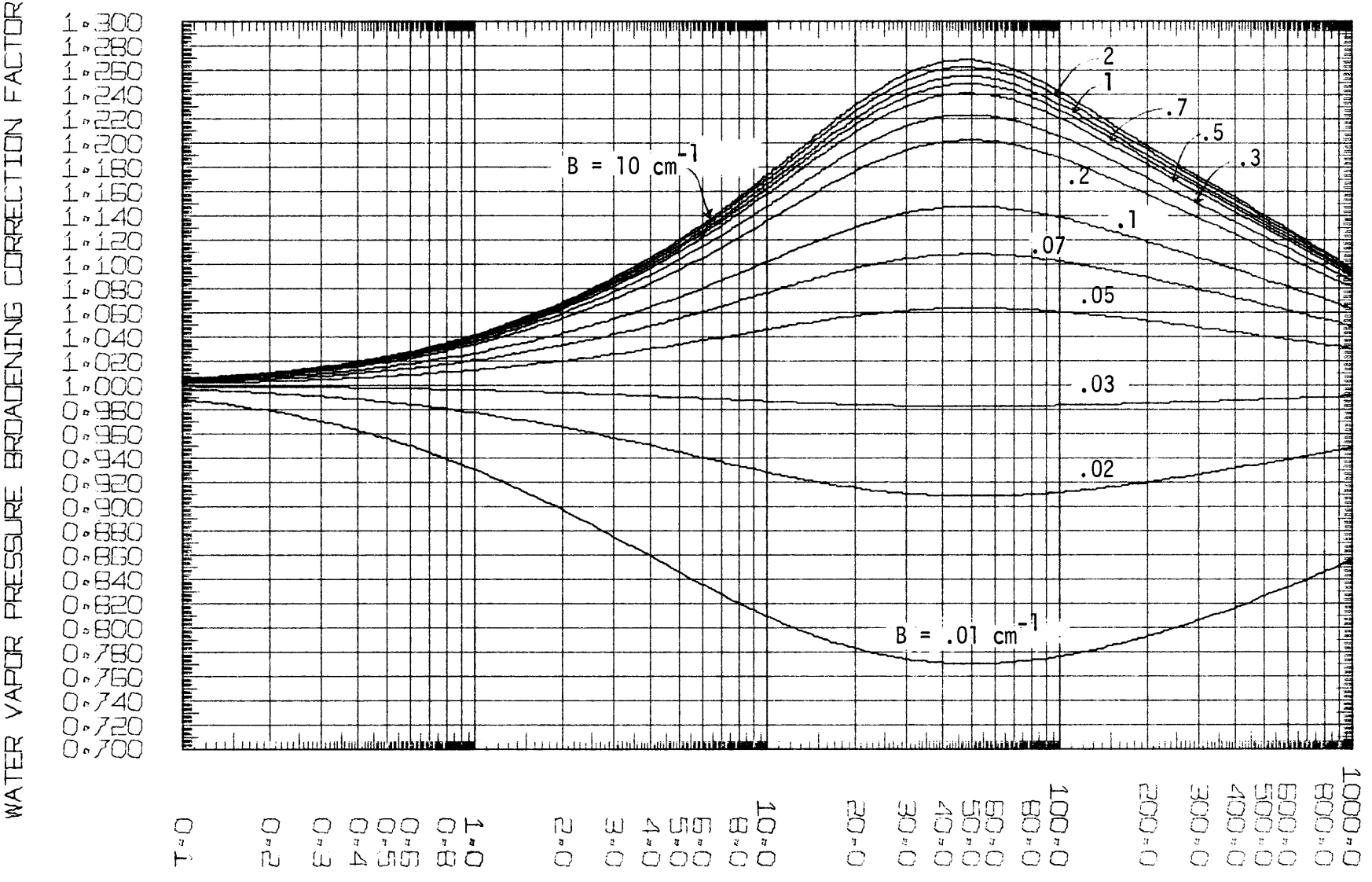
WATER VAPOR PRESSURE BROADENING CORRECTION FACTOR
1.300
1.280
1.260
1.240
1.220
1.200
1.180
1.160
1.140
1.120
1.100
1.080
1.060
1.040
1.020
1.000
0.980
0.960
0.940
0.920
0.900
0.880
0.860
0.840
0.820
0.800
0.780
0.760
0.740
0.720
0.700
B = 10 cm-1
2
1
.7
.5
.3
.2
.1
.07
.05
.03
.02
B = .01 cm-1
0.1
0.2
0.3
0.4
0.5
0.6
0.8
1.0
2.0
3.0
4.0
5.0
6.0
8.0
10.0
20.0
30.0
40.0
50.0
60.0
80.0
100.0
200.0
300.0
400.0
500.0
600.0
800.0
1000.0
PL CM-ATM-, TEMP= 2000 K, B(2000) = 0.0601 PW + 0.0333 PT

Figure 5.4-5

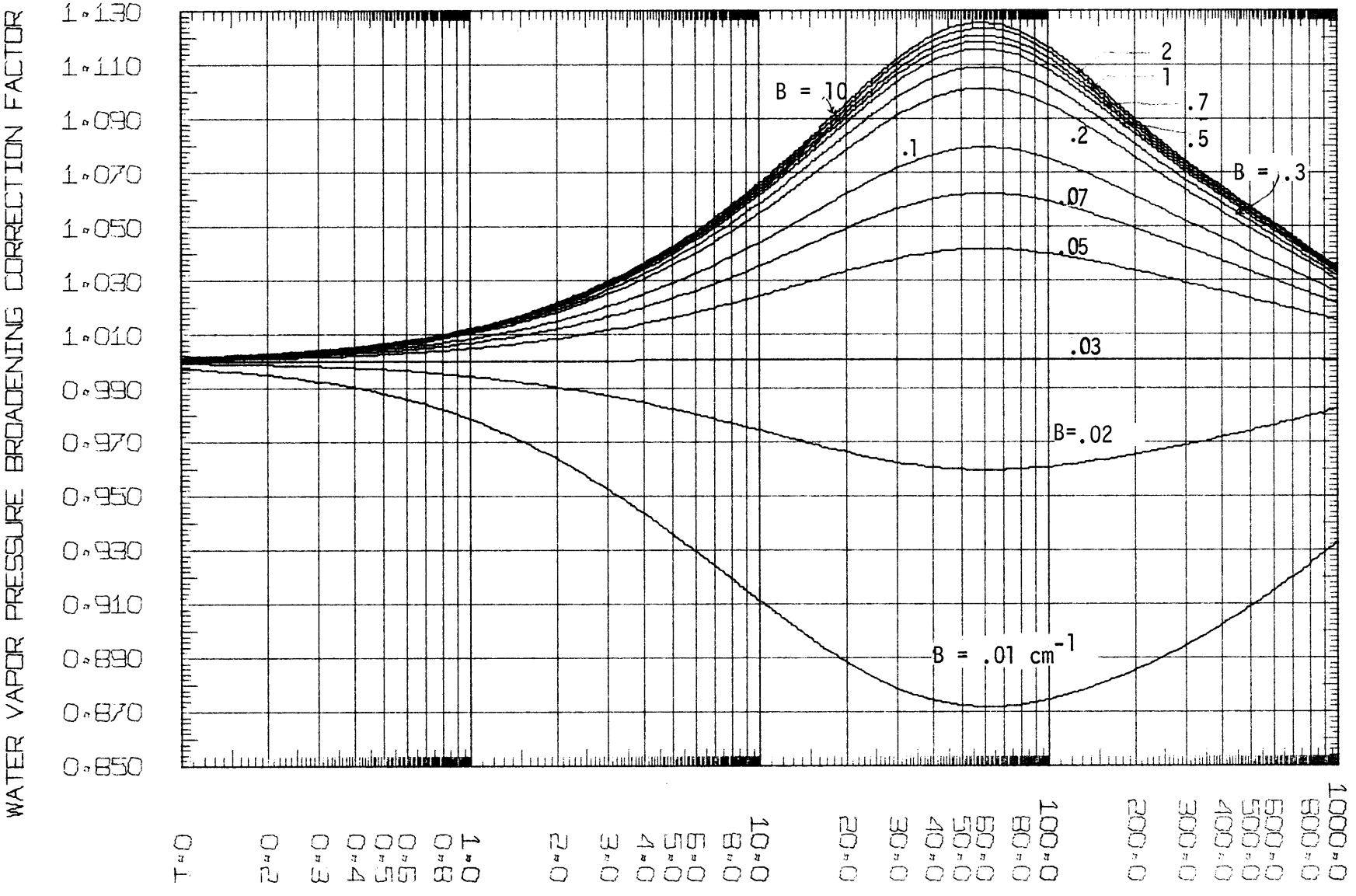

Figure 5.4-6 PL CM-ATM-,TEMP= 2500 K,B(2500) = 0.0480 PW + 0.0297 PT

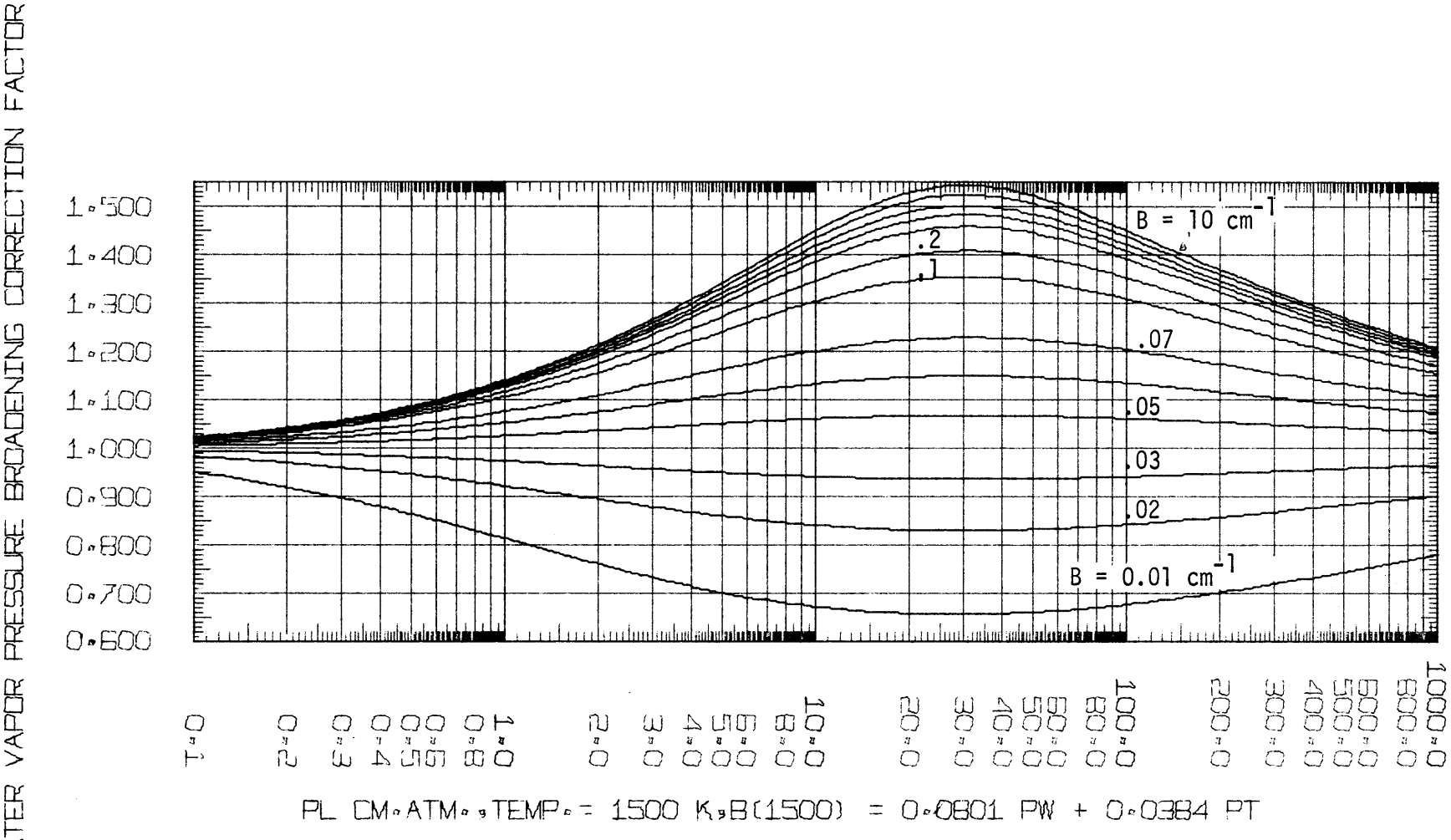
WATER VAPOR PRESSURE BROADENING CORRECTION FACTOR
1.500
1.400
1.300
1.200
1.100
1.000
0.900
0.800
0.700
0.600
B = 10 cm-1
.2
.1
.07
.05
.03
.02
B = 0.01 cm-1
0.1
0.2
0.3
0.4
0.5
0.6
0.8
1.0
2.0
3.0
4.0
5.0
6.0
8.0
10.0
20.0
30.0
40.0
50.0
60.0
80.0
100.0
200.0
300.0
400.0
500.0
600.0
800.0
1000.0
PL CM-ATM, TEMP = 1500 K, B(1500) = 0.0801 PW + 0.0384 PT

Figure 5.4-7

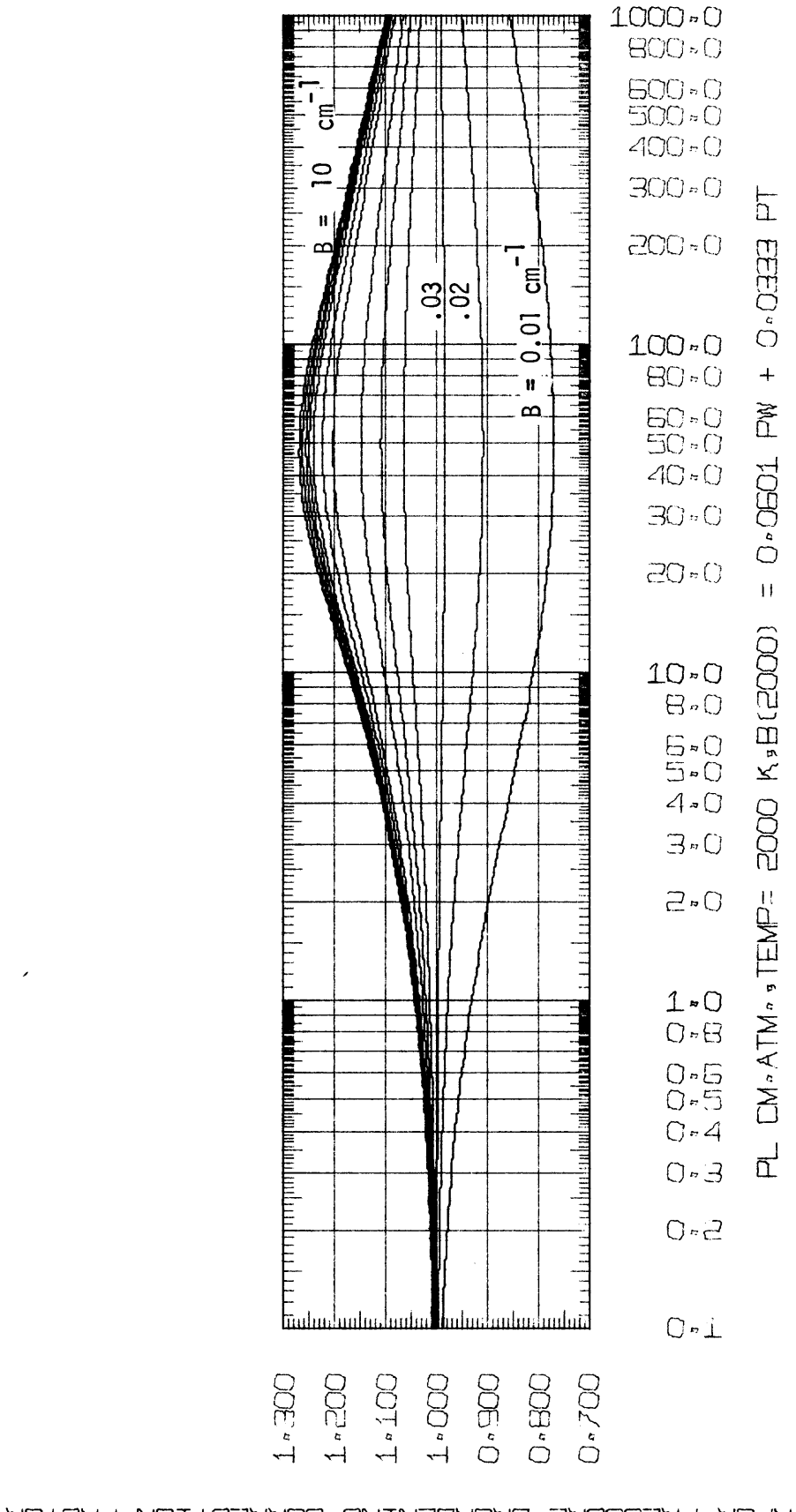
WATER VAPOR PRESSURE BROADENING CORRECTION FACTOR
1.300
1.200
1.100
1.000
0.900
0.800
0.700
B = 10 cm⁻¹
.03
.02
B = 0.01 cm⁻¹
1000.0
800.0
600.0
500.0
400.0
300.0
200.0
100.0
80.0
60.0
50.0
40.0
30.0
20.0
10.0
8.00
6.00
5.00
4.00
3.00
2.00
1.80
1.60
1.50
1.40
1.30
1.20
1.10
1.00
0.90
0.80
0.70
0.60
0.50
0.40
0.30
0.20
0.1
PL CM.ATM, TEMP= 2000 K, B(2000) = 0.0601 PW + 0.0333 PT

Figure 5.4-8

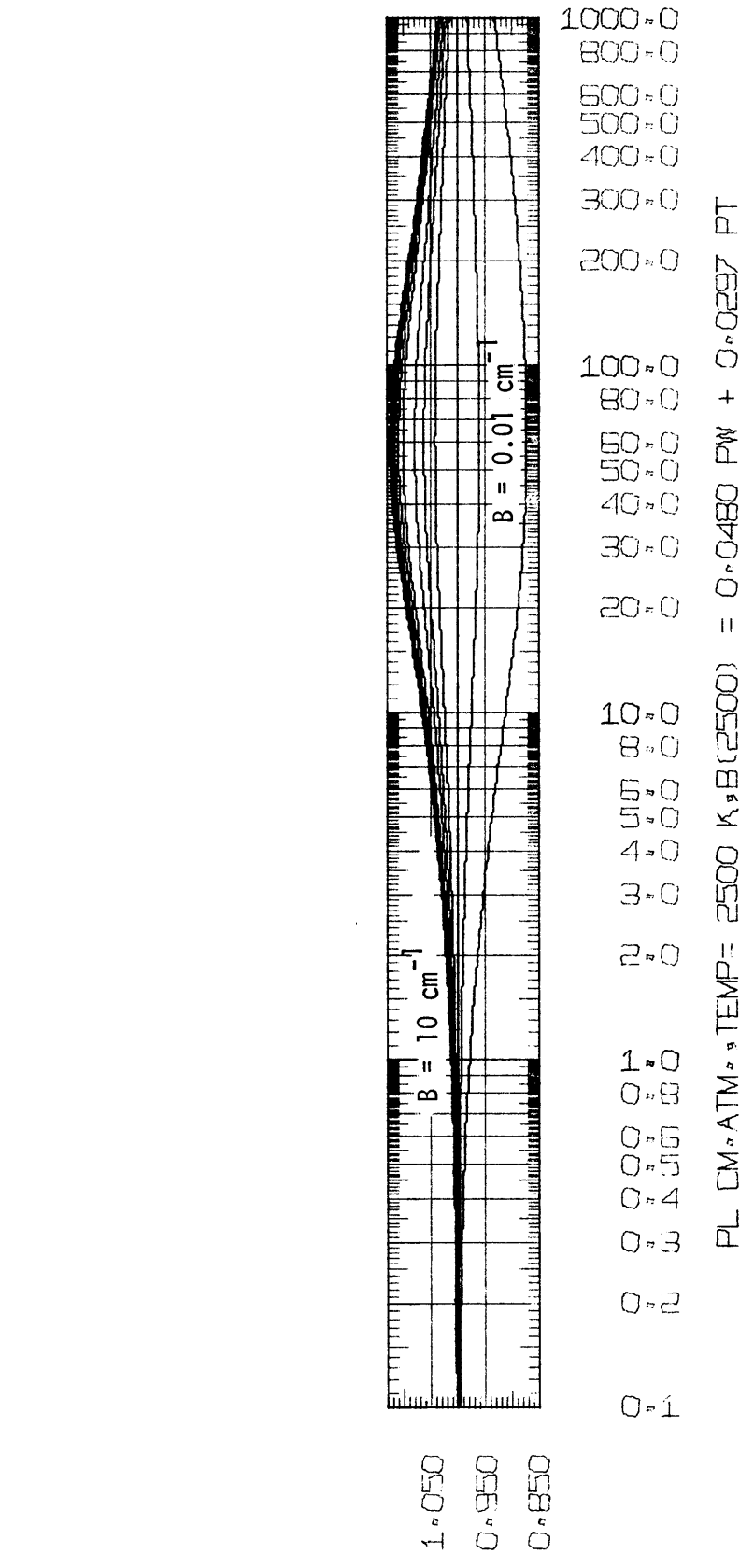
WATER VAPOR PRESSURE BROADENING CORRECTION FACTOR
1.050
0.950
0.850
B = 10 cm⁻¹
B = 0.01 cm⁻¹
0.1
0.2
0.3
0.4
0.56
0.8
1.0
2.0
3.0
4.0
5.5
8.0
10.0
20.0
30.0
40.0
50.0
60.0
80.0
100.0
200.0
300.0
400.0
500.0
600.0
800.0
1000.0
PL CM.ATM.,TEMP= 2500 K,B(2500) = 0.0480 PW + 0.0297 PT

Figure 5.4-9

six temperatures in Figures 5.4-10 through 5.4-15. All six graphs are plotted using the same scale on both axis to give the reader a better feel of the decrease in the magnitude, and importance of the pressure broadening with increased temperature. No curves are presented for a p_w of 0.02 atm. at temperatures of 2000 and 2500 K.

To get the correction factor at temperatures other than those for which the charts are given, it is presumed that the reader will use linear interpolation of C_F v.s. T using the correction factors at the nearest two temperatures. To estimate the error introduced by the use of linear interpolation the correction factors at pL's of 1, 10 and 100 cm. atm., p_w's of 0.04, 0.1 and 0.2 atm. are plotted against the temperature in Figure 5.4-16, which illustrates the importance of presenting a chart at 750 K. The figure also shows that the use of linear interpolation will introduce a maximum error in C_F of less than a couple of percent.

An example of the application of the working charts is the case of a gas turbine combustor at 1500 K at 20 atm. total pressure and a 15 cm. chamber. Assuming a 10 percent mole fraction of water vapor gives

$p_w = 2$ atm., $p_wL = 30$ cm. atm. at 1500 K

$$B_{1500} = 0.0801\ p_w + 0.0384\ P_t$$

$$= 0.0801 * 2 + 0.0384 * 20 = 0.928\ cm^{-1}$$

Next the correction factor is read from Figure 5.4-5 at $p_wL = 30$ cm. atm. and B = 0.928 as 1.235 approximately. This indicates that pressure broadening is responsible for an increase of 23.5 percent in the water vapor emissivity when the total pressure increased from 1 to 20 atm.

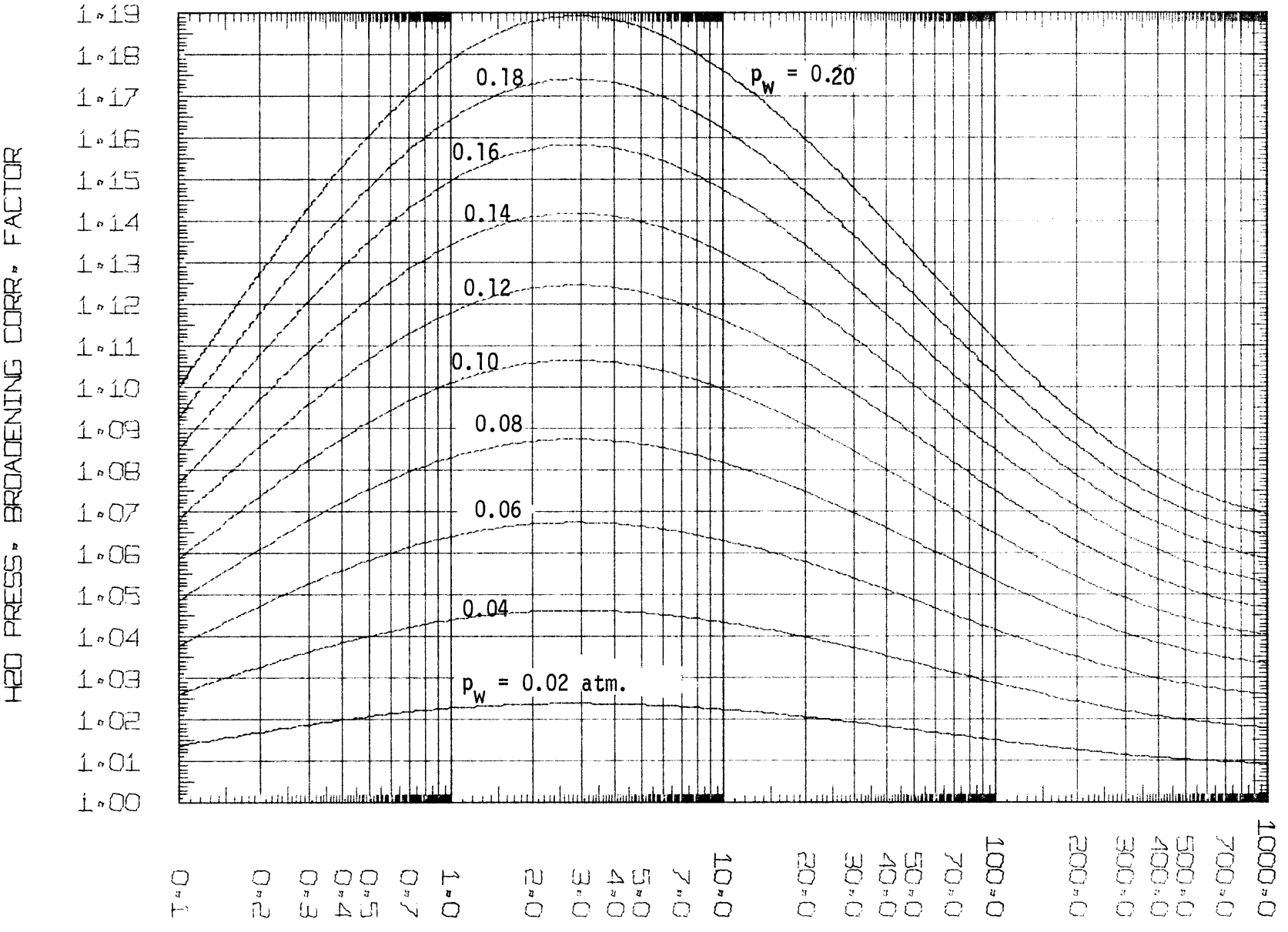
H2O PRESS. BROADENING CORR. FACTOR
1.19
1.18
1.17
1.16
1.15
1.14
1.13
1.12
1.11
1.10
1.09
1.08
1.07
1.06
1.05
1.04
1.03
1.02
1.01
1.00
0.18
0.16
0.14
0.12
0.10
0.08
0.06
0.04
p_w = 0.20
p_w = 0.02 atm.
0.1
0.2
0.3
0.4
0.5
0.7
1.0
2.0
3.0
4.0
5.0
7.0
10.0
20.0
30.0
40.0
50.0
70.0
100.0
200.0
300.0
400.0
500.0
700.0
1000.0
PL CM-ATM, TEMP= 500 K , P_t = 1 atm.

Figure 5.4-10

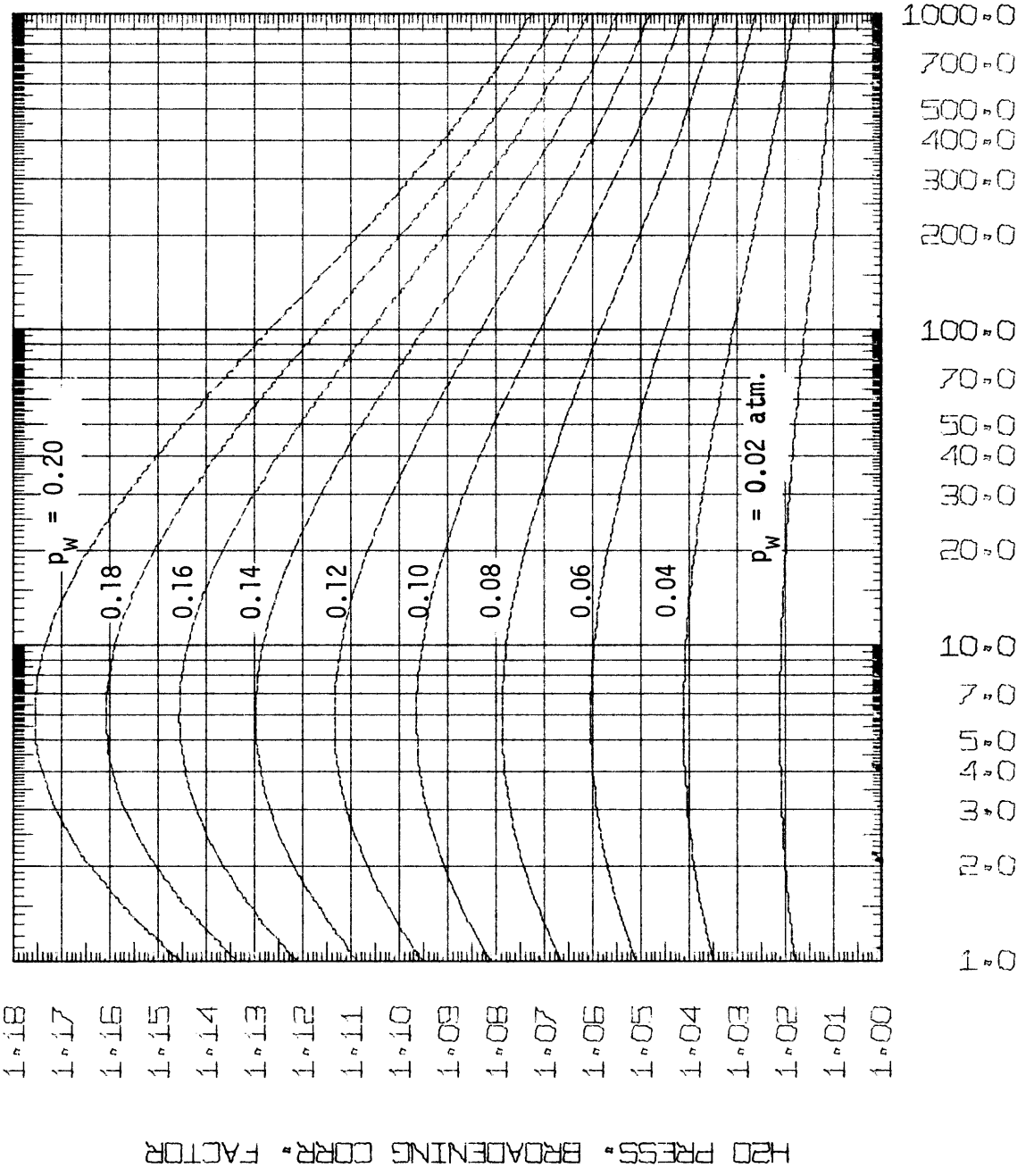
H2O PRESS. BROADENING CORR. FACTOR
1.18
1.17
1.16
1.15
1.14
1.13
1.12
1.11
1.10
1.09
1.08
1.07
1.06
1.05
1.04
1.03
1.02
1.01
1.00
PL CM.ATM. TEMP= 750 K.PT= 1. ATM.
1000.0
700.0
500.0
400.0
300.0
200.0
100.0
70.0
50.0
40.0
30.0
20.0
10.0
7.0
5.0
4.0
3.0
2.0
1.0
p_w = 0.20
0.18
0.16
0.14
0.12
0.10
0.08
0.06
0.04
p_w = 0.02 atm.

Figure 5.4-11

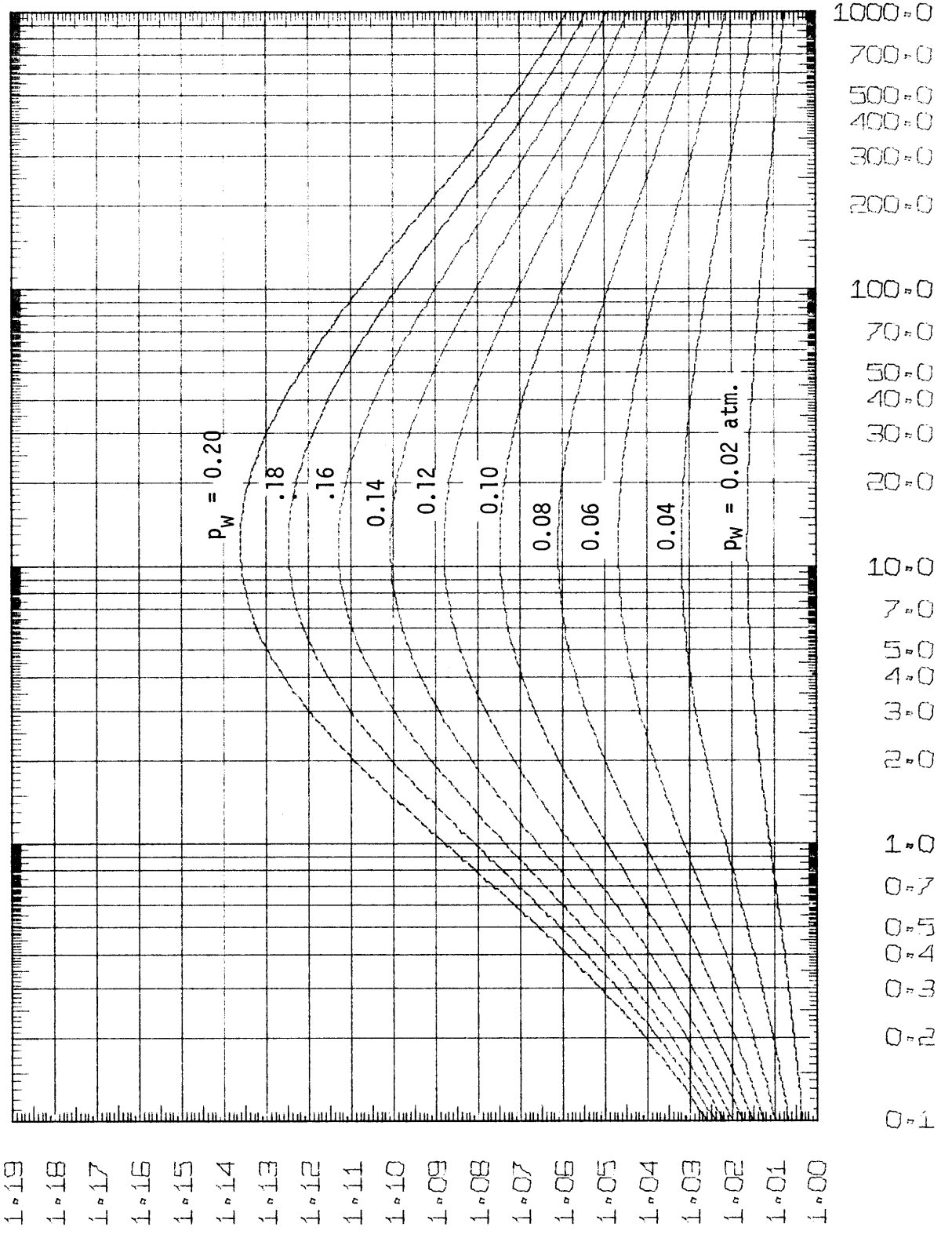
H2O PRESS. BROADENING CORR. FACTOR
1.19
1.18
1.17
1.16
1.15
1.14
1.13
1.12
1.11
1.10
1.09
1.08
1.07
1.06
1.05
1.04
1.03
1.02
1.01
1.00
P_w = 0.20
.18
.16
0.14
0.12
0.10
0.08
0.06
0.04
P_w = 0.02 atm.
1000.0
700.0
500.0
400.0
300.0
200.0
100.0
70.0
50.0
40.0
30.0
20.0
10.0
7.0
5.0
4.0
3.0
2.0
1.0
0.7
0.5
0.4
0.3
0.2
0.1
PL CM-ATM, TEMP=1000 K , P_t = 1 atm.

Figure 5.4-12

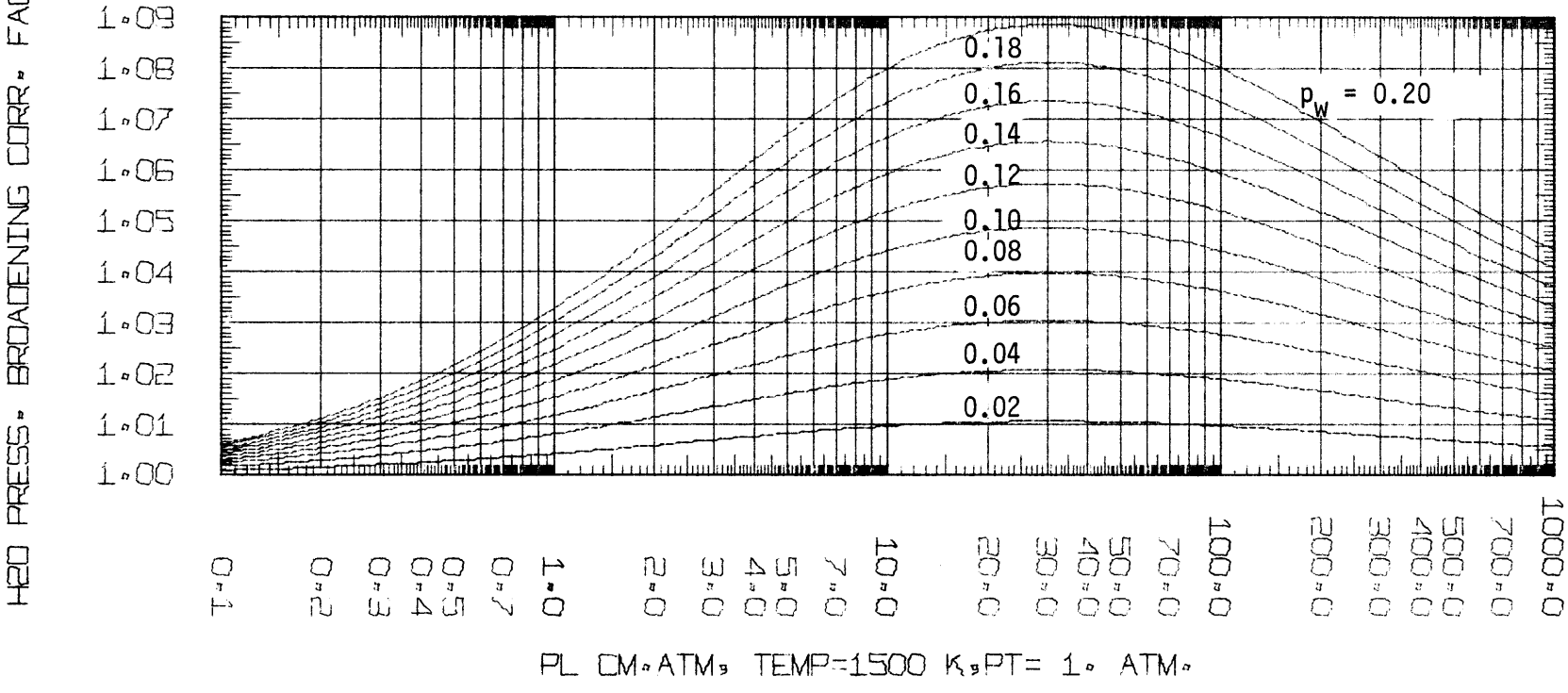
H2O PRESS. BROADENING CORR. FACTOR
1.09
1.08
1.07
1.06
1.05
1.04
1.03
1.02
1.01
1.00
0.18
0.16
0.14
0.12
0.10
0.08
0.06
0.04
0.02
p_w = 0.20
0.1
0.2
0.3
0.4
0.5
0.7
1.0
2.0
3.0
4.0
5.0
7.0
10.0
20.0
30.0
40.0
50.0
70.0
100.0
200.0
300.0
400.0
500.0
700.0
1000.0
PL CM.ATM, TEMP=1500 K,PT= 1. ATM.

Figure 5.4-13

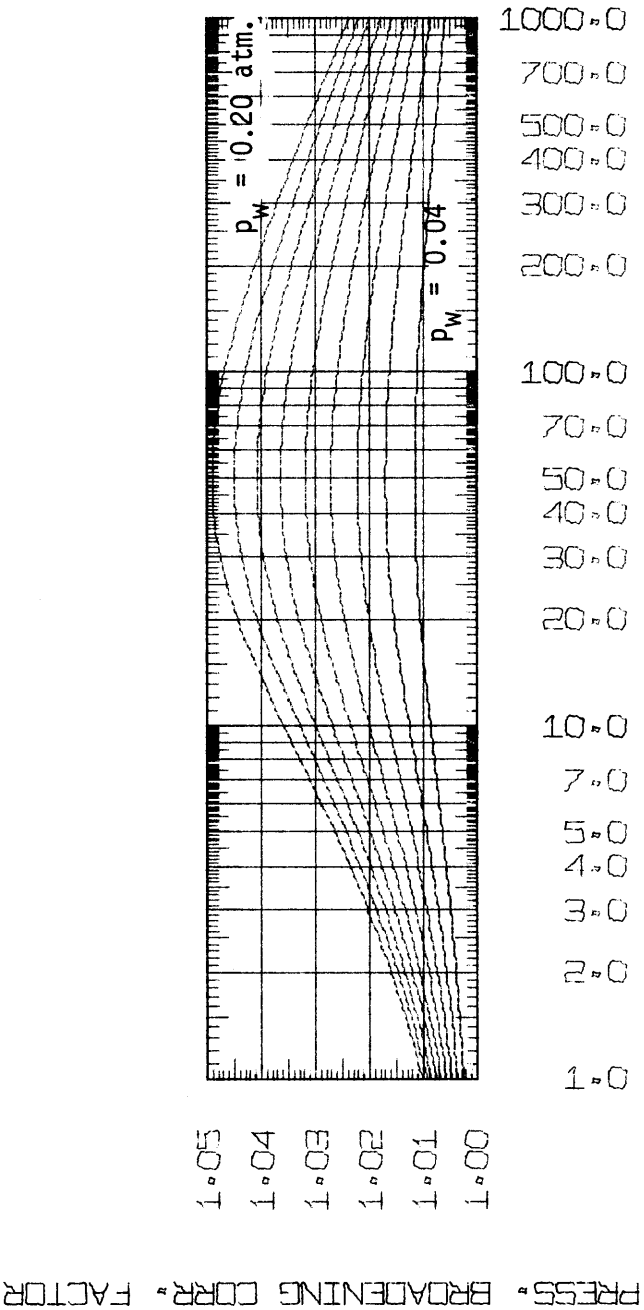
P_w = 0.20 atm.
P_w = 0.04
1000.0
700.0
500.0
400.0
300.0
200.0
100.0
70.0
50.0
40.0
30.0
20.0
10.0
7.0
5.0
4.0
3.0
2.0
1.0
1.05
1.04
1.03
1.02
1.01
1.00
PL CM.ATM, TEMP=2000 K, PT= 1. ATM.
H2O PRESS. BROADENING CORR. FACTOR

Figure 5.4-14

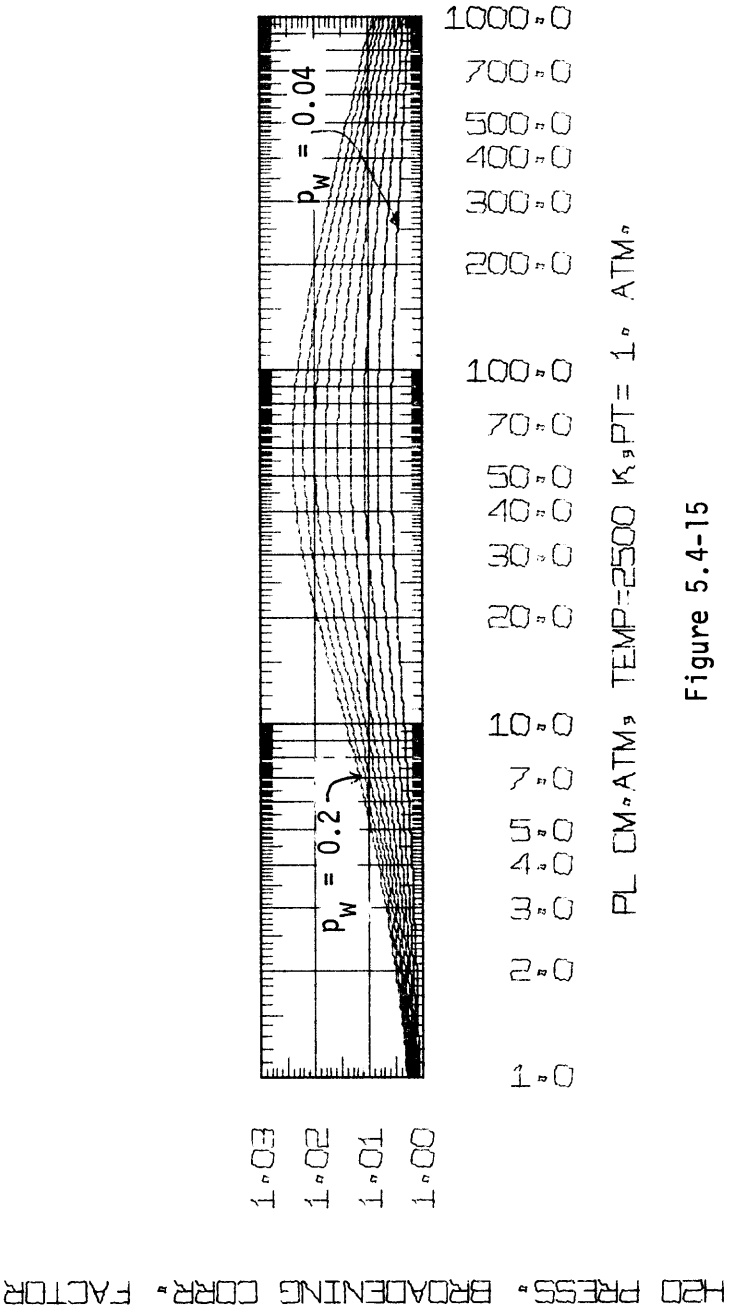
H2O PRESS. BROADENING CORR. FACTOR
1.03
1.02
1.01
1.00
p_w = 0.2
p_w = 0.04
PL CM.ATM, TEMP=2500 K,PT= 1. ATM.
1000.0
700.0
500.0
400.0
300.0
200.0
100.0
70.0
50.0
40.0
30.0
20.0
10.0
7.0
5.0
4.0
3.0
2.0
1.0

Figure 5.4-15

EFFECT OF TEMPERATURE ON WATER
VAPOR PRESSURE CORRECTION FACTOR

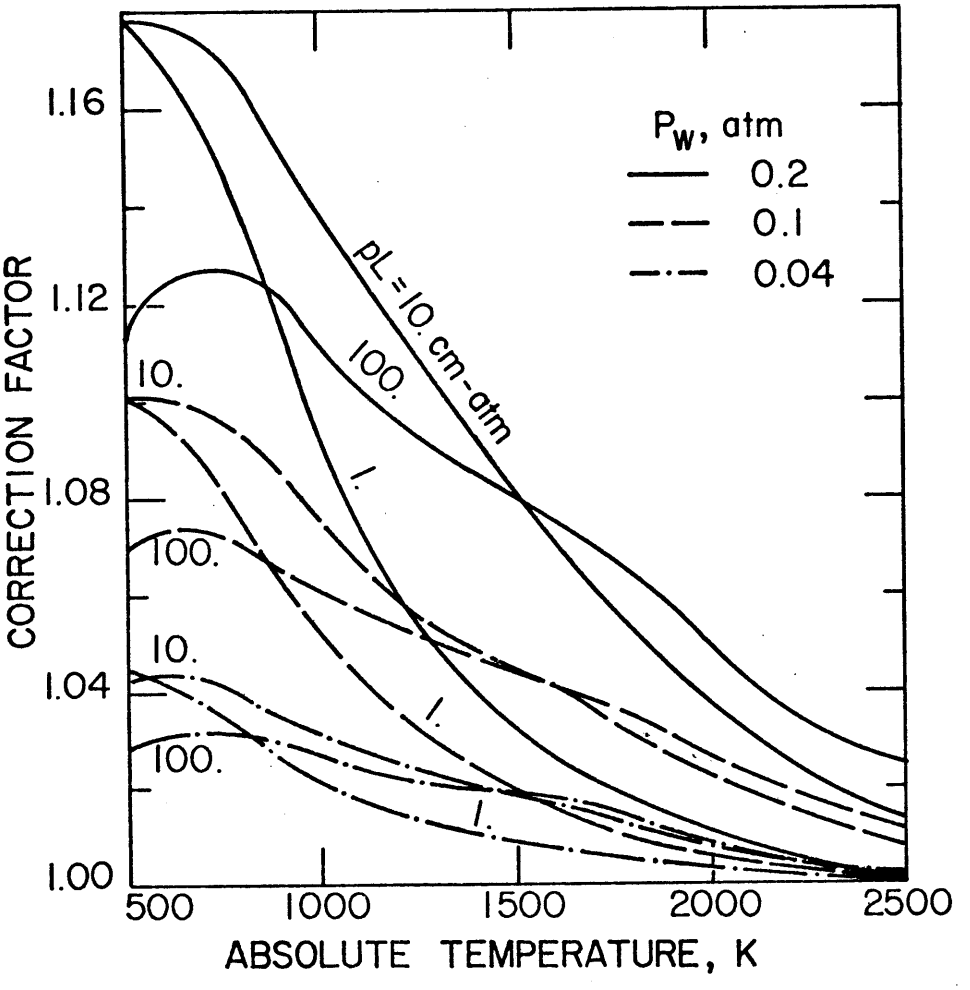

Figure 5.4-16

5.5. Overlap Correction Results and Discussion

Spectral emissivities of water vapor and carbon dioxide gases were measured at elevated temperatures by Ferriso et al. (1964). But since both gases were optically thin, the overlap correction was practically zero.

The classic example of the overlap correction is the chart developed by Hottel by cross plotting data calculated by Eckert from then available low-temperature low-resolution absorption spectra of water vapor and carbon dioxide . Comparison of the present computed overlap corrections and the Eckert charts at temperatures of 260 F (400 K), 1000 F (811 K) and 1700 F (1200 K) and $p_{c+w}L$'s of .75, 1, 1.5, 2, 3 and 5 ft. atm. are shown in Figures 5.5-1, 5.5-2 and 5.5-3 respectively. The curves show agreement generally on the location of the maximum of the curves. At 260 F and $p_w/(p_w+p_c)$ of 0.5 or less the computed $\Delta\varepsilon$ are consistently higher than Eckerts. At $p_w/(p_w + p_c)$ of 0.6 and above the computed values are higher than Eckert's at pL less than 1.5 ft. atm., and are lower at higher pL's.

At 1000 F the computed overlap corrections are higher than Eckert's values at pL's greater than 2 ft. atm. At 1700 F the computed overlap corrections are lower than Eckert's values at pL's less than 3 ft. atm. The important point here is that the disagreement between the two sets of curves is never more than 50% at all temperatures and pL's of 0.75 and higher. Considering that Eckert charts were published by Hottel to be a temporary measure of the overlap correction disagreements of this magnitude are not surprising.

Millard (1935) measured the radiation of illuminating gas in the

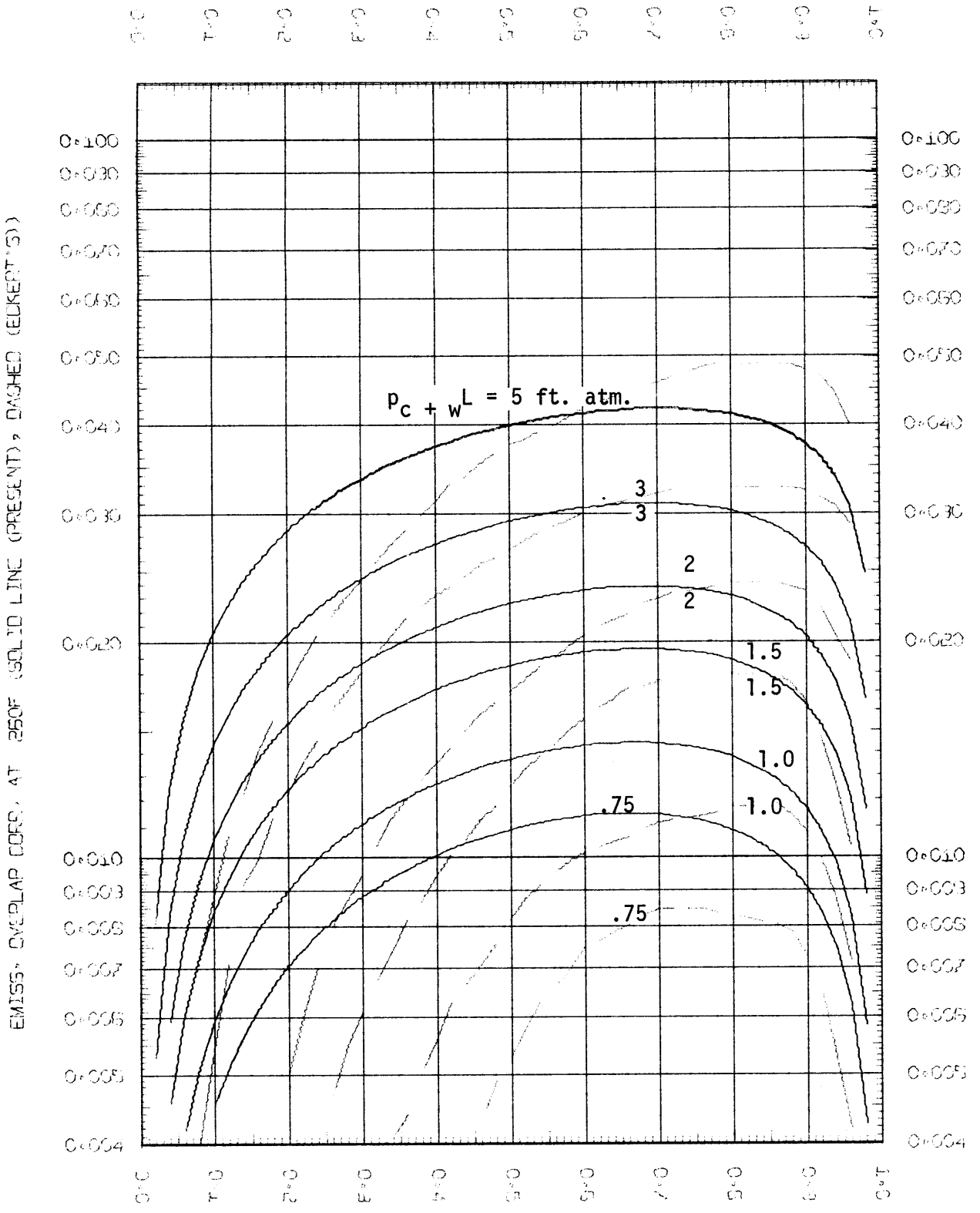

Figure 5.5-1

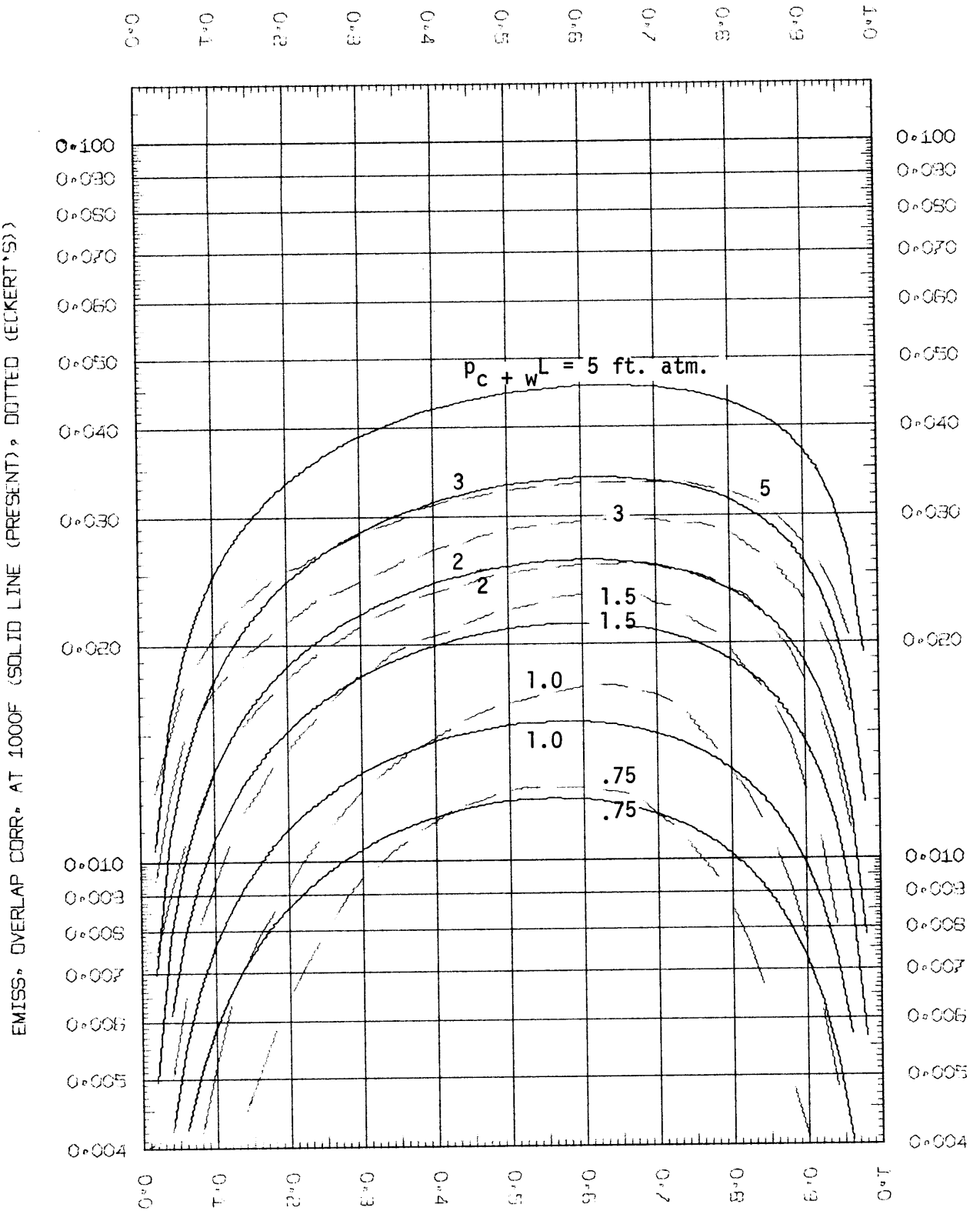
EMISS. OVERLAP CORR. AT 1000F (SOLID LINE (PRESENT), DOTTED (ECKERT'S))
PW/(PW+PC) (CURVES ARE FOR PL=5.FT.ATM. (TOP),3,,2,,1.5,1. AND 0.75 (BOTTOM))
$p_c + w^L$ = 5 ft. atm.
5
3
3
2
2
1.5
1.5
1.0
1.0
.75
.75
0.0
0.1
0.2
0.3
0.4
0.5
0.6
0.7
0.8
0.9
1.0
0.100
0.090
0.080
0.070
0.060
0.050
0.040
0.030
0.020
0.010
0.009
0.008
0.007
0.006
0.005
0.004

Figure 5.5-2

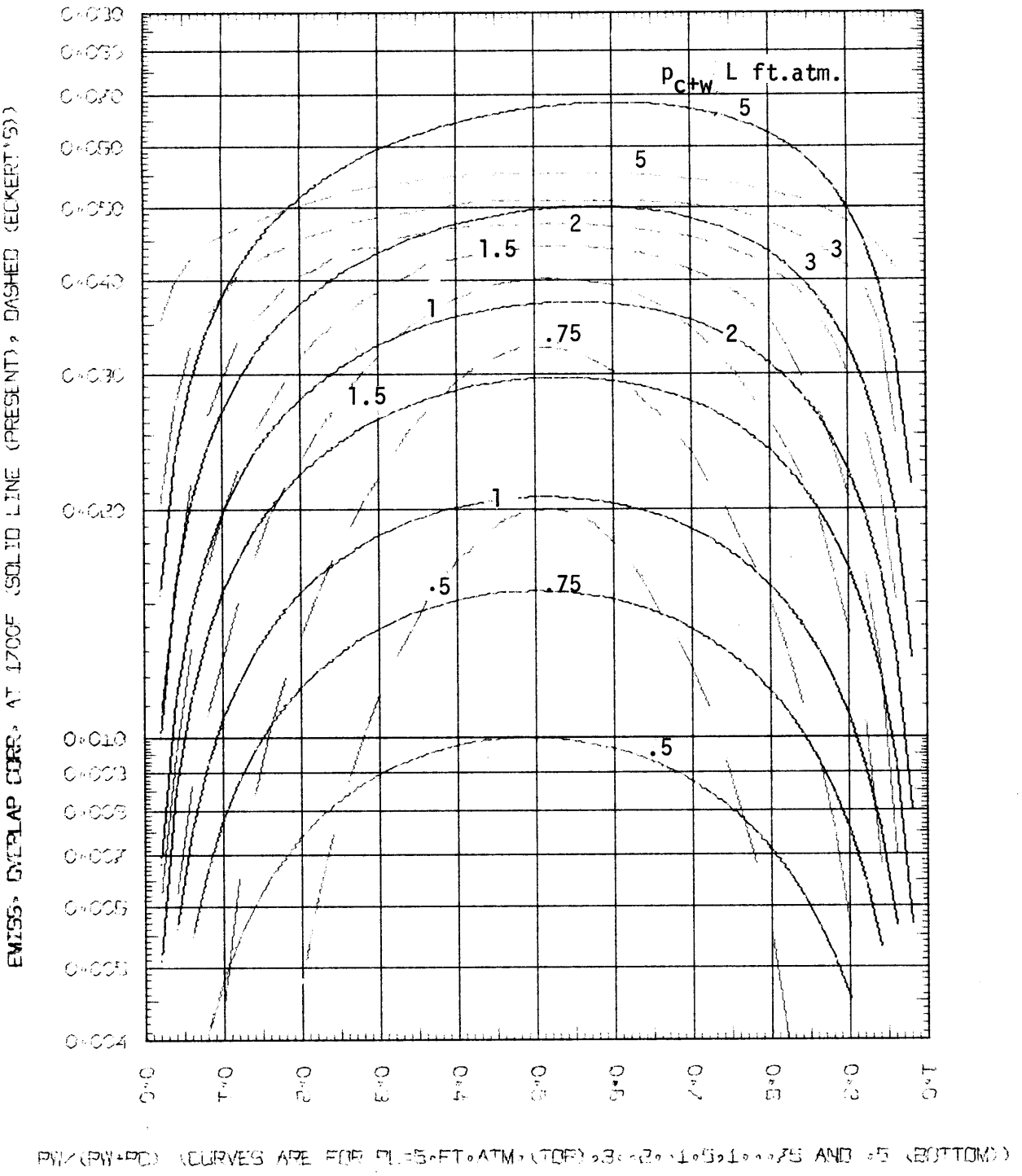
p_{c+w} L ft.atm.
5
5
3
3
2
2
1.5
1.5
1
1
.75
.75
.5
.5
0.040
0.030
0.020
0.010
0.0
1.0
2.0
3.0
4.0
5.0
6.0
7.0
8.0
9.0
1.0
PW/(PW+PD) (CURVES ARE FOR PL=5 FT-ATM, (TOP) 3, 2, 1.5, 1, .75 AND .5 (BOTTOM))

Figure 5.5-3

temperature range 2500 to 2800 F. A comparison of the computed mixture emissivity using the present model and the emissivities calculated from his radiation measurements is shown in Figure 5.5-4 for temperatures of 2500, 2600, 2700, and 2800 F and pL of .06 to 0.12 ft. atm., P_t = 1 atm. and $p_w/(p_w + p_c)$ = 0.705. The present computed values are consistently higher than Millard's measurements, which might have suffered from the presence of temperature gradients in the flames and the presence of simultaneous temperature and concentration gradients at the edges. It is also possible that Millard's partial pressure reported values were in error due to dissociation at the high temperature range of his experiments.

Fishenden (1936) ran experiments to determine the effect of the partial and total pressure on the absorption of high temperature radiation by carbon dioxide and water vapor. Her measured emissivity of a mixture containing 20% water vapor and 7.5% carbon dioxide at pL's of 0.2 and 0.3 ft. atm. and at 600 to 1600 F are compared to the present mixture emissivities computed at the same conditions in Figure 5.5-5, which shows a considerable scatter in her data. It could be due to her use of a chamber confined by rock salt windows, according to Egbert (1942). Other sources of errors in her measurements are the presence of simultaneous temperature and concentration gradients at the edges, the presence of moist air between her radiating chamber and the radiometer, considerable temperature gradient along her line of sight and high stray radiation making her results not fully reliable. These early data on total emissivities do not provide a critical test of the validity of the overlap correction factor.

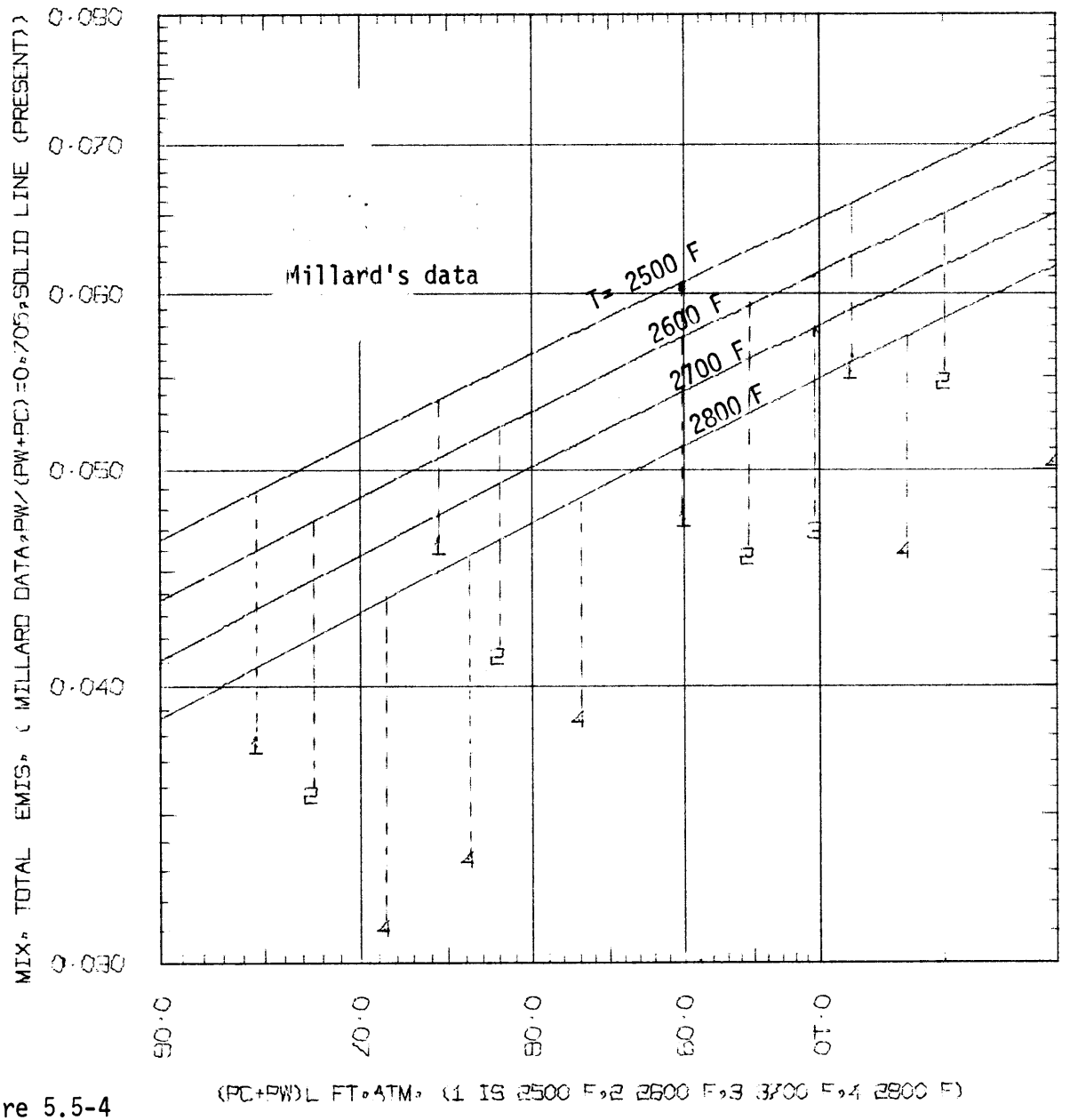
MIX, TOTAL EMIS, (MILLARD DATA,PW/(PW+PC)=0.705,SOLID LINE (PRESENT))
0.080
0.070
0.060
0.050
0.040
0.030
Millard's data
T= 2500 F
2600 F
2700 F
2800 F
90.0
70.0
80.0
60.0
50.0
(PC+PW)L FT.ATM, (1 IS 2500 F,2 2600 F,3 2700 F,4 2800 F)

Figure 5.5-4

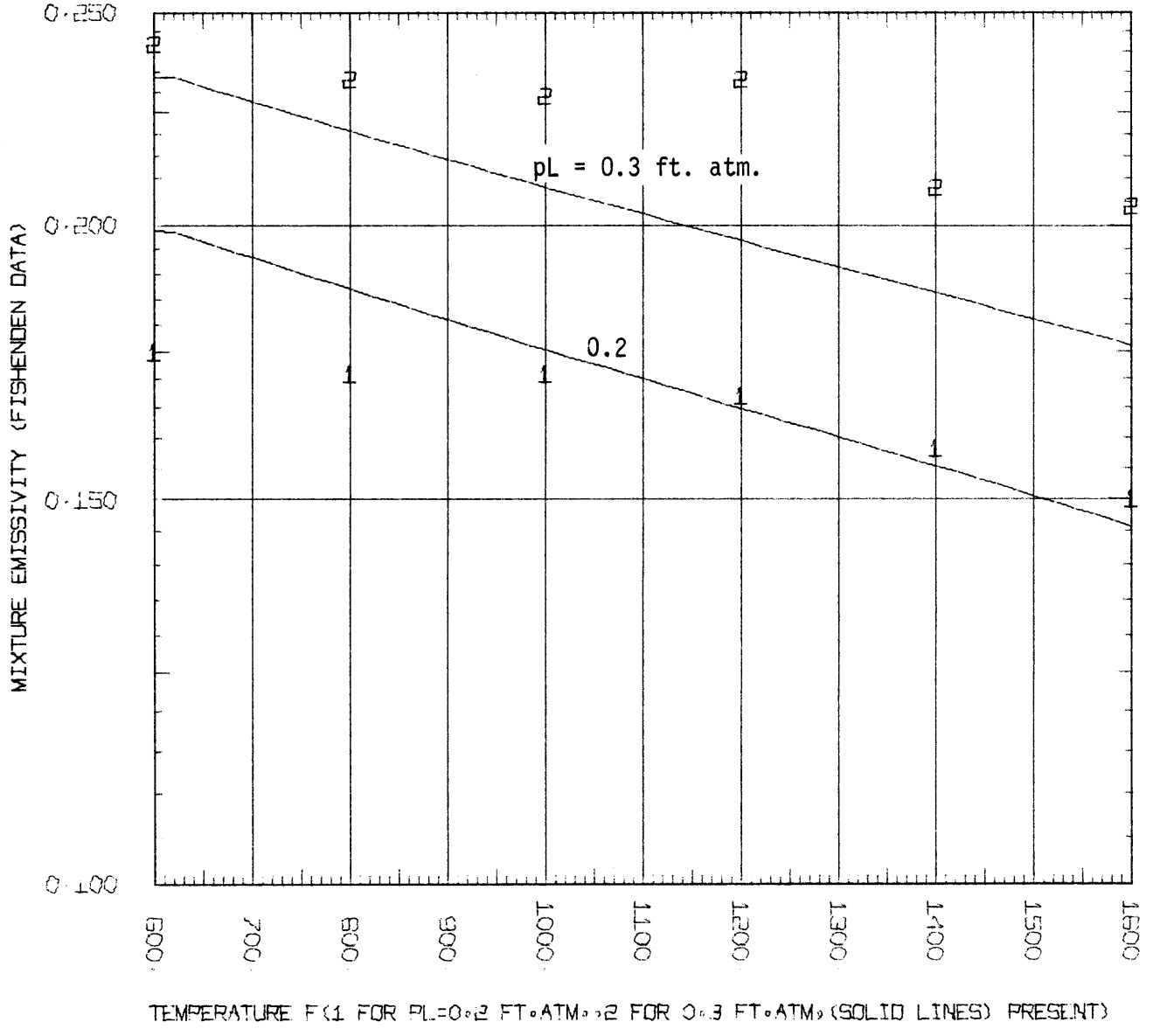
0.250
0.200
0.150
0.100
MIXTURE EMISSIVITY (FISHENDEN DATA)
pL = 0.3 ft. atm.
0.2
600
700
800
900
1000
1100
1200
1300
1400
1500
1600
TEMPERATURE F(1 FOR PL=0.2 FT.ATM., 2 FOR 0.3 FT.ATM.) (SOLID LINES) PRESENT)

Figure 5.5-5

Hines and Edwards (1968) investigated the use of band model for calculation of absorption of radiation by mixtures of water vapor, carbon dioxide and nitrogen as an inert gas. Their results are shown in Table 5.5-1, which include the results of Hottel, "HOTTEL", modified Hottel,"MOD HCH", Penner and Varanasi, "P + V" and the present computed absorptivities, emissivities and overlap corrections of the mixtures. Hines and Edwards absorptivities and overlap corrections are denoted "BAND" while those based on summing experimentally measured band absorptions are denoted "EXPTL". The "HOTTEL" values were the values of gas absorptivities predicted for the experimental conditions by the graphical correlations of Hottel and Egbert (1942) and listed by Hines and Edwards. Hines and Edwards modified Hottel's extrapolated data to include contributions of the medium strength bands 1.87 and 1.38 microns of water vapor and the 2.0 micron band of carbon dioxide. This was done by replacing the absorptivity overlap correction of Hottel by one calculated by Hines and Edwards using the approximations of Penner and Varanasi (1966).

i.e. MOD HCH α = (HCH α) + (HCH $\Delta\alpha$) - (H + E $\Delta\alpha$)

e.g. for Run No. 1 at 982 R and 1.042 atm.

Modified Hottel absorptivity =

0.195 + 0.029 - 0.13 = 0.211

The "P + V" values are overlap corrections calculated by Hines and Edwards based on the model of Penner and Varanasi (1966) in which they used harmonic oscillator approximations and rigid rotator band profiles.

For computation purposes the source temperature was taken as 1700 F (2160 R). The table shows good agreements in general between the present

Table 5.5-1

COMPARISON OF ABSORPTIVITIES AND ABSORPTIVITIES OVERLAP CORRECTIONS OF CARBON DIOXIDE AND WATER VAPOR MIXTURES

RUN NO	1	2	5	6	12	13	15
P ATM	1.042	1.098	1.093	1.070	1.14	1.178	1.17
TEMP R	982	990	990	1475	988	1470	1002
MOLE FRACTIONS OF WATER	.258	.051	.241	.250	.101	.100	.752
CO2	.254	.249	.046	.249	.099	.098	.248
ABSORBING MATTER (P(C) + P(W)) L FT.ATM	.686	.423	.403	.643	.292	.299	1.5
RATIO OF P(W)/ (P(W) + P(C))	.5037	.17	.838	.5005	.504	.505	.751
ABSORPTIVITIES							
EXPTL.	.233	.138	.206	.206	.150	.143	.332
BAND	.218	.131	.196	.197	.150	.144	.324
HOTTEL	.195	.125	.170	.190	.135	.130	.325
MOD HCH	.211	.131	.175	.204	.148	.139	.327
PRESENT	.189	.122	.169	.205	.133	.147	.298
ABSORPTIVITIES OVERLAP CORRECTIONS							
HOTTEL	.029	.011	.011	.026	.018	.013	.033
P+V	.021	.016	.006	.017	.013	.010	.029
BAND	.013	.005	.006	.012	.005	.004	.031
PRESENT	.014	.006	.006	.014	.006	.006	.026
EMISSIVITIES							
BAND	.368	.203	.348	.285	.256	.191	.520
PRESENT	.306	.190	.274	.269	.217	.195	.460

absorptivities and the values listed for others. The agreement is better for higher gas temperatures (1470 and 1475 R). In comparing the absorptivities overlap corrections it is clear that the agreement is excellent between the present values and those recently published by Edwards and Hines. Both sets are in good agreement with Penner and Varanasi corrections when the water vapor mole fraction is three or more times that of carbon dioxide. The agreement of the present overlap corrections with those of Edwards and Hines and of Penner and Varanasi is important inasmuch as it provides an independent check of the present values.

The best agreement between the four sets of overlap corrections occurs at $p_c + p_w \simeq 1$ atm. and $p_w/p_c \simeq 3$. This is because the overlap correction of Hottel closely represent conditions in which the partial pressure of water vapor and $(p_c + p_w)L$ are high enough to cause the water vapor to act as a black body over the 2.7 micron band of carbon dioxide.

It is possible to conclude from the above mentioned comparisons that the present model is suitable for the computation of overlap corrections. The standard conditions of zero partial pressure of water vapor, zero partial pressure of carbon dioxide, and a total pressure of one atmosphere were selected. The overlap corrections is, therefore, a function of the gas absolute temperature, the ratio of p_w/p_c and the $(p_c + p_w)L$ product. Presentation of the overlap corrections, therefore, requires a family of families of curves. In order to cover the widest possible range, the results of the present computed overlap corrections are presented in several plots. The solid lines in Figure 5.5-6

represent the computed overlap corrections for an equimolal mixture of water vapor and carbon dioxide plotted against the temperature from 300 to 2500 K for pL's of 20, 50, 100, 200, and 500 cm. atm. The dashed lines are for $p_w/p_c = 2$. Figures 5.5-7 and 5.5-8 are the same type of plot for p_w/p_c values of 1/3, 4, 1/9, and 9 respectively; two families are plotted on the same figure.

Figure 5.5-9 is a plot of the overlap correction against the fraction $p_w/(p_w + p_c)$ for pL's of 20, 50, 100, 200, and 500 cm. atm. at 500 K. Figures 5.5-10, 5.5-11, 5.5-12 and 5.5-13 are the same type of plots of the overlap correction against the water vapor fractions for temperatures of 1000, 1500, 2000, and 2500 K. The low temperature end of the curves (less than 1000 K) is a strong function of the spectral data of the water vapor rotation band and of the fifteen micron band of carbon dioxide. It was pointed out earlier that the water vapor rotation band spectral constants tabulated by General Dynamics were not adequate at 300 and 600 K. The spectral tabulation of McClatchey was used at 300 K and the constants at 600 K were obtained by interpolation. If and when better spectral data of the water vapor rotation band become available, it will be possible to update the charts in the range $T < 1000$ K.

Two approximations to the overlap correction were investigated. The first is the grey gas approximation in which the overlap correction becomes the product of the individual emissivities or absorptivities. For temperatures of 278 to 2500 K, pL's of 3 to 240 cm. atm. the Grey gas overlap corrections were off by a factor ranging from 2 to 60, but the maximum deviation in the mixture emissivities was about 11%.

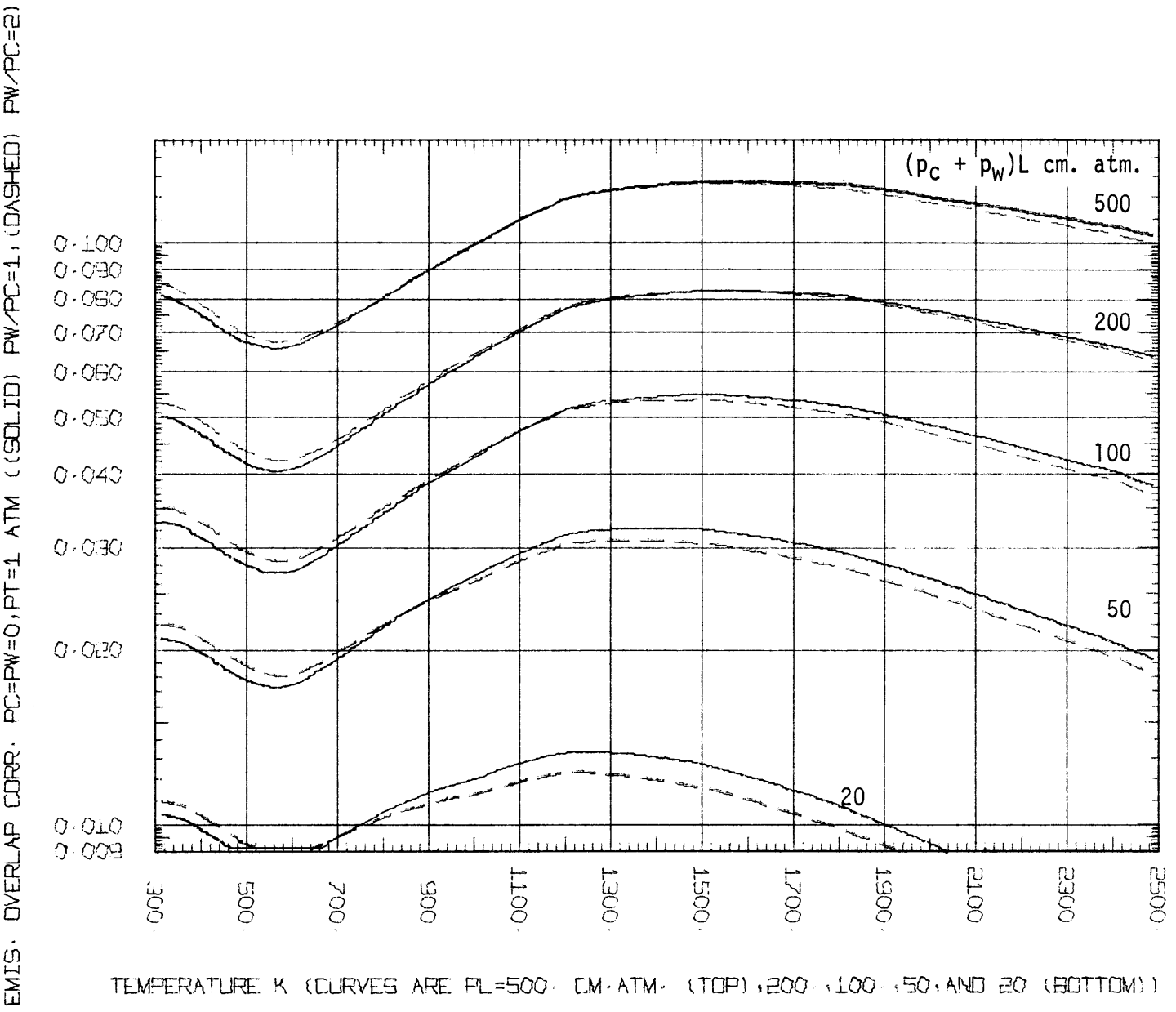
EMIS. OVERLAP CORR. PC=PW=0,PT=1 ATM ((SOLID) PW/PC=1,(DASHED) PW/PC=2)
0.100
0.090
0.080
0.070
0.060
0.050
0.040
0.030
0.020
0.010
0.000
300
500
700
900
1100
1300
1500
1700
1900
2100
2300
2500
TEMPERATURE K (CURVES ARE PL=500 CM-ATM- (TOP),200 ,100 ,50,AND 20 (BOTTOM))
$(p_c + p_w)L$ cm. atm.
500
200
100
50
20

Figure 5.5-6

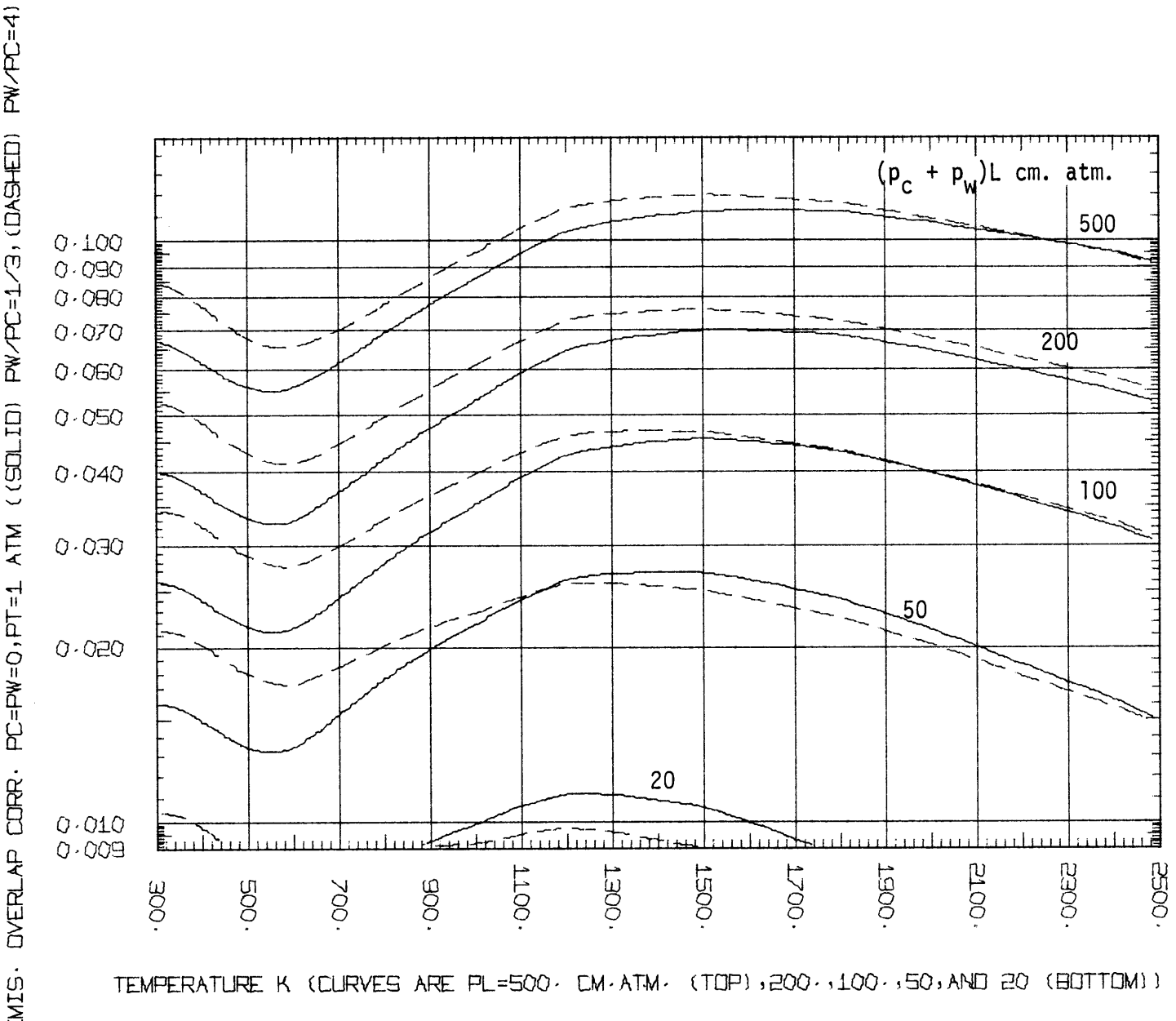
EMIS. OVERLAP CORR. PC=PW=0,PT=1 ATM ((SOLID) PW/PC=1/3,(DASHED) PW/PC=4)
0.100
0.090
0.080
0.070
0.060
0.050
0.040
0.030
0.020
0.010
0.009
$(p_c + p_w)L$ cm. atm.
500
200
100
50
20
300.
500.
700.
900.
1100.
1300.
1500.
1700.
1900.
2100.
2300.
2500.
TEMPERATURE K (CURVES ARE PL=500. CM.ATM. (TOP),200.,100.,50,AND 20 (BOTTOM))

Figure 5.5-7

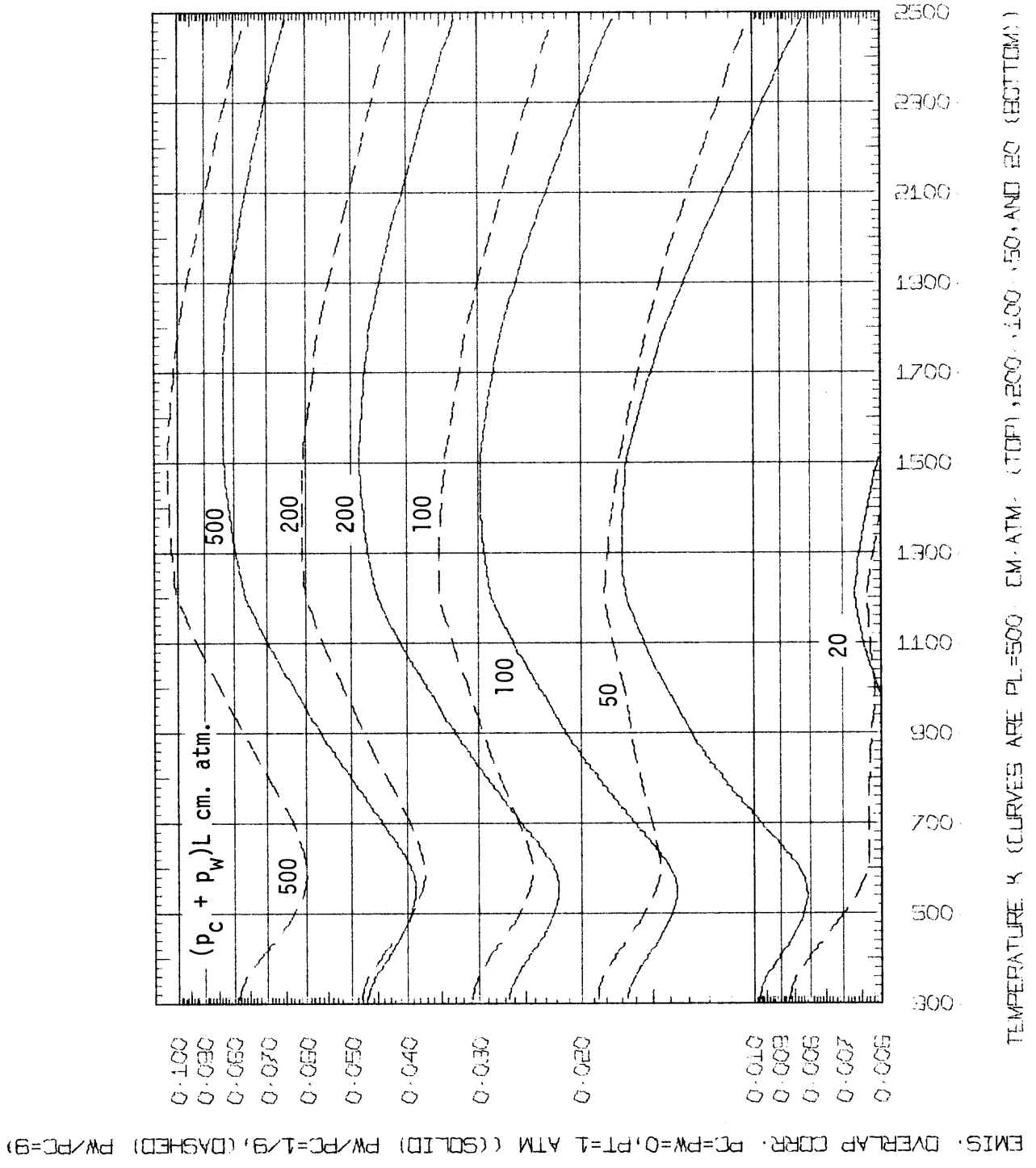
EMIS. OVERLAP CORR. PC=PW=0,PT=1 ATM ((SOLID) PW/PC=1/9, (DASHED) PW/PC=9)
0.100
0.080
0.060
0.070
0.090
0.050
0.040
0.030
0.020
0.010
0.008
0.006
0.007
0.005
TEMPERATURE K (CURVES ARE PL=500 CM-ATM (TOP),200,100,50,AND 20 (BOTTOM))
2500
2300
2100
1900
1700
1500
1300
1100
900
700
500
300
$(p_c + p_w)L$ cm. atm.
500
200
200
100
100
50
20

Figure 5.5-8

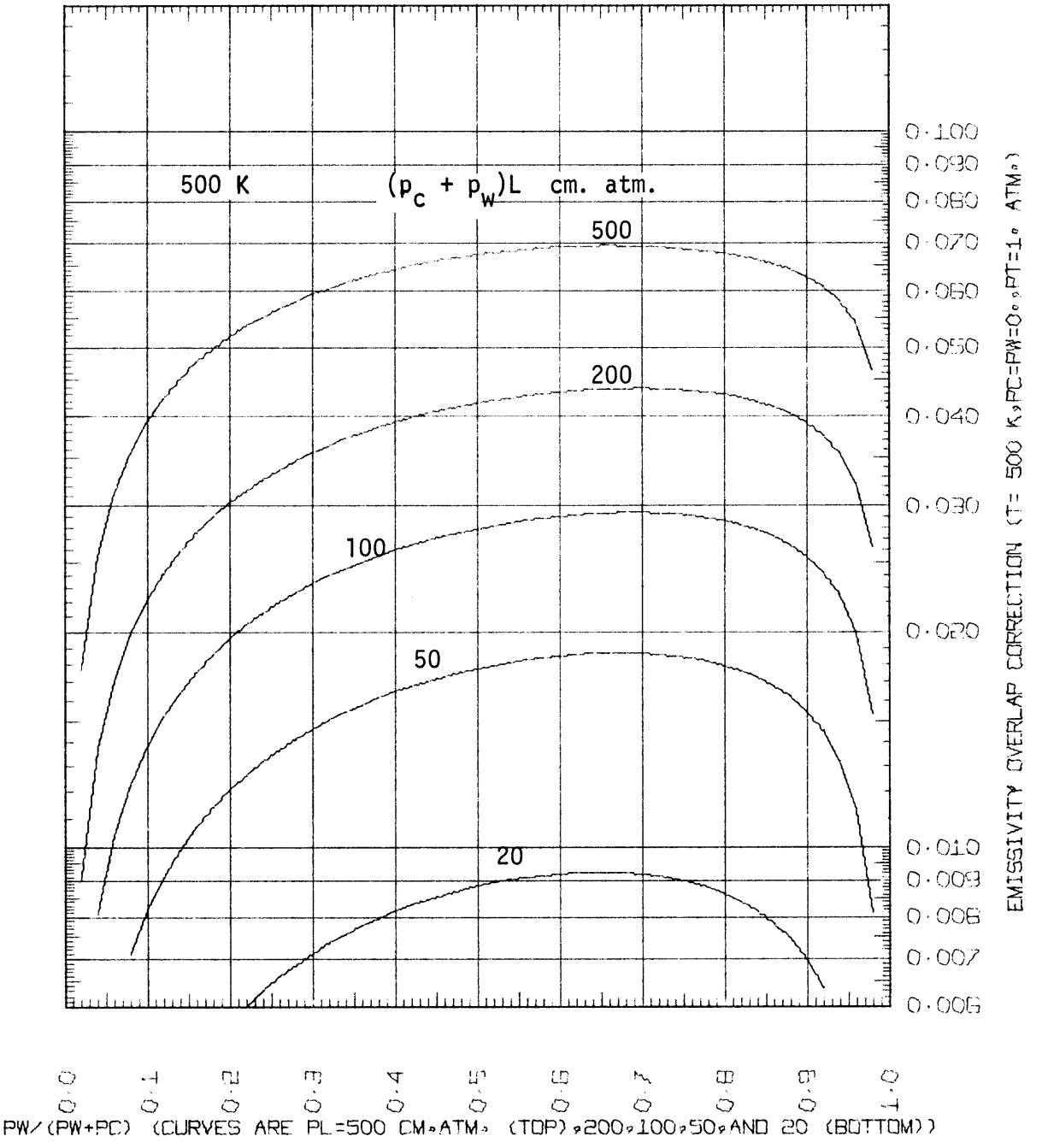
500 K
$(p_c + p_w)L$ cm. atm.
500
200
100
50
20
0.100
0.090
0.080
0.070
0.060
0.050
0.040
0.030
0.020
0.010
0.009
0.008
0.007
0.006
EMISSIVITY OVERLAP CORRECTION (T= 500 K, PC=PW=0., PT=1. ATM.)
0.0
0.1
0.2
0.3
0.4
0.5
0.6
0.7
0.8
0.9
1.0
PW/(PW+PC) (CURVES ARE PL=500 CM.ATM. (TOP), 200, 100, 50, AND 20 (BOTTOM))

Figure 5.5-9

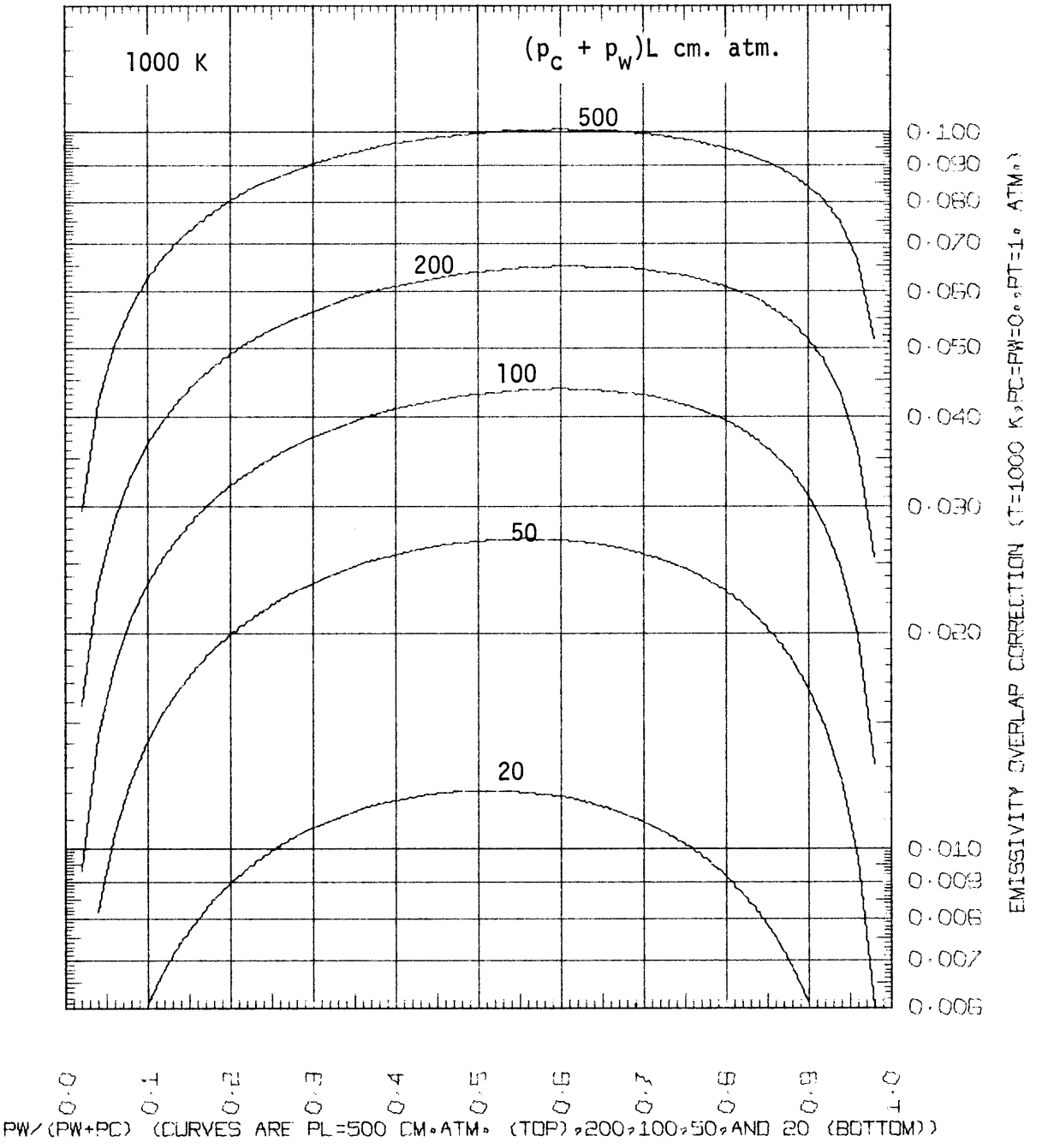
1000 K
$(p_c + p_w)L$ cm. atm.
500
200
100
50
20
0.100
0.090
0.080
0.070
0.060
0.050
0.040
0.030
0.020
0.010
0.009
0.008
0.007
0.006
EMISSIVITY OVERLAP CORRECTION (T=1000 K, PC=PW=0., PT=1. ATM.)
0.0
0.1
0.2
0.3
0.4
0.5
0.6
0.7
0.8
0.9
1.0
PW/(PW+PC) (CURVES ARE PL=500 CM.ATM. (TOP), 200, 100, 50, AND 20 (BOTTOM))

Figure 5.5-10

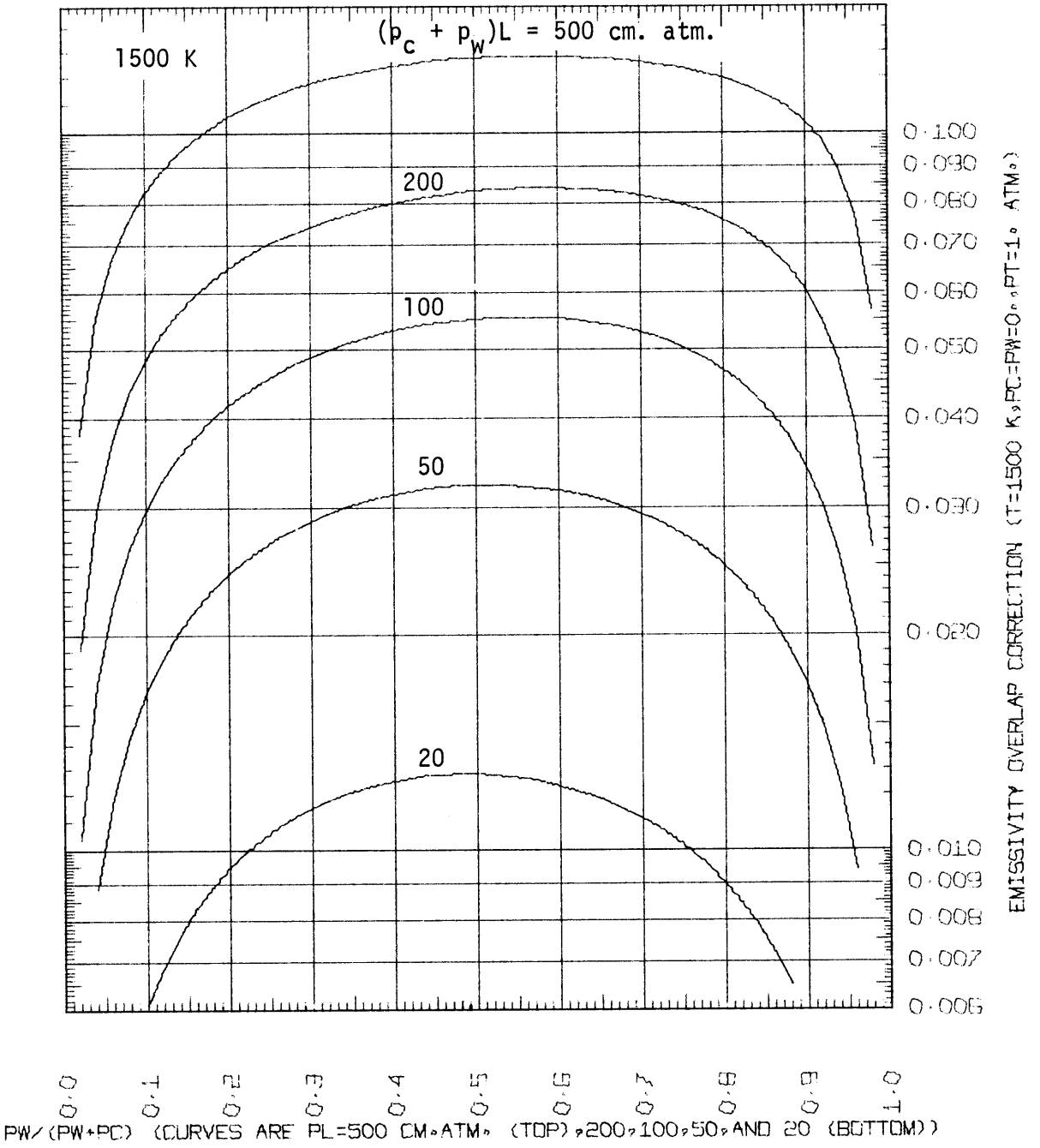
1500 K
$(p_c + p_w)L$ = 500 cm. atm.
200
100
50
20
0.100
0.090
0.080
0.070
0.060
0.050
0.040
0.030
0.020
0.010
0.009
0.008
0.007
0.006
EMISSIVITY OVERLAP CORRECTION (T=1500 K,PC=PW=0.,PT=1. ATM.)
0.0
0.1
0.2
0.3
0.4
0.5
0.6
0.7
0.8
0.9
1.0
PW/(PW+PC) (CURVES ARE PL=500 CM.ATM. (TOP),200,100,50,AND 20 (BOTTOM))

Figure 5.5-11

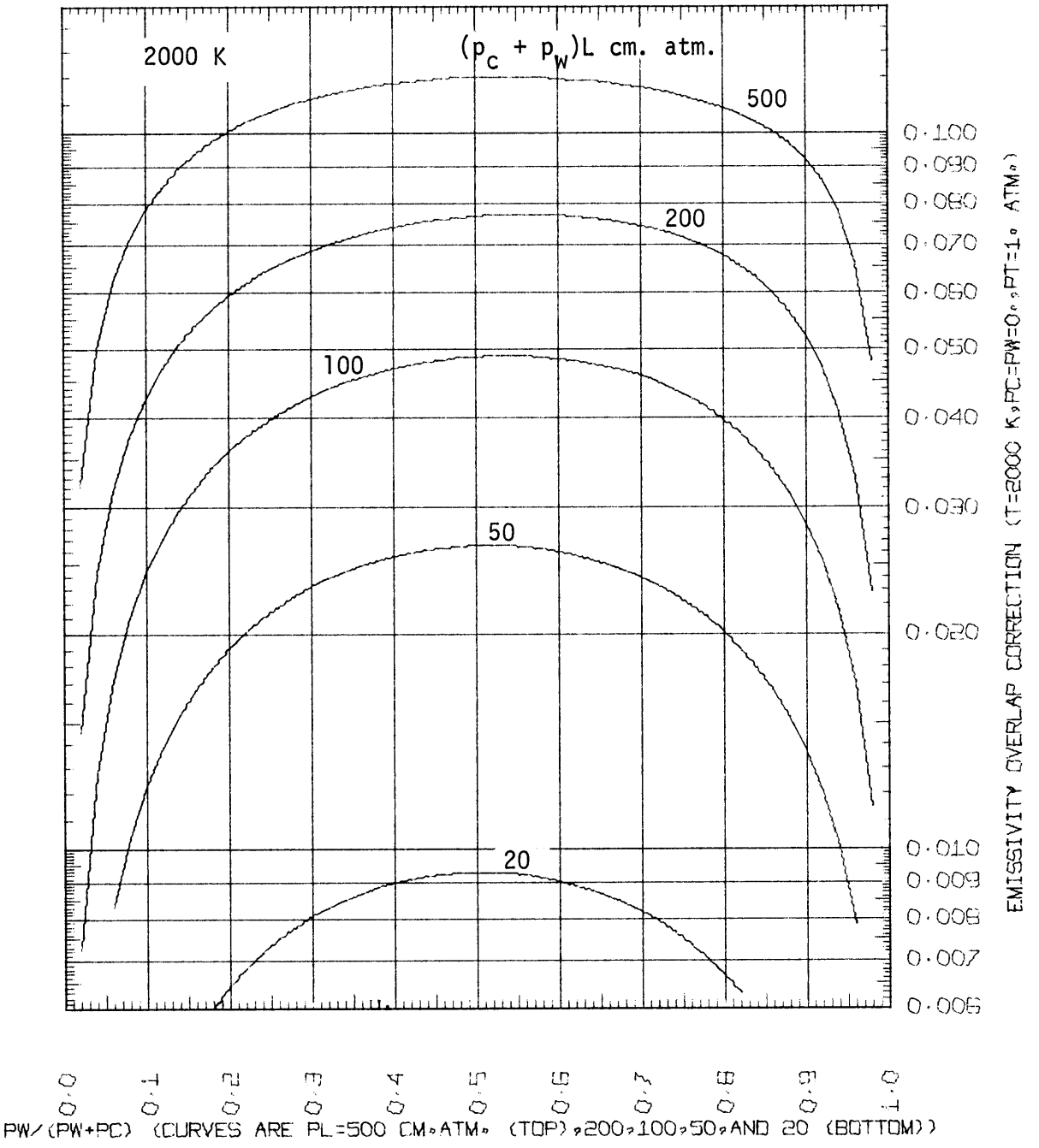
2000 K
$(p_c + p_w)L$ cm. atm.
500
200
100
50
20
0·100
0·090
0·080
0·070
0·060
0·050
0·040
0·030
0·020
0·010
0·009
0·008
0·007
0·006
EMISSIVITY OVERLAP CORRECTION (T=2000 K, PC=PW=0, PT=1. ATM.)
0.0
0.1
0.2
0.3
0.4
0.5
0.6
0.7
0.8
0.9
1.0
PW/(PW+PC) (CURVES ARE PL=500 CM-ATM, (TOP), 200, 100, 50, AND 20 (BOTTOM))

Figure 5.5-12

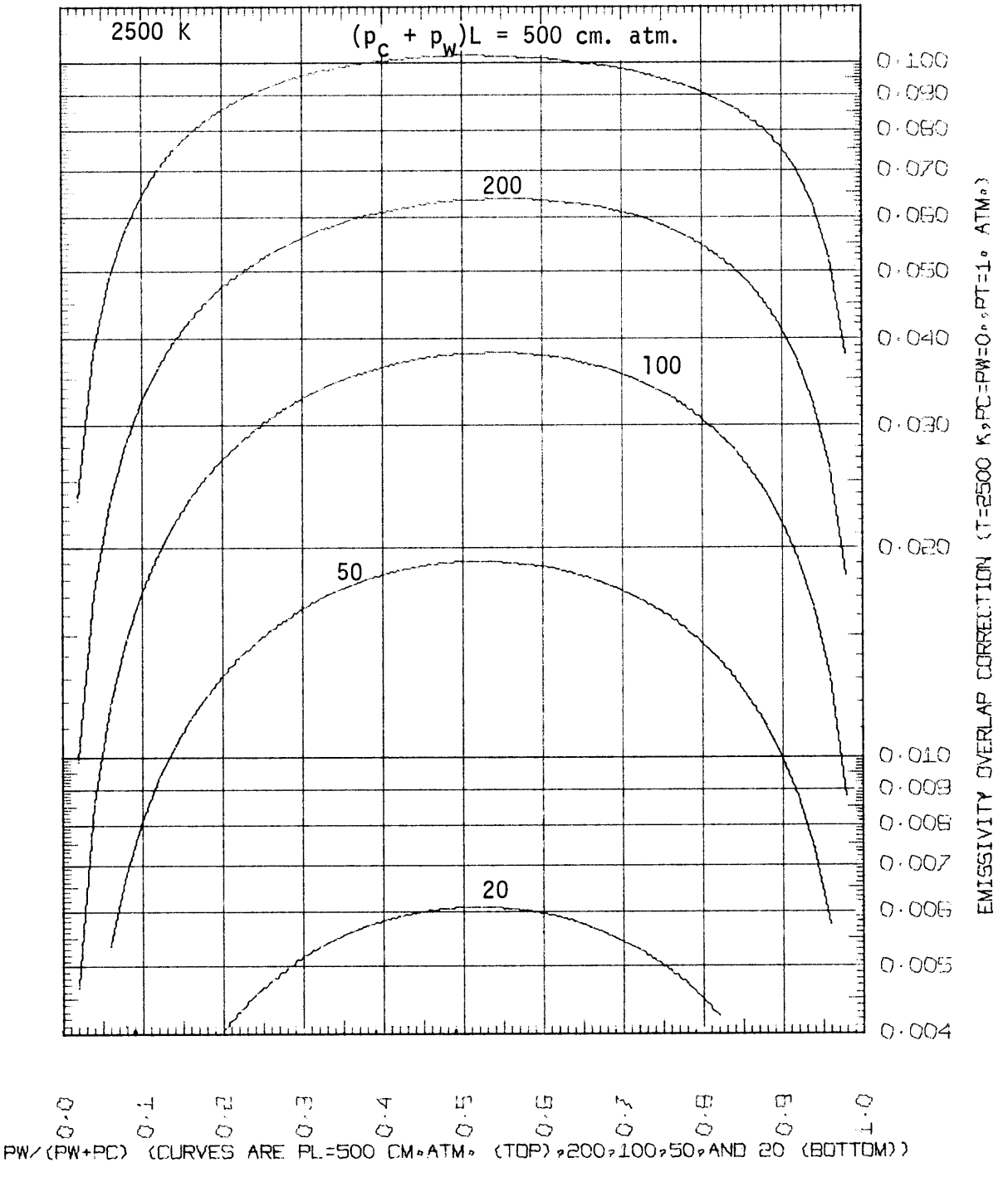
2500 K
$(p_c + p_w)L$ = 500 cm. atm.
200
100
50
20
0.100
0.090
0.080
0.070
0.060
0.050
0.040
0.030
0.020
0.010
0.009
0.008
0.007
0.006
0.005
0.004
EMISSIVITY OVERLAP CORRECTION (T=2500 K, PC=PW=0., PT=1. ATM.)
0.0
0.1
0.2
0.3
0.4
0.5
0.6
0.7
0.8
0.9
1.0
PW/(PW+PC) (CURVES ARE PL=500 CM.ATM. (TOP), 200, 100, 50, AND 20 (BOTTOM))

Figure 5.5-13

The second approximation was that of Hadvig (1964) who found that the product $\varepsilon_{c + w} T$ was a function of $(p_c + p_w)L$ only over a restricted temperature range and pL ranges. At temperatures of 1500, 2000, 2500, and 3500 R and pL ranging from 0.2 to 4 ft. atm. the deviation of mixture emissivities calculated using Hadvig's approximation and the present computed emissivities was within 20 percent.

5.6. Pressure Broadening Correction of Overlap Correction and Emissitivy of Mixture

The overlap correction and/or the emissivity of gaseous mixtures of carbon dioxide and water vapor is a function of the gas temperature, the $(p_c + p_w)$ L product, the ratio of p_w/p_c, the partial pressure of water vapor (or carbon dioxide) and the total pressure. Therefore, five variables are needed to define the overlap correction. The overlap correction charts presented in Section 5.5 were calculated at standard conditions of $p_w = 0$, $p_c = 0$, $P_t = 1$ atm. Some form of correction factor has to be used when using the charts at non standard conditions. Denoting the correction factor $C_{\Delta\varepsilon}$ it may be defined as

$$C_{\Delta\varepsilon} = \frac{\Delta\varepsilon \text{ at } p_w = p_w,\ p_c = p_c,\ P_t = P_t}{\Delta\varepsilon \text{ at } p_w = 0,\ p_c = 0,\ P_t = 1 \text{ atm}} \text{ at same T and } (p_c + p_w)L \tag{5.6-1}$$

$$C_{\Delta\varepsilon} = C_{\Delta\varepsilon}\left(T,\ (p_c + p_w)L,\ \frac{p_w}{p_w + p_c},\ p_w,\ P_t\right) \tag{5.6-2}$$

Alternatively a correction factor of the mixture emissivity may be defined as

$$C_{\varepsilon_{mix}} = \frac{\varepsilon_{mix} \text{ at } p_w = p_w,\ p_c = p_c,\ P_t = P_t}{\varepsilon_{mix} \text{ at } p_w = 0,\ p_c = 0,\ P_t = 1 \text{ atm}} \text{ at same T and } (p_c + p_w)\ L \tag{5.6-3}$$

$$C_{\varepsilon_{mix}} = C_{\varepsilon_{mix}}\left(T,\ (p_c + p_w)L,\ \frac{p_w}{p_w + p_c},\ p_w,\ P_t\right) \tag{5.6-4}$$

In theory a family of families of families of families of curves are needed for graphical presentation of either correction factor. A four generation family can be generated with the present model, but the computation time required to generate such a family is unreasonably large. It is the intention here to present, and justify, the use of an approximate method.

The effect of pressure broadening on overlap correction should be more than its effect on the emissivities of individual gases, especially at temperatures below 800 K when most of the contribution to the overlap correction is from the overlapping region of the wings of the fifteen micron band of carbon dioxide and the rotation band of water vapor. This is because broadening increases the strength of the wings of each gas; therefore, the broadening of the individual bands will greatly increase the wave length region in which overlap is important. In the case of the 2.7 micron band where the carbon dioxide band is completely contained within that of water vapor the broadening effect would not probably be a strong function of pressure and may even decrease with increasing pressure as a consequence of the decrease in the effective absorption coefficient of the water vapor band in the region of overlap. The proposed approximate pressure broadening correction factor of the overlap correction is given by

$$C_{\Delta_\varepsilon} = C_{\varepsilon_w} C_{\varepsilon_C} \qquad (5.6\text{-}4)$$

and the mixture emissivity would, therefore, be given by

$$\varepsilon_{mix} = C_{\varepsilon_w} \varepsilon_{w_0} + C_{\varepsilon_C} \varepsilon_{C_0} - C_{\varepsilon_w} C_{\varepsilon_C} \Delta\varepsilon_0 \qquad (5.6\text{-}5)$$

Equations (5.6-4) and (5.6-5) would be exact if the gases were grey.

To show the validity of the approximation Figure 5.6-1 shows the effect of temperature on three types of computed correction factors, $C_{\Delta\varepsilon}$ exact, $C_{\Delta\varepsilon}$ proposed (grey gas) and $C_{\varepsilon_{mix}}$ at P_t = 1 atm., $p_w = p_c = 0.5$, $p_{c+w}L$ = 4 ft. atm. in a temperature range of 500 to 3500 R (278 to 1944 K). As anticipated, the exact $C_{\Delta\varepsilon}$ is larger than the proposed grey gas approximation $C_{\varepsilon_w} C_{\varepsilon_C}$ at temperatures below 1500 R (833 K). For temperatures above 1500 R the approximation seems to be good.

EFFECT OF TEMPERATURE ON PRESSURE BROADENNING OF THE OVERLAP CORRECTION AND MIXTURE EMISSIVITY

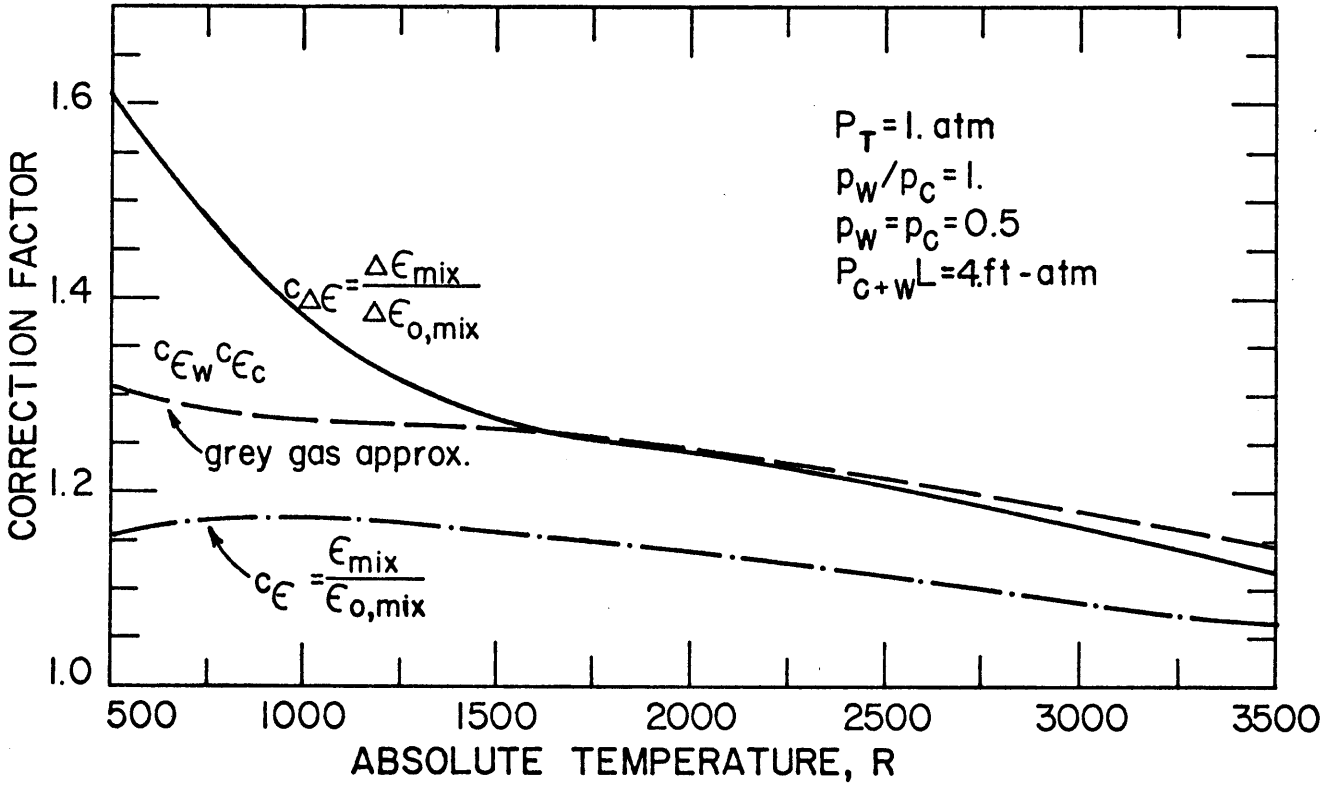

Figure 5.6-1

In the temperature range 500 to 1500 R the present approximation may be used with the understanding that it may underestimate the correction factor.

The effect of partial pressure variation on the computed exact correction factor to the overlap correction, the computed proposed grey gas approximate correction factor to the overlap correction and the computed exact correction factor to the emissivity of the mixture is shown in Figure 5.6-2 for a temperature of 1500 K, pL = 50 cm. atm., p_c/p_w = 1 and P_t = 1 atm. The figure shows the close agreement of the present proposed approximation. Figure 5.6-3 shows the computed effect of total pressure on the three types of corrections for an equimolal mixture of carbon dioxide and water vapor, pL = 50 cm. atm. and zero partial pressures of water vapor and carbon dioxide. An increase in the total pressure from 1 atm. to 20 atm., in the range of turbines increases the overlap correction and the mixture emissivity by about 56 and 25 percent respectively. The present proposed approximation results in an increase of about fifty percent in the overlap correction and twenty-six percent in mixture emissivity.

The above comparison indicates the importance of the pressure broadening correction for the overlap corrections. In spite of the very limited comparisons shown in the present investigation the use of the grey gas approximation proposed in the present study and represented by equations 5.6-4 and 5.6-5 is recommended with caution. It is to be regarded as a preliminary estimate of the correction.

An example of the application of the proposed grey gas approximation is the case of a gas turbine combustor at 1500 K at 20 atm. total pressure and a 15 cm. chamber. The results of calculations in

EFFECT OF WATER VAPOR PARTIAL PRESSURE ON PRESSURE BROADENNING OF THE OVERLAP CORRECTION AND MIXTURE EMISSIVITY

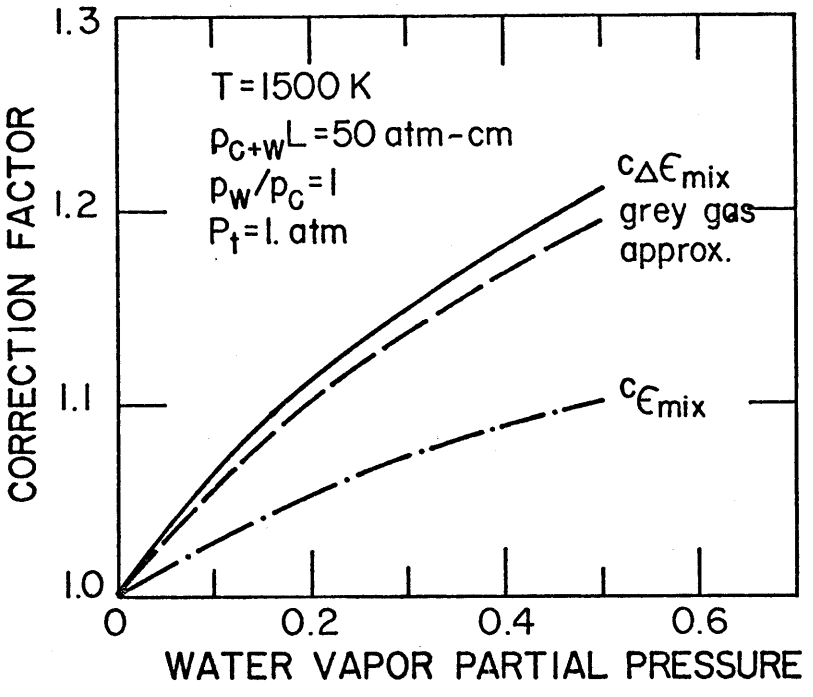

Figure 5.6-2

EFFECT OF TOTAL PRESURE ON PRESSURE BROADENNING
OF THE OVERLAP CORRECTION AND MIXTURE EMISSIVITY

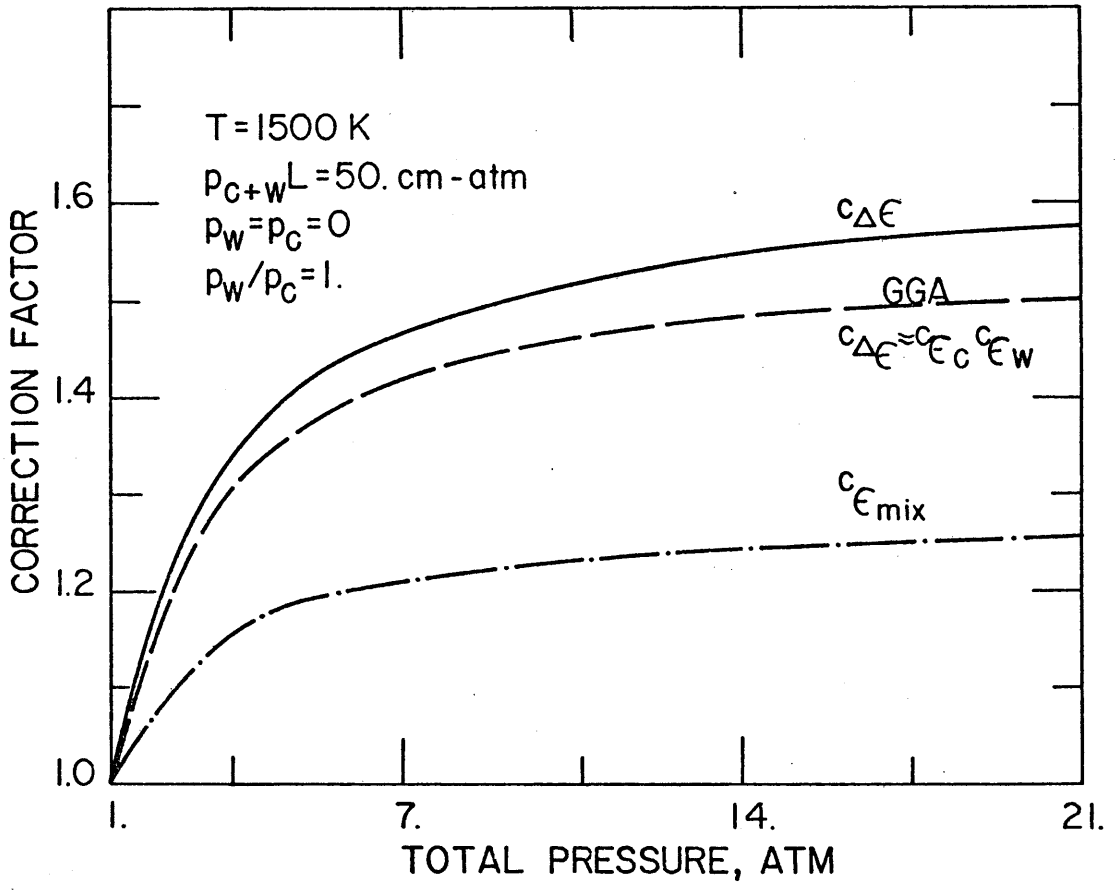

Figure 5.6-3

sections 5.2 and 5.4 are the following

Water Vapor	Carbon Dioxide
p_w = 2 atm.	p_c = 2 atm.
p_wL = 30 cm. atm.	p_cL = 30 cm. atm.
$\varepsilon_{w,\,0}$ = 0.173 (v.s. .16 from HCH charts) (from Figure 5.3-5)	$\varepsilon_{c,\,0}$ = 0.124 (v.s. .13 from old charts) (from Figure 5.1-4)
$B_{H_2O,\,1500}$ = 0.928 cm^{-1}	$B_{CO_2,\,1500}$ = 0.614 cm^{-1}
C_{ε_w} = 1.235	C_{ε_C} = 1.0125
ε_w = 1.235 * 0.173 = 0.2138	ε_c = 1.0125 * 0.124 = 0.125

the overlap correction may be read from the solid lines in Figure 5.5- 6 at 1500 K. The values obtained are $\Delta\varepsilon$ = 0.0125 at pL = 20 cm. atm. and 0.0321 at pL - 50 cm. atm. Using a power relation of $\Delta\varepsilon$ v.s. pL gives

$$\frac{\Delta\varepsilon_1}{\Delta\varepsilon_2} = \left(\frac{pL_1}{pL_2}\right)^n , \qquad (5.2\text{-}6)$$

substitution gives

$$\frac{0.0231}{0.0125} = \left(\frac{50}{20}\right)^n \rightarrow n \simeq 1.029, \qquad (5.6\text{-}7)$$

i.e. the relation of $\Delta\varepsilon$ to pL in the range of pL = 20 to 50 cm. atm. is almost linear.

$$\frac{\Delta\varepsilon_{30}}{\Delta\varepsilon_{20}} = \left(\frac{30}{20}\right)^{1.029}$$

and $\Delta\varepsilon_{30}$ = 1.518 * 0.0125 = 0.0189 (v.s. 0.04 from old Eckert charts)

therefore, $\Delta\varepsilon_0$ = 0.0089 (5.6-8)

and $\varepsilon_{mix,\,0} = \varepsilon_{w,\,0} + \varepsilon_{C,\,0} - \Delta\varepsilon_0$

$$= 0.173 + 0.124 - 0.0189 = 0.278 \qquad (5.6\text{-}9)$$

(v.s. 0.16 + 0.13 - 0.04 = 0.25 ,or 11% difference using the old charts)

Using the present proposed approximation

$$\Delta\varepsilon = C_{\varepsilon_w} C_{\varepsilon_C} \Delta\varepsilon_0 = 1.235 * 1.0125 * 0.0189 = 0.0236 \qquad (5.6\text{-}10)$$

and

$$\varepsilon_{mix} = 0.214 + 0.125 - 0.0236 = 0.315 \qquad (5.6\text{-}11)$$

the ratio

$$\frac{\varepsilon_{mix}}{\varepsilon_{mix,\,0}} = \frac{0.315}{0.278} = 1.135 \qquad (5.6\text{-}12)$$

Had we not made any pressure broadening correction to $\Delta\varepsilon$ the final answer of the mixture emissivity would have been

$$\varepsilon_{mix} \tilde{=} 0.214 + 0.125 - 0.0189 = 0.320 \qquad (5.6\text{-}13)$$

which is about 1.6 percent above the recommended value of equations 5.6-4 and 5.6-5 and 5.6-11.

6. Conclusions and Recommendations

1. Modified carbon dioxide emissivity charts have been developed at $p_c = 0$ and $P_t = 1$ atm. combining results of recent spectral measurements with early total emissivity charts.
2. Pressure Broadening correcting factor of carbon dioxide have been calculated for a wide range of partial and total pressures and temperatures of 500, 1000, 1500, 2000 and 2500 K.
3. Updated water vapor emissivity charts are developed in the region where the total emissivity data are well established. The data at low pL's and high temperatures is uncertain and additional experimental data are needed to resolve discrepancies.
4. Pressure Broadening correction factor charts of water vapor have been presented in a general working plot form and in Engineering form at $P_t = 1$ atm and p_w's of 0.02 to 0.20 atm. and temperatures of 500, 750, 1000, 1500, 2000, and 2500 K; linear interpolation of C_F against T between charts temperatures was shown to introduce a maximum error of less than a couple of percent.
5. Overlap correction charts for the superimposed radiation of water vapor and carbon dioxide have been developed to cover temperatures of 300 to 2500 K, pL's of 20 to 500 cm. atm. and $p_w/(p_w+p_c) = 0$ to 1 at standard corrections of $p_w = p_c = 0$ and $P_t = 1$ atm. An approximation of the pressure broadening correction of the overlap correction has been shown to provide a good preliminary estimate of the correction at pressures other than one atmosphere and at finite partial pressures of carbon dioxide and water vapor.

NOMENCLATURE

a	fine structure parameter = b/d
A	equivalent width of a band
b	line half width i.e. half the width of the spectral line in units of wave number when the absorption coefficient reaches half its maximum value
b_e	equivalent line half width
b_0	line half width at one atmosphere
d	spectral line spacing cm^{-1}
$E(w)$	spectral radiance
$E^0(w)$	spectral radiance of a black body
I	modified Bessel function
I_0	I of order zero
I_1	I of order one
l or L	length in ft. or cm. as specified
k	absorption coefficient
k_w	monochromatic absorption coefficient
$\overline{k}$	average k
n	coefficient
p	partial pressure in atmosphere
P or P_t	total pressure in atm.
P_e	equivalent pressure
s	distance
S	line strength: describes the area under the k_w - w curve
S_e	equivalent line strength

T	temperature, generally in absolute degrees, i.e. K or R
T_g	gas temperature
T_s	source temperature
u	absorbing matter = pL in units of cm. atm.
Y	mole fraction
α	absorptivity
α_w or $\alpha(w)$	spectral absorptivity
α_c	carbon dioxide absorptivity
α_w	water vapor absorptivity
β	band strength, i.e. total absorptivity for a unit absorbing matter
γ	self broadening coefficient, i.e. $\gamma_x = b_x/b_N$
ε	emissivity
ε_w or $\varepsilon(w)$	spectral emissivity
π	constant = 3.1415916
ρ	density of absorbing matter
σ	Stefan - Boltzman constant
τ	transmissivity
τ_w or $\tau(w)$	spectral transmissitivy
w	wave number cm^{-1}
Δw	wave number interval cm^{-1}
w_0	characteristic wave number

R E F E R E N C E S

AKHUNOV,N.KH.,K.B. PANFILOVICH AND A.G. USMANOV(1972)
'EXPERIMENTAL STUDY OF THE EMISSIVITY OF CARBON DIOXIDE AT HIGH PRESSURES.',TRANSLATED FRON RUSSIAN, HIGH TEMPERATURE, VOL 9 , NO. 4, P643

BARSLAU, N. (MARCH 1972)
'OVERLAP EMISSIVITY OF CARBON DIOXIDE AND WATER VAPOR IN THE FIFTEEN MICRON SPECTRAL REGION ', IBM J. RES. DEVELOP.,VOL 16,NO. 2, P180

BEN-ARYEH,Y. (1967)
APPL. OPTICS, VOL 6, P1049

BENEDICT,W.S. (1956)
'THEORETICAL STUDIES OF INFRARED SPECTRA OF ATMOSPHERIC GASES',FINAL REPORT, AF19(604)-1001, JOHN HOPKINS APPL. PHYS. LAB.,BALTIMORE, MARYLAND.

BENEDICT,W.S. AND R.F. CALFEE (1967)
'LINE PARAMETERS FOR THE 1.9 AND 6.3 MICRON WATER WATER VAPOR BANDS.',ESSA PROFESSIONAL PAPER NO. 2

BENEDICT, W.S., AND L.D. KAPLAN (1959)
J. CHEM. PHYS. VOL 30, P388

BENEDICT, W.S., AND L.D. KAPLAN (1964)
'CALCULATION OF LINE WIDTH IN H2O-H2O AND H2O COLLISIONS' J. QUANT. SPECTROSC. RAD. TRANSFER , VOL 4, P 453

BENEDICT,W.S. AND E.K. PLYLER(1954)
'ENERGY TRANSFER IN HOT GASES',U.S. GOVT. PRINTING OFFICE, WASHINGTON, D.C., P57

BREEZE,J.C. AND C.C. FERRISO(1964)
'INTEGRATED INTENSITY MEASUREMENTS OF THE 1.9 MICRON BANDS OF CARBON DIOXIDE IN THE TEMPERATURE RANGE 1400 TO 2500 K', J. CHEM. PHYS.,VOL 40,NO. 5, P 1276

BREEZE,J.C. AND C.C. FERRISO (1964)
J. CHEM. PHYS., VOL 41, P 3420

BREEZE,J.C. AND C.C. FERRISO (1963)
J. CHEM. PHYS., VOL. 39, P 2619

BREEZE,J.C.,C.C. FERRISO, C.B. LUDWIG AND W. MALKMUS (1965)
'TEMPERATURE DEPENDENCE OF THE TOTAL INTEGRATED INTENSITY OF THE VIBRATIONAL-ROTATIONAL BAND SYSTEMS', J. CHEM. PHYS., VOL 42, NO. 1, P402

BROOKS, F.A. (1939)
BULL. AMER. MET. SOC. ,VOL.20, P433

BROOKS, F.A. (1941)
'OBSERVATION OF ATMOSPHERIC RADIATION', PAPERS IN PHYSICAL OCEANOGRAPHY AND METEOROLOGY, PUBLISHED BY MIT AND WOODS HOLE OCEANOGRAPHIC INSTITUTION, VOL.8, NO.2

BURCH,D.E.,D.A. GRYVNAK AND R.R. PATTY (1964)
'ABSORPTION BY CARBON DIOXIDE BETWEEN 4500 AND 5400 RECIPROCAL CM.', SCI. REPT. NO. U-2955,AERONUTRONIC DIV. OF PHILCO, NEWPORT BEACH, CALIF.

BURCH,D.E., D.A. GRYVNAK AND R.R. PATTY (1966)
SCI. REPRT. NO. V-3704, AERONUTRONIC DIV. OF PHILCO NEWPORT BEACH, CALIF.

BURCH,D.E.,D.A. GRYVNAK AND R.R. PATTY (1967)
J. OPT. SOC. AM. , VOL 57, P 885

BURCH,D.E.,D.A. GRYVNAK,E.B. SINGELTON,W.L. FRANCE AND D. WILLIAMS (1962)
'INFRARED ABSORPTION BY CARBON DIOXIDE,WATER VAPOR AND MINOR ATMOSPHERIC CONSTITUENTS',AFCRL RES. REPRT. AFCRL-62-698, AIR FORCE CAMBRIDGE RES. LAB.,BEDFORD, MASS.

BURCH,D.E.,D.A. GRYVNAK AND D. WILLIAMS (1962)
'ABSORPTION LINE BROADENING IN THE INFRARED', APPL. OPT. VOL 1, P 359

BURCH,D.E.,D.A. GRYVNAK AND D. WILLIAMS (1962)
'TOTAL ABSORPTANCE OF CARBON DIOXIDE IN THE INFRARED APPL. OPT. VOL 1,NO. 6, PP759-765

CALFEE,R.F. AND W.S. BENEDICT (1966)
'CARBON DIOXIDE SPECTRAL LINE POSITIONS AND INTENSITIES CALCULATED FOR THE 2.05 AND 2.7 MICRON REGIONS', NBS TECH. NOTE NO. 332, U.S. GOVT. PRINTING OFFICE, WASHINGTON, D.C.

DRAYSON,S.R. (1968)
'METHODS OF CALCULATING ATMOSPHERIC TRANSMISSION FUNCTIONS', PROCEEDINGS OF A SPECIALISTS CONFERENCE ON MOLECULAR RADIATION, MARSHALL SPACE FLIGHT CENTER, HUNTSVILLE, ALA.,OCT. 5-6,1967,NASA TM X-53711, P 36

EBERHARDT,J.E. (1936)
'HEAT TRANSMISSION IN CONTINUOUS METAL-HEATING FURNACES' ,SC.D. THESIS, CHEM.ENG.,MIT,CAMB.,MASS.

EBERHARDT,J.E. AND P.C. HOTTEL (1936)

'HEAT TRANSMISSION IN STEEL REHEATING FURNACES', TRANS. ASME VOL.58, P185

ECHIGO,R.N.,NISHIWAKI AND M. HIRATA (1967)
'EVALUATION OF BAND EMISSIVITIES OF CARBON DIOXIDE AND WATER VAPOR',BULL. OF JAP. SOC. OF MECH.ENG.,

VOL 10, NO. 40, P671

ECKERT, E (1937)
'MESSUNG DER GESAMTSTRAHLUNG VON WASSERDAMPF UND KOHLENSAURE IN MISCHUNG MIT NICHTSTRAHLENDEN GASEN BEI TEMPERATUREN BIS ZU 1300 C', FORSCHUNG AUF DEM GEBIETE DES INGENIEURWESENS, BEILAGE NO. 387,VOL.8,P1,(DEC.)

ECKERT,E. AND E. SCHMIDT (1937)
' DIE WARMESTRAHLUNG VON WASSERDAMPFIN MISCHUNG MIT NICHTSTRAHLENDEN GASEN', FORSCHUNG AUF DEN GEBIETE DES INGENIEURWESENS, VOL. 8, P87

EDWARDS, D.K. (1960)
'ABSORPTION BY INFRARED BANDS OF CARBON DIOXIDE GAS AT ELEVATED PRESSURES AND TEMPERATURES', J. OPT. SOC. AM., VOL 50, NO.6, P 617

EDWARDS, D.K. (1963)
'STUDIES OF INFRARED RADIATION IN GASES' FINAL REPORT NSFG11968, REPORT NO. 62-65, UNIV. OF CALIFORNIA, LOS ANGELES, CALIF. (JAN.)

EDWARDS D.K.,AND A. BALAKRISHNAN (1973)
'THERMAL RADIATION BY COMBUSTION GASES'
INT. J. HEAT MASS TRANS. VOL 16, PP25-40,PERGAMON PRESS

EDWARDS, D.K. AND W.A. MENARD (1964)
'CORRELATIONS OF ABSORPTION BY METHANE AND CARBON DIOXIDE GASES', APPLIED OPTICS, VOL 3, NO.7, PP 847-852, (JULY)

EGBERT,R.E. (1942)
'HEAT TRANSMISSION BY RADIATION FROM GASES', SC.D. THESIS, CHEM.ENG., MIT, CAMB., MASS.

EGGERS,D.F. AND B.L. CRAWFORD (1951)
J. CHEM. PHYS., VOL. 19, P 1554

ELSASSER, W.M. (1940)
'AN ATMOSPHERIC RADIATION CHART AND ITS USE',QUAR. JOUR. ROY. METE. SOC., VOL. 66, SUPPL. P41

ELSASSER, W.M. (1941)
'A HEAT RADIATION TELESCOPE AND THE MEASUREMENT OF THE INFRARED EMISSION OF THE ATMOSPHERE', MONTHLY WEATHER REVIEW, VOL. 69, P1, JAN.

ELSASSER, W.M. (1942)
'HEAT TRANSFER BY INFRARED RADIATION IN THE ATMOSPHERE',HARVARD METEOROLOGICAL STUDIES NO. 6, HARVARD UNIVERSITY,BLUE HILL OBSERVATORY,MILTON,MASS.

FAHRENFORT,J.(1963)
'INFRARED SPECTROSCOPY AND MOLECULAR STRUCTURE', M. DAVIS ED., ELSEVIER,AMESTERDAM, P377

FALCKENBERG, G. (1936,1938,1939)
MET. ZEITS, VOL 53, P 172(1936), VOL 55,P174 (1938), VOL. 56, P72 (1939), VOL 56, P415 (1939)

FERRISO,C.C. (1962)
J. CHEM. PHYS., VOL. 37, P 1955

FERRISO,C.C. AND C.B. LUDWIG (1964)
J. OPT. SOC. AM., VOL 54, P 657

FERRISO,C.C. AND C.B. LUDWIG (1964)
J. CHEM. PHYS., VOL 41, P 1668

FERRISO,C.C. AND C.B. LUDWIG (1964)
JCP, VOL 41, P 1668

FERRISO,C.C. AND C.B. LUDWIG (1964)
'SPECTRAL EMISSIVITIES AND INTEGRATED INTENSITIES

OF THE 2.7 MICRON WATER BAND BETWEEN 530 AND 2200 K', JOURNAL OF QUANTITATIVE SPECTROSCOPY AND RADIATIVE TRANSFER, VOL 4, PP 215-227.

FERRISO, C.C., C.B. LUDWIG, AND L. ACTON (1966)
'SPECTRAL-EMISSIVITY MEASUREMENTS OF THE 4.3 MICRON CARBON DIOXIDE BAND BETWEEN 2650 K AND 3000 K', J. OPT. SOC. AM. ,VOL 56, NO.2, P171 (FEB)

FERRISO,C.C.,C.B. LUDWIG AND J.A.L. THOMSON (1966)
'EMPIRICALLY DETERMINED INFRARED ABSORPTION COEFFICIENTS OF WATER VAPOR FROM 300 K TO 3000 K',JQSRT, VOL 6, PP 241-275.

FISHENDEN,M. (1936)
'RADIATION FROM NON-LUMINOUS COMBUSTION GASES', ENGINEERING, VOL. 142, P684, DECEMBER

FLORNES,B.J. (1962)
'INFRARED ABSORPTION OF WATER-VAPOR-NITROGEN GAS MIXTURES AT ELEVATED TEMPERATURES', M.S. THESIS. UNIV. OF CALIF., LOS ANGELES.

FUES,O. (1927)
Z. PHYSIK, VOL. 46, P519

GATES,D.M.,R.F. CALFEE, D.W. HANSEN AND W.S. BENEDICT (1964)
'LINE PARAMETERS AND COMPUTED SPECTRA FOR WATER VAPOR BANDS AT 2.7 MICRON.', NATIONAL BUREAU OF STANDARDS MONOGRAPH NO. 71.

GOLDMAN,A. AND U.P. OPPENHEIM (1965)
'EMISSIVITY OF WATER VAPOR AT 1200 K IN THE 1.9 AND 2.7 MICRON REGIONS', J. OP. SOC. AM., VOL 55, NO. 7, P 794.

GOLDMAN,A. AND U.P. OPPENHEIM (1966)
APPLIED OPTICS, VOL. 5, P 1073

GOLDSTEIN,R. (1964)
'MEASUREMENT OF INFRARED ABSORPTION BY WATER VAPOR AT TEMPERATURES TO 1000 K.',JOURNAL OF QUANTITATIVE SPECTROSCOPY AND RADIATIVE TRANSFER, VOL 4,PP 343-352

GOODY, R.M. (1954)
'THE PHYSICS OF THE STRATOSPHERE,' PP 161-163, CAMBRIDGE UNIVERSITY PRESS, CAMBRIDGE.

GOODY, R.M. (1964)
ATMOSPHERIC RADIATION VOL. I. THEORETICAL BASIS. OXFORD UNIVERSITY PRESS.

GUERRIERI,S.A. (1932)
S.M. THESIS IN CHEM. ENG.,M.I.T.,CAMBRIDGE, MASS.

HARWARD,C.N. AND R.R. PATTY (1968)
J. OPT. SOC. AM., VOL 58, P 188

HERTZ G. (1911)
'UBER DAS ULTRAROT ABSORPTIONSPEKTRUM DER

KOHLENSAURE IN SEINER ABHANGIGKEIT VON DRUCK UND PARTIALDRUCK ',BERICHTE DER DEUTSCHEN PHYSIKALISCHEN GESELLSCHAFT,VERHANDLUNGEN, VOL 13, P617

HETTNER ET. AL. (1923)
ANNALEN DER PHYS.,VOL 55, P 476, AS CITED IN GUERRIERE (1932)

HINES, W.S. (1964)
'INFRARED RADIATION ABSORPTION STUDIES WITH MIXTURES OF WATER VAPOR, CARBON DIOXIDE AND NITROGEN', M.S. THESIS, UCLA, CALIF.

HINES, W.S. AND D.K. EDWARDS (1968)
'INFRARED ABSORPTIVITIES OF MIXTURES OF CO2 AND WATER VAPOR', CHEM. ENG. PROG. SYMP. SER. NO. 82, VOL 64, PP 173-180

HOTTEL, H.C. (1954)
IN 'HEAT TRANSMISSION.' (W.H. MCADAMS). 3RD EDITION, CHAP. 4. MCGRAW-HILL, NEW YORK.

HOTTEL, H.C. (1961)
J. INST. FUEL. ,VOL 34, P22

HOTTEL, H.C. AND R.B. EGBERT (1941)
'THE RADIATION OF FURNACE GASES', TRANS. ASME, VOL. 63, P297, MAY

HOTTEL, H.C., AND R.B. EGBERT (1942)
'RADIANT HEAT TRANSMISSION FROM WATER VAPOR.' AMER. INSTITUTE OF CHEM. ENGINEERS, VOL. 38, NO.3.

HOTTEL, H.C. AND H.G. MANGELSDORF (1935)
'HEAT TRANSMISSION BY RADIATION FROM NON-LUMINOUS GASES II. EXPERIMENTAL STUDY OF CARBON DIOXIDE AND WATER VAPOR', TRANS. A.I.CH.E.,VOL.31, P517

HOTTEL, H.C., AND A.F. SAROFIM (1967)
'RADIATIVE TRANSFER' MCGRAW-HILL, NEW YORK.

HOTTEL, H.C. AND V.C. SMITH (1935)
'RADIATION FROM NONLUMINOUS FLAMES', TRAN. ASME, PRO-57-4, P463

HOWARD,J.N.,D.E. BURCH AND D. WILLIAMS (1956)
'INFRARED TRANSMISSION OF SYNTHETIC ATMOSPHERES', JOURNAL OF THE OPTICAL SOCIETY OF AMERICA, VOL 46, NO. 3, P186

HOWARD,J.N.,D.E. BURCH AND D. WILLIAMS (1956)
J. OPT. SOC. AM. , VOL 46, NO. 4, P 237

HOWARD,J.N.,D.E. BURCH AND D. WILLIAMS (1956)
J. OPT. SOC. AM. , VOL 46, NO. 4, P 242

HOWARD,J.N.,D.E. BURCH AND D. WILLIAMS (1956)
J. OPT. SOC. AM. , VOL 46, NO. 5,P 334

JAFFE,J.H. AND W.S. BENEDICT (1963)
JQSRT, VOL 3, P 87

KAPLAN,L.D. (1947)
J. CHEM. PHYS., VOL 15, P 868

KAPLAN,L.D. AND D.F. EGGERS JR. (1956)
J. CHEM. PHYS., VOL 25, P 876

KOSTKOWSKI,H.J. (1954)
THESIS DISSERTATION, THE JOHN HOPKINS UNIV., BALT., MARYLAND, AS CITED BY MALKMUS,LUDWIG AND FERRISO(1966)

KUNITOMO,T.,M.OSUMI AND T. TAMBARA (1974)
'THE NARROW BAND MODEL PARAMETRRS OF THE CARBON DIOXIDE 4.3 MICRON BAND', INT. HT. TR. CONF.,FIFTH PROC.,JAPAN, VOL 1, PAPER R1.2

LECKNER, B. (1971)
'THE SPECTRAL AND TOTAL EMISSIVITY OF CARBON DIOXIDE' COMBUSTION AND FLAME VOL 17, P37

LECKNER, B. (1972)
'SPECTRAL AND TOTAL EMISSIVITY OF WATER VAPOR AND CARBON DIOXIDE',COMBUSTION AND FLAME,VOL 19, P 33

LOWDER, J.E. (1971)
JQSRT, VOL. 11, P 153

LUDWIG,C.B. AND C.C. FERRISO (1967)
'PREDICTION OF TOTAL EMISSIVITY OF NITROGEN BROADENED AND SELF BROADENED HOT WATER VAPOR ',JQSRT, VOL. 7, PP 7-26

LUDWIG,C.B.,C.C. FERRISO AND C.N. ABEYTA (1965)
'SPECTRAL EMISSIVITIES AND INTEGRATED INTENSITIES OF THE 6.3 MICRON FUNDEMENTAL BAND OF WATER VAPOR.', JQSRT, VOL 5, PP 281-290

LUDWIG,C.B.,C.C. FERRISO AND L. ACTON (1966)
'HIGH-TEMPERATURE SPECTRAL EMISSIVITIES AND TOTAL INTENSITIES OF THE 15 MICRON BAND SYSTEM OF CARBON DIOXIDE ', J. OPT. SOC. AM., VOL. 56,NO. 12, P 1685

LUDWIG,C.B.,C.C. FERRISO,W. MALKMUS AND F.P. BOYNTON (1965)
'HIGH-TEMPERATURE SPECTRA OF THE PURE ROTATIONAL BAND OF WATER VAPOR.', JQSRT, VOL 5, NO. 5, PP 697-714

LUDWIG, C.B. ET AL. (1966)
'STUDY ON EXHAUST PLUME RADIATION PREDICTION.' GENERAL DYNAMICS/CONVAIR, REPORTS DBE 66-017, 001A.

LUDWIG, C.B. ET AL. (1968)
'STUDY ON EXHAUST PLUME RADIATION PREDICTION.'
GENERAL DYNAMICS CORP., N.A.S.A., CR-61233.

LUDWIG,C.B. AND W. MALKMUS (1968)
'BAND MODEL REPRESENTATIONS FOR HIGH TEMPERATURE WATER VAPOR AND CARBON DIOXIDE', PROCEEDINGS OF A SPECIALISTS CONFERENCE ON MOLECULAR RADIATION, MARSHALL SPACE FLIGHT CENTER, HUNTSVILLE, ALA.,OCT. 5-6,1967, NASA TM X-53711, P 19

LUDWIG,C.B., W. MALKMUS, J.E. REARDON AND J.A.L. THOMSON (1973), 'HANDBOOK OF INFRARED RADIATION FROM COMBUSTION GASES',EDITORS R. GOULARD AND J.A.L. THOMSON, NASA SP-3080 WASHINGTON, D.C.

MADDEN, R.P. (1961)
J. CHEM. PHYS., VOL. 35, P 2083

MALKMUS, W. (1963)
'INFRARED EMISSIVITY OF CARBON DIOXIDE (4.3 MICRON BAND)', J. OPT. SOC. AM., VOL 53,NO. 8, P 951

MALKMUS W. (1964)
'INFRARED EMISSIVITY OF CARBON DIOXIDE (2.7 MICRON BAND)', J. OPT. SOC. AM., VOL.54, NO.6, P751

MALKMUS W. (1967)
'CRITERIA FOR ACCURACY OF MEASUREMENT OF LINE INTENSITIES AND MEAN ABSORPTION COEFFICIENTS', APPLIED OPTICS, VOL 6,NO. 2, P 349

MALKMUS,W.,C.B. LUDWIG AND C.C. FERRISO (1966)
'TEMPERATURE DEPENDENCE OF THE TOTAL INTENSITY OF DIFFERENCE-BAND SYSTEMS. THE 10 MICRON BAND SYSTEM OF CARBON DIOXIDE ', J. CHEM. PHYS., VOL. 45, NO. 11,P3953

MALKMUS W., AND A. THOMSON (1962)
'INFRARED EMISSIVITY OF DIATOMIC GASES FOR THE ANHARMONIC VIBRATING-ROTATOR MODEL', J. QUANTA. SPECTROSC. RAD. TRANSFER, VOL 2, P 17

MARTIN,P.E. AND E.F. BARKER (1932)
PHYS. REV., VOL. 41, P 291

MCCLATCHEY,R.A.,W.S. BENEDICT,S.A. CLOUGH, D.E. BURCH, R.F. CALFEE,K. FOX,L.S. ROTHMAN AND J.S. GARING (1973)
'AFCRL ATMOSPHERIC ABSORPTION LINE PARAMETERS COMPILATION', AFCRL-TR-73-0096, AFCRL, BEDFORD, MASS.

MCCLATCHEY,R.A.,R.W. FENN,J.E.A. SELBY,F.E. VOLZ AND J.S. GARING (1972)
'OPTICAL PROPERTIES OF THE ATMOSPHERE.',THIRD EDITION, AFCRL-72-0497, BEDFORD,MASS.

MCCUBBIN,T.K.,R. DARONE AND J. SORRELL (1966)
APPL. PHYS. LETTERS, VOL. 8, P118

MENARD, W.A. (1964)
'BAND AND LINE STRUCTURE MODELS FOR CORRELATION OF GASEOUS RADIATION ', M.S. THESIS, UNIV. OF CAL.,L.A.

MILLARD, J.E. (1935)
'THE RADIATING CHARACTERISTICS OF A PREMIXED GAS BURNER FLAME ',M.S. THESIS, CHEM.END.,(SUPV. H.C.HOTTEL) MIT, CAMBRIDGE, MASS.

NELSON, K.E. (1959)
'EXPERIMENTAL DETERMINATION OF BAND ABSORPTIVITY OF WATER VAPOR AT ELEVATED PRESSURES AND TEMPERATURES', M.S. THESIS, UNIV. OF CAL., BERKELEY

NICOLET, W.E. (1962)
'EXPERIMENTAL DETERMINATION OF THE BAND ABSORPTION OF CARBON DIOXIDE GAS AT ELEVATED TEMPERATURES AND SUBATMOSPHERIC PRESSURES',M.S. THESIS, U. OF CAL.,L.A.

OPPENHEIM,U.P. AND Y. BEN ARYEH (1963)
J. OPT. SOC. AM., VOL 53, P344

OVEREND,J.,M.J. YOUNGQUIST,E.C. CURTIS AND B. CRAWFORD (1959)
J. CHEM. PHYS., VOL. 30, P 532

PALMER,C.H. (1957)
J. OPT. SOC. AM., VOL 47, P1024, 1028, 1054, 367

PALMER,C.H. (1959)
J. OPT. SOC. AM. , VOL. 49, P 1139

PALMER, C.H. (1960)
'EXPERIMENTAL TRANSMISSION FUNCTIONS FOR THE PURE ROTATION BAND OF WATER VAPOR', J. OPT. SOC. AM.,VOL 50, NO. 12, P 1232

PATCH,R.W. (1965)
PH.D. THESIS, CALIF. INST. OF TECH.,PASADENA,CALIF.

PATCH,R.W. (1965)
'ABSOLUTE INTENSITY MEASUREMENTS FOR THE 2.7 MICRON BAND OF WATER VAPOR IN A SHOCK TUBE', JQSRT, VOL. 5, NO. 1, PP 137-164

PENNER, S.S. (1952)
AS CITED IN MALKMUS, LUDWIG AND FERRISO (1966)

PENNER, S.S. (1959)
'QUANTITATIVE MOLECULAR SPECTROSCOPY AND GAS EMISSIVITIES', ADDISON-WESLEY, READING, MASS.

PENNER,S.S. AND P. VARANASI (1966)
'EFFECT OF PARTIAL OVERLAPPING OF SPECTRAL LINES ON THE TOTAL EMISSIVITY OF WATER VAPOR-CARBON DIOXIDE MIXTURES (T GREATER THAN 800 K)',JQSRT, VOL 6, NO.2, P181

PLASS,G.N. (1952)
J. METEOROL., VOL. 9, P 429

PLASS, G.N. (1958)
'MODELS FOR SPECTRAL BAND ABSORPTION',J. OPT. SOC. AM., VOL. 48, P 690

PLASS, G.N. (1959)
'SPECTRAL EMISSIVITY OF CARBON DIOXIDE FROM 1800. TO 2400 RECIPROCAL CM.', J. OPT. SOC. AM., VOL. 49, NO.8, P 821

PLASS, G.N. (1960)
'USEFUL REPRESENTATION FOR THE MEASUREMENTS OF SPECTRAL BAND ABSORPTION', J. OPT. SOC. AM., VOL. 50, P 868

PLYLER,E.K.,E.D. TIDWELL AND W.S. BENEDICT (1962)
J. OPT. SOC. AM., VOL. 52, P 1017

RASOOL, S.I. (1964)
'INTENSITIES OF 9.4 MICRON AND 10.4 MICRON CARBON DIOXIDE BANDS', PROC. INTERN. SYMP. ASTROPHYS.,12 TH, LIEGE,1963, P 55

ROSENBERG JR.,C.W.,N.H. PRATT,AND K.N.C. BRAY (1970)
JQSRT, VOL 10, P 1155

RUBENS, H. AND E. LADENBURG (1905)
'UBER DAS LANGWELLIGE ABSORPTIONS-SPEKTRUM DER KOHLENSAURE', VERHANDLUNGEN DER DEUTSCHEN PHYSIKALISCHEN GESELLSCHAFT, VOL. 7, P170

SAROFIM, A.F. (1961)
'RADIANT HEAT TRANSMISSION IN ENCLOSURES ',SC.D. THESIS, CHEM. ENG., (SUPV. H.C. HOTTEL), MIT, CAMBRIDGE MASS.

SCHACK,K. (1970)
'BERECHNUNG DER STRAHLUNG VON WASSERDAMPF UND KOHLENDIOXID',CHEMIE INGENIEUR TECHNIK,VOL 42,NO. 2

SCHACK,K. (1971)
'ZUR BERECHNUNG DER WASSERDAMPFSTRAHLUNG',CHEMIE INGENIEUR TECHNIK, VOL 43, NO. 21

SCHMIDT, E. (1932)
'MESSUNG DER GESAMTSTRAHLUNG DES WASSERDAMPFES BEI TEMPERATUREN BIS 1000 C.', FORSCHUNG AUF DEM GEBIETE DES INGENIEURWESENS, VOL.3, P57

SCHMIDT, H. (1913)
ANN. PHYS., VOL '2, P415

SCHURIN,B. (1960)
'CALCULATED BAND INTENSITIES FOR CARBON DIOXIDE FROM INFRARED DISPERSION DATA', J. CHEM. PHYS., VOL. 33, NO. 6, P 1878

SELBY,J.E.A. AND R.M. MCCLATCHEY (1972)
'ATMOSPHERIC TRANSMITTANCE FROM 0.25 TO 28.5 MICRONS. COMPUTER CODE LOWTRAN 2.', AFCRL-72-0745, BEDFORD, MASS.

SMITH, W.L. (1969)
'A POLYNOMIAL REPRESENTATION OF CARBON DIOXIDE AND WATER VAPOR TRANSMISSION ', ESSA TECHNICAL REPORT NESC 47, NATIONAL ENVIRONMENTAL SATELLITE CENTER, WASHINGTON , D.C.

SPACE SCIENCE LABORATORY (1966)
'STUDY ON EXHAUST PLUME RADIATION PREDICTIONS', INTERIM PROGRESS REPORT,PARTS 1 AND 2, GENERAL DYNAMICS CONVAIR,SAN DIEGO, CAL., REPRT. GD/C-DBE-66-001 AND GD/C-DBE-66-001 A

SPACE SCIENCE LABORATORY, (1967)
STUDY ON EXHAUST PLUME RADIATION PREDICTIONS, NOV. 1967 GENERAL DYNAMICS CONVAIR, SAN DIEGO, CALIF.

STAUFFER,F.R. AND T.E. WALSH (1966)
'TRANSMITTANCE OF WATER VAPOR 14 TO 20 MICRONS.', J. OPT. SOC. AM., VOL 56, NO. 3, P 401

STULL,V.R.,P.J. WYATT AND G.N. PLASS (1964)
'THE INFRARED TRANSMITTANCE OF CARBON DIOXIDE',
APPLIED OPTICS, VOL 3, NO. 2, P 243

TEJWANI,G.D.T. AND P. VARANASI (1970)
'APPROXIMATE MEAN ABSORPTION COEFFICIENTS IN THE
SPECTRUM OF WATER VAPOR BETWEEN 10 AND 22 MICRON AT

ELEVATED TEMPERATURES', JQSRT, VOL 10, P 373-388

THOMSON, J.A.L. (1967)
AS CITED IN HOTTEL AND SAROFIM (1967)

THOMSON,J.A.L. (1968)
'RADIATION MODEL FOR NON SCATTERING ROCKET EXHAUST
GASES ', PROC. OF A SPECIALISTS CONFERENCE ON MOLECULAR
RADIATION,MARSHALL SPACE FLIGHT CENTER,HUNTSVILLE,ALA.
OCT. 5-6,1967, NASA TM X-53711, P 137

THORNDIKE, A.M. (1947)
J. CHEM. PHYS., VOL. 15, P 868

TIEN, C.L. (1967)
'THERMAL RADIATION PROPERETIES OF GASES', REPORT
NO. TS-67-1, THERMAL SYSTEMS DIVISION, UNIV. OF
CALIFORNIA, BERKELEY.

TINGWALT,C. (1934)
'DIE ABSORPTION DER KOHLENSAURE IM GEBIET DER BANDE
2.7 MICRONS ZWISCHEN 300 UND 1100 ABSOLUT', PHYS. ZEIT
VOL. 35, P 715

TINGWALT,C. (1938)
'DIE ABSORPTION DER KOHLENSAURE IM GEBIET DER BANDE
4.3 MICRONS ZWISCHEN 300 UND 1000 ABSOLUT',PHYS. ZEIT,
VOL. 39, P 1

TOURIN, R.H. (1961)
'SOME SPECTRAL EMISSIVITIES OF WATER VAPOR IN THE
2.7 MICRON REGION', J. OPT. SOC. AM., VOL 51, P 1225

TOURIN,R.H. (1961)
'MEASUREMENTS OF THE INFRARED SPECTRAL EMISSIVITIES
OF HOT CARBON DIOXIDE IN THE 4.3 MICRON REGION', J.
OPT. SOC. AM., VOL 51, P 175

TOURIN, R.H. (1961)
'SPECTRAL EMISSIVITIES OF HOT CARBON-DIOXIDE-WATER-
VAPOR MIXTURES IN THE 2.7 MICRON REGION',J.OPT. SOC.
AM., VOL 51, P 799

VARANASI,P. AND J.L. LAUDER (1966)
' A REDETERMINATION OF THE INTEGRATED INTENSITY OF THE 15 MICRON BANDS OF CARBON DIOXIDE ', JQSRT, VOL. 6, P 127

WEBER,D.R. (1959)
AS CITED BY S.S. PENNER (1959)

WEBER,D.R.,J. HOLM AND S.S. PENNER (1951)
J. CHEM. PHYS., VOL 19, P 1554

WOLK, M. (1967)

'THE STRENGTH OF THE PRESSURE-BROADENED CARBON DIOXIDE BANDS AT 15 MICRON BY DIGITAL INTEGRATION OF SPECTRA ', JQSRT, VOL. 7, PP 1-5

WYATT, P.J., V.R. STULL AND G.N. PLASS (1964)
'THE INFRARED TRANSMITTANCE OF WATER VAPOR.', APPLIED OPTICS, VOL 3, NO. 2, P 229

YAMAMOTO,G. AND T. SASAMORI (1958)
SCI. REPTS.,TOHUKU UNIV., FIFTH SER., VOL. 10,NO. 2 JULY